Role of C-type natriuretic peptide in cardiac structure and function

A thesis submitted in partial fulfilment for the Degree of
Doctor of Philosophy in Queen Mary University of London

Sandy Min Yin Chu

Translational Medicine and Therapeutics
Heart Centre
William Harvey Research Institute
Barts and The London, School of Medicine and Dentistry
Queen Mary University of London
Charterhouse Square
London EC1M 6BQ

Statement of originality

I, Sandy Min Yin Chu, confirm that the research included within this thesis is my own work or that where it has been carried out in collaboration with, or supported by others, that this is duly acknowledged below and my contribution indicated. Previously published material is also acknowledged below.

I attest that I have exercised reasonable care to ensure that the work is original, and does not to the best of my knowledge break any UK law, infringe any third party's copyright or other Intellectual Property Right, or contain any confidential material.

I accept that the College has the right to use plagiarism detection software to check the electronic version of the thesis.

I confirm that this thesis has not been previously submitted for the award of a degree by this or any other university.

The copyright of this thesis rests with the author and no quotation from it or information derived from it may be published without the prior written consent of the author.

Signature:

Date: 18.05.2018

Abstract

Introduction:

C-type natriuretic peptide (CNP) is synthesised and released by the endothelium and plays a vital role in the maintenance of vascular homeostasis (Moyes et al., 2014). However, a similar regulatory role of endogenous CNP in the heart has yet to be elucidated. Therefore, I have used three unique mouse strains with endothelium (Tie^2-Cre), cardiomyocyte (αMHC-Cre) and fibroblast (Col1α2-Cre)-restricted deletion of CNP to investigate if the peptide modulates coronary vascular reactivity and cardiac function.

Methods:

Langendorff isolated hearts were used to investigate the effect of CNP deletion on coronary vascular reactivity in response to the endothelium-dependent vasodilators bradykinin (10nmol) and acetylcholine (0.1-1nmol). Vasodilatation associated with reperfusion was investigated by transient cessation of flow (20-80 seconds). Ischaemia reperfusion (IR) injury (35 minutes ischaemia followed by 60 minutes reperfusion) was also investigated in cell-specific knockout (KO) animals. Isoprenaline (ISO; 20mg/kg/day, 7days)- and pressure overload (abdominal aortic constriction [AAC]; 6 weeks)-induced heart failure were used to study the effect of CNP deletion during cardiac stress, with cardiac function assessed by echocardiography. Cardiac fibrosis and hypertrophy were determined by picro-sirius red and wheat-germ agglutinin fluorescence staining, respectively. A subset of experiments was repeated in mice with global deletion of natriuretic peptide receptor-C (NPR-C) to delineate the signalling pathway triggered by CNP. Real time qPCR was used to determine hypertrophic and fibrotic gene expression in left ventricles isolated from mice subjected to AAC or sham. Neonatal cardiomyocytes were isolated to investigate angiotensin (Ang)II-induced hypertrophy.

Results:

Coronary endothelial reactivity was reduced in endothelial CNP (ecCNP) KO mice compared to wild type (WT) in response to bradykinin, acetylcholine and reperfusion-induced vasodilatation. These observations were paralleled in NPR-C KO animals. ecCNP KO did not exacerbate IR injury, whilst mice with cardiomyocyte-restricted deletion of CNP (cmCNP KO) and NPR-C KO animals exhibited a larger infarct size compared to WT. cmCNP KO mice also displayed greater cardiac dysfunction and fibrosis after ISO infusion or AAC compared

to WT; similar results were observed in fbCNP KO and NPR-C KO animals. Infusion of CNP (0.2mg/kg/day; osmotic mini-pump, s.c.) in WT, but not NPR-C KO, animals rescued the decline in cardiac function. CNP (1μM) administration in isolated cardiomyocyte also blunted Ang II-induced hypertrophy. Pro-hypertrophic and pro-fibrotic gene expression (ANP, β-MHC and MMP-2) was augmented in cmCNP KO and NPR-C KO mice compared to littermate controls following AAC.

Conclusions:

Endothelial, cardiomyocyte and fibroblast-derived CNP have distinct, complementary roles in the heart, modulating cardiac function by influencing coronary vascular tone and protecting against heart failure and IR injury. These protective effects of CNP are mediated, at least in part, via NPR-C activation. Developing CNP mimetics or selective NPR-C agonists could be a novel therapeutic intervention in cardiovascular disease.

Acknowledgements

First and foremost, I would like to thank my supervisors, Prof. Adrian Hobbs and Dr. Amie Moyes, for providing constant support, guidance and care throughout my PhD. Adrian has always kept his door open whether it was for work discussion or personal matters. I have been touched and motivated enormously by his kind words, which have been a good source of encouragement. He is the best supervisor/mentor a student could ever hope for. I will take away his work ethic and outlook to life with me and I wish our interaction will carry on beyond the PhD. Amie, my 'technical' mentor, taught me all the *in vivo* skills involved in this thesis. Her patience in teaching and her belief in me has given me confidence to expand my skill repertoire. I hereby wish her and the family a lovely future with their new-born daughter.

I also would like to thank the rest of the team in the Hobbs lab. I really appreciated the support and advice from Dr. Reshma Baliga that was always readily available. She always made sure that there were sweets to feed our little scientific brains! Dr. Aisah Aubdool is a very caring person who is always full of positive energy and ideas. I am always in awe of her endless knowledge and skills. Dr. Cristina Pérez-Ternero shared her thoughts and experience that encouraged me to be the best I can. Despite her busy schedule, she often offered to help (once even labelled all my qPCR tubes!). In addition, thanks for the random puns and jokes from Dr. Vanessa Lowe, Michael Preedy and Tara McConaghy that have brought a lot of laughter into the lab. No amount of words can express the gratitude that I have towards the entire Hobbs group for their friendship, guidance and encouragement throughout the years. A special thank you to Prof. Amrita Ahluwalia for the resources that enabled me to carry out the Langendorff experiments, which constitute a significant proportion of this thesis.

Last but not the least, I would like to thank my mum, Gui Ying Yang, and my brother, Andy Chu, who probably still don't quite get what I do but always supportive. This thesis marks the end of my student status and the beginning of a new challenge. I hope I have made you all feel proud.

This work was supported by the British Heart Foundation.

List of publications

Journal publication

Chu SM, Moyes AJ, Baliga RS, Aubdool AA, Hobbs AJ; 'C-type Natriuretic Peptide regulates cardiac structure and function.' Paper drafted for submission to European Heart Journal.

List of published abstracts

Chu SM, Moyes AJ, Hobbs AJ; 'C-type natriuretic peptide plays a fundamental role in cardiac function'. (**Oral** at British Pharmacology Society 2017; London, UK)

Moyes AJ, **Chu SM**, Baliga RS, Hobbs AJ; 'C-type Natriuretic Peptide regulates cardiac structure and function.' (**Oral** at cGMP conference 2017; Bamberg, Germany)

Chu SM, Moyes AJ, Hobbs AJ; The role of endogenous C-type natriuretic Peptide in cardiac function. (**Oral** at BHF 4-year PhD student conference 2016; Glasgow, Scotland)

Moyes AJ, **Chu SM**, Baliga RS, Hobbs AJ; Endothelial and Cardiomyocyte -derived C-type Natriuretic Peptide Coordinate Heart Structure and Function. (**Oral** at American Heart Association Scientific Sessions 2015; Orlando, USA)

Abbreviations

α-MHC	Alpha-myosin heavy chain
AAC	Abdominal aortic constriction
AC	Adenylyl cyclase
ACh	Acetylcholine
ACE	Angiotensin converting enzyme
ACEi	Angiotensin converting enzyme inhibitor
ADMA	Asymmetrical dimethylarginine
AIF	Apoptosis-induction factor
Ang I/II	Angiotensin I/II
ANP	Atrial natriuretic peptide
ApoE	Apolipoprotein E
ARB	Angiotensin II receptor blocker
AT_1R	Angiotensin II receptor
ATF-2	Activating transcription factor-2
ATP	Adenosine-5'-triphosphate
β-AR	Beta-adrenergic receptor
β-MHC	β-myosin heavy chain
BH_4	Tetrahydrobiopterin
BHF	British Heart Foundation
BK	Bradykinin
BK_{Ca}	Large conductance Ca^{2+} activated potassium channel
BNP	Brain natriuretic peptide
BP	Blood pressure
BS	Bovine serum

BW	Body weight
CaMK II	Calcium/calmodulin-dependent protein kinase II
cAMP	Cyclic adenosine-3',5'-monophosphate
cGMP	Cyclic guanosine-3',5'-monophosphate
CHD	Coronary heart disease
CHF	Chronic heart failure
cmCNP	Cardiomyocyte-derived CNP
CNP	C-type natriuretic peptide
COL1α2	Collagen 1-alpha-2
COX	Cyclooxygenase
CPP	Coronary perfusion pressure
CsA	Cyclosporin-A
CVD	Cardiovascular disease
CVS	Cardiovascular system
DAG	Diacylglycerol
DMEM	Dulbecco's Modified Eagle's Medium
DNA	Deoxyribonucleic acid
DNP	*Dendroaspis* natriuretic peptide
EC	Endothelial cell
ecCNP	Endothelial cell-derived CNP
ECG	Electrocardiogram
ECM	Extracellular matrix
EDHF	Endothelium-derived hyperpolarising factor
EDRF	Endothelium-derived relaxing factor
EF	Ejection fraction
ELSA	Enzyme-linked immunesorbent assay
eNOS (NOS 3)	Endothelial nitric oxide synthase

Epac	cAMP-activated guanine nucleotide exchange proteins
ERK1/2	Extracellular signal–regulated kinase 1/2
ET-1	Endothelin-1
fbCNP	Fibroblast-derived CNP
FGF-2	Fibroblast growth factor-2
FGFR	Fibroblast growth factor receptor
FRT	Flippase recognition target
FS	Fractional shortening
GC	Guanylyl cyclase
GH	Growth hormone
GIRK	G-protein coupled inwardly rectifying potassium channel
GPCR	G-protein coupled receptor
GSK3	Glycogen synthase kinase 3
GTP	Guanosine-5’-triphosphate
GWAS	Genome-wide association study
HBSS	Hank’s balance salt solution
HDAC 4	Histone deacetylase 4
HF	Heart failure
HFpEF	Heart failure with preserved ejection fraction
HFrEF	Heart failure with reduced ejection fraction
HR	Heart rate
HW	Heart weight
$I_{Ca(L)}$	L-type calcium current
I_f	Hyperpolarisation-activated (funny) current
IGF-1(R)	Insulin-like growth factor-1 (receptor)
IL-1	Interleukin-1
iNOS (NOS 2)	Inducible nitric oxide synthase

IR	Ischaemia reperfusion
ISO	Isoprenaline
JNK	c-Jun amino-terminal kinase
KO	knockout
LAD(CA)	Left anterior descending (coronary artery)
L-NAME	N^G-nitro-L-arginine methylester
LPS	Lipopolysaccharide
LV	Left ventricle
LVAW	left ventricular anterior wall
LVDP	Left ventricular developed pressure
LVID	Left ventricular internal diameter
LVPW	Left ventricular posterior wall
MABP	Mean arterial blood pressure
MAPK	Mitogen-activated protein kinase
MEF-2	Myocyte enhancer factor-2
MEK (MAP2K)	Mitogen-activated protein kinase kinase
MEKK (MAP3K)	Mitogen-activated protein kinase kinase kinase
MI	Myocardial infarction
mitoK$_{ATP}$	Mitochondrial ATP-dependent potassium
MLK	Mixed lineage kinase
MLC	Myosin light chain
MLCP	Myosin light chain phosphatase
mRNA	Messenger ribonucleic acid
MRTF	myocardin-related transcription factor
MSB	Martius scarlet blue staining
mPTP	Mitochondrial permeability transition pore
NADPH	Nicotinamide adenine dinucleotide phosphate

NEP	Neutral endopeptidase
NFAT	Nuclear factor of activated T cells
nNOS (NOS1)	Neuronal nitric oxide synthase
NO	Nitric oxide
NOS	Nitric oxide synthase
NPR	Natriuretic peptide receptor
NSAIDs	Non-steroid anti-inflammatory drugs
NSTEMI	Non-ST-elevation myocardial infarction
NTproBNP	N-terminal proBNP
PBS	Phosphate-buffered saline
PCI	Percutaneous coronary intervention
PCR	Polymerase chain reaction
PDE	Phosphodiesterase
PDGF(R)	Platelet-derived growth factor (receptor)
pGC	Particulate guanylyl cyclase
PGI_2	Prostacyclin
PI3K	Phosphatidylinositol-3-kinase
PKA	cAMP-dependent protein kinase
PKB (Akt)	Protein kinase B
PKC	Protein kinase C
PKG/cGK	cGMP-depending protein kinase
PLB	Phospholamban
PLC-β	Phospholipase C-β
PTx	*Pertussis toxin*
RAAS	Renin-aldosterone-angiotensin system
RGS	Regulator of G-protein signalling
RNA	Ribonucleic acid

ROS	Reactive oxygen species
RT	Reverse transcription
RyR	Ryanodine receptor
SAN	Sinoatrial node
SEM	Standard error of the mean
SERCA	Sarco/endoplasmic reticulum calcium ATPase
sGC	Soluble guanylyl cyclase
SHR	Spontaneous hypertensive rat
SNP	Sodium nitroprusside
STEMI	ST-elevation myocardial infarction
T3	Tri-iodothyronine
TAC	Transverse aortic constriction
TAK-1	Transforming growth factor-β activated kinase-1
TAM	Tamoxifen
TGF-β(R)	Transforming growth factor-β (receptor)
TNF-α	Tumour necrosis factor-α
TPF	1, 3, 5-triphenylformazan
TTC	Triphenyl tetrazolium chloride
VEGF-β	Vascular endothelial growth factor-β
VSMC	Vascular smooth muscle cell
WGA	Wheat germ agglutinin
WT	Wild type
XO	Xanthine oxidase
XOI	Xanthine oxidase inhibitor

Table of contents

List of figures

List of tables

Chapter 1 – Introduction

Chapter 1 – Introduction

1 Introduction

1.1 Cardiovascular disease

1.1.1 Background

Cardiovascular disease (CVD) is a group of disorders of the heart and blood vessels, including coronary heart disease (CHD), cerebrovascular disease, peripheral arterial disease, congenital heart disease, and deep vein thrombosis. CVDs are the leading cause of death worldwide. An estimated 17.7 million people died from CVD in 2015, representing 31% of all global deaths and this has been projected to increase to 23.3 million by 2030 (World Health Organisation, 2015). Of these, an estimated 42% were due to CHD. In the UK, almost 160,000 deaths resulted from CVD in 2015, which accounted for more than a quarter of all deaths, and around 7 million people are living with CVD (British Heart Foundation [BHF], 2017). Clinical care of CVD is costly and prolonged. The total annual health care cost of CVD in the UK is estimated at £9 billion. People with, or at risk of, CVD may exhibit one or more risk factors such as hypertension, diabetes, hyperlipidaemia or obesity. These individuals require early detection and management using counselling and medicines in order to effectively prevent premature deaths caused by CVD.

1.1.2 Coronary heart disease

CHD or ischaemic heart disease is the most common form of CVD. An estimated 2.3 million people are living with CHD in the UK (BHF statistics, 2017). It occurs when the coronary vessels that supply blood to the heart become narrowed by a build-up of fatty deposits, called atheroma. This narrowing reduces blood supply to the heart and causes pain and discomfort, an event called angina. Heart attack, also known as myocardial infarction (MI), occurs when an advanced atheroma ruptures in coronary arteries, causing reduced or no blood supply to the heart muscle (myocardium) beyond the lesion. This results in lack of oxygen and nutrient supply to myocardium and causes cell death. To minimise the damage to the myocardium, it is necessary to unblock the blood vessel using thrombolytic therapy, percutaneous coronary intervention (PCI; i.e. balloon angioplasty), or coronary artery bypass as soon as possible. However, the process of reperfusion itself can aggravate myocardial injury. This phenomenon is termed myocardial ischaemia reperfusion (IR) injury

and pre-clinical models suggest this could account up to 50% of the final infarct size (Yellon and Hausenloy, 2007).

1.1.3 Chronic heart failure

Chronic heart failure (CHF) is a condition where cardiac output cannot meet the demand of the body's needs at normal filling pressure. Over half a million patients are diagnosed with CHF every year in the UK (BHF statistics, 2017). CHF most commonly results from myocardium damage caused by MI or prolonged hypertension, but can also stem from faulty heart valves, infection (e.g. myocarditis) or genetic deficiency (i.e. cardiomyopathies) (Yousef et al., 2000, Appenzeller et al., 2011, Morales and Hershberger, 2017).

The improvement in therapeutic intervention in MI has led to more patients surviving and living longer after the event. Accordingly, the occurrence of post-MI CHF continues to rise. The progression of the CHF phenotype in these patients involves complex and progressive ventricular remodelling that entails dilatation of the left ventricle (LV) and formation of scar. These can be driven by molecular and cellular transformation in cardiomyocytes, fibroblasts and neurohormonal pathways.

Untreated hypertension causes LV remodelling that can eventually leads to CHF (David C. Dugdale, 2012). Hypertension mainly results from increased peripheral vascular resistance and/or a reduction in compliance, which causes an elevation of cardiac afterload. To accommodate the increased afterload, the LV has to generate a greater force of contraction that overcomes the elevated aortic pressure. The heart achieves this by increasing wall thickness and becoming distended. This adaptive structural remodelling is termed compensatory or concentric (physiological) cardiac hypertrophy (Heineke and Molkentin, 2006). However, when the remodelling is no longer able to compensate or the magnitude of the overload increases further, a relentless deterioration of cardiac structure and function ensues. This includes dilatation of the LV chamber, contractility reduces, and cardiac output consequentially declines (Heineke and Molkentin, 2006). This is termed decompensatory or eccentric LV hypertrophy. This chronic myocardial remodelling is characterised by myocyte loss due to necrosis and apoptosis, cardiomyocyte hypertrophy, re-expression of a fetal gene profile and increases in extra-cellular matrix (ECM)/fibrosis.

Clinically, patients are often grouped based on their LV ejection fraction (EF), HF with preserved EF (HFpEF) ≥50%, and HF with reduced EF (HFrEF) <50% (Noordali et al., 2018). HFpEF tends to occur in older, hypertensive patients with multiple cardiovascular comorbidities including the metabolic syndrome, diabetes mellitus, obesity, and

endothelial dysfunction (Burchfield et al., 2013). Recent published guideline in the diagnosis of HFpEF includes a normal LVEF coupled with raised LV end-diastolic pressure due to diastolic dysfunction, left atrial enlargement, LV hypertrophy and/or elevation of plasma natriuretic peptides (Burchfield et al., 2013).

HFrEF typically occurs in patients who have suffered acute myocardial damage (e.g. MI), chronic haemodynamic stress (e.g. hypertension and valvular heart disease), or results from autoimmune/infective causes (Noordali et al., 2018). A severe reduction in EF is the consequence of contractile impairment, maladaptive cardiac remodelling, and dysfunctional vasculoventricular coupling (Noordali et al., 2018). The fall in cardiac output results in end-organ hypoperfusion (e.g renal hypoperfusion) and baro-reflex impairment, which leads to activation of neurohormonal compensatory mechanisms (Jackson et al., 2000). These mechanisms include activation of the renin-angiotensin-aldosterone system (RAAS) that results in vasoconstriction, stimulates the release of noradrenaline from sympathetic nerve terminals and inhibits vagal tone. The release of aldosterone leads to the retention of salt and water that increases blood volume. Together, the activation of RAAS increases preload that augments systolic pressure according to the Frank-Starling mechanism. Activation of the sympathetic nervous system increases cardiac inotropy, chronotropy and lusitropy in order to maintain cardiac output. However, sustained sympathetic activation has deleterious effect, causing a further deterioration in cardiac function. In addition, excessive sympathetic activation is also associated with myocyte apoptosis and necrosis, and hypertrophy. Interestingly, Larsen *et al*. (2016) has shown that cross-culturing healthy sympathetic neurons onto diseased myocytes rescues the aberrant cAMP response of the myocyte and vice versa, diseased neuron cultured with healthy myocyte leads to the development of an increased cAMP response (Larsen et al., 2016). This suggests that the sympathetic neurons are the dominant drivers of β-adrenergic hyperactivity in myocardial pathology.

Many existing therapeutics licensed to treat HFrEF and are aimed at correcting volume-overload (e.g. diuretics), alter haemodynamics (e.g. vasodilators and inotropic agents), and reduce neurohormonal activation (e.g. β-adrenergic blockers and angiotensin converting enzyme inhibitors (ACEi)). Large clinical trials such as CONSENSUS (1987a) and SOLVD (Yusuf et al., 1991) have shown that the ACEi, enalapril, reduces mortality and improves symptoms in patients with CHF. β-blockers are also associated with survival benefits (CIBIS-II (1999a), MERIT-HF (1999b)). However, to date, there are no evidence-based therapies for HFpEF and the prognosis of both forms of HF remains poor (Noordali et al., 2018). No

therapeutic intervention directly prevents or reverses LV remodelling but rather they reduce symptoms, which entails a five year mortality of almost 50% (Mahjoub et al., 2008). Therefore, more effective therapeutic strategies are needed in the prevention and treatment of CHF.

In the recent past, the understanding of cyclic guanosine-3',5'- monophosphate (cGMP) signalling mediated by nitric oxide (NO) or natriuretic peptides in the cardiovascular system (CVS) has been significantly advanced and has shown to be an effective therapeutic target. For example, the VICTORIA trial has recently commenced to investigate vericiguat, a novel oral soluble guanylyl cyclase (sGC) stimulator (the enzyme responsible for cGMP synthesis in response to NO), in patients with HFrEF (Armstrong et al., 2018); LCZ696 (Sacubitril/valsartan), a novel combined inhibitor of neprilysin (neutral endopeptidase) and angiotensin receptor blocker (ARB), has been shown to be more effective than ARB or ACEi alone in the PARAMETER (Williams et al., 2017) and PARADIGM-HF studies (McMurray et al., 2014), respectively. A phase II clinical trial, PARAMOUNT, involving patients with HFpEF has also demonstrated LCZ696 reduces NT-proBNP, a well-established HF biomarker, to a greater extent than valsartan (Solomon et al., 2012), but whether this effect will translate into an improved outcome requires a larger scale prospective trial.

1.2 Regulation of cardiac remodelling

1.2.1 Physiological and pathological remodelling

Cardiac remodelling/hypertrophy refers to the changes in size, shape, structure and function of the heart. It can be broadly classified as physiological hypertrophy, for example, due to chronic exercise or pregnancy, and pathological hypertrophy as a result of hypertension or cardiac injury (Bernardo et al., 2010). Physiological hypertrophy is reversible and characterised by normal cardiac morphology, i.e. no fibrosis and apoptosis, normal or enhanced cardiac function (Bernardo et al., 2010). At the molecular level, physiological cardiac remodelling is associated with well-established signalling pathways, including vascular endothelial growth factor B (VEGF-B), growth hormone (GH), insulin-like growth factor (IGF)-1, and the thyroid hormone tri-iodothyronine (T3). These pathways essentially control angiogenesis, cardiomyocyte contractility, sarcomere remodelling, metabolic and mitochondrial adaptations, and cell survival (Wu et al., 2017b). Moreover, this hypertrophy is associated with no changes in the expression of known pathological biomarkers such as atrial natriuretic peptide (ANP) and brain natriuretic peptide (BNP), β-

myosin heavy chain (β-MHC) and sarcoendoplasmic reticulum Ca^{2+}-ATPase (SERCA) (Wu et al., 2017b).

In contrast, pathological remodelling is irreversible and associated with ventricular hypertrophy, fibrosis and chamber dilatation (Bernardo et al., 2010). These adverse changes cause a decline in systolic and/or diastolic function of the heart, leading to reduced cardiac output and HF. In pressure overload diseases, such as aortic stenosis and hypertension, the heart initially develops concentric hypertrophy to reduce wall stress and increase systolic pressure. This involves cardiomyocytes increasing in thickness and the formation of a parallel assembly of sarcomeres (Grossman et al., 1975). In volume overload diseases, such as dilated cardiomyopathy and MI, the loss of cardiomyocytes and scar formation leads to eccentric hypertrophy with sarcomeres increase in a serial fashion to accommodate the greater ventricular volumes (Wu et al., 2017b). Although the initial 'compensatory' stage is beneficial in order to maintain cardiac output, the changes in gene transcription, protein synthesis and function, metabolism and cardiomyocyte survival eventually lead to an increase in cardiac fibrosis, contractile dysfunction, ventricular dilatation, and transforms the heart into a maladaptive phase and HF (Figure 1). Furthermore, cardiac hypertrophy is also an independent risk factor for MI, arrhythmia and sudden cardiac death (Messerli and Ketelhut, 1991) and thus, understanding the molecular mechanisms responsible for cardiac hypertrophy have been of great interest to identify new therapeutic target to prevent or reverse cardiac remodelling and HF.

1.2.2 Mechanisms of pathological hypertrophy

The enlargement of cardiac myocytes involves a series of intercellular molecular events that includes activation of signalling pathways that lead to changes in gene expression and results in an increase in protein synthesis and myocyte size (Heineke and Molkentin, 2006). Vasoactive factors such as Ang II, endothelin (ET)-1 and noradrenaline are released in response to a pathological stimulus such as pressure overload (Bernardo et al., 2010). These hormones bind to cognate G-protein coupled receptors (GPCRs), which activate downstream signalling proteins, including phospholipase C (PLC), mitogen activated protein kinases (MAPKs), protein kinase C (PKC) and PKA. Key molecular mechanisms involved in cardiomyocyte hypertrophy during cardiac remodelling are shown in **Figure 2**.

1.2.2.1 Mitogen activated protein kinases (MAPKs)

Studies in mice with cardiac-specific overexpression of G_q reported a pathological hypertrophic phenotype associated with cardiac dysfunction and premature death (Mende

et al., 1998, Wettschureck et al., 2001). Whereas, mice lacking G_q in cardiomyocytes are resistant to the development of hypertrophy in response to pressure-overload (Wettschureck et al., 2001). These studies provide evidence that G_q-mediated pathways are involved in cardiac hypertrophy. MAPKs are a group of signalling proteins that lie downstream of G_q activation (Bernardo et al., 2010). MAPK activation is observed at different stages of heart disease progression, including hypertrophic cardiomyopathy, dilated cardiomyopathy, and IR injury in human and animal models (Wang, 2007). The MAPK cascade involves at least three protein kinases activated in series that include a MAPK kinase kinase (MEK2), MAPK kinase (MEK1) and a terminal MAPK. The three best-characterised distal MAPKs are extracellular signal-regulated kinases (ERK)1/2, the c-Jun amino-terminal kinase (JNKs) and the p38 kinases, which have all been implicated in pathological remodelling (Wang, 2007). These kinases are regulated by an activation loop that contains a tyrosine/threonine (TxY) motif, which needs to be phosphorylated in order to lock the kinase domain in a catalytically competent conformation. Studies have shown that the levels of the phosphorylated state of these three types of kinase are elevated in response to Ang II, ET-1 and noradrenaline in cultured cardiac myocytes, as well as in the pressure-overload model and patients with HF (Yamazaki et al., 1993b, Sugden and Clerk, 1998, Cook et al., 1999, Esposito et al., 2001).

1.2.2.1.1 Ras-raf-MEK-ERK1/2 pathway

Ras is a small guanosine-5'-triphosphate (GTP)-binding protein that transduces signals from calcium channels, membrane tyrosine kinase receptor (e.g. VEGFR and FGFR) and GPCRs (e.g. adrenoceptor and Ang II receptor), causing Raf activation and subsequent translocates from the membrane to the cytoplasm (Wang, 2007). This in turn activates MEK1 and sequentially ERK1/2 activation that has long been known to underlie cell hypertrophy and proliferation via gene regulation (Wang, 2007). In patients with hypertrophic cardiomyopathy, a positive correlation between Ras expression and the severity of hypertrophy has been observed (Kai et al., 1998). In addition, an endogenous inhibitor of the ERK1/2 pathway, sprouty-1, is induced in patients during hypertrophy regression after implementation of a left ventricular assist device (Huebert et al., 2004). These observations underscore a role for the ERK1/2 pathway in ventricular remodelling. Interestingly, the downstream signalling of Ras may have an ERK1/2-independent component. Transgenic mouse studies have shown that a gain-of-function mutation of MEK1 promotes compensatory hypertrophy (Bueno et al., 2000), whereas, constitutively activated v-12-H-Ras mutant develops pathological remodelling (Zheng et al., 2004). These different

observations indicate MEK-ERK1/2 is not the sole downstream target of Ras and the activation of ERK1/2-independent pathway(s) is likely to be critical to the transition from compensated to decompensated cardiac remodelling. In addition, Kehat *et al*. (2011) have shown that adult myocytes from mice with a cardiac deletion of ERK1/2 develop eccentric cardiac hypertrophy (lengthening), whereas cardiomyocytes from MEK1 transgenic mice exhibit concentric growth (width thickening) (Kehat et al., 2011). These findings further suggest the ERK1/2 signalling pathway coordinates eccentric and concentric growth of the heart.

1.2.2.1.2 JNK pathway

Activation of the JNK cascade involves triggering of the upstream MEKK1, MEKK2, MEKK3, and mixed lineage (MLK) 2 and 3 kinases. These subsequently phosphorylate and activate MKK4 and MKK7 that in turn phosphorylate JNK. Increased activity of JNK is found in the myocardium of HF patients secondary to ischaemic heart disease, indicating the JNK pathway may be involved in human cardiac pathology (Cook et al., 1999). Petrich *et al*. (2004) demonstrated that cardiac-specific activation of the JNK pathway in mice results in a marked increase in fetal gene expression, contractile dysfunction and premature death from CHF (Petrich et al., 2004). Moreover, specific activation of the JNK pathway by MKK7 in cardiac myocytes also induces hypertrophy, including an increase in cell size, augmented expression of ANP and impairment of sarcomere organization (Wang et al., 1998b). In sharp contrast, mice with selective deletion of JNK1 exhibit a significant reduction in fractional shortening (FS) associated with marked inflammatory infiltration after 3 and 7 days of pressure-overload, followed by a steady progression of cardiac dysfunction after 12 weeks that becomes indistinguishable from WT (Tachibana et al., 2006). This demonstrated that JNK1 prevents early deterioration of cardiac function in response to hemodynamic stress. Furthermore, targeted deletion of MEK4 or MEKK1, upstream kinases of JNK, in myocytes results in ventricular hypertrophy, elevated levels of apoptosis, fibrosis and inflammatory lesions compared to control animals, leading to HF and higher mortality (Liu et al., 2009, Sadoshima et al., 2002). Taken together, these conflicting data indicate JNK activation can be protective or exacerbate cardiac remodeling depending on the duration and the type of stimuli.

1.2.2.1.3 p-38 pathway

The p38 MAPK is a highly conserved stress-signaling pathway and consists of four isoforms: p38α, p38β, p38δ and p38γ (Martin et al., 2015). All four isoforms are expressed in the

murine heart but with higher expression of p38α and p38γ compared to p38β and p38δ (Martin et al., 2015). Phosphorylation of p38 has been implicated in the regulation of cardiac gene expression, myocyte apoptosis, myocyte proliferation and hypertrophy, inflammatory responses, contractility, energy metabolism, and vasoreactivity (Wang, 2007). The role of the p38 MAPK pathway has been extensively investigated in ischaemic heart disease (Clark et al., 2007). It has been reported that inhibition of p38 is protective against ischaemia-induced injury (Schneider et al., 2001, Clark et al., 2007). A further study showed reduced activation of p38 by steric obstruction of Cys-119/Cys-162, the cysteine residues close to the MKK3 docking domain, attenuates H_2O_2-induced hypercontracture following IR injury in isolated murine heart (Bassi et al., 2017). In addition, patients with ischaemic heart disease have elevated p38-MAPK activity in the myocardium (Cook et al., 1999), indicating a potential interventional target. A randomized phase II trial of a p38-MAPK inhibitor, Losmapimod, in non-ST elevation myocardial infarction (NSTEMI) patients showed the compound is well tolerated, improved EF and plasma BNP levels were lower compared to placebo (Newby et al., 2014).

In vivo studies have reported that p38 activation by gene transfer of the activated upstream kinases of p38 (MAPK kinase 3/6 [MKK3/6]) has a negative inotropic effect and causes diastolic dysfunction accompanied by enhanced matrix remodeling (Liao et al., 2001). A similar cardio-depressant effect is observed in isolated hearts from mice lacking MKK3, in which p38 activation contributes to tumour necrosis factor (TNF)-α-induced contractile dysfunction (Bellahcene et al., 2006).

On the other hand, evidence for a role of the p38 pathway in cardiac hypertrophy is highly controversial. Activation of p38 by over-expressing MKK3 and MKK6 in cultured cardiomyocytes results in characteristic hypertrophic responses (Wang et al., 1998a). Whereas, animals with cardiac-specific overexpression of MKK6 exhibit less myocardial damage and better functional recovery after IR injury (Martindale et al., 2005). In accord, transgenic mice expressing dominant-negative mutants of MKK3, MKK6, and p38α exhibit enhanced cardiac hypertrophy in response to cardiac stress, including aortic banding, Ang II infusion and isoprenaline (ISO) infusion (Braz et al., 2003). In addition, cardiac-restricted p38 KO mice exhibit significant cardiac fibrosis and enhanced cardiac apoptosis in response to pressure-overload (Nishida et al., 2004), indicating p38 activation contributes to cardiomyocyte survival pathway. However, some studies reported inhibition of p38 activity reduces ISO-induced ischaemic myocardial injury (Li et al., 2004b) and preserves systolic function in MI-induced HF but concomitantly leads to increase in cardiac hypertrophy (See

et al., 2004, Ren et al., 2005). This suggests p38 activity contributes to the progression of HF but not through aggravated hypertrophy. Though, evidence suggests that $P38_{\gamma}$ can contributes to hypertrophy in response to pressure overload by disinhibition of calpain via phosphorylation of calpastatin, resulting in calcineurin activation and subsequently, nuclear factor of activated T cells (NFAT) translocation and pro-hypertrophic gene expression (Clark, 2018).

1.2.2.2 Calcium signaling associated with cardiac hypertrophy

Intracellular Ca^{2+} regulates many cellular processes, especially contraction and hypertrophy (McDonald, 2011). The best-characterised calcium-dependent signalling proteins are calcineurin and calcium/calmodulin-dependent protein kinase II (CaMKII).

1.2.2.2.1 Calcineurin/NFAT

Activation of calcineurin by Ca^{2+} leads to dephosphorylation of NFAT transcription factors, promoting nuclear translocation, and association with other transcription factors such as GATA4 and myocyte enhancer factor 2 (MEF2) to regulate cardiac gene expression (Molkentin et al., 1998). Calcineurin activity is increased in patients with hypertrophied or failing hearts (Haq et al., 2001) and also in ventricular muscle explanted from human failing heart in response to hypertrophic stimuli such as ET-1 and Ang II (Li et al., 2005). In animal studies, calcineurin activity is increased in perfused heart preparation subjected to acute pressure-overload, and following aortic banding (Zou et al., 2001, Saito et al., 2003). Furthermore, transgenic mice with a constitutively active form of calcineurin develop marked pathological hypertrophy that progresses to dilated cardiomyopathy with profound interstitial fibrosis and sudden death (Molkentin et al., 1998). This can be prevented by pharmacological inhibition of calcineurin (Molkentin et al., 1998). Similarly, transgenic mice that overexpress a cardiac-specific dominant negative mutant of calcineurin exhibit a blunted hypertrophic response to pressure-overload compared to WT controls (Zou et al., 2001). Interestingly, when NFAT-luciferase reporter mice are subjected to both physiological and pathological stimuli, NFAT-luciferase reporter activity is only upregulated in response to pathological stress (Wilkins et al., 2004). Taken together, these studies suggest that calcineurin/NFAT plays a critical role in pathological hypertrophy.

1.2.2.2.2 CaMKII

Upregulation of CaMKII has been implicated in cardiac hypertrophy and HF (Anderson, 2005). Transgenic mice with overexpression of cardiac-specific CaMKII exhibit a genetic

profile associated with cardiac remodelling and HF (i.e. increased mRNA expression of ANP, β-MHC and α-skeletal actin, decreased expression of α-MHC, SERCA2a and phospholamban (PLB)) (Zhang et al., 2003). These mice also develop a dilated cardiomyopathy with reduced FS and die prematurely (Zhang et al., 2003). Consistent with these data, inhibition of CaMKII prevents maladaptive remodelling and cardiac dysfunction from excessive β-adrenergic receptor (β-AR) stimulation and MI (Zhang et al., 2005b). Moreover, cardiac-specific deletion of CaMKIIδ (the major isoform expressed in the heart) protects against cardiac hypertrophy and fibrosis in response to pressure overload (Backs et al., 2009). Ventricular lysates from these transgenic mice contain reduced histone deacetylase 4 (HDAC 4) activity, a protein that suppresses MEF2 (Backs et al., 2009). This study supports the idea that CaMKII mediates cardiac hypertrophy by inducing phosphorylation of HDAC4, which in turn dissociates from MEF2, causing MEF2 activation and hypertrophic gene expression (Backs and Olson, 2006, Kim et al., 2008).

1.2.2.3 PI3K-Akt-GSK-3β pathway

1.2.2.3.1 Phosphoinositide 3-kinase (PI3K)

Evidence obtained from transgenic strains indicates that PI3K activity is implicated in cardiac hypertrophy. Mice expressing a cardiac-specific constitutively active form of PI3K have a 20% increase in heart size, whereas hearts from mice with a dominant negative form of PI3K are 17% smaller compared to controls (Shioi et al., 2000, McMullen et al., 2003). These observations indicate an important role of PI3K in the growth of the heart. Furthermore, when adult mice with down-regulated PI3K activity are subjected to chronic swimming training, an attenuated hypertrophic response is observed; surprisingly however, these mice are not resistant to cardiac remodeling in response to pressure overload (McMullen et al., 2003, McMullen et al., 2007). This implies that PI3K is essential for physiological remodeling of the heart but not involved in pathological hypertrophy. In addition, insulin-like growth factor 1 (IGF1) is thought to trigger physiological heart growth and over-expressing the IGF1 receptor (IGF1R) leads to enlargement of the heart without histopathology (McMullen et al., 2004). Double transgenic mice over-expressing the IGF1 receptor and dominant negative PI3K are not significantly different from a phenotypic standpoint compared to dominant negative PI3K transgenic animals *per se* (McMullen et al., 2004), indicating physiological cardiac remodeling stimulated by IGF1 depends on PI3K signaling.

1.2.2.3.2 Akt

Akt, also known as protein kinase B (PKB), is a well-characterised target of PI3K (Matsui and Rosenzweig, 2005). There are three isoforms of Akt, Akt1, Akt2 and Akt3, of which only Akt1 and Akt2 are highly expressed in the heart (Abeyrathna and Su, 2015). The functional role of Akt in cardiac hypertrophy is controversial. Some transgenic mice studies showed overexpression of Akt improves contractility and protects again IR injury, but others reported massive cardiac dilatation and premature death (Condorelli et al., 2002, Matsui et al., 2002). This discrepancy is probably because Akt can be activated by both receptor tyrosine kinases (e.g. IGF-1R) and GPCRs (Bernardo et al., 2010). Thus, depending on the initiating stimulus, the resulting downstream signalling via Akt will be different. However, Akt1 KO mice exhibit a reduced hypertrophic response to swim training but not to pressure overload (DeBosch et al., 2006). This finding is in parallel with the phenotype of down regulation of PI3K, indicating Akt primarily underpins physiological hypertrophy.

1.2.2.3.3 Glycogen synthase kinase (GSK3)

GSK3 is a ubiquitously expressed, constitutively active serine/threonine kinase that is negatively regulated by Akt. GSK3 consist of two isoforms: GSK3α and GSK3β (Cheng et al., 2011). Although both isoforms are expressed in the heart (Henry and Killilea, 1994), most studies have been conducted to investigate the role GSK3β since it was among the first negative regulators of cardiac hypertrophy to be identified (Haq et al., 2000, Badorff et al., 2002, Morisco et al., 2000). It is evident that GSK3β negatively regulates cardiac hypertrophy in response to ISO, ET-1 and Fas signaling so removing the inhibitory constrain of GSK3β on gene transcription by hypertrophic stimuli is an important mechanism for the development of cardiac remodeling (Hardt and Sadoshima, 2002). GSK3β directly phosphorylates and stimulates nuclear export of GATA4, preventing gene transcription. Numerous cardiac hypertrophy genetic markers are critically regulated by GATA4 and other GATA family transcription factors, for example, ANP, BNP, α-MHC, cardiac troponin I, platelet-derived growth factor receptor (PDGFR) and Ang II type 1 receptor (Hardt and Sadoshima, 2002, Charron et al., 1999). Therefore, the regulation of GATA4 by GSK3β plays a critical role influencing the pathogenesis of cardiac hypertrophy.

GSK3β also negatively regulates cardiac growth by exerting inhibitory effects on the nuclear translocation of NFAT, thereby prevents NFAT-mediated gene transcription (Haq et al., 2000). Since NFAT is stimulated by calcineurin, GSK3β counteracts calcineurin signaling;

thus, inhibition of GSK3β by Akt invokes cross talk between the two pathways and exacerbates the hypertrophic response mediated by the calcineurin/NFAT cascade.

1.2.2.3.4 Protein kinase C

PKC is one of the key signal transducers downstream of $G\alpha_q$ in response to hypertrophic stimuli (Dorn and Force, 2005). There are at least 12 isoforms of PKC and 4 are known to be involved in cardiac hypertrophy (α, β, δ and ε) (Singh et al., 2017). Studies of myocardial hypertrophy or HF have reported that upregulation of the α and β isoforms is likely to cause maladaptive hypertrophy via Ras activation, whereas δ and ε phosphorylation leads to physiological remodelling (Dorn and Force, 2005). Braz *et al*. (2002) have shown that only the PKCα isoform is able to induce hypertrophic growth of neonatal cardiomyocytes and inhibition of PKCα abolishes agonist-mediated hypertrophy. However, *in vivo* studies of PKCα overexpression have demonstrated no effect of PKCα on cardiac hypertrophy but instead, deletion of PKCα protects against HF by improve cardiac contractility, while overexpression diminishes it (Braz et al., 2004). In accord, inhibition of PKCα activity in pathological hypertrophy improves systolic and diastolic function, indicating PKCα is a negative regulator of cardiac contractility (Hahn et al., 2003).

To give the role of PKC a human context, PKC activity and expression are elevated in HF patients (Simonis et al., 2007). These observations are in agreement with cardiac-specific overexpression of PKCβ displaying cardiac dysfunction and fibrosis (Wakasaki et al., 1997). However, PKCβ KO mice exhibit similar cardiac hypertrophy in response to phenylephrine and aortic-banding compared to control mice, demonstrating PKCβ is not necessary for the development of pathological hypertrophic responses (Roman et al., 2001).

1.2.3 Mechanism of cardiac fibrosis

1.2.3.1 Overview

An important hallmark of pathological hypertrophy and HF is cardiac fibrosis, which is characterised by excessive deposition of ECM proteins in the myocardium, leading to cardiac stiffening, arrhythmia, systolic and diastolic dysfunction (Creemers and Pinto, 2011). It is evident that increased ECM is directly induced by mechanical overload (Bishop and Lindahl, 1999), a phenomenon that is probably beneficial initially for accommodating the growth of the myocardium. However, chronic pressure overload leads to excessive collagen deposition that stiffens the ventricles, causing both systolic and diastolic dysfunction, impairs the cardiac conduction system, and can lead to hypoxia by reducing

capillary density and increasing oxygen diffusion distance (Sabbah et al., 1995, Jalil et al., 1988). Further, a study in spontaneous hypertensive rat (SHR) has shown that the transition from compensated hypertrophy to decompensated HF is closely correlated with increases in interstitial fibrosis (Boluyt and Bing, 2000). Drug treatments that prevent or reverse gene expression associated with ECM in the SHR heart improve myocardial function and survival (Boluyt and Bing, 2000). The components contributing to sensing and transducing the mechanical stress into biochemical events are facilitated by the fibroblast, involving the cytoskeleton of the cell, integrins and stretch-activated channels (Creemers and Pinto, 2011). Although the understanding of the mechanism responsible for the transition of the normal scaring process to excessive collagen accumulation is incomplete, there is evidence for the involvement of hormones such as Ang II, ET-1, and catecholamines, or locally produced growth factors, such as fibroblast growth factor 2 (FGF2), PDGF and transforming growth factor (TGF)-β are involved (Spinale, 2007, Manabe et al., 2002)(Figure 3).

1.2.3.2 TGF-β

In mammals, three isoforms of TGF-β has been discovered: TGF-β1, TGF-β2 and TGF-β3 (Heger et al., 2016). Although all three isoforms are expressed in the heart, only TGF-β1 is upregulated during pressure overload-induced hypertrophy (Li and Brooks, 1997). Thus, cardiac fibrosis studies have focused on the TGF-β1 isoform using genetic mouse models. Mice with overexpression of TGF-β1 develop cardiac morphology comprising increased myocyte size and interstitial fibrosis (Rosenkranz et al., 2002). Whilst, heterozygous TGF-$\beta1^{+/-}$ deficient mice appear to ameliorate age associated myocardial fibrosis and improve LV compliance (Brooks and Conrad, 2000). In this regard, inhibition of TGF-β1 by a specific neutralising antibody prevents the collagen mRNA induction, myocardial fibrosis and diastolic dysfunction (Kuwahara et al., 2002).

In human studies, the expression of TGF-β1 is elevated in the failing heart (Fielitz et al., 2001) and blockade of Ang II signalling has been shown to lower the levels of TGF-β (Agarwal et al., 2002). This is in agreement with the observation that HF patients administered ACEi or ARB display a reduction in ECM protein accumulation in the heart (Agarwal et al., 2002). This beneficial effect is most likely mediated via inhibition of TGF-β and its downstream cascade (Creemers and Pinto, 2011, Rosenkranz, 2004). Imaging-genomic analyses of primary human fibroblast has revealed that upregulation of interleukin (IL)-11 is the dominant transcriptional response to TGF-β1 and required for its pro-fibrotic effect (Schafer et al., 2017). Mice with overexpression of IL-11 display an enhanced fibrotic

response when exposed to pre-clinical HF models, whilst IL-11 KO animals resist the pathology (Schafer et al., 2017). Taken together, these findings suggest targeting TGF-β and its downstream signalling might be a new therapeutic approach to prevent diastolic dysfunction and cardiac fibrosis.

1.2.3.3 TGF-β downstream signalling

1.2.3.3.1 Smad

TGF-β exerts its biological effects via binding to its cognate receptor types 1 and 2 (TGFβR1 and TGFβR2) (Brand and Schneider, 1995). Activation of the receptors upon ligand binding leads to phosphorylation of Smad proteins, which subsequently translocate into the nucleus where they act as transcription factors (Creemers and Pinto, 2011). Studies from human mesangial cells have demonstrated that Smad proteins bind primarily to collagen type 1 promoter, mediating TGF-β1-induced collagen deposition (Poncelet and Schnaper, 2001).

1.2.3.3.2 Rho/ROCK

There is also evidence that TGF-β induces translocation of myocardin-related transcription factor (MRTF)-A, which promotes the transition of fibroblasts into myofibroblasts, via Rho/ROCK signalling (Small et al., 2010). In addition, fibrosis and scar formation in MRTF-A KO mice subjected to MI or Ang II is diminished compared to control animals and this is attributed to a reduction in gene expression driving fibrosis, including collagen 1α2 (Col1α2) and elastin (Small et al., 2010). In concert with the idea that Rho kinase signalling is involved in the development of cardiac fibrosis, Kagiyama *et al*. demonstrated that Rho kinase activity is increased in cardiac fibrosis, and that a specific Rho kinase inhibitor (fasudil) attenuates collagen accumulation (Kagiyama et al., 2010).

1.2.3.3.3 TAK1/p38

TGF-β-induced fibrosis can also be mediated via phosphorylation of activating transcription factor 2 (ATF-2; also known as CREB-BP1) through TGF-β-activated kinase-1 (TAK1) and p38 signalling (Sano et al., 1999, Rosenkranz, 2004). In aortic banded mice, the expression levels of TGF-β and TAK1 activity are upregulated and overexpression of TAK1 is sufficient to induce cardiac hypertrophy and fibrosis, leading to severe cardiac dysfunction (Zhang et al., 2000). However, these transgenic mice were generated via a cardiomyocyte-specific promoter; thus, the observed fibrotic response may have been a secondary effect facilitated by growth factors released from the hypertrophic myocardium.

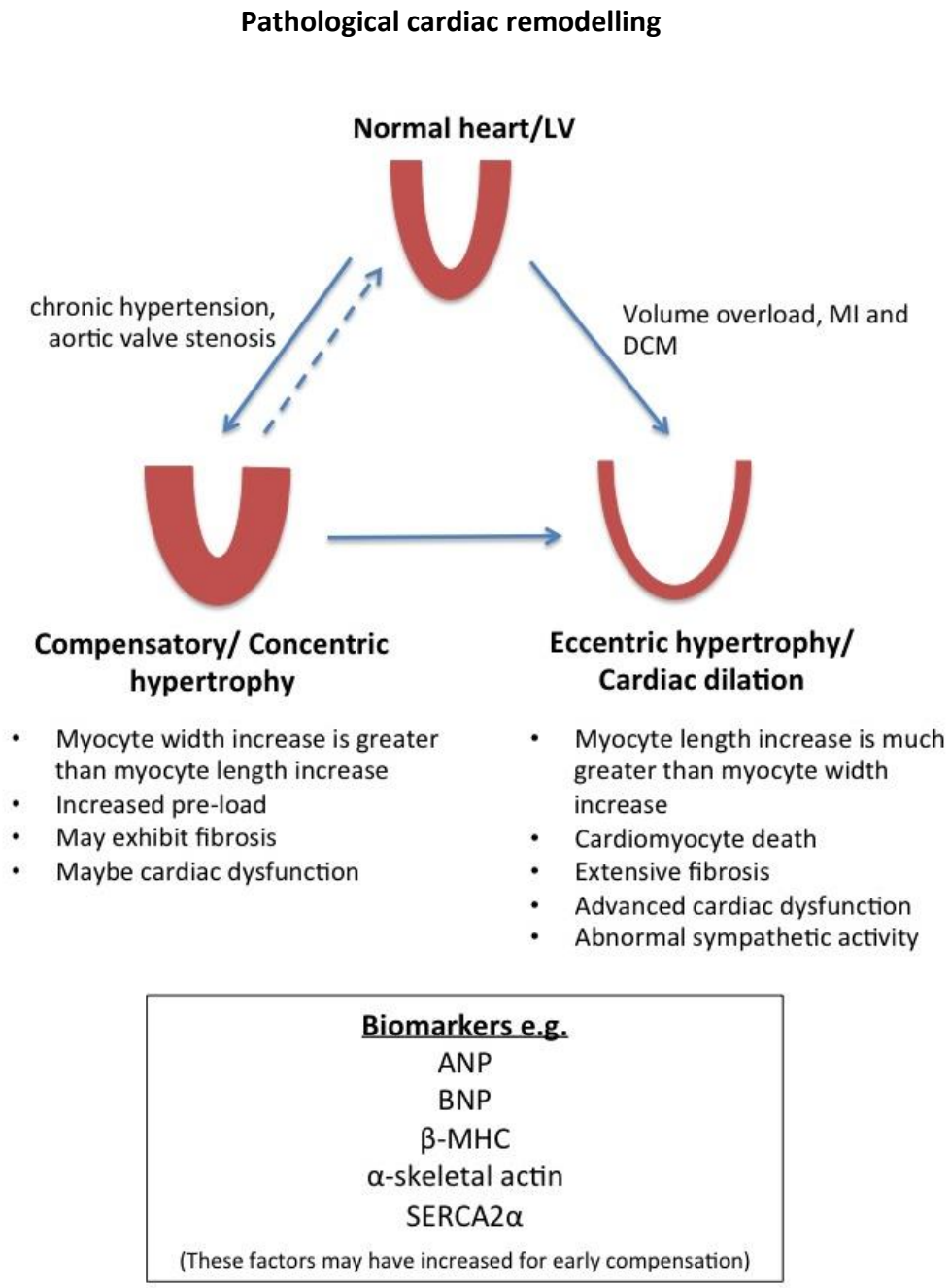

Figure 1. Pathological cardiac remodelling.

Pathological remodelling can be classified as concentric hypertrophy, in which the ventricular wall thickens reducing chamber diameter, and eccentric hypertrophy, in which the ventricular wall thins and the chamber dilates. Concentric hypertrophy can develop into cardiac dilation in advanced pathological conditions. Biomarkers such as atrial natriuretic peptide (ANP), brain natriuretic peptide (BNP) and β-myosin heavy chain (β-MHC) are up-regulated, whereas the expression of sarco/endoplasmic reticulum calcium ATPase (SERCA)2α is down-regulated in cardiac remodelling. LV, left ventricle; MI, myocardial infarction; DCM, dilated cardiomyopathy.

Cardiac hypertrophic pathways

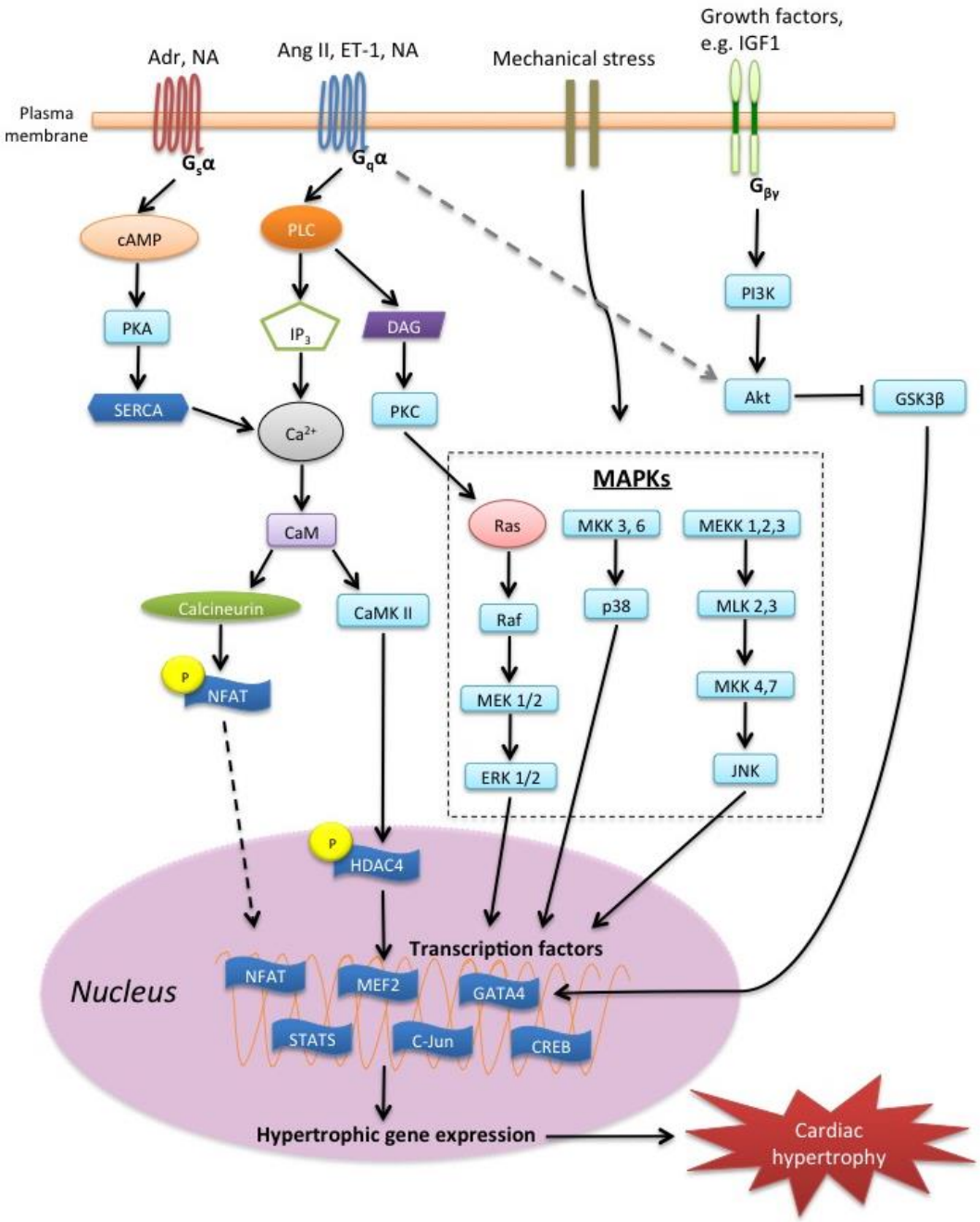

Figure 2. Cardiac hypertrophic pathways.

A schematic depicting the major pathways and transcription factors involve in cardiac hypertrophy. Adr, adrenaline; NA, noradrenaline; Ang II, angiotensin II; ET-1, endothelin-1; IGF-1, insulin-growth factor-1; PKA, protein kinase A; SERCA, sarco/endoplasmic reticulum calcium ATPase; PLC, phospholipase C; IP_3, inositol trisphosphate; CaM, calmodulin, CaMK II, calcium/calmodulin dependent protein kinase II; NFAT, nuclear factor of activated T cells; DAG, diacylglycerol; PKC, protein kinase C; PI3K, phosphoinositide 3-kinase; GSK3β, glycogen synthase kinase 3β; MAPKs, mitogen activated protein kinases; ERK, extracellular signal-regulated kinase; MEK, MAPK kinase, MLK, mix lineage kinase; HDCA, histone deacetylse; MEF2, myocyte enhancer factor-2.

Cardiac fibrotic pathways

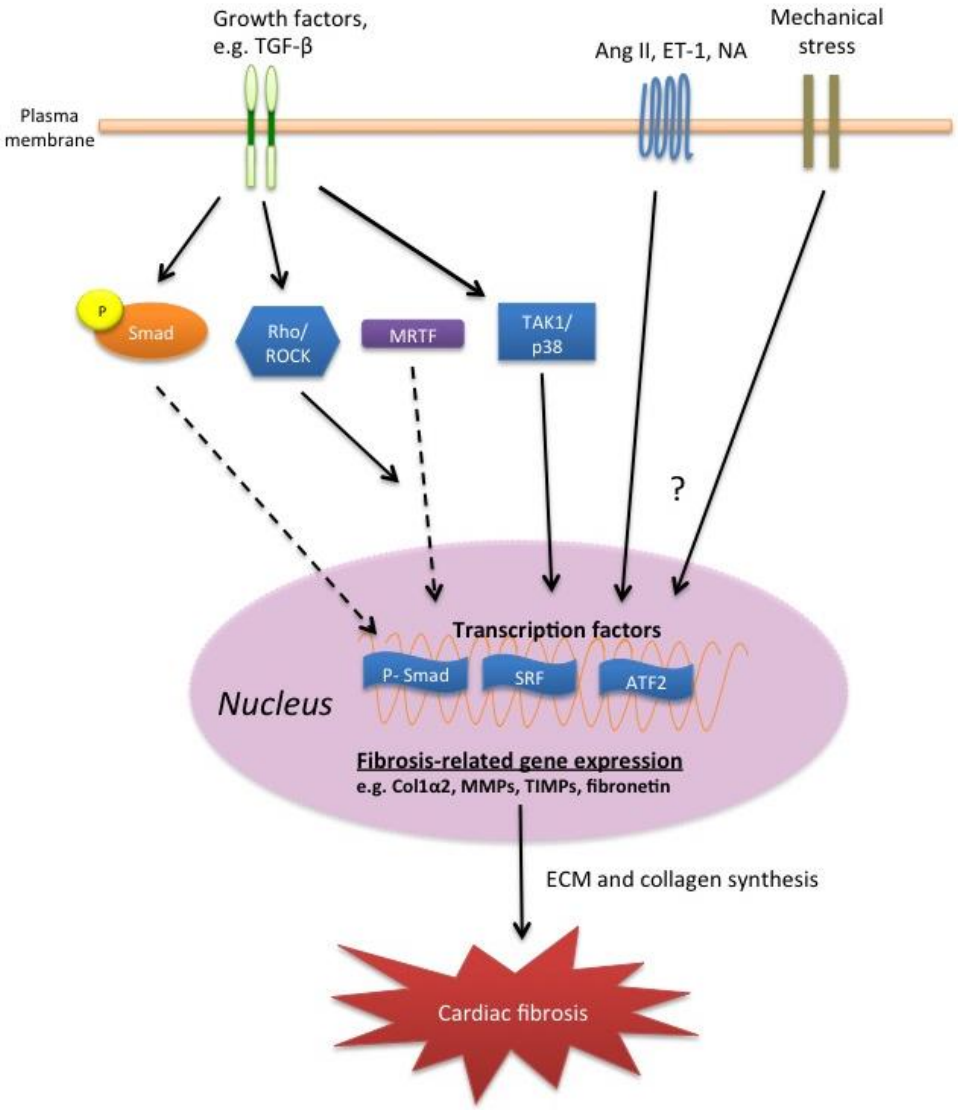

Figure 3. Cardiac fibrotic pathways.

A schematic depicting the major pathways and transcription factors involve in cardiac fibrosis. TGF-β, transforming growth factor-β; NA, noradrenaline; Ang II, angiotensin II; ET-1, endothelin-1; MRTF, myocardin-related transcription factor; TAK1, TGF-β-activated kinase-1; ATF-2, activating transcription factor 2; ECM, extracellular matrix.

1.3 Ischaemia reperfusion injury

1.3.1 Overview

Under normal circumstances, myocytes respire aerobically and hence if blood supply to the myocardium is cut off (e.g. as a result of CHD), the cells switch to rely on anaerobic respiration i.e. glycolysis (Powers et al., 2007). This results in in-sufficient energy production, acidosis, the build-up of toxic metabolites and oxidative stress (Hausenloy and Yellon, 2013). When the ischaemic period is extended beyond 20 minutes, some of the cardiac cells become irreversibly damaged and infarcted (Downey, 1990). Revascularisation of the culprit vessel using thrombolytic therapy or primary PCI is key to minimising infarct size (Hausenloy and Yellon, 2013). However, the process of reperfusion *per se* can aggravate the cellular injury already inflicted during the ischaemic period and thus, reperfusion can provoke both protective and harmful consequences. This phenomenon is termed myocardial IR injury. Since the final infarct size is the main determinant of mortality and morbidity (Sorensson et al., 2013, Terkelsen et al., 2009), it is important to investigate the molecular mechanism(s) behind IR injury and potential strategies to reduce the infarct size and the subsequent myocardial remodelling.

1.3.2 Harmful mediators contributing to IR injury

Several harmful mediators have been identified that can promote myocardial injury in response to reperfusion. These include oxygen and calcium paradoxes, rapid normalisation of pH and osmolality, the opening of a mitochondrial permeability transition pore (mPTP), and inflammation.

1.3.2.1 Intracellular calcium overload

A prolonged period of ischaemia results in high intracellular calcium concentration ($[Ca^{2+}]_i$) (Hausenloy and Yellon, 2013). Upon reperfusion, ATP production resumes and activates SERCA on the mitochondrial membrane that removes the excess $[Ca^{2+}]_i$ into the mitochondria (Siegmund et al., 1997). Na^+/Ca^{2+} exchangers on the cell membrane are also activated to pump out Ca^{2+} using the energy from the inward movement of Na^+ down its electrochemical gradient (Piper et al., 2003); three Na^+ ions enter and one Ca^{2+} ion leaves the cell. This leads to an increase in $[Na^+]_i$ that activates the Na^+/K^+ ATPase to remove three Na^+ ions whilst transporting two K^+ ions into the cell. If this pump is damaged during ischaemia, Na^+ ions accumulate in the cytosol that reduce the efficacy of the Na^+/Ca^{2+} exchanger, or even reverses its direction, causing enhancement of Ca^{2+} overload (Inserte et

al., 2002, Schafer et al., 2001). The elevated $[Ca^{2+}]_i$ also leads to hypercontracture of the myocardium, resulting in irreversible shortening of the myocytes and induces cytoskeleton structural injury (Yellon and Hausenloy, 2007).

1.3.2.2 pH and osmolality correction

Myocytes respire anaerobically during ischaemia, which causes the production of lactic acid and reduces interstitial and intracellular space pH (Hausenloy and Yellon, 2013). Restoration of flow flushes away the accumulated extracellular $[H^+]$, creating a high proton gradient between the intracellular and extracellular environment (Frank et al., 2012). This activates the Na^+/H^+ exchanger that drives outward movement of one H^+ ion for exchange with one Na^+ ion. The Na^+/HCO_3^- co-transporter is also activated by the higher Na^+ content, neutralising the intracellular acidic environment by HCO_3^- binds to the excess H^+ to form carbonic acid, which then dissociates into carbon dioxide and water. Consequently, the transporters increase intracellular Na^+ that lowers the Na^+ gradient. This reduces the efficiency of the Na^+/Ca^{2+} exchanger that can aggravate calcium overload (see section 1.3.2.1). This implies that a reduction in the proton gradient upon reperfusion would be beneficial and experimental reperfusion with acidic buffer is potentially cardioprotective (Bond et al., 1991). However, in clinical studies, the use of a Na^+/H^+ exchanger inhibitor at the start of reperfusion to delay restoration of physiological pH does not limit infarct size or improve clinical outcome (Zeymer et al., 2001).

Another factor that causes cell death upon reperfusion is osmolality (Piper et al., 1998). Cytosolic Na^+ overload and many end products of anaerobic metabolism accumulate in the interstitial and intracellular space during ischaemia (Piper et al., 1998) Reperfusion rapidly washes out the extracellular molecules, creating a high osmolality gradient. This causes an inward movement of water that can results in cell swelling, rupture and necrosis (Piper et al., 1998).

1.3.2.3 Opening of mitochondria permeability transition pore

The mitochondria permeability transition pore (mPTP) is a non-selective channel on the inner membrane of mitochondria that allows molecules smaller than 1500 kDa to pass through (Piper et al., 1998). During ischaemia, the mPTP remains shut but opens at the start of reperfusion in response to mitochondrial calcium overload, ATP depletion, oxidative stress and restoration of physiological pH (Kim et al., 2006a, Griffiths and Halestrap, 1995). The opening of the mPTP leads to collapse of the mitochondrial membrane potential and influx of molecules, causing organelle swelling and rupture

(Honda et al., 2005). Mitochondrial materials such as cytochrome C and apoptosis-induction factors (AIF) can also be released and initiate apoptosis (Honda et al., 2005). Thus, inhibiting the opening of the mPTP is an important new target for cardioprotection during reperfusion. The first proof-of-concept clinical trial was carried out by Piot *et al*. (2008), in which 58 patients presenting with acute ST segment elevation myocardial infarction (STEMI) were randomized to receive a single intravenous bolus of either Cyclosporin-A (CsA; 2.5 mg/kg), an immunosuppressant that inhibits mPTP opening, or placebo, 10 min prior to primary PCI. It was reported that the release of creatine kinase (an indicator of myocardial injury) was significantly reduced in the CsA group as compared with the control group (Piot et al., 2008). In a follow-up cardiac magnetic resonance study, it was demonstrated that MI size was also significantly reduced, accompanied by less adverse cardiac remodelling and improved EF in the CsA group compared to control patients at both 5 days and 6 months after the infarction (Mewton et al., 2010). However, in another larger clinical trial, CYCLosporinE A in Reperfused Acute Myocardial Infarction (CYCLE), patients received a single intravenous CsA bolus just before primary PCI did not have improved clinical outcomes or LV remodelling up to 6 months compared to the control group (Ottani et al., 2016).

1.3.2.4 Generation of reactive oxygen species

The transition of ischaemia to re-oxygenation generates reactive oxygen species (ROS), primarily superoxide (O_2^-), hydrogen peroxide (H_2O_2), hypochlorous acid (HClO) and hydroxyl radicals (OH^-). These highly reactive molecules represent a double-edged sword; moderate levels of ROS production lead to an ischaemic preconditioning-like effect encompassing decreased Ca^{2+} load, increased GPCR and mitochondrial ATP-dependent potassium (mitoK_{ATP}) channel activities, and decreased apoptotic signalling and mPTP opening (Bagheri et al., 2016). On the other hand, excess ROS production can directly cause damage to cellular DNA, oxidative injury to membrane lipids, damage enzyme complexes in the mitochondrial respiratory chain that results in ATP depletion and cytochrome C release, and activate stress response pathways (Bagheri et al., 2016). Ultimately, these deleterious effects provoke apoptosis and necrosis. Therefore, limiting the amount of ROS production represents an important therapeutic target to limit the extent of IR injury. These include xanthine oxidase (XO), nicotinamide adenine dinucleotide phosphate (NADPH) oxidase, mitochondria, and uncoupled nitric oxide synthase (NOS) (Granger and Kvietys, 2015).

XO is a mammalian form of xanthine oxidoreductase that catalyses purine metabolism i.e. the hydroxylation of xanthine to uric acid and generates ROS. Treatment strategies employing the xanthine oxidase inhibitors (XOI), allopurinol and oxypurinol, have proven to effectively inhibit XO activity and reduces ROS production, and exhibit cardioprotective effects against IR injury and HF in animal models (Puett et al., 1987, Haga et al., 2017, Naumova et al., 2006, Ukai et al., 2001). Moreover, a meta-analysis of randomised controlled trials has reported that XOI may reduce the incidence of adverse CV outcomes (Bredemeier et al., 2018). However, XO is also required for the reduction of nitrite to NO, which may be beneficial (Ghosh et al., 2013).

NO derived from NOS or from pharmaceutical administration of NO-donors is cardioprotective against IR injury in animal models and humans via its anti-oxidant and anti-inflammatory effects (Schulz et al., 2004, Duranski et al., 2005, Phillips et al., 2009). However, when NOS is 'uncoupled', e.g. as a result of IR injury, superoxide production increases and reduces NO generation (Bendall et al., 2014). Reductions in the levels of tetrahydrobiopterin (BH_4), a cofactor of NOS required for NO synthesis, have been shown to associate with NOS uncoupling and ROS production in IR models (Dumitrescu et al., 2007). BH_4 supplementation or substrates for BH_4 biosynthesis (sepiaterin and folate) can re-couple NOS and ameliorate IR-induced cardiac inflammation and myocardial damage, and improve cardiac function (Yamashiro et al., 2002, Tiefenbacher et al., 2003, Moens et al., 2008). However, clinical trials have been largely disappointing probably due to limited endothelial uptake, failure to act on specific site(s) of target cells or systemic oxidation of BH_4 (Cunnington et al., 2012).

1.3.2.5 Inflammation

Cardiac repair after ischaemic myocardial damage relies on the activation of the immune system that serves to clear the wound of dead cells, produce mediators triggering fibroblast growth and matrix formation, and to promote angiogenesis (Bonaventura et al., 2016). These processes are finely regulated by the production of cytokines, chemokines and growth factors (Frangogiannis, 2012). Dysregulation of any of the immune components may extend injury and accentuate adverse remodelling in cardiac injury. Therefore, to understanding the cellular inflammatory events during reperfusion and healing are important for potential therapeutic interventions by selectively inhibiting injury and promoting repair (e.g. resolution of inflammation) (Bonaventura et al., 2016).

The inflammatory response in the infarcted area involves up-regulation of endothelial adhesion molecules, increased permeability of the microvascular wall, and up-regulation of cytokines and chemokines which eventually lead to extravasation of activated cells into the injured site (Bonaventura et al., 2016). The infiltrated leukocytes produce ROS beyond the initiation of the inflammatory cascade, which causes further cardiac injury (Bonaventura et al., 2016). Studies targeting the process of leukocyte infiltration by inhibiting expression of adhesion molecules have shown a significant reduction in infarct size (Yamazaki et al., 1993a, Tojo et al., 1996). Also, studies investigating macrophage polarisation in the infarcted lesion have promoted interest in this area (Horckmans et al., 2017, Hulsmans et al., 2016, Nahrendorf and Swirski, 2013). It is largely agreed that the M1 macrophage is pro-inflammatory and destructive, whereas the M2 macrophage is anti-inflammatory and reparative (Boag et al., 2017). Thus, promoting M1 to M2 macrophage transition might be beneficial.

Coronary endothelial P-selectin is upregulated in cardiac IR injury (Thomas et al., 2010) and its interaction with leukocytes plays an important role in cell adhesion and the subsequent cellular infiltration. Studies have reported that P-selectin deficient mice or administration of an anti-P-selectin antibody results in a significantly smaller cardiac infarction in an *in vivo* MI model compared to controls (Palazzo et al., 1998, Tojo et al., 1996). Furthermore, antibodies against neutrophil adhesion protein CD18 also limit myocardial infarct size and preserve LV function in many species, including murine, canine and primates (Arai et al., 1996, Aversano et al., 1995, Ma et al., 1991, Lefer et al., 1993). However, these protective effects of a CD18 antibody did not translate to clinical benefits (LIMIT AMI, HALT MI, and FESTIVAL) with no modification in infarct size (Baran et al., 2001, Faxon et al., 2002, Rusnak et al., 2001). One possible explanation for the discrepancy between animal studies and human trials could be due to the longer duration of ischaemia period in patients (>2 hours), resulting in endothelial barrier leakage that circumvents the positive effect of blocking adhesion molecules, permitting neutrophils to migrate into the intravascular structure. This hypothesis is supported by a rabbit study in which a CD18 antibody reduced infarct size in the group subjected to 30 minutes ischaemia but not 45 minutes (Williams et al., 1994).

1.4 The importance of the endothelium in cardiovascular homeostasis

1.4.1 Overview of endothelial function

Although the endothelium is just a cell mono-layer that overlays the vascular smooth muscle, it plays an essential role in the maintenance of vascular homeostasis. It releases

numerous vasoactive mediators in response to neurohormonal substances (e.g. bradykinin (BK), thrombin, ATP and substance P), and physical stimuli (i.e. shear stress) (Rajendran et al., 2013, Busse et al., 2002). The most well-established endothelium-derived relaxant mediators are NO and prostacyclin (PGI_2). Together, they provide cardiovascular protection by regulating vascular tone, protect from oxidative stress, are anti-proliferative, and provide an anti-adhesive and anti-aggregatory vessel surface that prevents inflammation and thrombosis (Deanfield et al., 2007) (Figure 4). The loss of these protective functions is termed endothelium dysfunction and is thought to both initiate and exacerbate cardiovascular disorders associated with vasoconstriction, thrombosis and inflammation (Godo and Shimokawa, 2017). Indeed, evaluation of endothelial function in humans (e.g. flow mediated dilatation) has attracted much attention in the clinical settings because it can serve as an excellent prognostic marker for adverse cardiovascular events (Morimoto et al., 2016, Deanfield et al., 2007).

1.4.2 Nitric oxide

In 1980, Furchgott and Zawadzki discovered that a humoral factor released by the endothelium relaxed the underlying smooth muscle and termed this endothelium-derived relaxing factor (EDRF). A few years later, Furchgott and Ignarro independently identified NO as responsible for the vascular smooth muscle relaxation elicited by EDRF (Ignarro et al., 1987). In the same year, Moncada and co-workers also demonstrated that the release of NO from endothelial cells induced vasorelaxation indistinguishable from EDRF, confirming NO is responsible for the bioactivity of this factor (Palmer et al., 1987).

NO is synthesised from L-arginine by NOS. There are three isoforms of NOS: neuronal NOS (nNOS or NOS 1), inducible NOS (iNOS or NOS 2) and endothelial NOS (eNOS or NOS 3) (Chen et al., 2017). nNOS and eNOS are constitutively active, whereas iNOS is upregulated in response to pro-inflammatory stimuli such as lipopolysaccharide (LPS). The production of NO by eNOS in endothelial cells diffuses into the adjacent vascular smooth muscle cells (VSMCs), activating soluble guanylyl cyclase (sGC) which catalyses the conversion of GTP to cGMP. In turn, cGMP mediates biological effects via activation of cGMP-regulated ion channels, cGMP-binding phosphodiesterases (PDEs) and cGMP-dependent protein kinase (PKG or cGK) (Tsai and Kass, 2009). In VSMCs, PKG mediates relaxation via reducing intracellular calcium concentrations by activating Ca^{2+} ATPase on the cell membrane and sarcoplasmic reticulum, hyperpolarising the cell membrane by opening large conductance Ca^{2+} activated potassium (BK_{Ca}) channels, and upregulating myosin light chain phosphatase

(MLCP) activity that dephosphorylates myosin light chain, thus inhibiting contraction (Gewaltig and Kojda, 2002).

Shear stress is one of the most important stimuli for the release of NO. This endothelial mechanotransduction system plays a prominent role in health and disease as it translates the physical force changes on the internal surface of the endothelial layer throughout the CVS into numerous downstream signalling pathways in response to diverse physiological demands in the body, i.e. matching organ perfusion with cardiac output (Baratchi et al., 2017, Kim et al., 2017). Many published reports emphasize the distinct role of steady laminar flow or pulsatile shear stress being atheroprotective by triggering endothelial release of PGI_2 and NO, whereas disturbed flow or oscillatory shear stress stimulates proinflammatory signalling and leads to the development of atherosclerotic lesions (Abe and Berk, 2014, Zhou et al., 2014). In fact, atheroma often appears in branch points of the vessels where oscillatory shear stress occurs concomitant with low NO production (Libby, 2002).

1.4.3 Prostacyclin

PGI_2 shares some common biological activities with NO in the CVS, including vasodilatation, anti-platelet and anti-inflammatory properties. PGI_2 elicits vasodilatation via activation of prostacyclin receptors (IP) on the smooth muscle cell membrane that are coupled to adenylyl cyclase (AC). AC catalyses the conversion of ATP to cyclic adenosine-3',5'-monophosphate (cAMP) and leads to the activation of cAMP-dependent protein kinase (PKA). Similar to PKG phosphorylation, PKA mediates vasodilatation via reducing intracellular calcium concentrations and the calcium sensitivity of the contractile machinery (Morgado et al., 2012).

PGI_2 is synthesised from arachidonic acid by cyclo-oxygenase (COX). There are two isoforms: COX-1 and COX-2. COX-1 is widely distributed and constitutively expressed in nearly all cell types whilst COX-2 expression is induced by pro-inflammatory and proliferative stimuli, paralleling iNOS (Vane and Botting, 1998). It has been suggested that PGI_2 production in endothelial cells is dependent on COX-2 induction (Schmedtje et al., 1997, Grosser et al., 2006, Yu et al., 2012) and may account for the increased cardiovascular risk associated with the use of COX-2 specific inhibitors and non-steroid anti-inflammatory drugs (NSAIDs) (Solomon et al., 2004, Mukherjee et al., 2001, Yu et al., 2012, McGettigan and Henry, 2011). However, a recent study has demonstrated that under physiological conditions it is COX-1 and not COX-2 that drives PGI_2 production in the CVS

(Kirkby et al., 2012). Thus, the reason why COX-2 inhibitors increase adverse cardiovascular events needs to be revisited. It has been reported that COX-2 has a defined role in renal function and regulates blood pressure (BP) (Khan et al., 2002), which could provide a possible reason for the adverse cardiovascular effect with the use of COX-2 inhibitors. In addition, a recent study has revealed that COX-2 inhibition elevates renal production of asymmetrical dimethylarginine (ADMA), an endogenous NOS inhibitor (Ahmetaj-Shala et al., 2015). Thereby, COX-2 inhibitors reduce cardioprotective NO production.

1.4.4 Endothelium-derived hyperpolarizing factors

Another family of mediators, that are distinct from the bioactivity of NO and PGI_2, also play an important role in the regulation of vascular tone. These are termed endothelium-derived hyperpolarising factors (EDHFs) (Garland et al., 1995). As named, they are factors released from the endothelial cell that causes hyperpolarisation in the adjacent VSMCs resulting in vasodilatation. Many candidates for EDHF have been proposed, including H_2O_2, cytochrome P450 metabolites, anandamide, K^+ ions and C-type natriuretic peptide (CNP) (Ahluwalia and Hobbs, 2005); but each of the individual candidates for EDHF remains debatable and varies across different vascular beds and species. In conduit vessels, EDHF may provide a secondary/back-up system to NO, but the importance of EDHF as a vasorelaxant is more apparent in the resistance vasculature (Shimokawa et al., 1996). Since resistant vessels are one of the main determinants of systemic BP (i.e. peripheral vascular resistance), altered EDHF responses are associated with hypertension. Interestingly, double KO of eNOS and COX-1 in female mice has no effect on mean arterial blood pressure (MABP) whereas male double knockout mice are hypertensive (Scotland et al., 2005). These observations demonstrate that EDHF plays an important role in regulating BP in females, whereas males rely on NO and PGI_2 predominately. This also possibly explains the cardioprotective phenotype seen in pre-menopausal females when compared to age-matched male counterparts (McCulloch and Randall, 1998, Moyes et al., 2014). Furthermore, EDHF-mediated responses are altered in various other pathological conditions, including aging, atherosclerosis, IR injury and CHF (Fujii et al., 1993, Selemidis and Cocks, 2002, Chan and Woodman, 1999, Malmsjo et al., 1999). Common treatments for CVDs, such ACEi, restore the EDHF response and improve endothelium dysfunction (Goto et al., 2000), which suggests activation of the EDHF pathway contributes to the observed beneficial effect of such therapeutic interventions.

Pathways of endothelial (dys)function

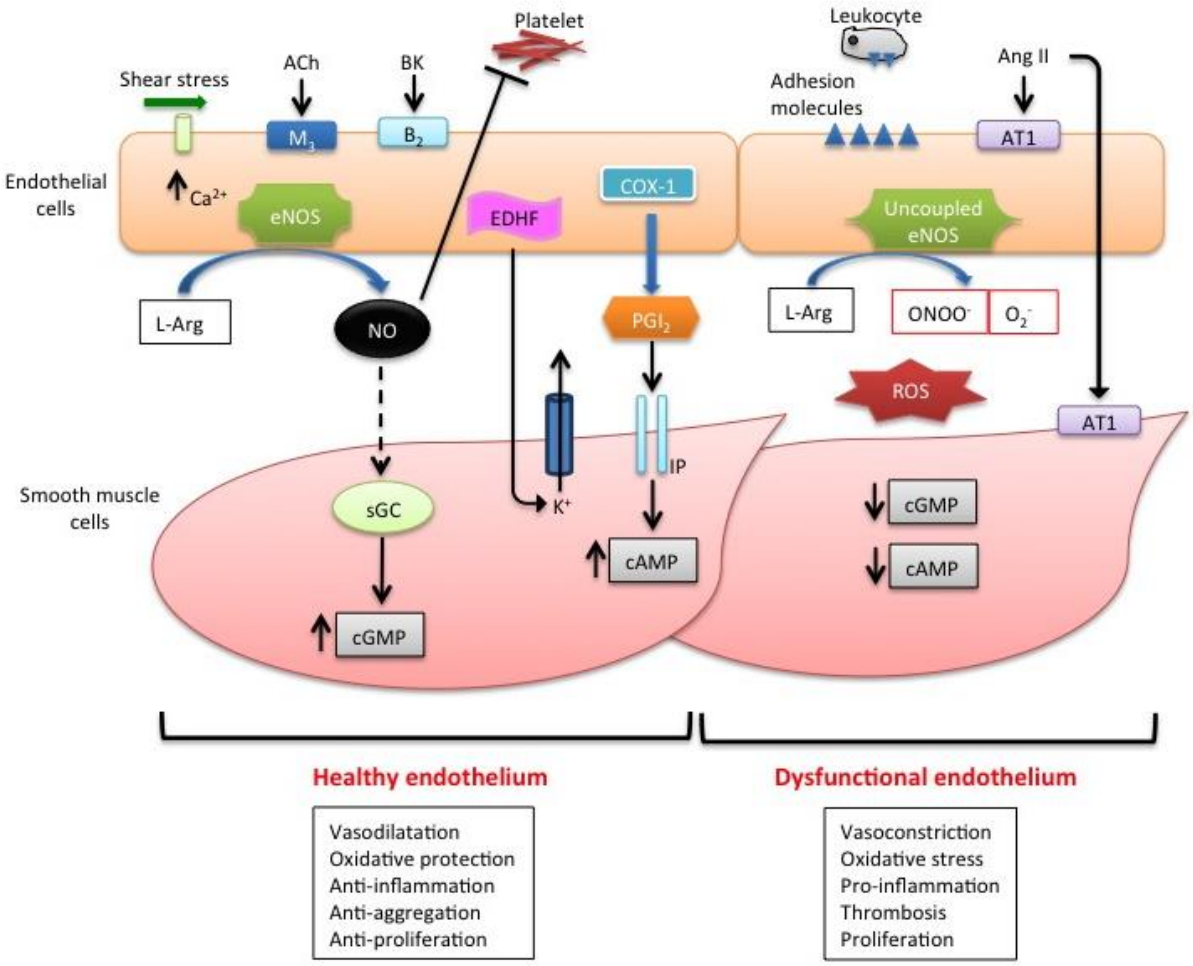

Figure 4. Pathways of endothelial (dys)function.

Healthy endothelium releases numerous vasoactive mediators in response to neurohormonal substances and shear-stress. Nitric oxide (NO), prostacyclin (PGI_2) and endothelium-derived hyperpolarising factor (EDHF) regulates vascular homeostasis by mediating vasodilatation, protects against oxidative stress, provides anti-inflammatory and anti-aggregatory vessel surface. In dysfunctional endothelium, endothelial nitric oxide synthase (eNOS) becomes uncoupled, diminishes NO production and produces ROS, which increases vascular oxidative stress, augments expression of adhesion molecules and mediates vasoconstriction. ACh, acetylcholine; BK, bradykinin; Ang II, angiotensin II; COX-1, cyclo-oxygenase-1; eNOS, endothelial nitric oxide synthase; L-Arg, L-arginine; sGC, soluble guanylyl cyclase; ROS, reactive oxygen species.

1.5 Natriuretic peptides

1.5.1 Overview of the natriuretic peptide family

Three main mammalian natriuretic peptides have been discovered: ANP, BNP and CNP. In addition, *Dendroaspis* natriuretic peptide (DNP) has been isolated from the venom of *Dendroaspis angusticeps*, and urodilatin has been found in human urine that is produced by renal tubular cells from the *Nppa* gene (Del Ry et al., 2013). ANP and BNP are endocrine hormones secreted from the heart and regulate natriuresis, diuresis, BP, and maintain cardiac integrity (Del Ry et al., 2013, Lee and Burnett, 2007). Whereas, CNP is predominantly released from the endothelial layer of the blood vessels, but also expressed at a low level in the heart. Studies published by the Hobbs' group have shown that CNP plays a fundamental role in vascular homeostasis by contributing to EDHF activity, promoting an anti-atherosclerotic environment and inhibiting the development of aneurysm (Moyes et al., 2014).

1.5.2 Discovery

The work of de Bold *et. al* (1981) provided the first comprehensive physiological characterisation of the ability of atrial tissue to induce a large diuretic and natriuretic response in the rat (de Bold et al., 1981). The group injected supernatant of atrial homogenates intravenously into non-diuretic rats, causing a rapid increase in sodium and chloride excretion, and urine volume. This work led to the discovery of ANP. Subsequently, Sudoh *et. al* isolated an analogous peptide from porcine brain and named it BNP (Sudoh et al., 1988). However, in the subsequent year it was shown that cardiac ventricles are the major source of circulating BNP (Saito et al., 1989). In 1990, Sudoh *et. al* isolated a third member of the natriuretic peptide family from porcine brain, which they termed CNP. Following the discovery of CNP, Burnett's group showed this member of the natriuretic peptide family is synthesised and released by endothelial cells and has vasoactive properties (Stingo et al., 1992).

1.5.3 Structure and synthesis

All natriuretic peptides are produced as preprohormones that are cleaved to generate prohormones. These are subsequently processed into biologically active peptides (D'Souza et al., 2004). Each natriuretic peptide consists of a 17 amino acid disulphide ring structure that is critical for receptor binding and 11 of the amino acids in the cyclic structure are conserved across the three peptides (Del Ry et al., 2013). ANP and BNP possess 5- and 6-

amino acid residues on the carboxyl terminal extension, respectively, but CNP completely lacks this tail. These are thought to be important in receptor selectivity (D'Souza et al., 2004) (Figure 5).

1.5.4 Atrial natriuretic peptide

The human ANP gene (*Nppa*) is located on chromosome 1 and contains three exons and two introns, encoding a 151-amino acid preprohormone (Song et al., 2015). Proteolytic processing removes the signal peptide to form a 126-amino acid prohormone (pro-ANP) that is stored in dense granules in the atrial myocyte (Ruskoaho, 1992). During the secretory process, corin, a cardiac serine protease, cleaves proANP to the biologically active 28-amino acid mature ANP (C-terminal) and a 98-amino acid fragment (N-terminal proANP) (Yan et al., 2000). ANP is released into the circulation in response to atrial wall stretch resulting from increased intravascular volume (Potter et al., 2006). ANP is a potent vasodilator and has natriuretic and diuretic properties through its actions on renal tubules and inhibition of the RAAS (Rubattu et al., 2013). Thus, it is an important anti-hypertensive and anti-hypovolemic factor. Furthermore, studies have shown that ANP KO mice exhibit exaggerated cardiac remodelling in response to pressure or volume overload (Li et al., 2008, Mori et al., 2004). A synthetic ANP analogue, carperitide, reduces BP and increase cardiac output by causing vasodilatation, natriuresis, and inhibits RAAS. This drug is used as therapeutic in HF (Rubattu et al., 2013).

1.5.5 Brian natriuretic peptide

BNP is a 32-amino acid polypeptide synthesised and secreted from cardiac tissue, predominantly the ventricles. The human BNP gene (*Nppb*) is located on chromosome 1 and consists of two exons and one intron (Song et al., 2015). It encodes a preprohormone of 134-amino acid that is cleaved into a 108-amino acid prohormone ($proBNP_{1-108}$) by removing the signal peptide. This is subsequently processed into the mature biologically active 32-amino acid C-terminal peptide and a 76-amino acid N-terminal fragment (NT-proBNP) (Sudoh et al., 1989). In contrast to ANP, BNP is not stored but synthesised *de novo* in the ventricles upon volume overload that is sensed by cardiac wall stretch (Potter et al., 2006). Plasma levels of BNP are normally low but markedly increased upon pathophysiological conditions such as HF. Thus, particularly NT-proBNP, has been used as a diagnostic and prognostic biomarker of cardiac dysfunction (Aspromonte et al., 2017). Mice with BNP deletion exhibit an augmented fibrotic lesion in response to pressure-overload compared to WT controls, suggesting BNP is an anti-fibrotic factor.

1.5.6 C-type natriuretic peptide

CNP is the most highly conserved natriuretic peptide across species, including humans, rodents, reptiles and fish (Del Ry et al., 2006b). In addition, studies of the lineage of natriuretic peptide genes have suggested that ANP and BNP originated from CNP via gene duplication (Inoue et al., 2003). The human CNP gene (*Nppc*) is located on chromosome 2 and contains two exons and one intron (Ogawa et al., 1992). CNP is synthesised as pre-proCNP comprising 126 amino acids. The pre-proCNP is then cleaved into pro-CNP (103 amino acids) via the removal of signal peptide by signal peptidase. Pro-CNP is the form in which the peptide is stored. Subsequently, furin, a protein convertase that residents in the trans-Golgi network, cleaves pro-CNP to yield CNP-53. CNP-53 is then converted to biological active CNP-22 by an unidentified mechanism (Del Ry et al., 2006b) (Figure 6). Targeted disruption of CNP in mice causes severe dwarfism due to impairment of endochondral ossification, and high mortality before adulthood (Komatsu et al., 2002). Similar phenotypes are observed in humans with conditions involving inactivating mutations in CNP (Hisado-Oliva et al., 2018). Furthermore, several genome-wide association studies (GWAS) have established a relationship between *Nppc* and height (Estrada et al., 2009, Wood et al., 2014). This indicates that CNP is crucial for bone development and growth. Interestingly, the highest CNP expression in adult mice is found in the uterus and ovary (Stepan et al., 2000), and a function of CNP in reproduction has been demonstrated (Gutkowska et al., 1999). Other sites with significant expression of CNP mRNA include the CVS, skin, lungs, tongue, liver, kidney and stomach (Stepan et al., 2000). This wide distribution of CNP expression implies a multifunctional role for this peptide.

CNP is highly expressed in endothelial cells and acts in an autocrine/paracrine fashion. Several stimuli have been found to be important in triggering the release of CNP in endothelial cells. This includes pro-inflammatory cytokines such as TNF-α and interleukin (IL)-1, TGF-β, and LPS (Potter et al., 2006), as well as shear stress (Chun et al., 1997). In addition, ANP and BNP also strongly stimulate the production and secretion of CNP from the endothelium, suggesting the vascular actions of ANP and BNP may partly be mediated via CNP release (Nazario et al., 1995). In fact, CNP is more potent than ANP in inducing smooth muscle relaxation but does not elicit natriuretic and diuretic effects (Chen and Burnett, 1998). Furthermore, forearm vasodilatation in response to ANP administration is reduced in patients with HF compared to normal individuals (Hirooka et al., 1990), but the vasorelaxant effects of CNP in such patients are preserved (Nakamura et al., 1994). Taken

together, these observations suggest that CNP could be a good pharmacological target for managing CVDs (Clavell et al., 1993) without inducing an adverse drop in BP. However, the role of CNP in the pathophysiology of CVD, particularly in the heart, is yet to be fully elucidated.

1.5.7 Urodilatin

Urodilatin is a 32-amino acid peptide generated from alternative processing of ANP expressed in the kidney (Potter et al., 2006). It plays an important role in the regulation of sodium and water homeostasis and has vasorelaxant effects (Hirsch et al., 2006). In healthy volunteers, urodilatin dose-dependently reduces mean pulmonary arterial pressure and pulmonary capillary wedge pressure, and increases heart rate (HR) and cardiac index (Kentsch et al., 1992b), indicating urodilatin has beneficial effect in CVDs. These cardioprotective effects of urodilatin are also observed in patients with CHF (Kentsch et al., 1992a, Elsner et al., 1995).

The structure of natriuretic peptides

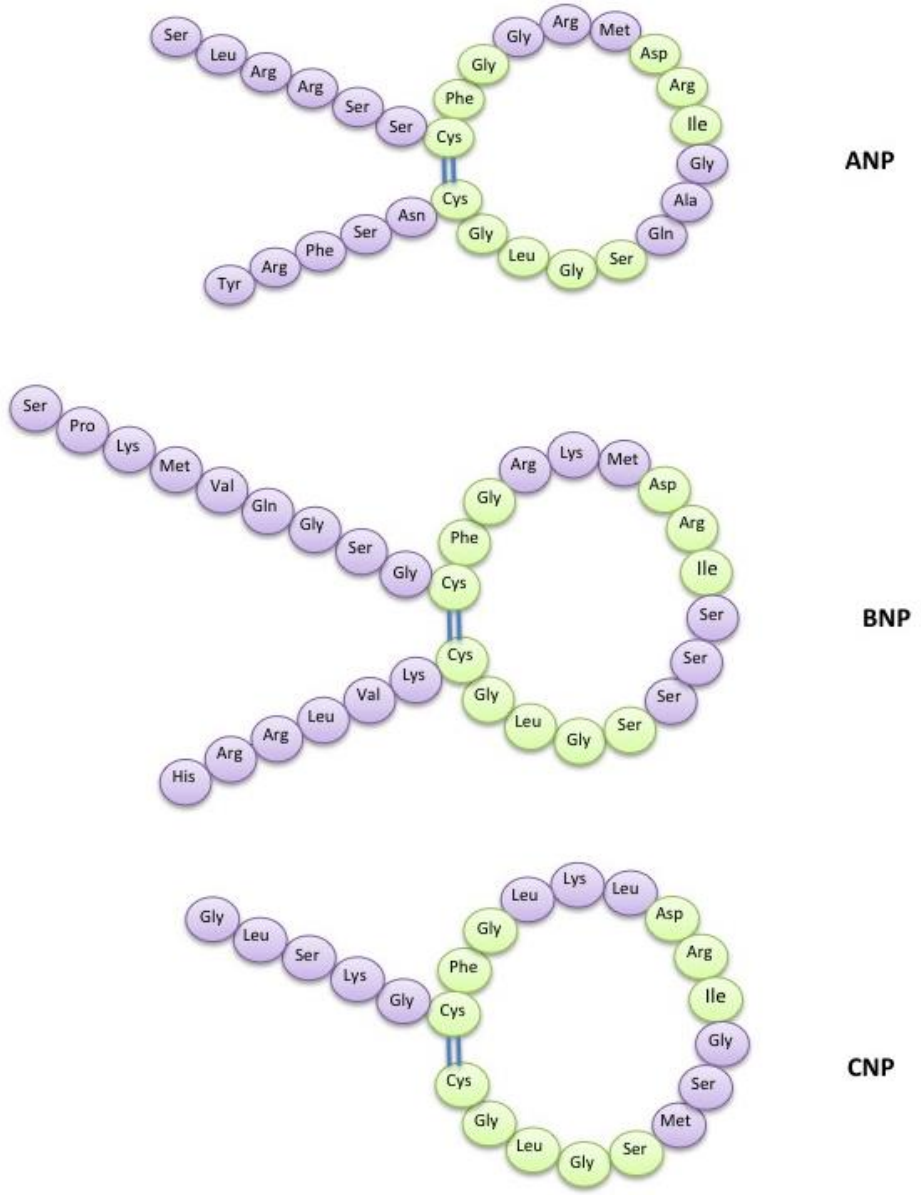

Figure 5. The structure of natriuretic peptides.

Atrial natriuretic peptide (ANP), brain natriuretic peptide (BNP), and C-type natriuretic peptide (CNP). Conserved amino acids are in green and disulphide bonds are indicated in straight lines.

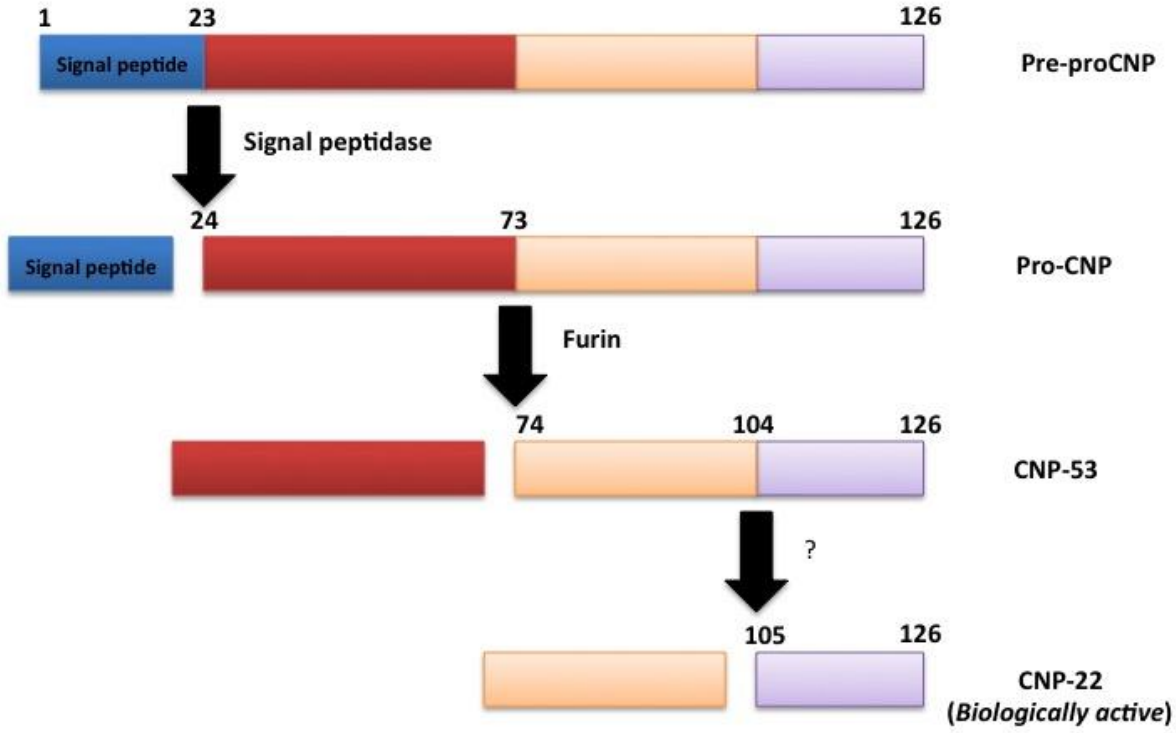

Figure 6. Biosynthesis of biologically active CNP-22.

The signal peptide is removed from pre-proCNP by signal peptidase, yielding pro-CNP, which is then cleaved by furin to produce CNP-53. CNP-53 is then converted into CNP-22 by an unknown mechanism.

1.6 Natriuretic peptide signalling and clinical significance

1.6.1 Overview of natriuretic peptide receptors

The biological effects of natriuretic peptides are mediated by binding of the peptides to a family of membrane spanning receptors, termed natriuretic peptide receptors (NPRs) (Potter et al., 2006). Three subtypes of NPRs have been found: NPR-A, NPR-B, and NPR-C. NPR-A and NPR-B are also known as GC-A and GC-B, respectively, representing particulate guanylyl cyclases (pGC). ANP and BNP are the primary ligands for NPR-A, whereas NPR-B is more selective for CNP (Potter, 2011a). NPR-C is the most abundant NPR in many tissues and it is known as a clearance receptor that removes natriuretic peptides from the circulation. Thus, the binding affinities of NPR-C for all three natriuretic peptides are relatively similar (Potter, 2011a).

NPRs are homodimeric and exhibit high homology, especially their N-terminal extracellular binding domain (Potter, 2011a). Both NPR-A and NPR-B have GC functionality at the C-terminus, which is normally inhibited by phosphorylation of the kinase homology domain (Koller et al., 1992). Receptor binding of the natriuretic peptides to their respective NPR causes conformational changes, which releases the inhibitory action of the kinase homology domain on the GC functionality resulting in cGMP synthesis, which underpins many of the biological activities of the peptides (Ogawa et al., 2004, Pagel-Langenickel et al., 2007)(Figure 7). The extracellular ligand-binding domain of NPR-C shares approximately 30% homology with NPR-A and NPR-B (Potter et al., 2009). However, NPR-C is devoid of kinase and GC activities but possesses a 37-amino acid intracellular N-terminal that has been shown to have a *Pertussis toxin* (PTx) sensitive G_i binding domain (Zhou and Murthy, 2003) (Figure 7).

1.6.2 Natriuretic peptide receptors A

NPR-A is the common receptor for ANP and BNP that is widely expressed in the CVS, predominantly in the cardiac atria and the ventricles, aorta and peripheral vasculature as well as in platelets, kidney and presynaptic fibres (Pandey, 2011). Activation of NPR-A by ANP or BNP elicits vasodilatation, natriuresis as well as decreases renin, vasopressin and aldosterone release (Lohmeier et al., 1995). Deletion of NPR-A in mice causes hypertension and leads to cardiac hypertrophy and fibrosis (Oliver et al., 1997), indicating the importance of the receptor in cardiovascular homeostasis.

1.6.3 Natriuretic peptide receptor B

In NPR-B expressing cells, only CNP can effectively stimulate GC activity (Ogawa et al., 1992). Although NPR-B is expressed in blood vessels, NPR-B KO mice do not exhibit hypertension (Tamura et al., 2004). However, absence of NPR-B leads to dwarfism due to impairment of endochondral ossification and female animals fail to develop a normal reproductive tract (Tamura et al., 2004). In humans, homozygous defects in NPR-B gene cause a severe skeletal dysplasia, acromesomelic dysplasia Maroteaux type (Bartels et al., 2004). This confirms CNP/NPR-B signalling is critical for bone development.

1.6.4 Natriuretic peptide receptor C

The extracellular domain of NPR-C shares ~30% homology with NPR-A and NPR-B and has a short 37 amino acid cytoplasmic domain (Anand-Srivastava, 2005). It is widely distributed throughout the body including vasculature, heart, kidney and the brain (Anand-Srivastava, 2005). The receptor density in these tissues is higher than NPR-A/B. In fact, NPR-C comprises about 94% of the natriuretic peptide receptor population on endothelial cells (Leitman et al., 1986). It has long been thought to solely acts as a clearance receptor due to an absence of a GC domain (Nussenzveig et al., 1990). However, two subtypes of NPR-C have been found. The 77-kDa protein is implicated in ligand clearance via receptor internalisation, whereas a 67-kDa protein has G_i protein coupling that is able to inhibit AC/cAMP cascade and activate PLC-β3 (Murthy et al., 2000, Li et al., 2014a) (Figure 7). NPR-C KO mice exhibit increased bone growth resulting in a hunched back, dome-shaped skull, elongated tail and limbs (Jaubert et al., 1999), probably due to reduced local clearance of CNP that over-stimulates NPR-B signalling. Although mice with NPR-B deletion are normotensive, NPR-C KO mice exhibit elevated BP (Moyes et al., 2014), suggesting NPR-C signalling is important in maintaining vascular function. It has been reported that NPR-C activation leads to the opening of G protein-gated inwardly rectifying potassium (GIRK) channels that causes hyperpolarisation of VSMCs, resulting in vasorelaxation (Chauhan et al., 2003).

1.6.5 Clinical trials of natriuretic peptides

Hobbs *et al*. (1996) conducted the first randomised, double-blinded, placebo-controlled clinical trial of synthetic human BNP, nesiritide, in patients with acute decompensated (AD)HF. The study demonstrated that bolus intravenous administration of BNP improves haemodynamics, and increases cardiac and stroke volume indices in a dose-dependent fashion (Hobbs et al., 1996). Other trials also showed continuous infusion of nesiritide in

ADHF patients is well tolerated and provides a rapid and sustained beneficial haemodynamic effect that is comparable with standard therapies such as intravenous diuretics, dobutamine, nitroglycerin and sodium nitroprusside (Mills et al., 1999, Colucci et al., 2000). Furthermore, the Vasodilation in the Management of Acute CHF (VMAC) study demonstrated nesiritide improves dyspnoea similarly to nitroglycerin with a greater reduction in pulmonary capillary wedge pressure (PCWP), which formed the basis for the Food and Drug Administration's approval of nesiritide in the US. The PRECEDENT study also indicated that nesiritide has greater haemodynamic effect without the undesired pro-arrrythmic and chronotropic effects associated with dobutamine (Burger et al., 2002). These studies demonstrated that nesiritide is a safer, short-term treatment for patients with ADHF. However, a meta-analysis suggested nesiritide significantly increases the risk of worsening renal function that is associated with poorer prognosis compared with control therapy (Sackner-Bernstein et al., 2005). Yet, the definition of worsening renal function used in these trials was elevations in serum creatinine. Blockade of RAAS by the action of nesiritide can lead to increases in creatinine levels, suggesting the 'worsening renal function' may reflect the haemodynamic effect, rather than renal injury. In addition, studies have shown that nesiritide has no impact on renal function and no association with short or long-term mortality (Witteles et al., 2007, Arora et al., 2006). Indeed, nesiritide administered to patients with left ventricular dysfunction undergoing coronary artery bypass grafting is associated with a significant reduced peak increase of serum creatinine, a smaller fall in glomerular filtration rate and a lower 180 day mortality (Mentzer et al., 2007). However, the ROSE Acute Heart Failure Trial, which was specifically designed to investigate the effect of low-dose nesiritide on renal function in patients with acute HF and renal dysfunction on diuretic therapy, demonstrated that nesiritide neither enhances decongestion nor improves renal function as indicated by urine volume and serum cystatin C measurements (Chen et al., 2013). In addition, serial outpatient nesiritide infusion does not provide clinical benefit over standard therapies in patients with advanced HF (Yancy et al., 2008). This fits well with the first large-scale randomised, placebo-controlled trial with over 7000 acute HF patients (ASCEND-HF trial). It demonstrated that nesiritide has no significant clinical benefits in addition to standard care, including neither increase nor decrease in death rate and rehospitalisation, no worsened renal function but associated with an increased occurrence of hypotension (O'Connor et al., 2011). The study, in part, agrees with the VMAS trial in that a significant effect on dyspnoea at 3 hours was observed as compared with placebo but the improvement was similar to that of intravenous

nitroglycerin, and no significant effect was observed at 24 hours. Taken together, there is no strong clinical evidence demonstrating nesiritide is superior to standard care. The inconsistencies reported from different clinical trials could be due to the patient population studied, analysis strategies, and whether nesiritide was compared to standard therapy or placebo. For example, the treated patients in the VMAS study were compared to placebo with no additional therapy unless worsening symptoms was observed, whereas in the ASCEND-HF trial, all patients received interventions and the effect of nesiritide was compared to the standard therapy.

Some clinical trials have been conducted to investigate the action of BNP in LV remodelling and function in patients with AMI. A proof-of-concept study involving 24 patients showed 72 hours infusion of BNP has beneficial effect on LVEF and reduced LV end-systolic volume (Chen et al., 2009). However, a phase II study, BELIEVE II, involving 60 patients with STEMI showed no significant effect of 3 days of nesiritide infusion on infarct size and cardiac function compared to placebo (Sangaralingham et al., 2013, Chen, 2014). Whilst, eight weeks of chronic subcutaneous infusion of BNP improves LV remodelling, LV systolic and diastolic volume index, LV filling pressure and Minnesota Living with Heart Failure scores in patients with HFrEF (Chen et al., 2012). Yet, this study was unable to determine clinical outcomes and whether BNP can delay progression of HF due to lack of long-term follow up of the patients. Furthermore, evidence suggests that NPR-A signalling is reduced whereas as NPR-B activation is increased in experimental models of HF and in human failing hearts (Dickey et al., 2007, Dickey et al., 2012, Tsutamoto et al., 1993, Matsumoto et al., 1999). In accord, immunocytochemistry has demonstrated a significant downregulation in the density of NPR-A in cardiomyocyte, endothelial cells and vascular smooth muscle of patients with ischaemic heart disease. Thus, increasing circulating active BNP may not necessarily confer cardiovascular benefits due to dysfunction/downregulation of NPRs in patients with HF. In contrast, an increase in NPR-C mRNA expression was observed in patients with HF (Kuhn et al., 2004), suggesting NPR-C activation may represents a feasible therapeutic target. In fact, sympathetic over-activation, which is associated with HF, is dampened by NPR-C signalling, possibly in a similar manner as β-blockers (Azer et al., 2012, Azer et al., 2014, Moghtadaei et al., 2017). Thus, targeting CNP/NPR-C signalling offers a theoretical advantage in treating HF.

1.7 Clearance of natriuretic peptides

1.7.1 Overview

Plasma levels of natriuretic peptides are regulated by the rate of synthesis, release and clearance from the circulation. Two main mechanisms contribute to the removal of the peptides: NPR-C mediated endocytosis or hydrolysis by neutral endopeptidase (NEP) (Potter, 2011b). The reported half-life for ANP is about 2.5 minutes in normal human subjects (Yandle et al., 1986) and about 20 minutes for BNP (Holmes et al., 1993). This parallels NEP sensitivity and NPR-C affinity, which are both lower for BNP (Potter, 2011b). CNP has the shortest half-life (~2 minutes) of all the natriuretic peptides in human (Hunt et al., 1994), probably due to the sensitivity to NEP degradation.

1.7.2 Endocytosis by NPR-C

NPR-C-mediated internalisation and degradation involves the binding of the peptides to the receptor, followed by endocytosis and lysosomal degradation. The ligand-free receptor is then rapidly recycled back to the plasma membrane (Potter, 2011b). The dissociation of natriuretic peptides from NPR-C is slower than the rate of internalisation, ensuring the bound peptide is delivered to the lysosome for degradation. NPR-C contains a single tyrosine (Tyr^{508}) amino acid in the cytoplasmic domain that has been suggested to be important in clathrin-dependent endocytosis (Cohen et al., 1996). However, NPR-C does not contain cytoplasmic internalisation motifs that are homologous to other receptors that are known to internalise via a clathrin-coated-pit dependent pathway (Cohen et al., 1996), hence the exact mechanism by which NPR-C-mediates endocytosis is still uncertain.

1.7.3 Neutral endopeptidase

NEP, also known as neprilysin, is a zinc-containing, membrane-bound, extracellular proteinase that cleaves substrates on the amino side of hydrophobic residues (Kerr and Kenny, 1974). It is widely distributed throughout the body including the heart, lungs, kidney and also found on the surface of endothelial cells, VSMCs, fibroblasts and myocytes (Vanderheyden et al., 2004). NEP cleaves ANP and CNP at multiple sites but the initial cleavage occurs between the conserved C^7 and F^8 residue, breaking the ring structure and inactivating the peptide (Potter, 2011b). Studies have been shown that BNP is a poorer substrate for NEP, which does not break between C^7 and F^8 but at M^5-V^6 near the N-terminal tail of the peptide (Kenny et al., 1993). This may contribute to the longer half-life of BNP.

The relative contribution of receptor-mediated and extracellular proteinase to natriuretic peptide inactivation has been studied. Charles *et al*. (1996) have shown that NPR-C blockade and NEP inhibition induce similar increases in ANP and BNP concentration under physiological conditions, indicating an equal contribution of enzymatic and receptor clearance pathway. However, during pathophysiological conditions where natriuretic peptide levels are raised and NPR-C may be saturated, NEP may play a major role in inactivation (Hashimoto et al., 1994).

Natriuretic peptide receptors and their respective downstream signalling pathways

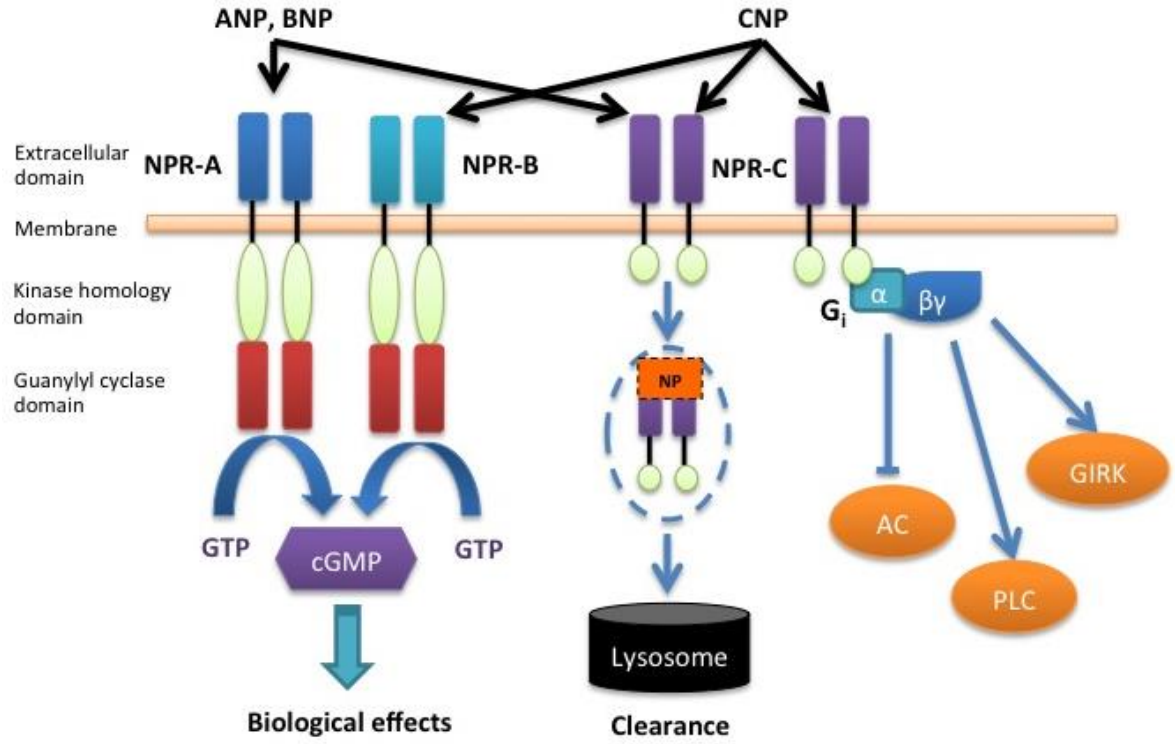

Figure 7. Natriuretic peptide receptors (NPRs) and their respective downstream signalling pathways.

NPR-A and –B are particulate guanylyl cyclase receptors that produce biological effects via cGMP production. NPR-C is a clearance receptor and has Gi-protein coupling. Its activation by CNP mediates biological signalling via inhibition of adenylyl cyclase (AC), activation of phospholipase-C (PLC) or opening of G protein-gated inwardly rectifying potassium channels (GIRK).

1.8 The role of CNP in the vascular system

1.8.1 Overview

The relatively high expression of CNP in endothelial cells and the presence of its receptor on the underlying smooth muscle cells suggest that CNP plays a role in vascular homeostasis (Stingo et al., 1992). Due to the low plasma levels of CNP, it is thought to act in a paracrine/autocrine fashion. In healthy human subjects, the plasma concentration of CNP is approximately 1 pg/ml (Igaki et al., 1996, Hama et al., 1994) and rises in pathological conditions, especially in patients with cardiovascular disorders (septic shock, 13 pg/ml (Hama et al., 1994); renal failure, 3 pg/ml (Igaki et al., 1996); CHF, 8 pg/ml (Del Ry et al., 2011a)), diabetes (9 pg/ml (Del Ry et al., 2011a)) and cirrhosis (5 pg/ml (Del Ry et al., 2011a)). In conditions of oxidative stress, such as atherosclerosis, NO bioavailability is reduced whilst CNP production is increased (Chun et al., 2000). These observations suggest CNP may play a protective, compensatory role to NO in maintaining endothelial function.

1.8.2 CNP in the regulation of vascular tone

CNP is widely reported as a potent vasodilator in various vascular beds of different species including human (Wiley and Davenport, 2001), pig (Barber et al., 1998), rat (Chauhan et al., 2003) and mouse (Madhani et al., 2003). In isolated porcine coronary arteries CNP evokes vasorelaxation by hyperpolarisation (Barton et al., 1998). Subsequently, Chauhan *et al*. (2003) showed that CNP and EDHF exhibit equivalent hyperpolarisation and relaxation responses in rat mesenteric artery that were blocked by well-characterised EDHF inhibitors. This provided the first evidence that CNP acts as an EDHF and regulates local vascular tone in parallel with NO and PGI_2. Correspondingly, mice lacking endothelium-derived CNP have reduced vasorelaxant responses to ACh compared to WT in the presence or absence of NO and PGI_2 blockade (Moyes et al., 2014). With the use of the selective NPR-C antagonist, M372049, it has been revealed that CNP acts on NPR-C leading to G_i-dependent activation of Ba^{2+}-sensitive GIRK channels and Na^+/K^+-ATPase in the VSMC, resulting in hyperpolarisation and vasorelaxation (Villar et al., 2007) (Figure 8). This mechanism represents a major component of EDHF-induced smooth muscle relaxation. However, activation of proteinase-activated receptor 2 (PAR_2) in the endothelium also mediates EDHF responses and this is not altered in mice deficient in the NPR-C gene (McGuire et al., 2004). Furthermore, vasodilator responses to CNP in capillaries are preserved in endothelial-restricted NPR-B KO mice but abolished in pericyte NPR-B KO (Spiranec et al., 2018). These

observations indicate CNP signalling is important in regulating different vascular cell types across various vascular beds.

1.8.3 CNP in the regulation of blood pressure

The ability of CNP to regulate vascular tone intimates that this peptide contributes to BP regulation. In a genetic association study, it has shown that a single-nucleotide polymorphism in the CNP gene associates with hypertension, particular in younger adults (Ono et al., 2002). GWAS have also shown that mutations in NPR-C and furin associate with higher BP (Ehret et al., 2011). This is consistent with animal studies that have revealed disruption of CNP production leads to a hypertensive phenotype in an allele dependent manner, particularly in female animals (Moyes et al., 2014).

1.8.4 Interaction between CNP and renin-aldosterone-angiotensin system

There is evidence that CNP contributes to the regulation of BP by interfering with the RAAS signalling in a manner akin to ANP. Ang II stimulates the secretion of ET-1, a process that is inhibited by CNP with a greater potency than ANP or BNP (Kohno et al., 1992). In human forearm blood flow studies, CNP inhibits Ang I-induced vasoconstriction but not Ang II, intimating that CNP inhibits ACE activity (Davidson et al., 1996). On the other hand, ramipril, an ACEi, increases CNP mRNA expression in the renal cortex (Walther et al., 2001), suggesting the use of ACEi not only inhibits the generation of Ang II but also increases CNP expression that could be cardioprotective. However, the overall diuretic and natriuretic effect of CNP is modest compared to ANP and BNP (Kalra et al., 2001).

1.8.5 CNP in vascular cell proliferation and remodeling

Atherosclerosis is a huge contributor to cardiovascular disorders including CHD, stroke and MI (Hansson, 2005). To promote endothelial regeneration whilst inhibiting VSMC proliferation is essential to prevent atherosclerosis, restenosis and maintain a healthy vasculature (Kipshidze et al., 2004, Losordo et al., 2003). Many studies have shown that CNP is a strong anti-proliferative agent and reduces intimal thickening via the NPR-B/cGMP cascade (Furuya et al., 1993, Doi et al., 2001, Ohno et al., 2002). Similar results were reported in different vascular beds and species, including rat and rabbit carotid artery (Furuya et al., 1993, Gaspari et al., 2000, Shinomiya et al., 1994), porcine coronary artery (Morishige et al., 2000) and porcine femoral artery (Pelisek et al., 2006). However, a study by Cahill *et al.* (1994) showed that CNP suppresses aortic smooth muscle cell proliferation via a cGMP-independent pathway involving NPR-C. This result is supported by recent

studies from the Hobbs' laboratory, using antagonists and NPR-C KO mice, demonstrating that NPR-C dependent ERK1/2 phosphorylation is responsible for the dual effect of CNP to inhibit VSMC proliferation but concomitantly augment endothelial cell growth (Khambata et al., 2011). These dual roles of CNP in vascular cell proliferation might represent an attractive therapeutic avenue in atherosclerosis and might provide an alternative agent to the existing drug eluting stents for patients undergoing PCI.

1.8.6 CNP in vascular inflammation and atherosclerosis

One of the early steps of atherogenesis is the rolling and adhesion of leukocytes to the endothelial surface through interaction of various cell adhesion molecules that are expressed on both leukocytes and endothelial cells (Libby, 2002). CNP has been shown to supress leukocyte rolling induced by acute inflammation or in a high basal leukocyte activation mouse model (i.e. eNOS KO mice). Genetically modified mice with endothelial CNP deletion exhibit increased basal leukocyte rolling, and apolipoprotein E (*ApoE*)/endothelial CNP double KO mice are more prone to the development of atherosclerotic plaque in the aorta compared with WT/ApoE KO littermate controls (Moyes et al., 2014). These findings provide strong evidence that CNP has anti-atherosclerotic properties.

Furthermore, CNP is expressed strongly in coronary atherosclerosis lesions, particularly in the endothelium, VSMCs and macrophages (Casco et al., 2002). Interestingly, the level of CNP expression correlates with the severity of human atherosclerotic lesions. Naruko *et al*. (1996) showed that CNP expression is present in the endothelial cells of non-lesional human coronary arterial segments, but is decreased in lesional segments (Naruko et al., 1996). Conversely, CNP levels are increased in VSMCs and macrophages of the lesion area but absent from healthy segments (Naruko et al., 1996, Casco et al., 2002). In addition, NPR-A is absent in the lesions but both NPR-B and NPR-C are expressed (Casco et al., 2002). Taken together, this evidence indicates an autocrine/paracrine action of CNP in modulating the progression of atherosclerotic disease via its anti-proliferative and anti-migratory action on VSMCs and macrophages, and maintenance of vasculature integrity.

EDHF/CNP-mediated vascular smooth muscle hyperpolarisation

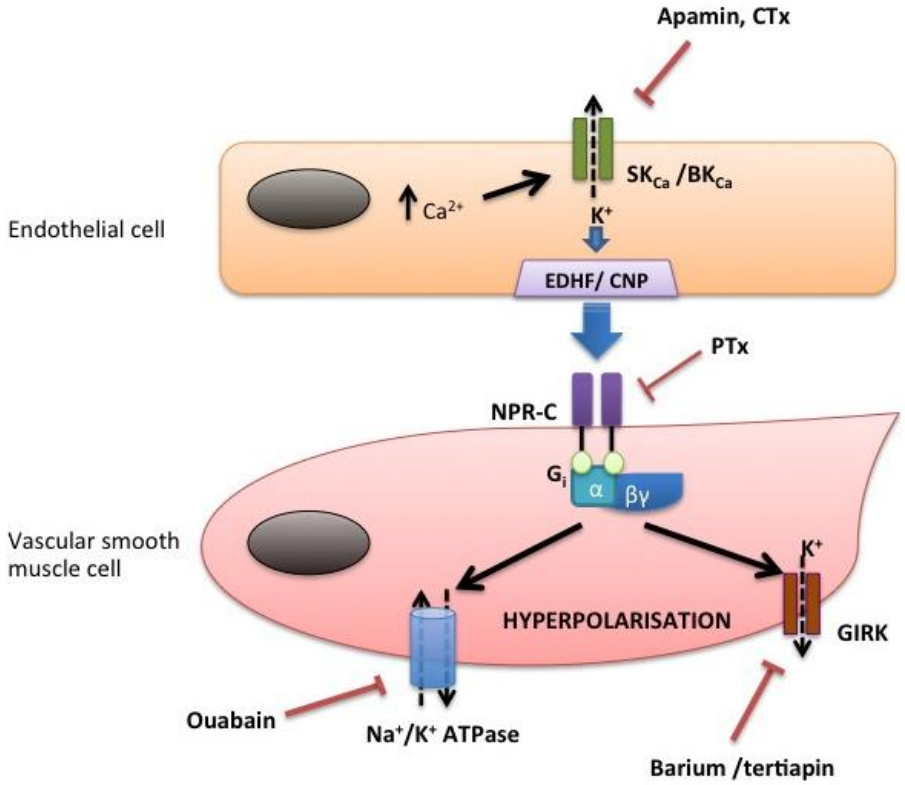

Figure 8. EDHF/CNP-mediated vascular smooth muscle hyperpolarisation.

EDHF/CNP is released in the endothelial cell upon activation of calcium-dependent potassium channel, SKCa. The release of CNP results in the activation of NPR-C on the vascular smooth muscle cell, which causes activation of Na^+/K^+ ATPase and G protein-gated inwardly rectifying potassium (GIRK) channels via G_i-coupling, leading to hyperpolarisation and vasorelaxation. SK_{Ca}, calcium activated small-conductance potassium channel; BK_{Ca}, calcium activated big-conductance potassium channel; CTx, charybdotoxin; PTx, pertussis toxin.

1.9 The role of CNP in cardiac function

1.9.1 CNP in cardiac pathologies

Early studies detected expression of all three types of NPR (NPR-A, -B and -C) in both rat and human hearts (Nunez et al., 1992). Subsequently, CNP mRNA was also found in rat hearts (Vollmar et al., 1993), confirming the production of CNP in the myocardium and hinting that it may contributes to the regulation of cardiac function. By measuring the difference in plasma levels of CNP between the aortic root and coronary sinus in patients with CHF, it has been confirmed that failing hearts produce CNP (Kalra et al., 2003, Del Ry et al., 2006a), and that plasma levels of CNP are related to disease severity (Del Ry et al., 2005). The expression of CNP mRNA is also significantly increased in ischaemic cardiomyopathy and inversely associated with LV function (Tarazon et al., 2014). Similarly, CNP mRNA expression is elevated in the fibrotic area of the infarct and border regions of the lesion (Soeki et al., 2005), indicating local CNP acts in an autocrine manner and may play an important part in cardiac fibrosis. In *in vivo* studies, CNP levels decrease as collagen deposition increases in aging rat (Ichiki et al., 2014, Sangaralingham et al., 2011), suggesting a reduction in CNP may contribute to fibrosis. These observations indicate CNP production and secretion in the heart may play an important role in pathophysiological processes, and may have a compensatory or potentiating effect on other cardioprotective mediators, such as NO and alternate natriuretic peptides. In addition, higher levels of CNP and NPR-B expression are observed in leukocytes of HF patients with respect to control subjects (Cabiati et al., 2012), indicating CNP may also influence cardiovascular disorders via anti-inflammatory activity (Wang et al., 2007).

Nevertheless, the physiological function of CNP in cardiac function remains to be elucidated due to lack of selective pharmacological tools and cell-specific gene deletion, since global CNP KO is lethal before mice reach adulthood (Chusho et al., 2001).

1.9.2 CNP in ischaemia-reperfusion injury

Numerous studies have shown a protective effect of pGC/cGMP/PKG activity in IR injury (Abdallah et al., 2005, Burley et al., 2007, Inserte et al., 2000, Jin et al., 2014), implying the activation of NPR-B by CNP is myocardial protective. However, cardiomyocytes respire anaerobically during ischaemia that results in intracellular acidosis, which blunts cGMP production via pGC signalling in this environment (Agullo et al., 2003). This suggests that a pGC/cGMP-independent protective pathway might be involved. The Hobbs' lab has

demonstrated in the isolated Langendorff heart that infusion of CNP prior to or following an ischaemic insult results in a 30-50% reduction in infarct size. The NPR-C agonist, $cANF^{4-23}$, mimicked this beneficial effect of CNP, indicating that NPR-C activation contributes to the CNP-mediated protective mechanism against IR injury (Hobbs et al., 2004). Furthermore, it has been suggested that the activation of NPR-C/G_i coupling exerts its biological action by recruiting PI3K/Akt cascade that in turn stimulates eNOS and NO production (Anand-Srivastava, 2005). This pathway is known to be protective in IR injury (Schulz et al., 2004). Thus, both cGMP-dependent (i.e. NPR-B) and –independent (i.e. NPR-C) mechanisms might underlie the cardioprotective effect of exogenous CNP.

1.9.3 CNP in the regulation of cardiac remodelling

Cardiac remodelling and fibrosis is a hallmark of end-stage HF that involves cardiac fibroblast proliferation, and changes in myocardial morphology and function (Wu et al., 2017b). Thus, to slow cardiac hypertrophy and fibrosis is a sought-after therapeutic option in CHF. To date, it is well established that ANP and BNP possess anti-hypertrophic and anti-fibrotic properties and improve cardiac function in the diseased heart (Tamura et al., 2000, Rosenkranz et al., 2003). However, their potent diuretic and natriuretic properties are a huge drawback to patients with unstable haemodynamics, dropping BP and impairing renal function (Vaduganathan et al., 2013). Interestingly, it has been reported that CNP has more potent anti-hypertrophic and anti-fibrotic actions than ANP (Horio et al., 2003), suggesting CNP may be a better pharmacological tool for CHF. Studies of CNP pharmacology have demonstrated that CNP attenuates an increase in cardiac hypertrophy and fibrosis, reduces LV enlargement in response to pressure-induced or ischaemia-induced HF (Soeki et al., 2005, Izumiya et al., 2012). In concert with these studies, mice with cardiac-restricted CNP-overexpression do not develop cardiac hypertrophy and fibrosis after MI, but no difference in infarct size was observed compared to WT (Wang et al., 2007). This indicates that CNP moderates the adverse cardiac remodelling process post-ischaemia. The protective mechanism of CNP is proposed to be attributed to CNP/NPR-B signalling as down-regulation of NPR-B signalling exhibits progressive cardiac hypertrophy without altering BP (Langenickel et al., 2006, Del Ry et al., 2008a). Yet, the ventricular expression of NPR-B is reduced in HF (Del Ry et al., 2008a), limiting the therapeutic potential of targeting NPR-B signalling. In addition, there is no evidence of increased fibrosis in animals with down-regulated NPR-B, while loss of NPR-C results in structural remodelling and fibrosis (Egom et al., 2014). These observations suggest that the anti-fibrotic action of CNP might be conveyed via NPR-C.

1.9.4 CNP in the control of heart rate

All three NPRs are expressed in the sinoatrial node (SAN) and atrium (Springer et al., 2012), suggesting natriuretic peptides have the ability to modulate HR and the cardiac conduction system. Early *in vivo* studies showed that CNP has positive chronotropic and inotropic effects via NPR-B signalling (Beaulieu et al., 1997, Hirose et al., 1998). Correspondingly, a recent study has shown that CNP increases HR via increasing L-type Ca^{2+} current ($I_{Ca(L)}$) and hyperpolarisation-activated current (I_f) (Springer et al., 2012). It is proposed that CNP regulates HR and conductivity by activating GC-linked NPR-B that increases cGMP concentration and inhibits PDE3 activity (Springer et al., 2012). Blockade of PDE3 would be expected to result in an increase of cAMP, which has positive chronotropic effect. However, Herring *et* al. (2001) reported a bradycardia effect of CNP via a cGMP/PDE3 dependent pathway, causing an increase of cAMP PKA-dependent phosphorylation of presynaptic N-type calcium channels. This leads to ACh release into the synapse and activates M_2 receptor on pacemaker cells that results in an enhanced vagal tone (Herring et al., 2001).

Rose *et al.* (2004) have demonstrated a negative chronotropic effect of CNP mediated by activation of NPR-C through G_i protein coupling in isolated SAN cells that leads to inhibition of L-type Ca^{2+} current (Rose et al., 2004). This group has also demonstrated a dual role of CNP in HR and SAN function by stimulating NPR-B and/or NPR-C in response to different levels of sympathetic drive (Azer et al., 2012). Under basal condition, CNP is able to increase HR, but this effect is not replicated by $cANF^{4-23}$, which suggests NPR-B is responsible for the positive chronotropic activity. In sharp contrast, CNP causes a reduction in HR in the presence of isoprenaline (ISO) and this effect is enhanced by NPR-B blockade, but abolished in NPR-C KO mice. These observations provide a definitive role for CNP in the SAN function and demonstrated CNP acts via NPR-B to increase HR under basal conditions but that this appears to switch to NPR-C signalling, probably via decrease in cAMP level, during sympathetic hyperactivity. In addition, NPR-C KO mice have elevated heart rate with reduction in parasympathetic activity and enhanced sympathetic activity, confirming NPR-C signalling modulates autonomic function (Moghtadaei et al., 2017). Furthermore, CNP can also reduce cardiac sympathetic neurotransmission by inhibiting the release of noradrenaline (Buttgereit et al., 2016). These biological actions of CNP on the sympathetic system may represent an important therapeutic target in CHF patients as damping sympathetic activity improves survival (Gheorghiade et al., 2003, Butler et al., 2006).

1.9.5 CNP in the control of cardiac contractility

Patients with CHF have elevated plasma levels of CNP that parallels clinical severity (Del Ry et al., 2005). Furthermore, clinical studies also reported a negative correlation between CNP and dP/dt in CHF patients, indicating CNP has a possible role in cardiac contractility (Del Ry et al., 2008b). In cardiac muscle preparations and isolated cardiomyocytes, CNP displays a positive lusitropic effect associated with a negative inotropic effect (Brusq et al., 1999, Nir et al., 2001, Zhang et al., 2005a). Whereas in the isolated perfused working heart, CNP exhibits a biphasic action with an immediate increase in inotropy and lusitropy, followed by a slowly developing negative inotropic effect (Pierkes et al., 2002, Wollert et al., 2003). These actions associate with PLB phosphorylation and activation of SERCA, and are mimicked by a cGMP-analogue (Pierkes et al., 2002), suggesting a cGMP-dependent pathway contributes to CNP bioactivity. In addition, cGMP-dependent protein kinase I (PKG I) overexpression enhances CNP-mediated cell shortening, systolic Ca^{2+} levels and accelerates Ca^{2+} decay (Wollert et al., 2003). Thus, it is plausible that CNP modulates cardiac contractility via the NPR-B/cGMP cascade.

1.10 cGMP and cAMP signalling in cardiac remodelling

1.10.1 Overview

cGMP and cAMP are second messengers conveying the biological activity of NO and natriuretic peptides, and the sympathetic system (Tsai and Kass, 2009). Different stimuli activating these cyclic nucleotides can mediates diverse cellular and physiological effects on the CVS depending on their concentration, localisation and duration of stimulation (Levy, 2013). For instance, acute elevation of cAMP increases intracellular Ca^{2+} that enhances contractility of the heart and cardiac output (Bobin et al., 2016). However, prolonged activation of cAMP activity due to sustained activation of adrenoceptors, as occurs in hypertension and HF, leads to maladaptive cardiac remodelling, apoptosis and arrhythmia (Bobin et al., 2016). Hence, modulation of cyclic nucleotide amplitude, duration and localisation is very important in determining the physiological responses. This is tightly regulated by the balance between the rate of cAMP and cGMP generation by AC and GC, respectively, and the rate of degradation by PDEs.

1.10.2 cAMP/PKA cascade in the heart

The stimulation of G_s protein coupled receptors, such as β-adrenoceptors, activates AC that syntheses cAMP, which in turn activates cAMP-dependent protein kinase A (PKA) (Bobin et

al., 2016). PKA phosphorylates various downstream proteins that regulate Ca^{2+} transient in cardiomyocytes in response to acute sympathetic stimulation, including sarcolemmal L-type Ca^{2+} channels, ryanodine receptors (RyR2), PLB (which controls the activity of SERCA2) and troponin I, leading to positive inotropic and lusitropic effects (Bobin et al., 2016). However, chronic activation of PKA suppresses GSK3β that releases numerous transcription factors from chronic inhibition (see section 1.8.4.3), leading to protein synthesis and maladaptive hypertrophy (Dorn and Force, 2005). In addition to PKA, cAMP-activated guanine nucleotide exchange proteins (Epacs) may also play an important role in remodelling (Bobin et al., 2016). A study has shown that Epac1 expression is increased in response to pressure-overload, and activation of Epac1 triggers the calcineurin/CaMKII signalling pathway that results in hypertrophic growth (Metrich et al., 2008). Thus, inhibition of the production of cAMP, i.e. by activating G_i protein coupled receptors, or increasing its rate of degradation by PDEs could be beneficial in CVDs.

1.10.3 cGMP/PKG cascade in the heart

It is widely agreed that elevation of cGMP is cardioprotective. Activation of sGC and pGC by NO and natriuretic peptides, respectively, leads to cGMP production.

1.10.3.1 The effector molecules of cGMP and its physiological action in the cardiovascular system

Two types of effector molecules of cGMP predominate in the CVS: cGMP-dependent protein kinases (PKG), and PDEs. A third type of cGMP effector is the cGMP-gated cation channel, which is found in retinal and olfactory neuro-epithelium and nephrons.

1.10.3.1.1 cGMP-dependent protein kinase

There are three isoforms of PKG. PKG-type Iα (PKG-Iα) is expressed in cardiac myocytes, PKG-Iβ is predominantly found in the endothelial cells, while VSMC expresses both isoforms. The third isoform is PKG-type II (PKG-II) that is found in the kidney, brain and intestine. All three isoforms are homodimers and each subunit consist of three functional domains – N-terminal, regulatory domain and a kinase domain. When cGMP binds to specific sites in the regulatory domain, PKG undergoes a conformational change that leads to the release of the N-terminal inhibition of the kinase domain. Subsequently, the kinase domain catalyses the phosphorylation of a serine/threonine residue of the target proteins.

The action of cGMP is often viewed as opposing cAMP activity, meaning cGMP has negative inotropy, anti-hypertrophic and anti-fibrotic effects. In isolated cardiomyocytes, cGMP

analogues modulate the contraction of electrically stimulated myocardium from WT control mice, but have no effect in the myocardium from cardiomyocyte-specific PKG-I null mice (Wegener et al., 2002), demonstrating cGMP/PKG-I signalling negatively modulates cardiac contractility. Moreover, it has been shown that inhibition of L-type Ca^{2+} channel and troponin I phosphorylation is responsible for the negative inotropic effect mediated by PKG (Yang et al., 2007).

The anti-hypertrophic role of cGMP has been demonstrated in numerous studies with genetic disruption of the cGMP pathway. Mice lacking eNOS develop cardiac hypertrophy and dysfunction (Wenzel et al., 2007, Li et al., 2004a, Flaherty et al., 2007). However, local ANP signalling can compensate for the loss of NO and prevent the development of hypertrophy in eNOS-deficient mice (Bubikat et al., 2005). Likewise, disruption of the cGMP pathway in the heart by cardiac-specific deletion of NPR-A leads to maladaptive hypertrophy with enhanced fibrosis and marked deterioration in cardiac function (Holtwick et al., 2003, Kuhn et al., 2002). These observations are also seen in mice with cardiomyocyte-restricted deletion of PKG-I and accompanied by diminished expression of SERCA2a and PLB that affects myocardial Ca^{2+} homeostasis (Frantz et al., 2013). Taken together, these studies illustrate that one of the potential molecular mechanisms by which ANP and/or BNP exert anti-hypertrophic effects is via regulation of intracellular Ca^{2+} through NPR-A-cGMP-PKG-I signalling that can consequently inhibit the Ca^{2+}-calcineurin-NFAT hypertrophic pathway (see section 1.2.2.2).

An anti-fibrotic effect of natriuretic peptide/pGC pathway has also been identified. It has been shown that ANP-cGMP-PKG signalling induces phosphorylation of Smad3 at a different site from TGF-β1 (Li et al., 2008). The resultant pSmad3 cannot translocate into the nucleus, thus, PKG disrupts TGF-β1-induced pro-fibrogenic gene expression (Li et al., 2008). Moreover, mice with ANP deficiency exhibit accelerated dilated cardiomyopathy with enhanced fibrosis and systolic dysfunction (Wang et al., 2014). Interestingly, these mice have marked increases in CNP and NPR-C expression, which may indicates CNP/NPR-C signalling is upregulated to play a compensational role when ANP production is diminished. It is known that activation of G_i protein coupled NPR-C can indirectly generate cGMP by activating eNOS via PI3K and Akt (Costa et al., 2006). Perhaps, CNP can exert cardioprotective effects via stimulating cGMP production and inhibiting excessive cAMP signalling through activation of NPR-B and/or NPR-C, respectively. Regardless, the patho/physiological signalling of CNP in cardiac function is still poorly understood.

1.10.3.1.2 Phosphodiesterases

cGMP and cAMP catabolism is regulated by PDEs. Since some non-selective PDEs can catabolise both cAMP and cGMP, the hydrolysis of one cyclic nucleotide can inhibit the activity of PDEs on the other cyclic nucleotide. This provides a cross-regulation of cAMP and cGMP signalling. For example, cGMP production following the activation of NPR-B binds to PDE3 and inhibits cAMP degradation, resulting in an increase of cAMP-mediated β-adrenoceptor signalling and contractility in both failing and non-failing hearts (Qvigstad et al., 2010, Meier et al., 2017). Whereas, PDE2 is stimulated by cGMP, leading to an increase in cAMP hydrolysis and protects against sympathetic over-stimulation (Mehel et al., 2013). Indeed, one plausible mechanism by which cGMP/PKG signalling mediates anti-hypertrophic effects is by inhibiting the calcineurin pathway that can activated by cAMP/PKA cascade (Tsai and Kass, 2009). Furthermore, PDE5 is specific for cGMP degradation. In HF models, studies reported PDE5 inhibition blunts β-adrenergic stimulation (Senzaki et al., 2001), protects against IR injury by targeting mitochondrial K_{ATP} channels (Ockaili et al., 2002) and reverses pre-established cardiac hypertrophy in pressure-overload model (Takimoto et al., 2005). Small scale clinical trials in HErEF patients have reported that PDE5 inhibitors improve cardiac function and exercise capacity (Lewis et al., 2007, Kim et al., 2015). However, the larger scale RELAX trial, in HFpEF patients showed neutral results with sildenafil administration (Redfield et al., 2013). One explanation could be that the natriuretic peptides levels are lower in HFpEF patients compared to HErEF (Bishu et al., 2012), which suggests limited natriuretic peptide activity. Thus, to enhance cGMP levels by PDE5 alone may not be adequate in HFpEF patients.

1.11 Hypothesis and aims

Despite the pharmacological evidence supporting a beneficial action of exogenous CNP in maintaining cardiac function in disorders such as MI and HF, there is no direct evidence for a physiological or pathological role for endogenous CNP. Thus, my PhD project was designed to investigate the hypothesis that 'endothelium-derived CNP (ecCNP), cardiomyocyte-derived CNP (cmCNP) and fibroblast-derived CNP (fbCNP) play a central role in regulating cardiac function in health and disease'. To test this hypothesis, I addressed the following specific aims:

1. To determine the role of ecCNP in the regulation of coronary vascular reactivity and explore if it has a protective effect in IR injury by comparing the cardiac phenotype of WT and ecCNP KO mice.

2. To investigate if deletion of CNP from cardiomyocytes affects the development of cardiac remodelling in experimental HF, and if this has a protective effect against IR injury, by comparing WT and cmCNP KO mice.
3. To investigate if deletion of CNP from fibroblasts affects the development of cardiac hypertrophy and fibrosis in HF by comparing WT and fbCNP KO mice.
4. To establish the NPR subtype(s) that confers the bioactivity of ecCNP, cmCNP and fbCNP identified in Aims 1, 2 and 3, respectively.
5. To identify the pro-hypertrophic and pro-fibrotic pathways that are inhibited by the NPR defined in Aim 4.

Chapter 2 – Methods

Chapter 2 – Methods

2 Methods

2.1 Animal models of cardiovascular disease

The greatest advantage of using mouse models is the availability of relevant transgenic or KO strains that provide an excellent tool for identifying a novel signalling pathway and, potentially, therapeutic target.

Many animal models of HF have been developed, including volume overload, pressure overload, rapid-pacing, drug-induced, ischaemia, and genetically modified (Patten and Hall-Porter, 2009). None of the models reproduces every aspect of human HF, but rather these have been developed to represent different characteristics of the disease. In addition, there is evidence that the nature of the stimulus for cardiac hypertrophy determines the type of hypertrophic responses and triggers different signalling pathways (Breckenridge, 2010). For instance, cardiac hypertrophic response to β-adrenoceptor overstimulation by ISO are not altered in PKG KO mice but loss of PKG causes a marked exacerbation of cardiac function in pressure-overload model (Frantz et al., 2013). Therefore, it is very important to choose the right model that signifies the pathology in question.

Although mouse models have many advantages, structural and electrophysiological differences with respect to the human CVS are important limitations (Doevendans et al., 1998).

2.1.1 Isoprenaline-induced heart failure

The sympathetic drive of the heart is regulated by the β-adrenergic system that leads to an increase in contractile force and HR; essentially increasing cardiac output in order to match the demand of the body (Vincent, 2008). This increased workload of the heart elevates cardiac oxygen consumption and may cause myocardial ischaemia and injury. Accumulating evidence illustrates that over-activation of the cardiac adrenergic system promotes myocardial hypertrophy and can be detrimental to the heart (Limbird and Vaughan, 1999). Indeed, a study by Strand et al (2006) has shown in men that plasma noradrenaline levels predict LV mass independently of systolic BP, suggesting a close link between chronic adrenergic activation and hypertrophy/HF (Strand et al., 2006). Moreover, excessive

endogenous catecholamines (β-adrenoceptor agonists) in the circulation are associated with myocardial tissue damage seen in patients with ischaemic heart disease, cardiac arrhythmias and sudden cardiac death (Nichtova et al., 2012). These observations are corroborated by the fact that chronic stimulation of cardiac β-adrenoceptors causes progressive myocyte dysfunction, necrosis and myocardial remodelling (Limbird and Vaughan, 1999). Mechanisms that underlie such damage have been proposed to include Ca^{2+} handling abnormalities, defects in energy production and utilisation, increased preload and afterload and altered signal transduction (Nichtova et al., 2012). Furthermore, the use of β-blockers provides time-dependent improvements in ventricular structure and function as well as reductions in HR and BP (Gillian Pocock, 2006). Considering these clinical findings, it is reasonable to employ an animal model of chronic administration of β-adrenoceptor agonist to investigate the deleterious effects of sympathetic over-activation upon cardiac structure changes and function, and thus, the progression to cardiac disease.

ISO is a synthetic catecholamine that activates the adrenergic system, causing severe cardiac stress. In the late 50s, Rona and Chappel showed that subcutaneous injection of ISO produces diffuse myocardial necrosis that is similar to infarct-like lesions without coronary vasculature damage (Rona et al., 1959). Further studies of acute injection of ISO have demonstrated that ISO-induced myocardial necrosis is time- and dose-dependent and eventually results in a progressive enlargement of the LV cavity that is out of proportion to mass (Teerlink et al., 1994). This morphology has been shown to be an important predictor of mortality in HF and MI patients (Teerlink et al., 1994). In later studies, continuous administration of ISO in rats using osmotic mini-pumps for 1-4 weeks was reported to result in an increase in heart weight of 30-70% (Osadchii, 2007). Similarly, sustained infusion of ISO also induces cardiac hypertrophy in mice (Oudit et al., 2003, Ozaki et al., 2002), rabbits (Kim et al., 2006b) and guinea pigs (Maisel et al., 1989). The development of ISO-mediated cardiac hypertrophy is associated with upregulation of foetal genes such as ANP, skeletal α-actin and β-MHC (Osadchii, 2007). With the use of β-adrenoceptor selective antagonists (β_1 and β_2), it has been found that β-stimulated cardiac hypertrophy is predominantly mediated via β_1 (Morisco et al., 2001, Tomita et al., 2003). More importantly, long-term exposure of isolated, cultured cardiac myocytes to ISO stimulates myocyte growth, suggesting that cardiac hypertrophy results from direct sympathetic stimulation rather than developed only as a compensation for myocyte loss due to necrosis (Luo et al., 2001, Tomita et al., 2003). In addition, there is evidence supporting the

activation of both the circulating and cardiac renin-angiotensin system is also involved in ISO-induced cardiac damage (Grimm et al., 1998, Leenen et al., 2001).

2.1.2 Pressure overload-induced heart failure

Pressure overload models have been the most common model to study the pathogenesis of hypertrophy, subcellular failure, and vascular changes. Transverse aortic constriction (TAC) or administrations of angiotensin II are the most widely used pressure-overload HF model. Rockman et al. first introduced the TAC mice model in 1991 for investigation of ANP expression in cardiac hypertrophy (Rockman et al., 1991). The sudden onset of hypertension achieved with TAC causes an approximately 50% increase in LV mass within 2 weeks (Patten and Hall-Porter, 2009), making this model an excellent choice to examine the utility of pharmacological or molecular interventions that may limit cardiac hypertrophy. However, the severity and time course of hypertension in humans occurs over many years, thus the acute onset of severe hypertension in this model lacks direct clinical relevance. Hence in recent years, more studies are conducted using abdominal aortic constriction (AAC) which induces less severe afterload and the disease progression arises over a longer period of time that more closely mimics the human situation.

While performing the TAC or AAC model demands some advanced surgical skills, the use of a vasoconstrictor, Ang II, provides an alternative, less invasive HF model. Ang II can be administrated by daily injections or via an osmotic mini-pump implanted subcutaneously. Interestingly, many recent pre-clinical and clinical studies have suggested that Ang II does not solely induce hypertension but also has direct bioactivity on myocardial remodelling, which can be prevented or reversed by Ang II antagonists (Williams, 2001, Kim et al., 1995). Enalapril, an ACEi, has been shown to reduce mortality in numerous clinical trials such as CONSENSUS (1987b)and SOLVD (1991) (Jong et al., 2003). These findings support Ang II having detrimental effects in cardiovascular pathologies. Furthermore, transgenic mice with myocardium-specific overexpression of angiotensinogen develop left and right ventricular hypertrophy without an increase in BP (Mazzolai et al., 2000). This study suggests that local production of Ang II in the myocardium conveys the hypertrophic response *in vivo*. Kim *et al*. (1995) also demonstrated that exogenous Ang II infusion in rats induces cardiac hypertrophy accompanied by an increase in the expression of hypertrophic genes such as β-MHC, fibronectin, TGF-β, type I and type III collagen. Normalisation with the use of vasodilator neither prevents cardiac hypertrophy nor decreases the level of foetal gene expressions. However, a selective Ang II receptor (AT_1R) antagonist, TCV-116,

abolishes these phenotypes (Kim et al., 1995), suggesting that Ang II causes cardiac remodelling via AT_1 signalling, independent of a systemic vascular effect. This work dovetails with the study of Harada *et* al. (1998) who demonstrated cardiac hypertrophy is induced by Ang II infusion in WT mice but not in AT_1 KO mice. However, the same study also reported that the development of cardiac hypertrophy in response to TAC model is not altered in mice with deletion of AT_1 signalling compared to control (Harada et al., 1998), implying that pressure overload-induced cardiac remodelling can be driven by an AT_1-independent mechanism and multiple hypertrophic pathways can be involved. Thus, the use of TAC and Ang II model should delineate two distinct cardiac hypertrophic pathways and might provide new insights into the development of novel therapeutic strategies for cardiac hypertrophy.

2.1.3 Myocardial infarction-induced heart failure

MI is one of the main causes of HF in patients. It occurs when an atherosclerotic plaque ruptures and blocks the coronary arteries supplying oxygen and nutrient to the myocardium (Dargie, 2005). This causes cardiomyocyte damage (infarct) that results in a decreased EF and an increased in LV end-diastolic pressure and volume. The increased wall stress may induce regional hypertrophy in non-infarcted areas, but wall thinning in the infarcted segments (Muthuramu et al., 2014). Thus, the degree of ventricular hypertrophy and remodelling is dependent on infarct size.

One of the pre-clinical models that mimic the human condition is permanent ligation of the left anterior descending coronary artery (LADCA). LADCA is the main vessel that supplies blood to the LV myocardium. Upon occlusion of the LADCA, the anterior wall of the LV and the anterior portion of the interventricular septum suffer ischaemia. This model has long been used in mice for the investigation of ventricular remodelling and HF post-MI. Fang Yang *et al*. (2002) examined the inflammatory response and cardiac remodelling in mice after MI for 6 months. They demonstrated that neutrophil infiltration peaks at 1-2 days after MI, while massive macrophage infiltration appears after 4 days. These inflammatory cells are responsible for ECM degradation and removal of necrotic tissue, which results in ventricular wall thinning and cardiac rupture (Yang et al., 2002). Lymphocyte infiltration, reaches a maximum at 1-2 weeks, and then decreases as proliferation of connective tissue increases. This implies that lymphocytes are important in the transition between inflammation and wound healing. An increase in LV internal diameter (LVID) and interstitial collagen deposition are also observed at 1-2 weeks after MI (Yang et al., 2002).

Interestingly, myocyte cross-sectional area remains constant from 4 months to 6 months while heart weight continues to increase, indicating that the hypertrophic process involves myocyte elongation and results in LV enlargement (Yang et al., 2002). This observation is comparable to end-stage human HF that is characterised by dilated, relatively thin-walled ventricles (Gerdes, 1997). More importantly, post-MI cardiac structural composition, LV dilatation and functional deterioration continues over 6 months in this model, allowing long-term studies of myocardial remodelling and drug intervention (Yang et al., 2002).

Another model of MI-induced HF is transient ligation of the LADCA. This model arguably more closely mimics IR injury in the clinical setting. It is different in terms of pathophysiological relevance compared to permanent ligation. The final infarct size resulting from the transient ligation model is exacerbated by myocardial salvage factors following reperfusion (Powers et al., 2007), whereas the infarct area is fixed in the permanent ligation model (Muthuramu et al., 2014). Therefore, the IR model is largely used to examine the short-term consequences of ischaemic injury and to explore the potential therapeutic interventions targeting reperfusion injury that could account for up to 50% of the final infarct size (Yellon and Hausenloy, 2007). Nevertheless, one major limitation of both permanent and transient ligation of the LAD is the accuracy of the ligature position for each repeated experiment that can affect the severity of MI.

2.2 Generation of genetically modified animals and genotyping

2.2.1 Generation of cell-restricted CNP KO mice

Cre/loxP technology was employed to generate conditional deletion of the CNP gene (*Nppc*) in C57BI6 mice (Figure 9). Cre-recombinase excises the region of DNA between two loxP sites. The loxP site is a 34bp nucleotide recognition sequence that can be inserted into both ends of an essential exon (or exons) in a gene of interest (Gu et al., 1994). The allele containing the gene flanked by LoxP sites is called the floxed allele and is phenotypically WT. Mice containing the floxed allele can then be bred to Cre expressing transgenic strains that have been developed using cell-specific promoters that are required to drive Cre expression, allowing cell-restricted deletion of the floxed genes.

2.2.2 Generation of ecCNP KO and cmCNP KO mice

To generate ecCNP KO mice, floxed CNP mice were mated with mice expressing Cre-recombinase under the control of the endothelium specific tyrosine protein kinase receptor (Tie2) promoter, as previously described (Moyes et al., 2014, Kisanuki et al., 2001). To

produce cmCNP KO animals, floxed CNP mice were bred to an α-MHC Cre-recombinase expressing mouse line (Agah et al., 1997).

2.2.3 Generation of tamoxifen-induced fbCNP KO mice

To generate fbCNP KO mice, a modified strategy was used compared to ec/cmCNP KO. Mice expressing collagen type I alpha 2-cre inducible estrogen receptor transgene (Col1α2-Cre-ERT; Jaxon laboratory, USA) (Zheng et al., 2002) were mated with floxed CNP mice. In this approach, Col1α2-Cre-ERT is ligated to a mutated ligand binding domain of the estrogen receptor that restricts transcription until tamoxifen is present (Hall et al., 2009). Therefore, it allows the timing of recombination to be regulated. To trigger the activity of Col1α2-Cre, the mice were given 40mg/kg/day of tamoxifen (Sigma-Aldrich, Poole, UK; T5648) for 5 consecutive days. Tamoxifen powder was weighed and dissolved in sunflower seed oil (Sigma-Aldrich, S5007) with 10% absolute ethanol. The solution was wrapped in foil to avoid light and heated on a heating block at 50-55°C for 5 minutes or until the tamoxifen was completely dissolved. 100µL of the tamoxifen solution was injected intra-peritoneally. Since tamoxifen can cause transient cardiac dysfunction (Koitabashi et al., 2009), both control (WT) and fbCNP KO mice received tamoxifen injections to ensure the observed effects were not due to tamoxifen toxicity. The effect of tamoxifen on cardiac function was also studied in a group of mice by echocardiography, followed up to 6 weeks after tamoxifen injection.

2.2.4 Global NPR-C KO mice

Global NPR-C KO mice were the kind gift of Prof. Oliver Smithies (University of North Carolina, USA; (Matsukawa et al., 1999)).

2.2.5 Genotyping of animals

Genomic DNA was prepared from ear biopsies for analysis by polymerase chain reaction (PCR) using standard cycling parameters. Mouse ear clip samples were digested overnight at 55°C using proteinase K (10mg/ml; Sigma-Aldrich, Poole, UK) and mouse ear-lysis reagent (0.3mg/ml; Viagen Biotech, Los Angeles, USA). The samples were then vortexed to make sure the tissue had completely broken down and heated at 85°C for 45 minutes to denature the proteinase K. Samples were stored at 4°C. A master mix was prepared for the PCR reactions composed of Biomix™ Red (Bioline 25006, London, UK), forward and reverse primers (Table 1) and ddH_2O. For the floxed gene genotyping, MyTaq™ Red Mix (Bioline 25044, London, UK) was used because MyTaq DNA polymerase has increased affinity for

DNA and thus, improves sensitivity and yield. For details of the master mix components see Table 2. 3µL of the DNA sample was added to 22µL of the master mix. The PCR thermal cycler conditions (Bio-Rad S1000, UK) for each reaction are described in Table 3. PCR products were loaded into the wells of an electrophoresis gel made of 2% agarose gel in TAE buffer (2.0M Tris Acetate and 100mM Na_2EDTA; Fisher Scientific, Loughborough, UK) containing Midori Green nuclei acid stain (5µL/100mL gel; NIPPON Genetics EUROPE GmbH). The gel was run for 1 hour at 100mV and the bands were visualised under UV light using Alphalmager (Alpha-Innotech, Kasendorf, Germany). Floxed animals were identified by a band of 956bp whereas non-floxed animals have a band of 842bp. The appearance of both floxed and non-floxed bands indicate heterozygous (Het) animals. In terms of genotyping for the Cre transgenes, the Tie^2-Cre band corresponds to 512bp, αMHC-Cre to 990bp, and Col1α2-Cre-ERT to 700bp. Mice with $flox^{+/+}$ and *Cre* positive (i.e. $Nppc^{flox/flox}$ Cre^{+}) represent CNP KO mice in each respective cell type, whereas $flox^{-/-}$ Cre positive or $flox^{+/+}$ *Cre* negative mice (i.e. $Nppc^{+/+}$ Cre^{+} *or* $Nppc^{flox/flox}$ *)* were used as WT controls. Global NPR-C KO mice were identified by a band at 413bp, WT at 250bp. The analyses of genotype by PCR/gel electrophoresis are shown in Figure 10.

Generation of cell-specific deletion of CNP using Cre/LoxP technology

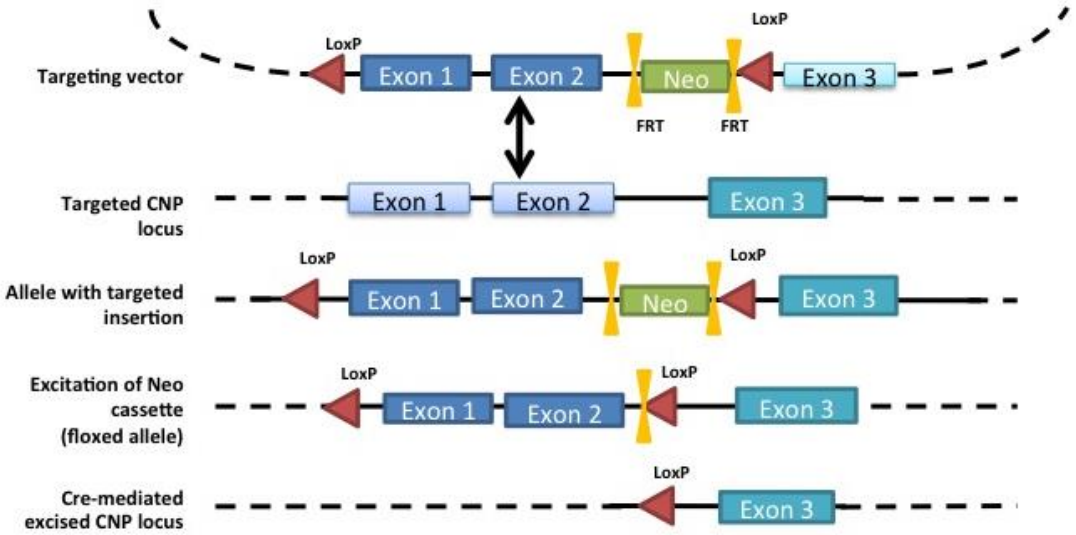

Figure 9. Generation of cell-specific deletion of CNP using Cre/LoxP technology.

LoxP sites were inserted into the CNP gene (exon 1 and 2). Firstly, chimeric mice were breed with LoxP-expressing mice. Flippase recognition target (FRT) sites were used to allow efficient removal of the neomycin cassette, resulting in the generation of *Nppc*$^{flox/flox}$ offspring. The resulting animal was then crossed with specific Cre recombinase-expressing mice in which expression is driven by cell-specific promoters.

Primer sequences used for genotyping

Target gene	Primer nucleic acid sequence
Floxed CNP	Forward: 5'-CCTTTATGCCAAGAGAACTTCCAGGAGG-3'
	Reverse: 5'-TCCTTCCTGACTTCCTTCTGCTCTCTATCC-3'
Tie^2 Cre	Forward: 5'-CCCTGTGCTCAGACAGAAATGAG-3'
	Reverse: 5'-CGCATAACCAGTGAAACAGCATTGC-3'
α-MHC Cre	Forward: 5'-CCAATTTACTGACCGTACACC-3'
	Reverse: 5'-GTTTCACTATCCAGGTTACGG-3'
Col1α-2 Cre	Forward: 5'-ATCCGAAAAGAAAACGTTGA-3'
	Reverse: 5'-ATCCAGGTTACGGATATAGT-3'
NPR-C	Forward: 5'-CTTGGATGTAGCGCACTATGTC-3'
	Reverse: 5'-CACAAGGACACGGAATACTC-3'
	NEO: 5'-ACGCGTCACCTTAATATGCG-3'

Table 1. The primer sequences used for genotyping cell-specific CNP KO and WT mice.

Components of the PCR reactions for genotyping

Target gene	Volume per reaction					
	Biomix Red (µL)	Forward Primer (µL)	Reverse Primer (µL)	NPR-C NEO (µL)	DNase free water (µL)	Sample DNA (µL)
Floxed CNP	12.5	0.08	0.08	-	9.34	3
Tie^2 Cre	12.5	2	2	-	5.5	3
α-MHC Cre	12.5	2.5	2.5	-	4.5	3
Col1α2-Cre	12.5	2.5	2.5	-	4.5	3
NPR-C	12.5	0.5	0.5	0.5	8	3

Table 2. Components of the PCR reactions for genotyping.

The total volume for each reaction was 25µL. The working stock concentrations for each primer were: floxed CNP, 100µM; Tie^2 Cre, 25µM; α-MHC Cre, 10µM; Col1α2α-Cre, 10µM; NPR-C, 2.5µM.

PCR thermal cycler conditions for genotyping target genes

Target gene	PCR step					
	Polymerase enzyme activation	Denaturation	Annealing	Polymerisation	Cycles	Extension
Floxed CNP	94°C 10mins	94°C 30s	60°C 1min	68°C 2mins	X 35	68°C 10mins
Tie^2 Cre	95°C 10mins	95°C 30s	58°C 1min	72°C 1min	X 40	72°C 10mins
α-MHC Cre	94°C 2mins	94°C 1mins	60°C 1min	72°C 1min	X 35	72°C 5min
Col Cre	93°C 1min	93°C 20s	68°C 3min	72°C 1min	X 30	72°C 5min
NPR-C	95°C 5mins	93°C 1mins	60°C 1min	72°C 1min	X 35	72°C 10mins

Table 3. The PCR thermal cycler conditions used for each genotyping target genes.

Analysis of DNA from genetically modified mice

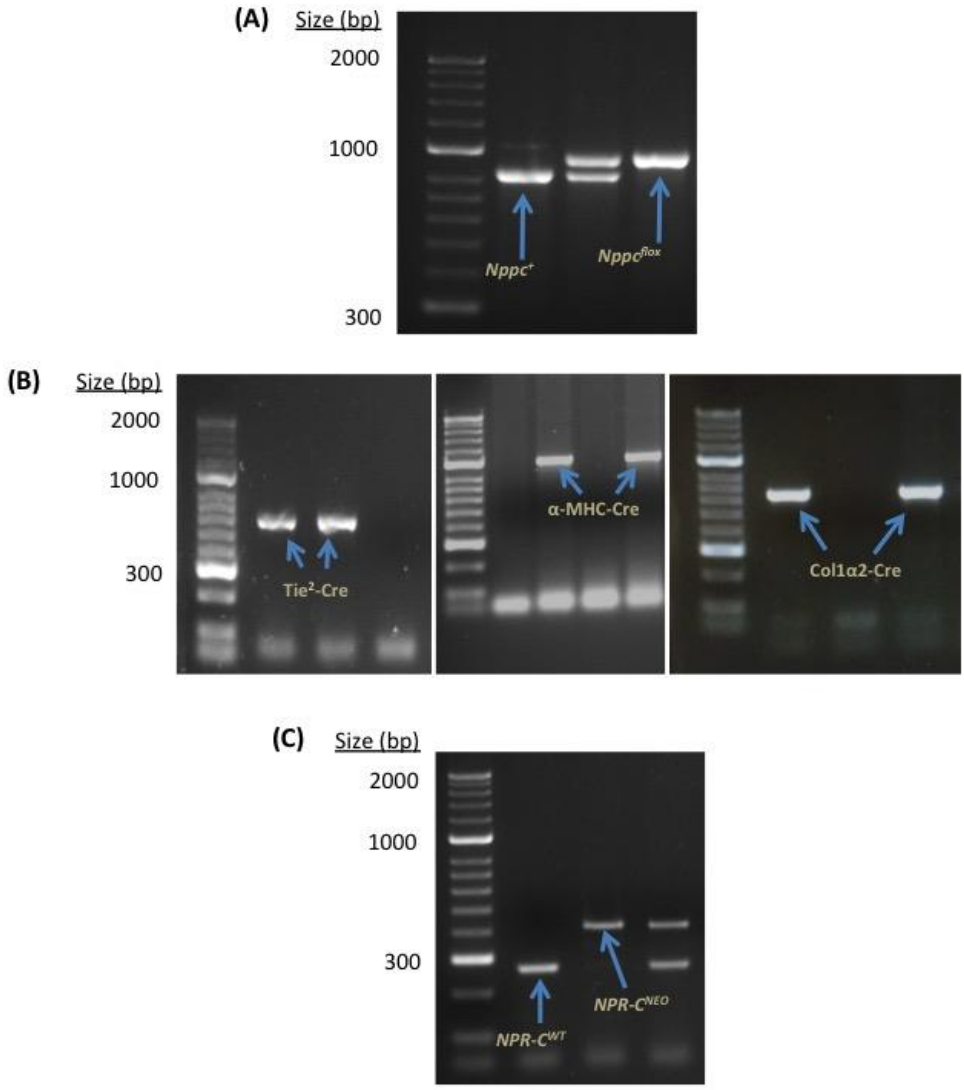

Figure 10. Analysis of DNA from the genetically modified mice.

(A) Floxed animals were identified by the band at position of 956bp and non-floxed animals has band position at 842bp. (B) Tie^2-Cre at position of 512, αMHC-Cre at position of 990bp, Col1α2-Cre at position 700bp. (C) NPR-C KO mice were identified by a band at position 413bp and WT at 250bp. Non-floxed mice or mice that do not have Cre expression are referred to as WT; the appearance of both floxed and non-floxed bands with Cre expression are referred to as heterozygous (Het) animals.

2.3 Langendorff isolated heart model

2.3.1 Overview of the Langendorff system

Even 100 years after its description, the Langendorff isolated heart system remains at the forefront of cardiovascular physiological and pharmacological studies. It represents a feasible and highly reproducible model for obtaining a broad spectrum of physiological data, including contractile function, coronary blood flow and cardiac metabolism, and pharmacological responses (Bell et al., 2011). With the emergence of genetically modified animals, the Langendorff perfused heart is a unique tool to study the impact of targeted deletion or upregulation of genes on the physiology of the heart and the coupled intracellular signalling. The Langendorff isolated heart model has also been widely used to investigate the pathophysiology of IR injury as it provides an easier, less technically demanding alternative to *in vivo* MI models. Hearts are retrogradely perfused via the aorta (i.e. opposite direction compared to the *in vivo* situation). Thus, the aortic valves are forced closed, and the perfusate is directed into the coronary system and the capillary beds of the myocardium. The perfusate leaves the heart via two venous drainages. The majority of the perfusate goes into the coronary sinus that lies within the posterior atrioventricular groove, which opens into the right atrium. The perfusate then passes through the tricuspid valve, into the right ventricle and leaves the heart via the pulmonary artery. In addition, a small proportion of the perfusate leaves the heart via the Thebesian veins, which directly drain into the chambers.

2.3.2 Materials

Krebs-Henseleit buffer solution was made fresh on a daily basis from its constituents: sodium chloride (NaCl; 118.5mM; Sigma-Aldrich, Poole, UK), potassium chloride (KCl; 4.7mM; BDH/VWR, Poole, UK), Magnesium sulphate ($MgSO_4$; 1.2mM; BDH/VWR, Poole, UK), potassium dihydrogen orthophosphate (KH_2PO_4, 1.2mM; BDH, Poole, UK), glucose (12mM; Sigma-Aldrich, Poole, UK), sodium bicarbonate ($NaHCO_3$; 25mM; Poole, UK), sodium pyruvate (2mM; Sigma-Aldrich, Poole, UK), and calcium chloride ($CaCl_2$; 1.7mM; VWR, Leicestershire, UK).

Vasoactive drugs used: N^G-nitro-L-arginine methylester (L-NAME; Sigma-Aldrich, Poole, UK), acetylcholine (ACh, Sigma-Aldrich, Poole, UK), bradykinin (BK, Sigma-Aldrich, Poole, UK), CNP (Gene-script, Piscataway, USA), sodium nitroprusside (SNP, Sigma-Aldrich, Poole, UK),

2.3.3 Langendorff isolated heart preparation

The isolated heart perfusion system used in this project was manufactured by Harvard Apparatus, UK. A schematic diagram of the system is shown in Figure 11. Firstly, mice were anti-coagulated with an intra-peritoneal injection of heparin (100µL, 5000unit/ml; LEO, Wrexham, UK) and then anaesthetised with isoflurane (3% in O_2; 100%w/w; Abbott Laboratories Ltd, Queenborough, UK). The adequacy of anaesthesia was confirmed with the absence of a pedal reflex. The hearts were quickly excised and immersed in ice-cold perfusion solution to prevent warm ischaemic injury. Subsequently, the hearts were mounted onto the perfusion system as fast as possible via the aorta for retrograde perfusion and fixed by ligature to the cannula (made using a 21-gauge needle with the sharp end snapped off and smoothed). In order to minimize air embolization (which damages the endothelial layer and affects pressure readings) during cannulation, the flow of perfusate via the aortic cannula was started prior to the mounting of the hearts. The Krebs-Henseleit buffer solution was gassed with 95% O_2/ 5% CO_2 (British Oxygen Company, BOC, Guildford, UK), pH 7.4 and the temperature maintained at 37°C by a water-jacketed chamber. A digital thermometer was used throughout the experiment to monitor the perfusate temperature. Constant flow mode was used in this project, which was set at 2mL/minute controlled by a peristaltic pump (MINIPULS3, Gilson) (Sutherland et al., 2003). The left atrium was removed and a fluid-filled balloon made of plastic film was inserted into the LV for recording of the left ventricular developed pressure (LVDP). The balloon was inflated in steps of 4µL until a total volume of 24µL for female or 28µL for male animals. These volumes have been demonstrated in previous studies to give a consistent LVDP reading without damaging the internal ventricular wall (Sutherland et al., 2003). HR was derived from the cycle of contraction per minute. Coronary perfusion pressure (CPP) and LVDP were monitored using a pressure transducer (HUGO TECH) connected to an amplifier (Power Lab 4/30, ADInstruments, UK), which was then recorded via LabChart 6.0 software.

2.3.4 Assessment of coronary vascular reactivity

Since constant flow mode was used, changes in the diameter (i.e. resistance) of the coronary vasculature were reflected by changes in CPP (Figure 12). After 10-15 minutes of stabilisation of the heart, perfusion was switched to Krebs-Henseleit buffer solution containing the NOS inhibitor, L-NAME (300µM). CPP increased with the addition of L-NAME, by approximately 50%, which gave a good indication of an intact endothelium (i.e. blockade of NO production). The hearts were further stabilised for 15 minutes before being

challenged with pharmacological agents. Any preparations that had a CPP higher than 100mmHg before exposure to L-NAME, and/or did not give a rise of 50% in CPP with L-NAME perfusion were deemed to be endothelium-denuded and excluded from the study.

2.3.4.1 Vasoactive drugs

The coronary reactivity was investigated, in the presence of L-NAME, by bolus addition of the endothelium-dependent vasodilators: BK (10nmol) and ACh (0.1, 0.3 and 1nmol), and endothelium-independent vasodilators: CNP (10nmol) and SNP (1nmol). A dose-response curve to BK cannot be constructed due to rapid desensitisation of the receptor (Gobeil et al., 2002). 10µL of each drug was administered by bolus injection with a Hamilton syringe (1702, Ghiroda, Romania). Each injection was at least 5 minutes apart in order for the cardiac function to return to baseline before adding the next dose or drug. 10ml of coronary effluent was collected from the apex of the hearts during the response to 1nmol ACh. This was immediately snap-frozen in liquid nitrogen and stored at -80°C for CNP bioassay. The coronary reactivity in response to each vasoactive drugs were quantified by the following equation:

$$\Delta CPP, \% = \frac{CPP\ at\ maximum\ relaxation - CPP\ at\ baseline}{CPP\ at\ baseline} \times 100$$

2.3.4.2 Vasodilatation associated with reperfusion

The release of CNP from endothelial cells in response to shear stress is well established in *in vitro* studies (Chun et al., 1997). The initial resumption of flow after a brief period of ischaemia can be used to mimic shear stress–induced release of endothelium-derived mediators, including CNP (Zatta and Headrick, 2005). The hearts were subjected to three occlusion periods (cessation of flow for 20, 40 and 80 seconds), in the presence of L-NAME. Similar to the drug addition protocol, occlusion periods were at least 5 minutes apart, allowing the CPP to return to baseline. The magnitude of vasodilatation associated with reperfusion was quantified by calculating area under the curve using the trapezium rule between the period of perfusion resumption and the point at which CPP returned to baseline (Figure 12).

Langendorff perfused heart model

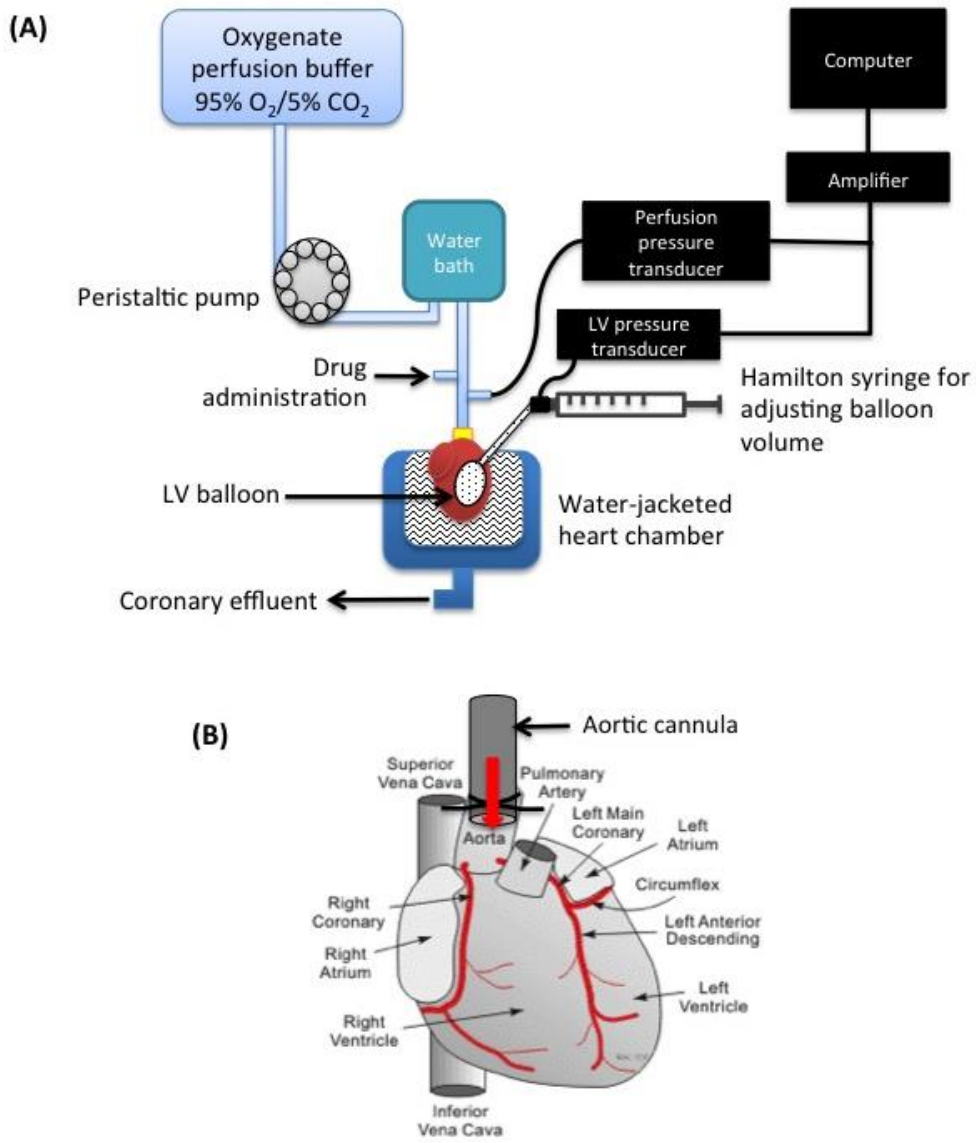

Figure 11. Simplified scheme of a Langendorff perfused heart model in constant flow.

(A) Schematic diagram of the Langendorff system. The heart is cannulated via the aorta and retrogradely perfused, and suspended within a warmed chamber. The flow rate is controlled by a peristaltic pump. The pipe work goes into the water-jacketed chamber to maintain the perfusate temperature at 37°C. One side arm of the perfusion cannula is used for drug administration and the other one is connected to a transducer for measuring coronary perfusion pressure (CPP). A left ventricle (LV) balloon is inserted to measure LV developed pressure (LVDP). Transducers are connected to an amplifier, which then transmits the data to a computer. (B) Diagram showing aortic cannulation (adapted from http://www.cvphysiology.com/Blood%20Flow/BF001). The perfusate (red arrow) enters the aorta via the cannula and closes the aortic valves, which forces the perfusate into the coronary system.

Assessment of coronary vascular reactivity and cardiac contractility

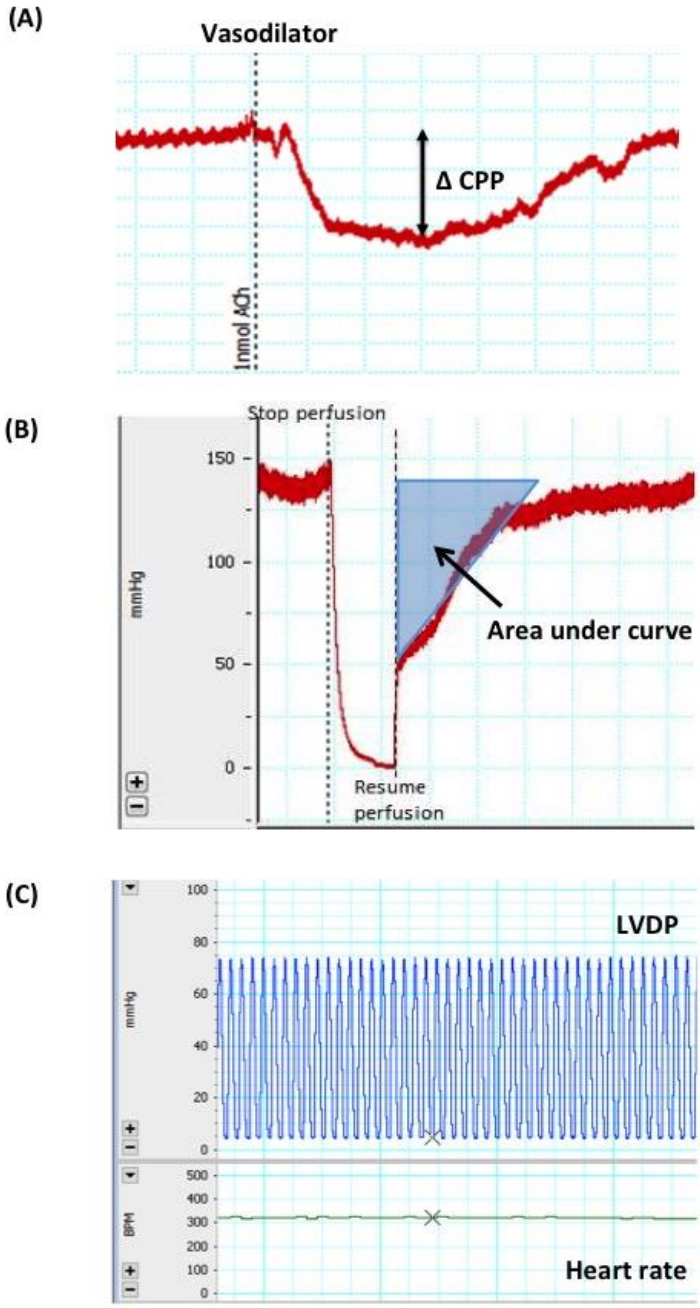

Figure 12. Assessment of coronary vascular reactivity and cardiac contractility.

(A) Example of a trace depicting a vasorelaxation in response to a vasodilator. Constant flow mode was used and thus, changes in the resistance of the coronary vasculature were reflected by changes in coronary perfusion pressure (CPP). (B) Example of a trace depicting vasodilatation associated with reperfusion. Perfusion was stopped and resumed after a transient period of ischaemia. Total area under the curve between the resumption of perfusion and returning of CPP to baseline (blue triangle) was calculated according to the trapezium rule. (C) Example of a trace for left ventricular developed pressure (LVDP) and heart rate assessment via a balloon inserted into the left ventricle.

2.3.5 Ischaemia reperfusion injury

The excised hearts were placed in Krebs solution at room temperature (instead of ice-cold solution) to avoid pre-conditioning of the hearts and then cannulated in an identical fashion to that described above. After 10-15 minutes of stabilisation of the heart, perfusion was stopped for 35 minutes to induce global ischaemia and then re-perfused for 60 minutes to create IR injury. During the ischaemic period, the hearts were maintained at 37°C by immersion in warm perfusion solution. After 60 minutes reperfusion, the hearts were removed from the system and placed at -20°C for 10 minutes to harden the tissue for slicing. This was cut into 1mm thick sections perpendicular to the long-axis of the heart using fixed razor blades. The heart sections were then incubated with 1% triphenyl tetrazolium chloride (TTC; Sigma-Aldrich, Poole, UK) in an enclosed shaker at 37°C for 15 minutes. TTC is a white compound that reduces to red TPF (1,3,5-triphenylformazan) in living tissues due to the activity of dehydrogenses; in areas of necrosis, dehydrogenases are either denatured or degraded so TTC is unable to be reduced in infarcted areas and remains white. The heart sections were then arranged on a plastic film and scanned (600dpi; CanoScan LiDE 700F, Canon, UK) on both sides. The infarcted regions were quantified using Image J and expressed as a percentage of infarcted area over total ventricular area.

2.3.6 CNP bioassay

The effluent collected from the Langendorff experiment was defrosted to room temperature. Peptides were extracted using C18 SEP-Columns according to the manufacturer's instructions (Phoenix Pharmaceuticals, Karlsruhe, Germany). The eluents were concentrated to dryness by a centrifugal concentrator overnight (Speedvac, Thermo Scientific, USA). Samples were then reconstituted in 125µL assay buffer and CNP-22 enzyme-linked immunosorbent assay (ELISA) performed according to the manufacturer's instructions (Phoenix Pharmaceuticals, USA, FEK-012-03). The kit has a sensitivity limit of 6.6pg/ml.

2.4 In vivo heart failure models

2.4.1 Materials

Isoprenaline hydrochloride (ISO, Sigma-Aldrich, Poole, UK), saline (NaCl, 0.9%w/v; Baxter healthcare, Norfolk, UK), ascorbic acid (Sigma-Aldrich, Poole, UK), Vetergesic (Centeur, Somerset, UK), isoflurane (100%w/w; Abbott Laboratories Ltd, Queenborough, UK),

Lidocaine hydrochloride (2.0%, w/v; LIGNOL ® Dechra, Skipton, UK), tissue adhesive (3M Vetbound, St.Paul, USA).

2.4.2 Recovery surgery

All the recovery surgeries were performed under a standard sterile environment, including the use of sterilised drapes, surgical groves and gown, heat-sterilised surgical tools, and the mouse was covered with sterile film only exposing the incision area. Mice were anaesthetised with isoflurane (2% in O_2) and laid on a heating plate (Physitemp, Norfolk, UK) to maintain temperature at 37°C via a TCAT-2LV controller (Physitemp, Norfolk, UK). Mice received 100µL of vetergesic (30mM; Centeur, Somerset, UK) subcutaneously at the beginning of the surgery. The hairs around incision area were removed by hair-removal cream (Veet; Hull, UK). 6.0 absorbable and non-absorbable sutures were used for internal and external stiches, respectively. Small amount of tissue adhesive was applied on the stiches to avoid wound opening and local anaesthetic (lidocaine) was smeared around the wound using cotton buds. 500µL of saline was injected subcutaneously before the mouse was left to recover on a heating mat. The health of the mice was monitored closely for 3 consecutive days after surgery.

2.4.3 Isoprenaline-induced heart failure

2.4.3.1 Overview of the experimental protocol

ISO was administrated subcutaneously via osmotic mini-pumps (model 1002, Alzet, DURECT corporation, Cupertino, CA). To establish a suitable dose and duration of the model, pilot studies of 20mg/kg/day and 30mg/kg/day of ISO infusion for 7 or 14 days were conducted in WT mice.

The pilot studies revealed that 20mg/kg/day for 7 days is a subpressor dose that causes mild/no change in cardiac function in WT but detects increased pathology in cmCNP KO mice. Echocardiography was performed under isoflurane anaesthesia (2% in O_2) at baseline prior to the induction of ISO and on the 7^{th} day of ISO treatment. The body weight of each mouse was determined before euthanisation. Blood samples were taken from the abdominal aorta and centrifuged for plasma collection (2 minutes at 13,000rpm). It was then frozen immediately in liquid nitrogen and stored at -80°C. Weight of the whole hearts and the LVs were recorded and preserved for histological staining.

2.4.3.2 Osmotic mini-pump preparation

ISO was dissolved in saline with 0.5% ascorbic acid to prevent oxidation. The mini-pumps were filled with 100µL of the ISO solution in a sterile environment and submerged in saline for 48 hours at 37°C for equilibration prior to implantation.

2.4.3.3 Surgical procedure of mini-pump implantation

Standard recovery surgery procedures were employed as described above. The hairs around the back of the neck were removed and a small opening made in the skin. With the use of a haemostat, the skin layer and the muscle layer were separated carefully down towards the side of the body, creating a 'pocket' for the mini-pump to be inserted. Small amount of saline were injected into the 'pocket' to facilitate the mini-pump placement. After placing the mini-pump into the body, the incision was closed with 6.0 non-absorbable sutures. Post-operative care was carried out as described above.

2.4.4 Radio-telemetric recording of haemodynamics and heart rate in response to isoprenaline

In order to examine the effect of ISO, a subset of animals were implanted with radio-telemetric transmitter (TA11PA-C10; Data Science International). MABP, HR and locomotor activity were recorded in conscious, freely moving mice before and after receiving ISO infusion. The probe was sterilised in gluteraldehyde (2%) overnight and rinsed in sterile saline prior to implantation. The surgery was done under standard recovery surgery procedure as described above. The mice were laid in a supine position and hairs around the neck were removed. A small incision was made, exposing the salivary glands. The glands were separated gently using fine forceps until the left carotid artery is visible. The artery then isolated from the surrounding tissues and clamped at the top and the bottom of the vessel to stop blood flow. A small cut on the vascular wall was made and the BP catheter inserted ensuring no air bubble formed. The tip of the catheter was placed into the aortic arch and secured in place with a suture. Subsequently, a subcutaneous pouch was made at the right flank for the transmitter body implantation. The animals were allowed 10 days of recovery before taken recordings. Data was recorded for 24 hours under 12 hour light/12 hour dark cycle. Samplings were acquired for 2 minutes every 15 minutes, and the average values for MABP, HR and locomotor activity were calculated for every time point (Dataquest Art Acquisition System).

2.4.5 Pressure overload-induced heart failure by abdominal aortic constriction

2.4.5.1 Overview of the experimental protocol

AAC was performed on male cmCNP KO, fbCNP KO, NPR-C KO and WT mice weighing 23-24g. Mice were randomly assigned to undergo either a sham surgical procedure or AAC. Cardiac function was measured by echocardiography and assessed at baseline prior to the aorta banding, and at 3 and 6 weeks after the surgical procedure (Figure 13). At termination, carotid MABP was measured under isoflurane anaesthesia (1.5% in O_2). Blood samples were taken by cardiac puncture and centrifuged for plasma collection (2 minutes at 13,000rpm), which was snap frozen in liquid nitrogen and stored at -80°C. The body weight, whole heart and LV weight were recorded. The LV were either snap frozen and stored at -80°C for further biochemical analyses or preserved (4% formaldehyde solution overnight then stored in 70% ethanol) for histology staining.

2.4.5.2 Surgical procedure of abdominal aortic constriction

Standard recovery surgery procedures were followed as described above. The coat between the sternum and the bladder was removed using hair removal cream. A small cut was made in the lower abdomen. The skin and the muscle layer towards the sternum were then separated using a haemostat. A midline incision was made and exposing the upper abdomen by pulling the skin to the sides. The stomach together with the spleen was then pulled out and clamped aside carefully. The organs were covered with a piece of moist gauze to avoid drying-out. The liver and the right kidney were pushed away slightly using a small ball of wet gauze to expose the abdominal aorta. After clearing of fat and connective tissue around the abdominal aorta, the vessel was ligated above the renal artery branches using 4.0 suture with an overlying blunted 25-gauge needle (Figure 13). The needle was then removed with care, leaving a discrete region of stenosis with the diameter approximately equal to the needle width (0.51mm), ~30% constriction of the aorta. Organs were placed back into the abdomen cavity gently and the wound was closed as described above. In mice subjected to sham surgery, the aorta was exposed and a 4.0 suture was pulled through without performing the ligation.

2.4.5.3 Acute mean arterial blood pressure measurement

After 6 weeks of AAC, the mice were subjected to carotid acute MABP measurement before being euthanised. The mice were anaesthetised (2% isoflurane in O_2) and placed supine on a thermostatically regulated heating mat at 37°C. A small incision was made at

the position of the salivary glands and the left common carotid artery was isolated. The top and bottom of the carotid artery were clamped and a very small cut on the artery wall performed. A cannula (0.28mm internal diameter; Critchley Electrical Products Pty Ltd, Castle Hill, Australia) filled with heparinised saline (100U/ml in 0.9% saline) was inserted into the artery carefully without inducing any air bubbles and secured in position with a 6-0 suture. The clamp at the bottom of the carotid artery was removed that allowed the detection of MABP using a calibrated in-line P23 XL transducer (Viggo-Spectramed, California, USA) and PowerLab system (ADInstruments, Oxford, UK) which was recorded on a computer running LabChart 6.0. The level of anaesthesia was reduced to 1.5% until the respiration rate reached 110±5 breath per minute before the MABP and HR measurements were taken (to minimise and standardise the effect of anaesthesia on MABP).

2.5 Echocardiography

A Vevo 770 ECHO system was employed in the studies of cmCNP KO and NPR-C KO mice; and a Vevo 3100 system was used in fbCNP KO studies. Mice were anaesthetised with isofluorane (3% in O_2) before transferred onto the ECHO stage and the isoflurane reduced to 2% (in O_2). Conduction gels were applied onto the four paws and attached to the ECG pads. The chest hair was removed with hair removal cream and cleaned thoroughly. A small amount of ECHO gel (Aquasonic, Parker; the Netherland) was applied on the chest and the ECHO probe was placed above the heart. The position of the probe and the angle of the stage were adjusted so that the entire long-axis of the LV was seen in a horizontal position on the computer screen. The mice were equilibrated on the stage for 10 minutes or until the HR reached 500±10bpm and the body temperature at 37°C. Three recordings of the B mode (longitudinal axis) and M-mode (cross-sectional axis immediately below the mitral valves) were made in each mouse. Analyses of the heart function were conducted on the M-mode with measurements of LV anterior wall (LVAW) and LV posterior wall (LVPW) thickness, and LV internal diameter (LVID) at diastole (d) and systole (s) (Figure 14). The EF and FS were calculated by the following equations:

$$EF\ (\%) = \frac{LV\ Vol;d - LV\ Vol;s}{LV\ Vol;d} \times 100$$

$$FS(\%) = \frac{LVID;d - LVID;s}{LVID;d} \times 100$$

$$Where:\ \ LV\ Vol;d = LVID;d^3 \times \frac{7.0}{2.4+LVID;d}\ ;\ \ LV\ Vol;s = LVID;s^3 \times \frac{7.0}{2.4+LVID;s}$$

Abdominal aortic constriction-induced heart failure

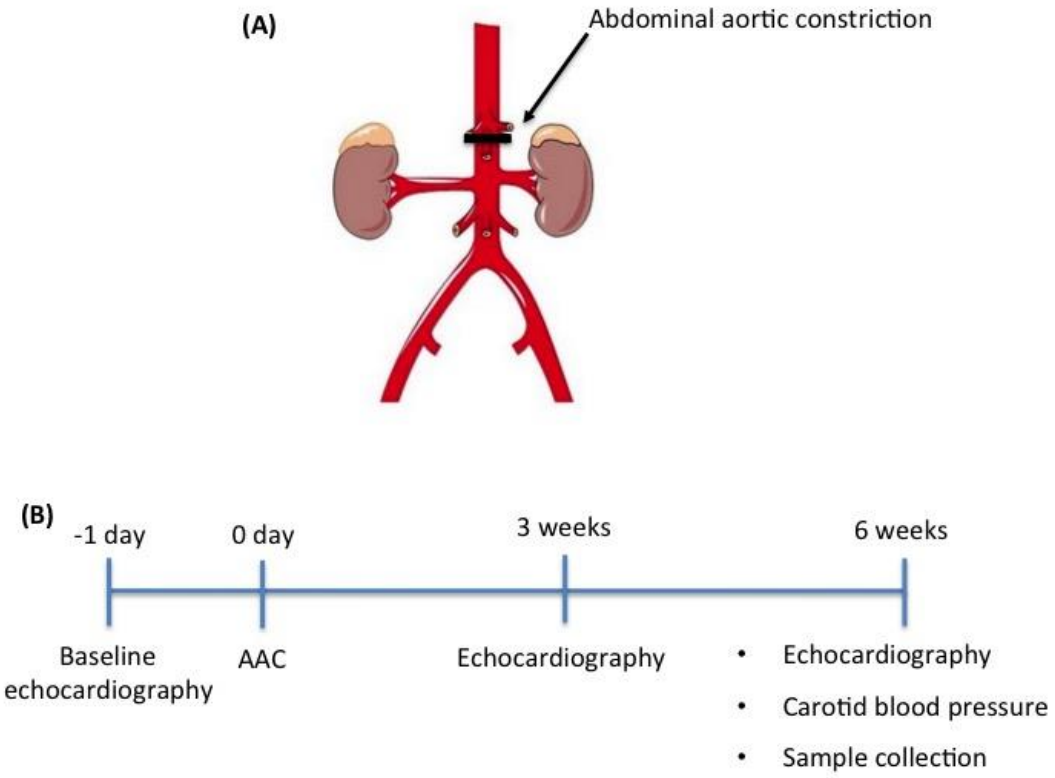

Figure 13. Abdominal aortic constriction-induced heart failure.

(A) An anatomical diagram showing the position of abdominal aortic constriction (AAC), above the renal arteries. (B) A timeline illustrating the AAC-induced heart failure protocol.

Echocardiography images using B-mode and M-mode

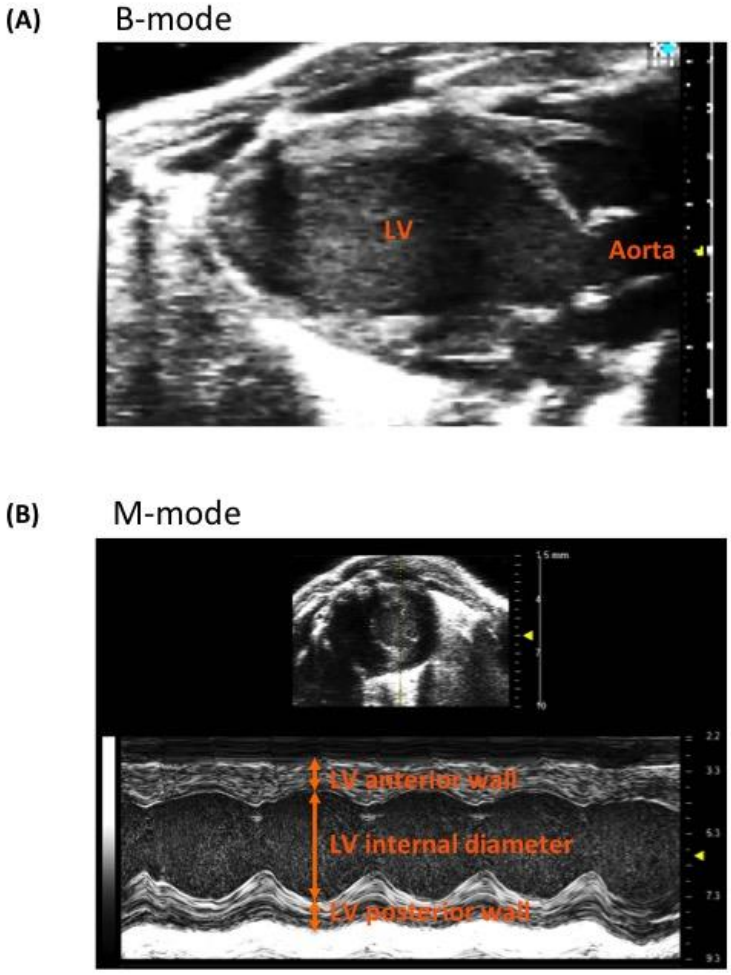

Figure 14. Example of echocardiography images using B-mode and M-mode.

(A) The long-axis of the left ventricle (LV) on B-mode. (B) The cross-sectional axis of the LV on M-mode. ECHO measurements on the M-mode trace are indicated, including the diameter of the LV anterior and posterior wall, and LV internal diameter.

2.6 Histology

2.6.1 Left ventricle fixation

The isolated LVs were cut transversely below the mitral valves, where the M-mode ECHO images were taken. They were then immersed in 4% formaldehyde (10% formalin, VWR, Leicestershire, UK) overnight and subsequently transferred to 70% ethanol (Fisher Scientific Ltd, Leicestershire, UK) and stored at 4°C until paraffin wax embedding and sectioning were performed.

2.6.2 Martius scarlet blue staining

Martius scarlet blue (MSB) staining was performed by the pathology department at the Royal London Hospital. This stains for fibrin (red), erythrocytes (yellow) and connective tissue (blue). Axioplot microscope (Zeiss, UK) was used to view and capture images at a magnification of X50 of the stained sections.

2.6.3 Picro-sirus red staining

Picro-sirus red (Polysciences, Germany) stains the cytoplasm of cells yellow and collagen (as an index of fibrosis) red. The tissue slides were firstly dewaxed and rehydrated by processing the slides through the following steps: 1) histoclear for 5 minutes; 2) 1:1 of histoclear and 100% ethanol for 5 minutes; 3) 100% ethanol for 3 minutes; 4) 95% ethanol for 3 minutes; 5) 70% ethanol for 3 minutes; 6) 50% ethanol for 3 minutes; 7) distilled water for 3 minutes. The tissue slides were then placed in solution A (phosphomolybdic acid) for 2 minutes, and then rinsed with distilled water, followed by Solution B (Pico-sirius red) for 60 minutes and solution C (0.1M HCl) for 1 minute. The slides were then dehydrated with 100% ethanol for 10 minutes followed by histoclear for another 10 minutes. The slides were mounted with DPX (Merck, a mixture of distyrene, a plasticizer, dissolved in toluene-xylene) and left to dry on a tray overnight. 8 images (2 images at each of the position of top, bottom, left and right of the LV slide) were taken using a light microscope (Nikon Eclipse TS100, Amsterdam, Netherland). The collagen deposition (as the percentage of total area) was quantified using Image J.

2.6.4 Wheat germ agglutinin fluorescence staining

In order to measure the ventricular myocyte size, tissue slides were stained with wheat germ agglutinin (WGA) alexafluor 647 (Invitrogen^{TM} Thermo Scientific, Paisley, UK). This lectin selectively binds to N-acetylglucosamine and N-acetylneuraminic acid (sialic acid)

residues in glycoproteins and hence, stains the cell membrane. The tissue slides were firstly dewaxed and rehydrated as described earlier (section 2.8.3). Antigen unmasking solution (Vector Laboratories Inc. (H3300), Peterborough, UK) was pre-boiled for 6 minutes in a microwave. The rehydrated tissue slides were then added into the solution and heated for a further 11 minutes. The tissue slides were then cooled in running water and washed with phosphate-buffered saline (PBS; pH7.4) three times, 5 minutes each. The slides were then dried and a square was drawn around the tissue using a water repellent pen. 200µL of WGA (1:500 dilution) was applied onto each tissue section and incubated in darkness at room temperature for 1 hour. The tissue slides were then washed three times with PBS, 5 minutes each, and mounted with ProLong™ Gold Antifade Mountant with DAPI (Thermo-Fisher Scientific, Leicestershire, UK). Images were taken on a Zeiss 710 confocal microscope (magnification X20) and the cardiomyocyte size was analysed with Image J.

2.7 Primary cell isolation and culture

2.7.1 Materials

Pierce™ primary cardiomyocyte isolation kit (Thermo Fisher Scientific, Leicestershire, UK), Dulbecco's Modified Eagle's Medium (DMEM) (Thermo-Fisher Scientific, Leicestershire, UK), heat inactivated bovine serum (BS; Life Technologies Ltd, Paisley, UK), and penicillin streptomycin (Pen/Strep; Sigma-Aldrich, Poole, UK).

2.7.2 Neonatal cardiomyocyte isolation and culture

Neonatal hearts were dissected from 2-3 day old mice and placed in 500µL of ice-cold Hank's balance salt solution (HBSS; Thermo-Fisher Scientific, Leicestershire, UK). The hearts were then minced into 1-3mm^3 pieces in a petri dish and transferred to 1.5mL tubes using a 1mL pipette. The tissues were washed twice with 500µL ice-cold HBSS to remove blood. 200µL of Cardiomyocyte Isolation Enzyme 1 (with papain) and 10µL of Cardiomyocyte Isolation Enzyme 2 (with thermolysin) were then added to each tube, mixed gently and incubated in 37°C for 30-35 minutes. The enzyme solutions were then removed gently and the tissues washed twice with 500µL ice cold HBSS. Subsequently, 0.5mL of complete DMEM (containing 10% BS and 1% Pen/Strep) were added and cells dissociated into a single cell suspension by pipetting up and down 25-30 times using a sterile 1mL pipette tip. 1mL of complete DMEM was then added to each tube to bring the total volume to 1.5mL. The cell suspension in each tube was seeded into two separate wells of a gelatine (0.1%) pre-coated 12-well plate (Corning Incorporated, UK) i.e. 0.75mL into each well, and topped

up with 0.25mL of complete DMEM to bring the total volume to 1mL. The plates were then incubated at 37°C in a 5% CO_2 incubator for 24 hours. After the incubation, the medium was replaced with fresh complete DMEM containing Cardiomyocyte Growth Supplement (1µL per ml of media). The cardiomyocytes were then further cultured for 3 days to become confluent. Beating cells that had striations with an irregular shape were identified as neonatal cardiomyocytes (Figure 15).

2.7.3 Hypertrophic analysis

The confluent cardiomyocytes were cultured in media with 0% BS and 1% Pen/Strep for 24 hours before treated with Ang II (1µM) ± CNP (1µM). Light microscopy images (x40; Nikon Eclipse TS100, Amsterdam, Netherland) of the beating neonatal cardiomyocytes were taken at 0 hour (baseline), 24 hours and 48 hours of Ang II treatment. The cardiomyocyte size was determined by measuring cell surface area using Image J. At least 40 cardiomyocytes from each well were measured to minimise bias.

2.7.4 Cardiac fibroblast isolation and culture

Hearts isolated from adult fbCNP KO and WT mice were washed in sterile ice-cold PBS to remove any blood. The hearts were placed on a sterile surface and cut into 1mm pieces, and transferred into a T75 flask using a sterile cell scraper. Tissues were spread around the flask and incubated for 25 minutes at room temperature. 20mL of media containing DMEM, 15% BS and 1% Pen/Strep were added into the flask without disturbing the tissues. The tissue flask were then incubated in a 37°C/5% CO_2 incubator for 7 days to allow cardiac fibroblasts to grow. The cells were then trypsinised by the following steps. First, old media was removed and washed twice with pre-warmed sterile PBS. 3mL trypsin was added into the flask and incubated at 37°C for 5 minutes for the cells to detach. 3mL of BS was then added to stop the trypsin activity. The cell suspension was transferred into a 15mL tube and centrifuged at 1000rpm for 5 minutes. The supernatant was removed and the cell pellet was transferred into a new T75 flask and incubated in 20mL complete DMEM for 10 days (media changed every 2-3 days) until the cardiac fibroblasts reached confluency. To collect the cells, the media was removed and replaced with 3mL of RLT buffer from the RNeasy mini kit (QIAGEN, Hilden, Germany) with 30µL of β-mercaptoethanol (Sigma-Aldrich, Poole, UK). Cells were then scrapped from the flask using a sterile cell scraper. The cell suspension were divided into two 1.5mL tubes, snap-frozen with liquid nitrogen and stored at -80°C.

Identification of neonatal cardiomyocytes

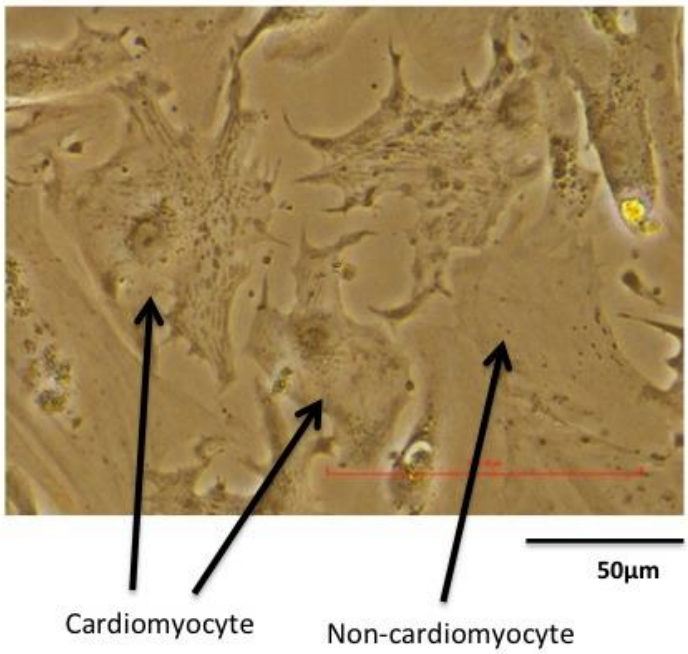

Figure 15. Identification of neonatal cardiomyocytes.

Neonatal cardiomyocytes beat spontaneously and are identified by their striation and irregular shape. The cardiomyocyte size was determined by the area of the cell using Image J.

2.8 Molecular biology

2.8.1 Materials

Ribonucleic acid (RNA) extraction from cells was undertaken using a QIAshredder (cat. 79656) and RNeasy mini kit (cat. 74106). For RNA isolation from tissues, RNeasy Fibrous Tissue Mini Kit (cat. 74704) was used. RNase-Free DNase Set (cat. 79254) was used to eliminate genomic DNA contamination in the samples. Generation of cDNA was achieved using a QuantiTect® Reverse Transcriptase kit (cat. 205313), and a QuantiTect® SYBR® Green PCR kit (cat. 204143) was used for qPCR reaction. All sourced from Qiagen (Hilden, Germany).

2.8.2 RNA extraction

2.8.2.1 RNA extraction from cardiac fibroblasts and cardiomyocytes

Total RNA extraction was performed according to the manufacturer's instructions using a RNeasy mini kit (cat. 74106; Qiagen; Hilden, Germany). Briefly, cells were thawed on ice and pipetted directly into a QIAshredder spin column placed in a 2mL collection tube, and centrifuged for 2 minutes at 14000rpm. One equal volume of 70% ethanol was added to the homogenised lysate and mixed well by pipetting. The samples then transferred to an RNAeasy spin column placed in a 2mL collection tube and centrifuged for 15 seconds at 14000rpm. In order to eliminate genomic DNA contamination, on-column DNAse digestion was performed using a RNase-free DNase Set (Qiagen, Hilden, Germany): 350µL of buffer RW1 solution was added into the RNeasy spin column and centrifuged for 15 seconds at 14000rpm. 10µL DNase I solution plus 70µL of buffer RDD were added directly to the RNeasy spin column membrane and incubated for 15 minutes at room temperature. The columns were then washed with 350µL of buffer RW1 and centrifuged for 15 seconds at 14000rpm. After further washes with 500µL of buffer RPE twice, the RNeasy spin columns then placed onto new collection tubes, and centrifuged for 1 minute at 14000rpm to eliminate any possible carryover of RPE. The columns were then placed in 1.5mL tubes for RNA collection. 30µL of RNase-free water were used to elute the RNA on the spin column membrane (centrifuged for 1 minute at 14000rpm). The eluents were re-applied onto the spin columns and centrifuged to obtain a higher concentration of RNA.

2.8.2.2 RNA extraction from tissue

RNA extraction from tissues was achieved with a RNeasy Fibrous Tissue Mini Kit (Qiagen, Hilden Germany) and performed according to the manufacturer's instruction. Organs were powdered using a pestle and mortar in liquid nitrogen. 25-30mg of tissue sample was dissociated in 300µL RLT buffer with 3µL β-mercaptoethanol (Sigma-Aldrich, Poole, UK) by agitation using a 1mL pipette. The cell suspension were then homogenised with a QIAshredder. 590µL of H_2O and 10µL of proteinase K were added to the homogenised cells and incubated at 55°C for 10 minutes followed by 3 minutes centrifugation at 14000rpm. The supernatant were transferred to 1.5mL tubes and 450uL of 100% ethanol was added and mix by pipetting. The mixture was then transferred to RNAeasy spin columns and spun at 14000rpm for 15 seconds for total RNA binding on the column membrane. The on-column genomic DNA elimination and RNA eluting steps were then performed as described above.

2.8.3 Measurement of RNA concentration and quality

The concentration and quality of RNA was determined using a Nano-drop®ND-1000 Spectrophotometer (Thermo-Fisher, Leicestershire, UK). Sample concentration in ng/uL was calculated based on absorbance at 260 nm. The ratio of sample absorbance at 260 and 280 nm (260/280) is used to assess the purity of RNA. A ratio of ~2.0 is generally accepted as "pure" for RNA. If the ratio is <1.8, it may indicate the presence of protein, phenol or other contaminants that absorb strongly at or near 280 nm, and the RNA sample was excluded. The ratio of sample absorbance at 260 and 230nm (260/230) is a secondary measure of nucleic acid purity. The 260/230 values for 'pure' nucleic acid are often higher than the respective 260/280 values and they are typically in the range of 1.8-2.2. If the ratio is appreciably lower, it may indicate the presence of ethanol or guanidine contamination (NanoDrop 1000 Spectrophotometer V3.8 User's Manual).

2.8.4 Complementary (c)DNA generation

Since the yield of total RNA extracted from neonatal cardiomyocytes was relatively low (approximately 40ng/µL), 250ng of RNA were used to generate cDNA. Whereas, the yields from cardiac fibroblast (approximately 200ng/µL) and tissues (>400ng/µL) were relatively high and thus, 1000ng of RNA were used to generate cDNA. First, genomic DNA elimination step was carried out by adding 2µL of gDNA wipeout buffer (Qiagen; Hilden, Germany) to 12µL of RNA samples and followed by an incubation of 2 minutes at 42°C. A reverse transcription (RT) master mix prepared according to Table 4 was then added to the

samples. A thermal cycler (Bio-Rad S1000^{TM}, UK) was used for the reverse transcription reaction (15 minutes at 42°C followed by 3 minutes at 95°C to inactivate Quantiscript Reverse Transcriptase). The cDNA products were stored at -20°C until proceeding to real-time quantitative (q)PCR.

2.8.5 Real-time quantitative PCR

2.8.5.1 cDNA dilution

Prior to the qPCR reaction, cDNA was diluted 1:40 with RNase-free water, except for the detection of the *Nppc* gene, in which cDNA was diluted 1:2 due to low mRNA expression.

2.8.5.2 qPCR reactions

The components for the qPCR master mix per reaction were prepared according to Table 5, and samples were prepared in triplicate. The qPCR reactions were facilitated by the 7900HT machine and the qPCR cycle conditions for 10µL sample are shown in Table 6. Using the SDS 2.4 software, the efficiency of the qPCR reaction was assessed by examining the melt curves for each reaction to exclude primer-dimer formation and to ensure that only one product was amplified. The threshold (manual Ct) for each detector was adjusted by placing the threshold line at the geometric phase along the amplification plot. The baseline for each detector was set manually to end before the amplification curve starts to rise. Details of the primers used are shown in Table 7. β-actin and RPL-19 were used as reference genes and relative gene expression were calculated using the $2^{-\Delta\Delta Ct}$ method (Livak and Schmittgen, 2001).

Master mix components for reverse transcription

Component	Volume per reaction (µL)
Reverse transcriptase	1
Reverse transcriptase buffer	4
Reverse transcriptase primer mix	1

Table 4. Master mix components for reverse transcription per reaction.

Master mix components for qPCR reaction

Component	Volume per reaction (µL)
SYBR green	5
Forward primer (10µM)	0.3
Reverse primer (10µM)	0.3
RNase-free water	2.4
Sample cDNA	2

Table 5. Master mix components for qPCR reaction per sample.

Real-time qPCR cycle conditions

qPCR cycle conditions			
	Temperature (°C)	Time (minute:second)	
Polymerase enzyme activation	95	15:00	
Denaturation	95	0:15	X45 cycles
Annealing	57	0:30	
Polymerisation	72	0:30	
Dissociation stage	95	0:15	
	60	0:15	

Table 6. qPCR cycle conditions.

Cardiac remodelling target genes and their primer sequence

Target gene	Primer nucleic acid sequence
CNP	Forward: 5'-AAAAGGGTGACAAGACTCCAGGCAG-3'
	Reverse: 5'-GGTGTTGTGTATTGCCAGTA-3'
ANP	Forward: 5'-GGATTTCAAGAACCTGCTAGACC-3'
	Reverse: 5'-GCAGAGCCCTCAGTTTGCT-3'
α-MHC	Forward: 5'-GCTGGAAGAAAAGCTCAAGAAGAAA-3'
	Reverse: 5'-TCTCTATCTGCACGGATGTGG-3'
β-MHC	Forward: 5'-CACCTACCAGACAGAGGAAGA-3'
	Reverse: 5'-GGAGCTGGGTAGCACAAGA-3'
SERCA2a	Forward: 5'-TGGAACCTTTGCCGCTCATTT-3'
	Reverse: 5'-CAGAGGCTGGTAGATGTGTT-3'
TGFβ1	Forward: 5'-TCAGACATTCGGGAAGCAGT-3'
	Reverse: 5'-GCCCTGTATTCCGTCTCCTTG-3'
MMP-2	Forward: 5'-GACAAGTTCTGGAGATACAATGAAGTG-3'
	Reverse: 5'-CAGGTTATCAGGGATGGCATTC-3'
Collagen type 1 α1	Forward: 5'-TCTGACTGGAAGAGCGGAGAG-3'
	Reverse: 5'-AGACGGCTGAGTAGGGAACA-3'
β-actin	Forward: 5'-GGCTGTATTCCCCTCCATCG-3'
	Reverse: 5'-CCAGTTGGTAACAATGCCATG-3'
RPL-19	Forward: 5'-GCTTGCCTCTAGTGTCCTCC-3'
	Reverse: 5'-TTGGCGATTTCATTGGTCTCA-3'

Table 7. List of cardiac remodelling target genes and their primer sequences for qPCR.

2.9 Data analysis

All data are reported as mean ± SEM, where n is the number of mice used. Statistical analyses were conducted using GraphPad Prism version 5 (GraphPad software, California, USA). For comparison of two groups of data, a two-tailed, unpaired Student's t-test was used. When comparing three or more groups of data one-way ANOVA followed by a Bonferroni multiple comparisons test was used. Two-way ANOVA was used to compare data influenced by two factors. Shapiro-Wilk test was used to test normality of data. For all tests, $p<0.05$ was considered statistically significant.

Chapter 3 – Results I

Chapter 3 – Results I

3 Results I

3.1 Introduction

The actions of EDHFs are of critical importance to cardiovascular physiology, especially when production of NO is compromised in diseases such as pulmonary hypertension and atherosclerosis (Luksha et al., 2009). Chauhan *et al*. 2003 originally reported that CNP is indistinguishable from EDHF in the regulation of vascular tone and blood flow in mesenteric resistance arteries. More recently, evidence showing CNP plays a critical role in regulating vascular homeostasis, by acting as an EDHF, maintaining vascular integrity and preventing atherogenesis has been provided by the generation of endothelial-specific CNP KO mice (Moyes et al., 2014, Nakao et al., 2017). Many groups have also demonstrated exogenous CNP is a potent coronary vasodilator (Wei et al., 1994, Wright et al., 1996, Hobbs et al., 2004) and protects against IR injury (Hobbs et al., 2004). During CHF, myocardial production and release of CNP is elevated as a function of clinical severity (Kalra et al., 2003, Del Ry et al., 2006a, Del Ry et al., 2005). In *in vivo* studies, IR injury and ventricular remodelling are aggravated in response to CNP genetic knockdown (Wu et al., 2017a). Whilst, pharmacological addition of CNP ameliorates IR injury (Jin et al., 2014, Hobbs et al., 2004, Soeki et al., 2005). These observations suggest CNP might be a potential therapeutic target for coronary artery disease and have beneficial effects in MI patients. Therefore, this thesis investigated a patho/physiological role of CNP in the regulation of coronary vascular function and in acute IR injury by utilising the Langendorff isolated heart model and cell-specific CNP KO mice (i.e. ecCNP and cmCNP KO).

Sex differences in the contribution of EDHF to the regulation of vascular activity have previously been reported (Scotland et al., 2005, Barber et al., 1998). Furthermore, endothelial dysfunction and a hypertensive phenotype are observed in female, but not male, ecCNP KO (Moyes et al., 2014). Thus, my work also investigated sex differences in endogenous CNP-mediated changes in coronary reactivity in ecCNP KO mice.

The mechanism by which CNP induces vasodilatation remains unclear and appears to vary between vascular beds. Early studies in aortic rings reported the activation of NPR-B upon CNP binding is responsible for relaxation of vascular smooth muscle via production of

cGMP (Drewett et al., 1995, Madhani et al., 2003). However, in smooth muscle restricted NPR-B KO mice, ACh-induced vasorelaxation is preserved in mesenteric vessels (Nakao et al., 2015), suggesting a NPR-B independent mechanism is involved. Accordingly, Villar *et al*. 2007 demonstrated that a selective NPR-C antagonist, M372049, inhibits CNP-induced vasodilatation in mesenteric arteries. Subsequently, Moyes *et al*. 2014 showed a hypertensive phenotype in NPR-C KO animals, but not in NPR-B KO (Nakao et al., 2015). These data imply NPR-C is the dominant receptor for CNP signalling in resistance vascular beds, and thus, I also explored the coronary vasoreactivity and IR injury in NPR-C KO mice in this project.

3.2 Characterisation of cell-specific CNP KO mouse

3.2.1 Endothelium-specific CNP KO mice

The characterisation of ecCNP KO mice under the tyrosine protein kinase receptor (Tie^2) promoter has been previously published and showed CNP expression is specifically reduced in the endothelial cells by 80% (Moyes et al., 2014).

3.2.2 Cardiomyocyte-specific CNP KO mice

CNP expression was deleted in cardiomyocytes via cell-specific excision of the *Nppc* gene using Cre-Lox technology (α-MHC-driven Cre) (Agah et al., 1997). CNP mRNA expression in whole hearts (analysed by qPCR) revealed almost 80% reduction in cmCNP KO mice compared to WT controls (Figure 16). In contrast, CNP mRNA expression in other organs was similar (lungs, liver, and kidney) across the genotypes. Expression of CNP mRNA in neonatal cardiomyocytes isolated from cmCNP KO mice was approximately 50% lower than WT littermates (Figure 16). This residual CNP expression is likely to be due to the impurity of the cell culture, with cardiomyocytes comprising approximately 60% of the total cell population (Figure 16). The percentage of cardiomyocytes was estimated by the number of cells that stained positive for the cardiomyocyte-specific marker Troponin T (ab8295; AbCam) in comparison to the total cell population (DAPI positive). Thus, a 50% reduction in CNP mRNA expression overall, in a cell population consisting of 60% cardiomyocytes, gives rise to an approximate 83% reduction in abundance, which closely matches the whole heart evaluation. These data confirm efficient and specific removal of the *Nppc* gene from cardiomyocytes. However, the baseline levels of ANP and BNP were not measured. The lost of CNP bioactivity may have been compensated for, in part, by an increase in the bioactivity

of other natriuretic peptides, although this would only results in an under-estimate of the (patho)physiological consequences of CNP deletion.

Characterisation of CNP expression in WT and cmCNP KO mice

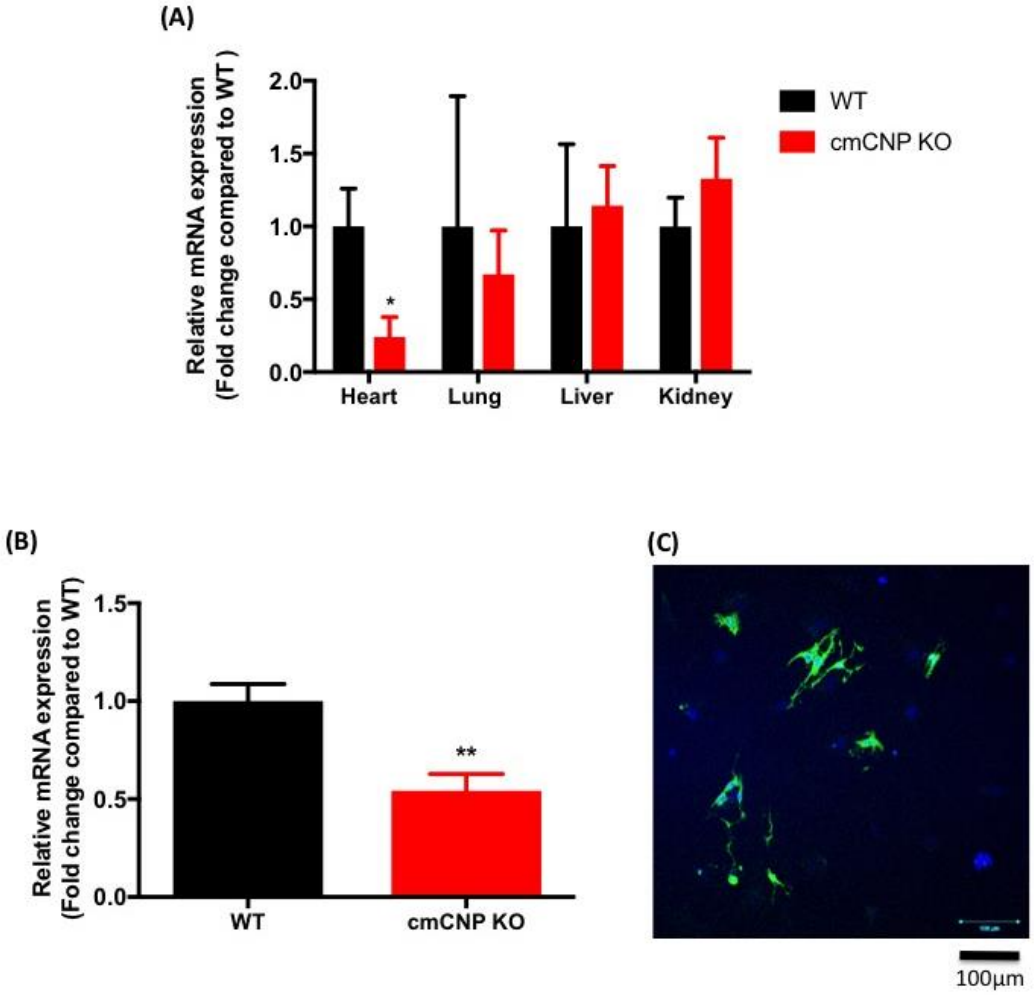

Figure 16. Characterisation of cmCNP KO mice.

qPCR analysis of CNP mRNA from different tissues in WT and cmCNP KO confirmed that the CNP gene had been deleted from the heart (A). qPCR analysis of CNP mRNA expression in neonatal cardiomyocytes also established that deletion of CNP is specific to cardiomyocytes (B). Isolated cardiomyocytes were stained with cardiac Troponin T (green) and DAPI (blue), demonstrating approximately 60% of the cultured cells were cardiomyocytes (C). Data are represented as the mean±SEM. n=4-6. *p<0.05, **p<0.01 (unpaired t-test), significantly different from corresponding WT littermates.

3.3 Coronary vascular reactivity in ecCNP KO mice

3.3.1 Baseline coronary perfusion

Baseline CPP was similar between WT and ecCNP KO mice in both females and males (female, 91.80±7.35mmHg vs. 95.32±8.72mmHg; male, 79.14±8.65mmHg vs. 77.69±10.00mmHg; p>0.05; n=8-10) (Figure 17). Coronary perfusion pressure increased in the presence of L-NAME (300μM) regardless of genotype or sex (female, WT 142.2±9.64mmHg, ecCNP KO 138.7±11.77mmHg; male, WT 126.6±8.57mmHg, ecCNP KO 144.3±6.06mmHg; *p*<0.001 compared to baseline; n=8-10) (Figure 17). This increase in CPP indicates the presence of an intact endothelium in the hearts studied, i.e. blockade of NO production from the endothelium.

3.3.2 Endothelium-dependent vasodilators

3.3.2.1 Bradykinin

The endothelium-dependent vasodilator BK (10nmol) produced an equivalent fall in CPP in hearts from female and male WT mice (female, ΔCPP=-31.68±2.682%; male, ΔCPP=-32.59 ±2.350%; *p*>0.05; n=7-9) (Figure 18). In female ecCNP KO animals the responsiveness to BK was significantly reduced (ΔCPP=-21.14±2.89%; *p*<0.05; n=7-9) (Figure 18). However, this blunted response to BK was not observed in male ecCNP KO (ΔCPP=-32.84±3.42%; *p*=0.95; n=7-8) compared to WT (Figure 18).

3.3.2.2 Acetylcholine

The mechanistically-distinct endothelium-dependent vasodilator, ACh (0.1nmol – 1nmol) produced a dose-dependent decrease in CPP in hearts from both WT and ecCNP KO animals (Figure 19). Unlike responses to BK, coronary reactivity in both male and female ecCNP KO was significantly blunted compared with WT controls (female, *p*<0.001; male, *p*<0.05, 2-way ANOVA; n=7-9) (Figure 19). In particular, the response to 1nmol ACh in female ecCNP KO was almost 50% lower than WT (ΔCPP=-30.12±5.82% vs. -50.40±2.92%; p<0.001; n=7-9).

3.3.2.3 Vasodilatation associated with reperfusion

CNP expression and secretion are upregulated in endothelial cells in response to shear-stress (Chun et al., 1997, Zhang et al., 1999). Thus, I also investigated if CNP contributes to shear-stress-induced vasodilatation in the coronary vasculature *ex vivo* by examining the magnitude of vasodilatation in response to reperfusion. The resumption of flow following

transient cessation of perfusion creates a shear force against the vessel wall and triggers the release of endothelium-derived mediators, such as CNP (Nakamura et al., 1994, Zatta and Headrick, 2005). The response to reperfusion following 80 seconds of zero flow was significantly reduced in hearts from female ecCNP KO mice compared to WT (WT, 2429±300 a.u vs. KO, 1493±280 a.u; p<0.05; n=6-8) (Figure 20), but not in male animals (WT, 4454±642 a.u; ecCNP KO 4125±575a.u; p>0.05; n=5-7) (Figure 20). However, the area under the curve was 50% higher in male compared to females across all three occlusion durations, regardless of genotype. This observation is probably due to the size difference of the hearts/coronary vasculature tree between sexes. Nevertheless, the heart size/body weight were similar between the genotypes within the same sex, suggesting the phenotype observed in female might be due to the loss of endothelial CNP production.

3.3.3 Endothelium-independent vasodilators

3.3.3.1 CNP

CNP (10nmol) was used to examine if vascular smooth muscle sensitivity altered in response to endothelial-specific deletion of CNP (i.e. in ecCNP KO mice). The coronary reactivity was comparable between WT and ecCNP KO mice in both sexes (female, WT ΔCPP=-11.96±1.838% vs. ecCNP KO ΔCPP = -9.769±1.274%, p>0.05; male, WT ΔCPP=-24.10±6.283% vs. ecCNP KO ΔCPP=-19.99±3.957%, p>0.05; n=6-9) (Figure 21). These data suggest that the responsiveness to CNP is not affected in ecCNP KO and that differences observed in endothelium-dependent vasodilator responses are due to lack of endothelial CNP production.

3.3.3.2 SNP

The NO donor SNP was employed to examine the sensitivity of the vascular smooth muscle in response to vasodilators mechanistically distinct to CNP. The vasorelaxant response to SNP was similar between WT and ecCNP KO (female, WT ΔCPP=-23.78±3.152% vs. ecCNP KO ΔCPP=-21.52±3.249%, p>0.05; male, WT ΔCPP=-41.64±3.228 vs. ecCNP KO ΔCPP=-37.65 ±3.356%, p>0.05; n=7-9) (Figure 21). These results indicate that the coronary vascular smooth muscle sensitivity to exogenous vasodilators is equivalent in all animals regardless of genotype.

3.3.4 Release of CNP from the coronary endothelium

In order to confirm that the difference observed between WT and ecCNP KO mice with respect to coronary vasodilatation was due to a diminished release of endothelial CNP in

response to ACh, the coronary effluent was collected immediately after bolus injection of ACh (1nmol) for CNP bioassay. Indeed, the concentration of CNP in the effluent of ecCNP KO hearts was significantly lower compared to WT (ecCNP KO, 0.459±0.111ng/mL vs. WT, 0.884±0.074ng/mL; $p<0.01$; n=4-7) (Figure 22). This observation confirms that CNP is released by the coronary endothelium in response to ACh, and substantiates the concept that the reduced vasoreactivity is due to the lack of endothelium-derived CNP. However, CNP production was not completely abolished in ecCNP KO mice (Figure 22). It is not clear if this is due to the release of CNP by other cardiac cells or just at the level of signal-noise ratio for this EIA.

Taking together, these observations demonstrate endothelium-derived CNP contributes to coronary reactivity in response to endothelium-dependent vasodilators and mechanical shear force, especially in females.

Baseline coronary perfusion in hearts from female and male WT and ecCNP KO mice in the absence and presence of L-NAME

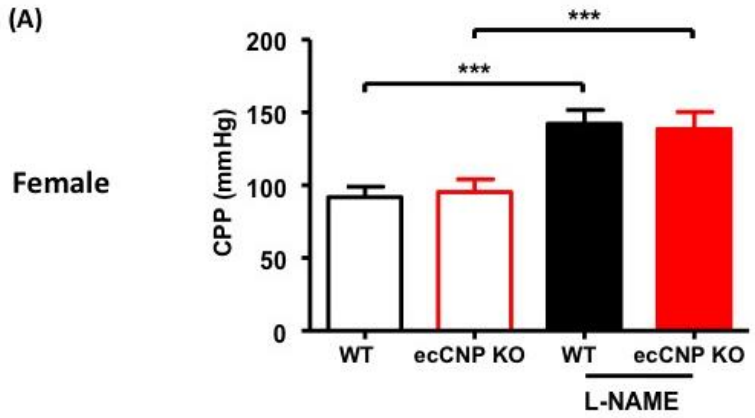

WT										Mean	SEM
Baseline	99.98	110.69	111.62	126.94	63.93	85.72	86.36	64.17	76.76	91.80	7.35
L-NAME	146.46	183.72	181.83	160.40	109.91	143.97	129.69	111.90	111.71	142.18	9.64

ecCNP KO									Mean	SEM
Baseline	143.09	84.54	74.68	103.30	104.29	106.54	82.43	63.6736	95.32	8.72
L-NAME	177.97	98.47	95.65	162.27	124.89	166.06	166.80	117.1853	138.66	11.77

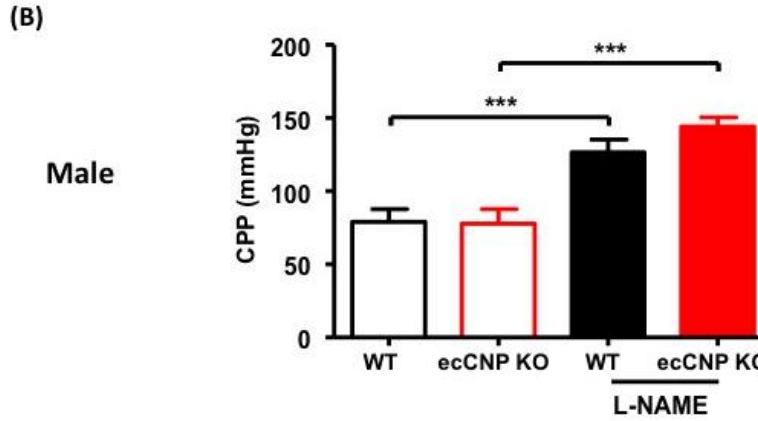

WT									Mean	SEM
Baseline	53.71	61.58	71.28	122.31	50.80	67.62	107.97	90.69	78.24	9.23
L-NAME	112.93	156.82	146.84	159.22	103.22	121.15	145.37	123.60	133.64	7.46

ecCNP KO									Mean	SEM
Baseline	52.60	50.10	125.13	112.01	72.08	55.05	66.54	87.99	77.69	9.99
L-NAME	139.40	160.79	143.70	154.70	154.26	146.73	105.38	149.66	144.33	6.06

Figure 17. Baseline coronary perfusion pressure in hearts from female and male WT and ecCNP KO mice in the absence and presence of L-NAME.

Coronary perfusion pressure (CPP) in the isolated hearts from WT and ecCNP KO in the absence and presence of L-NAME (300µM). (A) females and (B) males. Data are represented as the mean±SEM. n=8-10. ***p<0.001 (2-way ANOVA with Bonferroni *post-hoc* test), significantly different from corresponding WT littermates.

Coronary reactivity in hearts from female and male WT and ecCNP KO mice in response to bradykinin

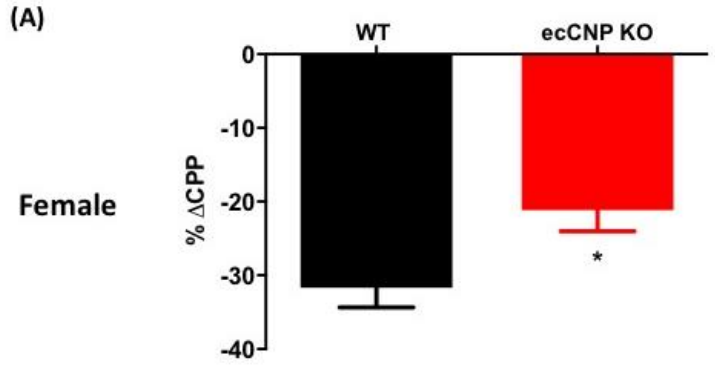

WT										Mean	SEM
baseline	146.95	182.70	158.60	107.11	128.82	133.18	113.25	106.99	166.61	138.24	9.10
relaxation	112.10	135.93	119.61	77.42	73.20	93.88	70.05	68.85	119.06	96.68	8.51
ΔCPP	-34.85	-46.77	-38.98	-29.70	-55.62	-39.30	-43.20	-38.14	-47.54	-41.57	2.56
% ΔCPP	-23.72	-25.60	-24.58	-27.72	-43.18	-29.51	-38.14	-35.65	-28.54	-31.68	2.68

ecCNP KO								Mean	SEM
baseline	177.56	96.20	97.36	159.86	129.44	160.38	165.81	140.95	12.66
relaxation	153.56	67.76	76.34	114.42	117.86	127.55	123.63	111.59	12.89
ΔCPP	-24.00	-28.44	-21.02	-45.44	-11.58	-32.83	-42.18	-29.36	28.85
% ΔCPP	-13.52	-29.56	-21.59	-28.43	-8.94	-20.47	-25.44	-21.14	2.89

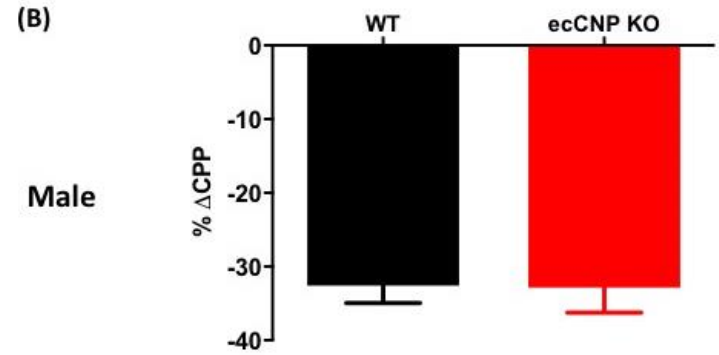

WT								Mean	SEM
baseline	106.02	146.84	150.39	103.01	121.67	146.00	128.09	128.86	7.44
relaxation	77.79	92.71	113.97	64.04	85.76	86.13	87.03	86.77	5.72
ΔCPP	28.23	54.13	36.42	38.97	35.91	59.87	41.07	42.09	4.18
% ΔCPP	26.63	36.86	24.22	37.83	29.51	41.01	32.06	32.59	2.35

ecCNP KO									Mean	SEM
baseline	139.75	154.58	143.54	154.71	165.67	81.74	108.31	148.83	137.14	9.92
relaxation	78.00	108.96	108.54	124.64	121.88	54.92	65.15	80.23	92.79	9.40
ΔCPP	61.75	45.62	35.01	30.07	43.79	26.83	43.16	68.59	44.35	5.16
% ΔCPP	44.18	29.51	24.39	19.43	26.43	32.82	39.85	46.09	32.84	3.42

Figure 18. Coronary reactivity in hearts from female and male WT and ecCNP KO mice in response to bradykinin.

Coronary endothelium-dependent relaxation to bradykinin (10nmol) in isolated hearts from female (A) and male (B) WT and ecCNP KO mice. Data are represented as the mean±SEM. n=7-9. *p<0.05 (unpaired t-test), significantly different from corresponding WT littermates.

Coronary reactivity in hearts from female and male WT and ecCNP KO mice in response to acetylcholine

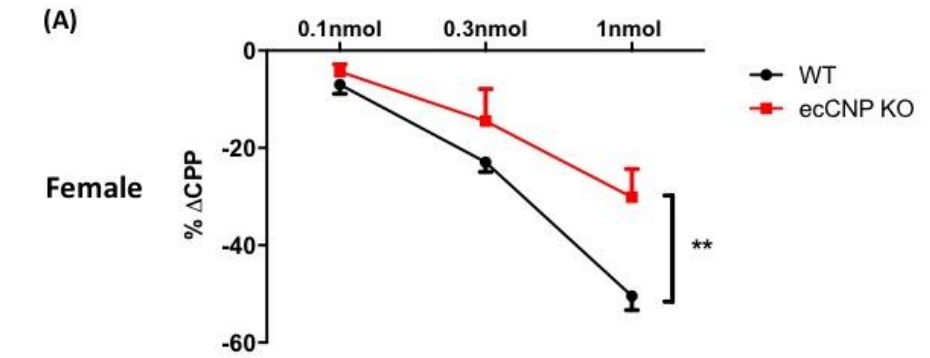

1nmol ACh

WT													Mean	SEM
baseline	147.17	136.31	93.41	143.07	135.69	150.60	130.16	151.43	141.61	127.86	115.02	108.16	131.71	5.20
relaxation	62.16	50.47	55.36	49.32	62.43	62.32	75.86	102.20	65.11	75.60	58.93	56.97	64.73	4.16
ΔCPP	-85.01	-85.84	-38.05	-93.74	-73.26	-88.27	-54.30	-49.24	-76.50	-52.26	-56.08	-51.19	-66.98	5.42
% ΔCPP	-57.76	-62.98	-40.73	-65.52	-53.99	-58.62	-41.72	-32.51	-54.02	-40.87	-48.76	-47.33	-50.40	2.92

ecCNP KO													Mean	SEM
baseline	142.43	107.83	166.35	155.73	127.82	140.27	96.37	153.64	134.19	139.01	163.92	109.73	136.44	6.51
relaxation	122.67	58.51	145.48	58.23	61.88	123.57	83.79	91.71	116.77	111.25	135.33	44.48	96.14	9.90
ΔCPP	-19.76	-49.33	-20.88	-97.50	-65.95	-16.70	-12.57	-61.93	-17.43	-27.76	-28.58	-65.25	-40.30	7.81
% ΔCPP	-13.87	-45.74	-12.55	-62.61	-51.59	-11.91	-13.05	-40.31	-12.99	-19.97	-17.44	-59.46	-30.12	5.82

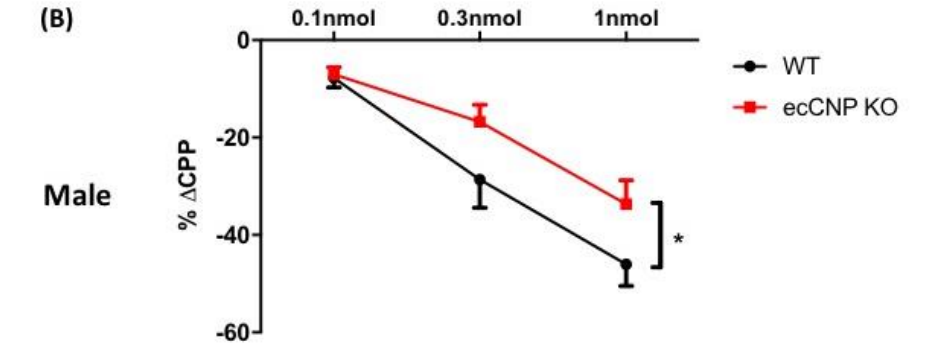

1nmol ACh

WT									Mean	SEM
baseline	105.34	175.99	101.10	102.65	103.52	132.80	133.36	120.92	121.96	9.05
relaxation	79.71	128.34	55.96	50.58	64.06	79.20	46.94	49.46	69.28	9.58
ΔCPP	-25.63	-47.65	-45.14	-52.07	-39.46	-53.61	-86.43	-71.46	-52.68	6.66
% ΔCPP	-24.33	-27.07	-44.65	-50.72	-38.12	-40.36	-64.81	-59.10	-46.00	5.05

ecCNP KO									Mean	SEM
baseline	145.07	159.60	148.04	144.35	145.25	141.02	68.49	91.80	117.63	129.03	10.12
relaxation	60.16	132.44	97.07	121.62	92.06	103.72	41.62	53.99	63.61	85.14	10.58
ΔCPP	-84.92	-27.16	-50.97	-22.73	-53.19	-37.30	-26.88	-37.82	-54.01	-43.89	6.48
% ΔCPP	-58.53	-17.02	-34.43	-15.75	-36.62	-26.45	-39.24	-41.19	-45.92	-33.65	4.56

Figure 19. Coronary reactivity in hearts from female and male WT and ecCNP KO mice in response to acetylcholine.

Coronary endothelium-dependent relaxation to acetylcholine (0.1-1nmol) in isolated hearts from female (A) and male (B) WT and ecCNP KO mice. Data are represented as the mean±SEM. n=8-12. *p<0.05 (2-way ANOVA with Bonferroni *post-hoc* test), significantly different from corresponding WT littermates.

Coronary reactivity in hearts from female and male WT and ecCNP KO mice in response to reperfusion

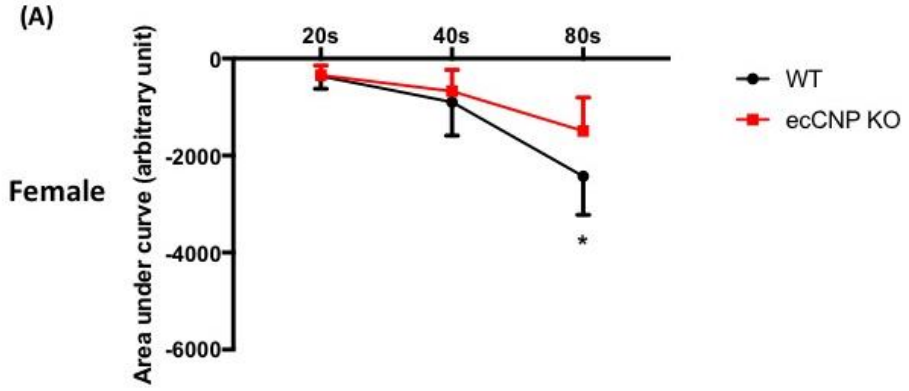

80s								Mean	SEM
WT	-3845.93	-1874.62	-1917.59	-2172.72	-1547.86	-2675.13	-2965.63	-2428.50	299.49
ecCNP KO	-974.94	-1280.72	-2655.39	-696.63	-1702.63	-1645.38		-1492.62	280.83

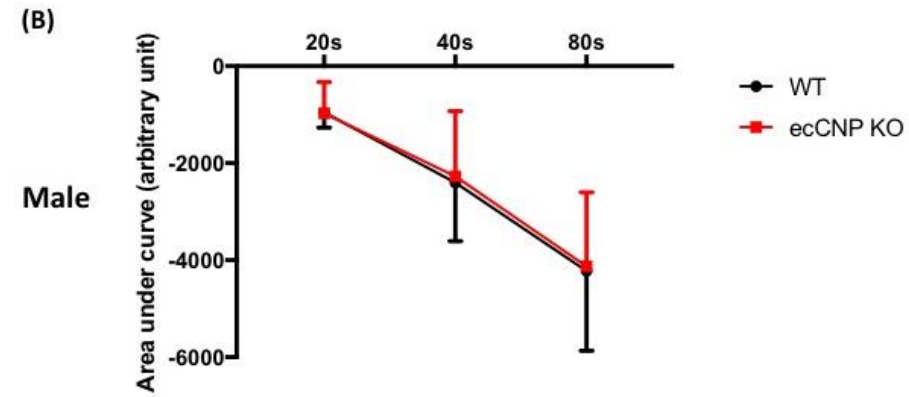

80s								Mean	SEM
WT	4568.85	5611.12	3885.29	1874.77	6465.00	4322.79		4454.64	642.63
ecCNP KO	5885.97	4395.64	1279.34	2989.67	4623.49	4955.78	4748.56	4125.49	575.05

Figure 20. Coronary reactivity in hearts from female and male WT and ecCNP KO mice in response to reperfusion.

Cessation of flow, 20, 40 or 80 seconds followed by reperfusion. (A) female, (B) male animals. Data are represented as the mean±SEM. n=6-7. *p<0.05 (2-way ANOVA with Bonferroni *post-hoc* test), significantly different from corresponding WT littermates.

Coronary reactivity in hearts from female and male WT and ecCNP KO mice in response to endothelium-independent vasodilators

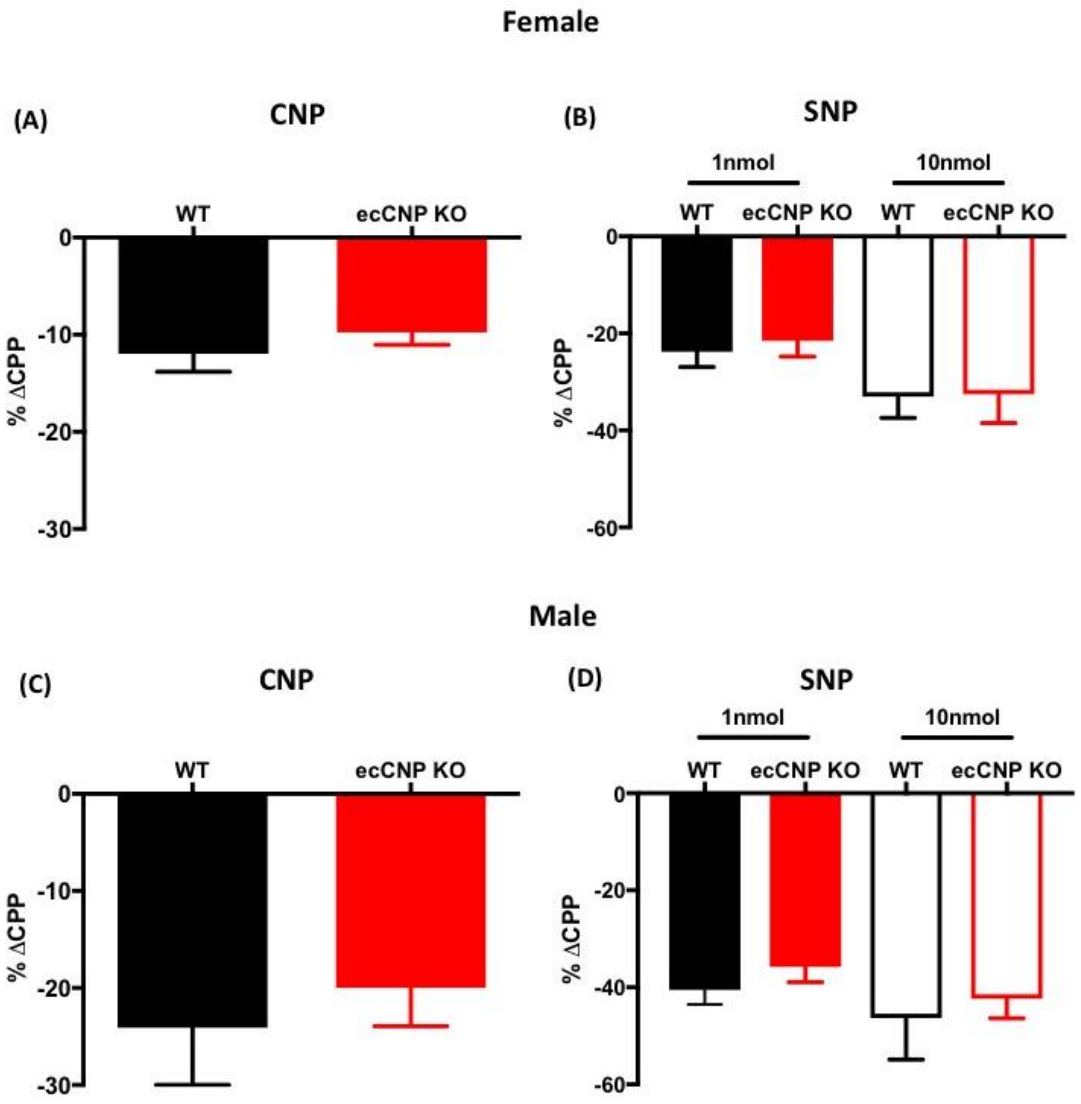

Figure 21. Coronary reactivity in hearts from female and male WT and ecCNP KO mice in response to endothelium-independent vasodilators.

(A) and (C), coronary endothelium-independent relaxation to CNP (10nmol) in female and male WT and ecCNP KO mice, respectively. (B) and (D), the response to SNP in female and male animals, respectively. Data are represented as the mean±SEM. n=6-9. Statistical analysis was by unpaired t-test.

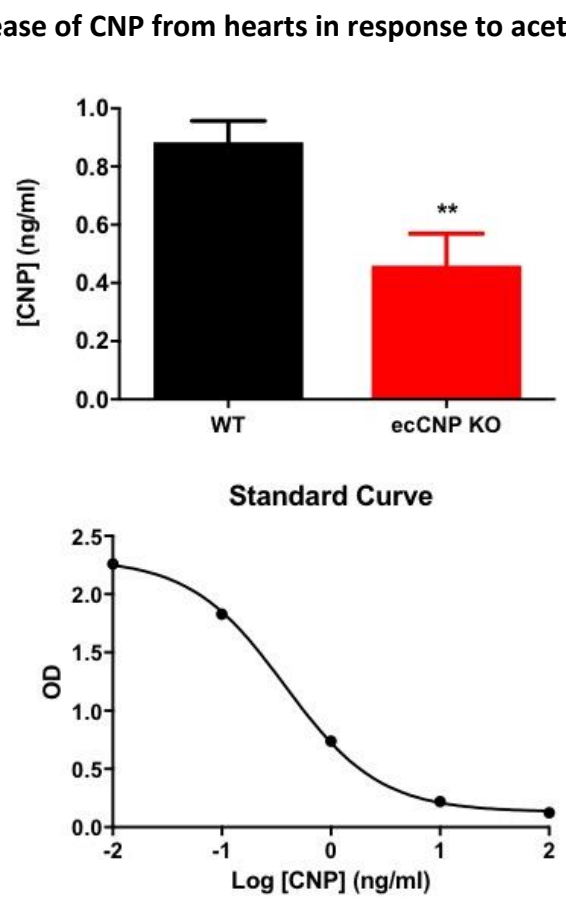

Figure 22. Release of CNP from hearts in response to acetylcholine.

Coronary perfusion effluent was collected following bolus injection of ACh (1nmol) in WT and ecCNP KO mice. Data are represented as the mean±SEM. n=4-7. ** p<0.01 (unpaired t-test), significantly different from corresponding WT littermates.

3.4 Ischaemia reperfusion injury

Having established that CNP release by the coronary endothelium regulates vascular function and local blood flow, I went on to investigate a potential cardioprotective effect of endothelial-derived CNP in IR injury. Previous studies have established that exogenous CNP (i.e. pharmacological administration) provides a protective effect against reperfusion injury (Hobbs et al., 2004). Baxter *et* al. (2004) also demonstrated myocardial ischemia is associated with rapid release of natriuretic peptide and induction of de novo peptide synthesis (Baxter, 2004). Herein, I investigated if endogenous release of CNP has protective function against IR injury and, if so, which source of CNP (i.e. cellular origin) proffers the most beneficial effect.

3.4.1 ecCNP KO mice in response to ischaemia reperfusion injury

After establishing the acute IR injury model, isolated hearts were subjected to 35 minutes global ischaemia followed by 60 minutes reperfusion; this results in an approximately 15% infarct size in WT animals (as measured by TTC staining). This relative small infarct induction was chosen because it was expected that abrogation of CNP would exacerbate IR injury. However, the infarct size was not significantly different between WT and ecCNP KO mice in both male and female animals, although there was a trend towards a larger infarct size in female ecCNP KO compared to littermate controls (male, WT 15.05±2.040% vs. ecCNP KO 14.66±2.498%, $p>0.05$, n=11; female WT, 18.96±2.17% vs. ecCNP KO 25.13±2.71%, $p=0.095$, n=7-8) (Figure 23 and Figure 24). The recovery of LVDP was lower in females than males but no difference was observed between genotypes (female, WT 13.78±1.742mmHg, ecCNP KO 16.96±4.241mmHg; male, WT 34.23±4.056mmHg, ecCNP KO 27.91±3.701mmHg; $p>0.05$; n=7-11) (Figure 23 and Figure 24).

3.4.2 cmCNP KO mice in response to ischaemia reperfusion injury

In contract to ecCNP KO, the hearts from cmCNP KO mice had a significantly greater infarct size in comparison to WT controls following IR, regardless of sex (Figure 25 and **Figure 26**). The infarct size in female WT was 12.73±1.15% vs. cmCNP KO 21.76±1.85%; $p<0.005$; n=5-8. The effect of male cmCNP KO in response to IR was even more striking; WT 13.02±1.70% vs. cmCNP KO 35.89±3.64; $p<0.0005$; n=8-12 (**Figure 26**). Accordingly, this larger infarct size in male cmCNP KO was accompanied by a much smaller recovery of LVDP compared to WT controls ($p<0.0005$; n=8-12) (**Figure 26**). The recovery of LVDP in female cmCNP KO was not significantly different to WT controls, probably due to a relatively small increase in infarct

size compared to the male cmCNP KO. These results suggest that cardiomyocyte-derived CNP is cardioprotective in a pre-clinical MI model.

IR injury in female WT and ecCNP KO mice

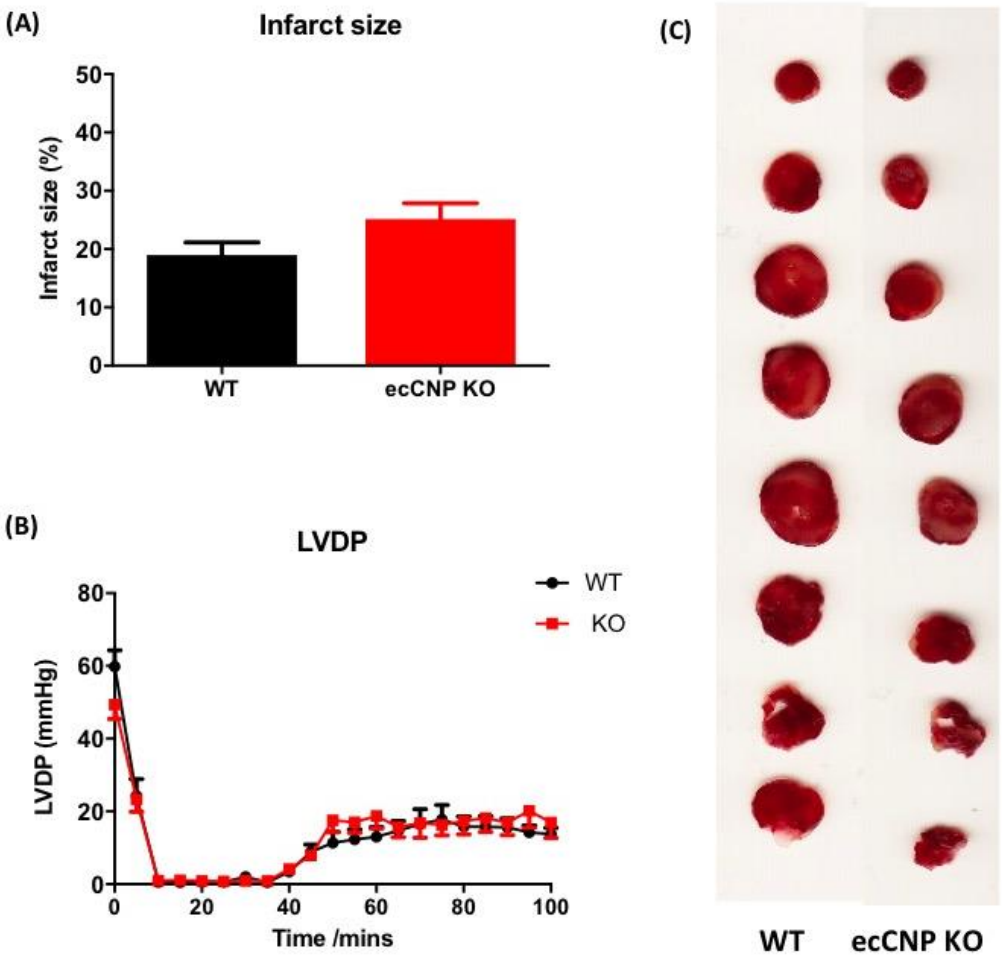

Figure 23. IR injury in female WT and ecCNP KO mice.

Infarct size (A) and left ventricular developed pressure (LVDP) (B) in isolated hearts from female WT and ecCNP KO mice subjected to 35 minutes ischaemia followed by 60 minutes reperfusion. Representative images of TTC staining for infarcted areas (white regions) are shown (C). Data are represented as the mean±SEM. n=7-8. Unpaired t-test and 2-way ANOVA was used to analyse infarct size and LVDP, respectively.

IR injury in male WT and ecCNP KO mice

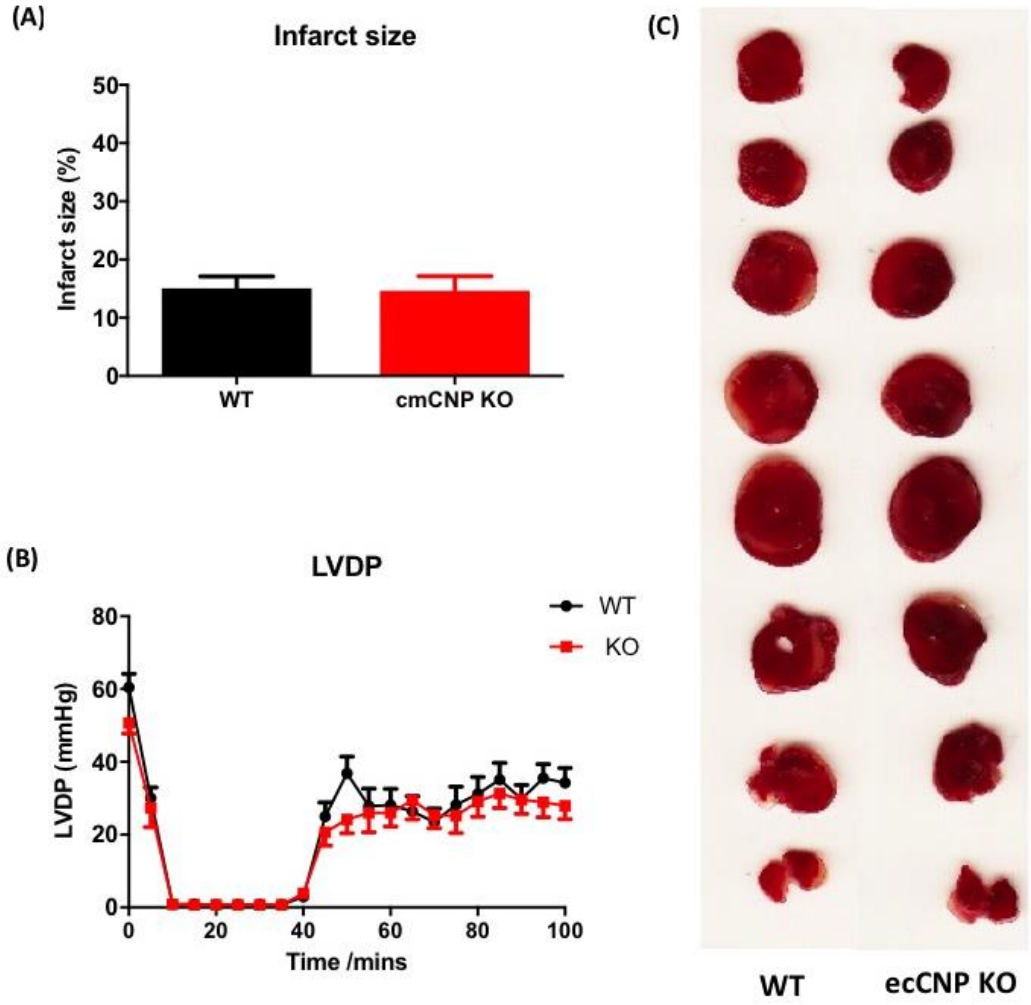

Figure 24. IR injury in male WT and ecCNP KO mice.

Infarct size (A) and left ventricular developed pressure (LVDP; B) in isolated hearts from male WT and ecCNP KO mice subjected to 35 minutes ischaemia followed by 60 minutes reperfusion. Representative images of TTC staining for infarcted areas (white regions) are shown (C). Data are represented as the mean±SEM. n=11. Unpaired t-test and 2-way ANOVA was used to analyse infarct size and LVDP, respectively.

IR injury in female WT and cmCNP KO mice

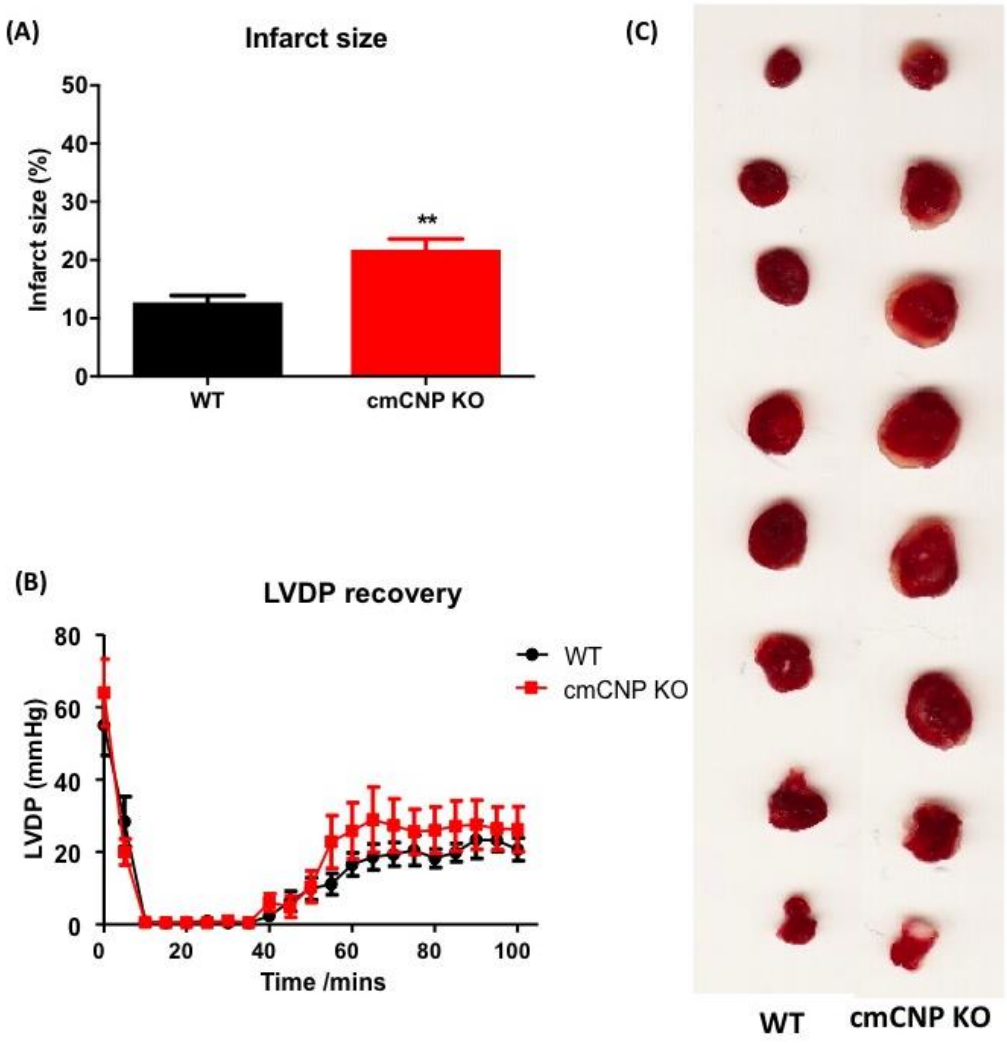

Figure 25. IR injury in female WT and cmCNP KO mice.

Infarct size (A) and left ventricular developed pressure (LVDP) (B) in isolated hearts from female WT and cmCNP KO mice subjected to 35 minutes ischaemia followed by 60 minutes reperfusion. Representative images of TTC staining for infarcted areas (white regions) are shown (C). Data are represented as the mean±SEM. n=5-8. Unpaired t-test and 2-way ANOVA was used to analyse infarct size and LVDP, respectively. ***p*<0.01, significantly different from corresponding WT littermates.

IR injury in male WT and cmCNP KO mice

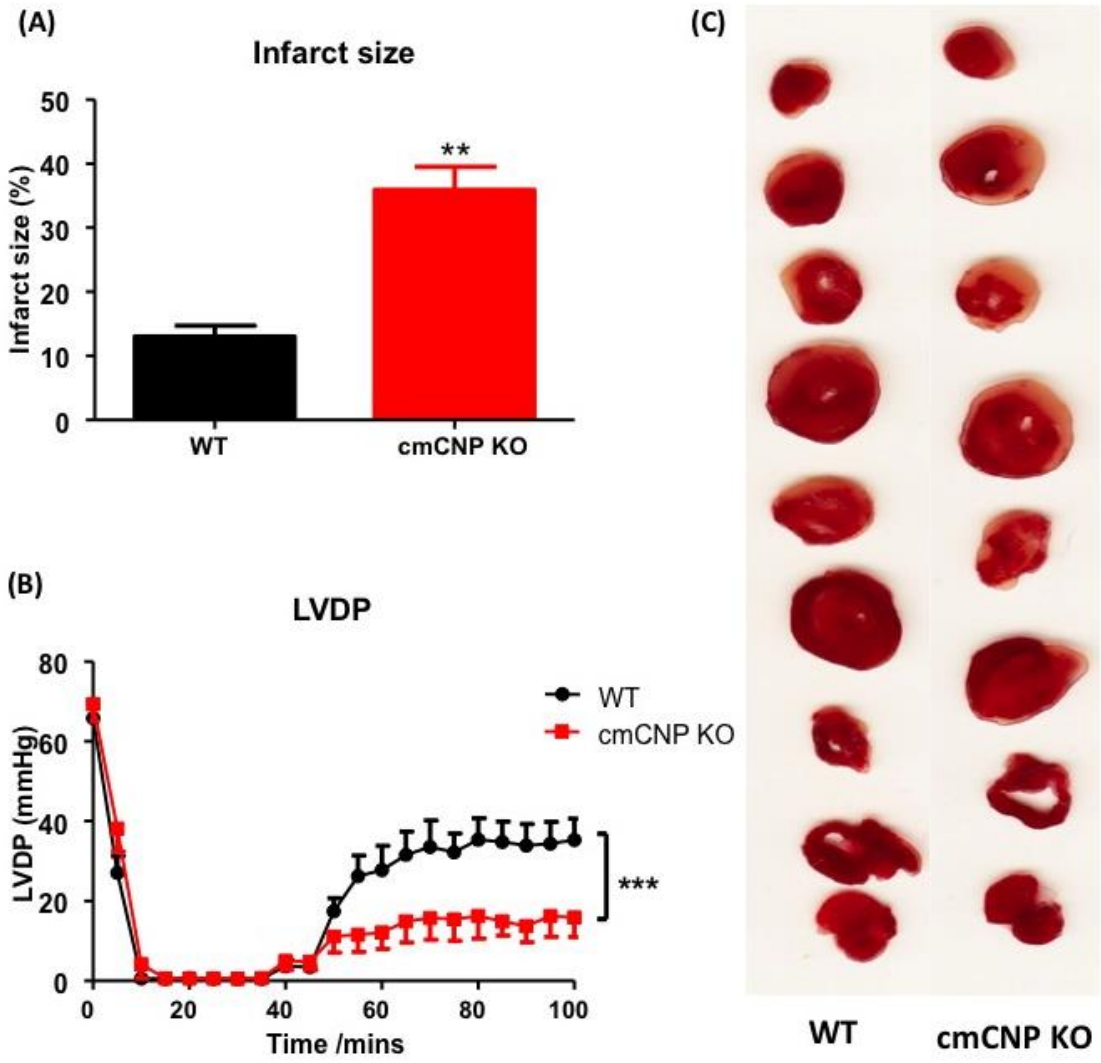

Figure 26. IR injury in male WT and cmCNP KO mice.

Infarct size (A) and left ventricular developed pressure (LVDP) (B) in isolated hearts from male WT and cmCNP KO mice subjected to 35 minutes ischaemia followed by 60 minutes reperfusion. Representative images of TTC staining for infarcted areas (white regions) are shown (C). Data are represented as the mean±SEM. n=8-12. Unpaired t-test and 2-way ANOVA was used to analyse infarct size and LVDP, respectively. ** $p<0.01$, *** $p<0.001$, significantly different from corresponding WT littermates.

3.5 Endothelium-derived CNP induces coronary vasorelaxation via NPR-C activation

3.5.1 Coronary reactivity in NPR-C KO mice

To identify the NPR responsible for conveying the vasorelaxant activity of CNP in the coronary vasculature, I employed male global NPR-C KO mice in the Langendorff isolated heart model. Similar to ecCNP KO mice, there was no difference in baseline CPP between WT and NPR-C KO animals (WT, 75.61±4.296mmHg vs. NPR-C KO, 77.13±6.654mmHg; p>0.05; n=5-8) (Figure 27). CPP was elevated by approximately 50% in response to L-NAME (300µM) in both genotypes (WT, 134.4±9.728mmHg vs. NPR-C KO, 125.6±15.53mmHg; p<0.001 compared to baseline; n=5-8) (Figure 27). The vasodilator response to BK (10nmol) was significantly reduced in NPR-C KO compared to littermate controls (WT, ΔCPP=-29.25±3.61% vs. NPR-C KO, ΔCPP=-11.15±2.57%; p<0.005; n=5-8) (Figure 28). Likewise, the responses to ACh (0.1-1nmol) were markedly reduced in mice lacking NPR-C (1nmol: WT, ΔCPP =-49.81±5.958% vs. NPR-C KO, ΔCPP=-23.27±6.364%; p<0.01; n=5-8) (Figure 28). Reactive hyperaemia (20-80 seconds) was also significantly blunted in NPR-C KO mice compared to WT (80 seconds: WT, 5163±572.1 a.u vs. NPR-C KO, 1779±385.9 a.u; p<0.001; n=5-6) (Figure 29). These observations illustrate NPR-C mediates CNP signalling in the coronary vasculature. The vasorelaxant potency of exogenous CNP (10nmol) was reduced in the deletion of NPR-C, but was not completely abolished (WT, ΔCPP=-27.10±6.698% vs. NPR-C KO, ΔCPP=-11.99±1.287%; p<0.05; n=5-7) (Figure 30), suggesting NPR-B may also play a part in mediating CNP-induced vasodilatation in the coronary vasculature.

3.5.2 Ischaemia reperfusion injury

Having identified cardiomyocyte-derived CNP is cardioprotective against IR injury, I repeated the IR model in male global NPR-C KO mice to explore if a similar phenotype was present, thereby supporting a role for NPR-C signalling in the beneficial effect of cardiomyocyte-derived CNP. Indeed, the effect of cmCNP KO animals in response to IR injury is recapitulated in NPR-C KO mice. The infarct size in NPR-C KO animals was almost 50% larger than WT controls (WT, 18.20±4.35% vs. NPR-C KO, 35.21±4.46%; p<0.05; n=7-8) (Figure 31), accompanied by a significantly lower recovery of LVDP (WT, 45.44±8.171mmHg vs. NPR-C KO, 16.48±5.397; p<0.001; n=5-7) (Figure 31). These data suggest activation of NPR-C is critical to the cardioprotective effect of CNP against IR injury.

Baseline coronary perfusion in hearts from male WT and NPR-C KO mice in the absence and presence of L-NAME

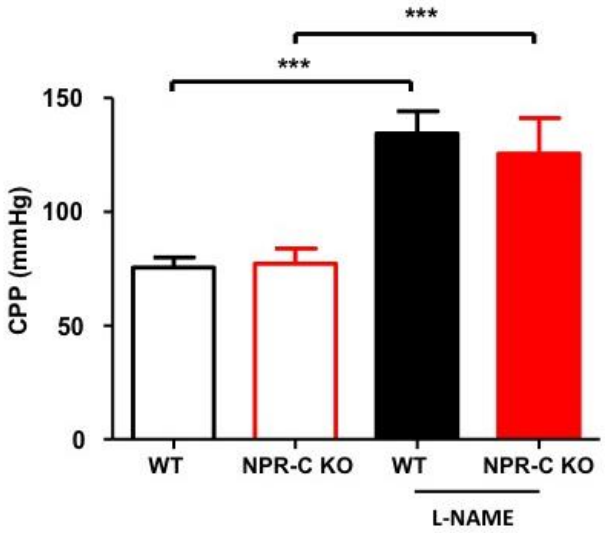

WT								Mean	SEM
baseline	74.37	73.87	73.20	80.10	58.23	86.21	96.16	77.45	4.48
L-NAME	174.19	178.03	112.50	124.33	132.67	128.40	123.44	139.08	9.85

NPR-C KO						Mean	SEM
baseline	76.45	91.56	70.01	56.44	91.21	77.13	6.65
L-NAME	175.52	138.09	93.59	91.84	129.08	125.62	15.53

Figure 27. Baseline coronary perfusion in hearts from male WT and NPR-C KO mice in the absence and presence of L-NAME

Baseline CPP in isolated hearts from WT and global NPR-C KO mice in the absence and presence of L-NAME (300µM). Data are represented as the mean±SEM. n=5-8. ***p<0.001 (2-way ANOVA with Bonferroni *post-hoc* test), significantly different from corresponding WT littermates.

Coronary reactivity in hearts from male WT and NPR-C KO mice in response to endothelium-dependent vasodilators

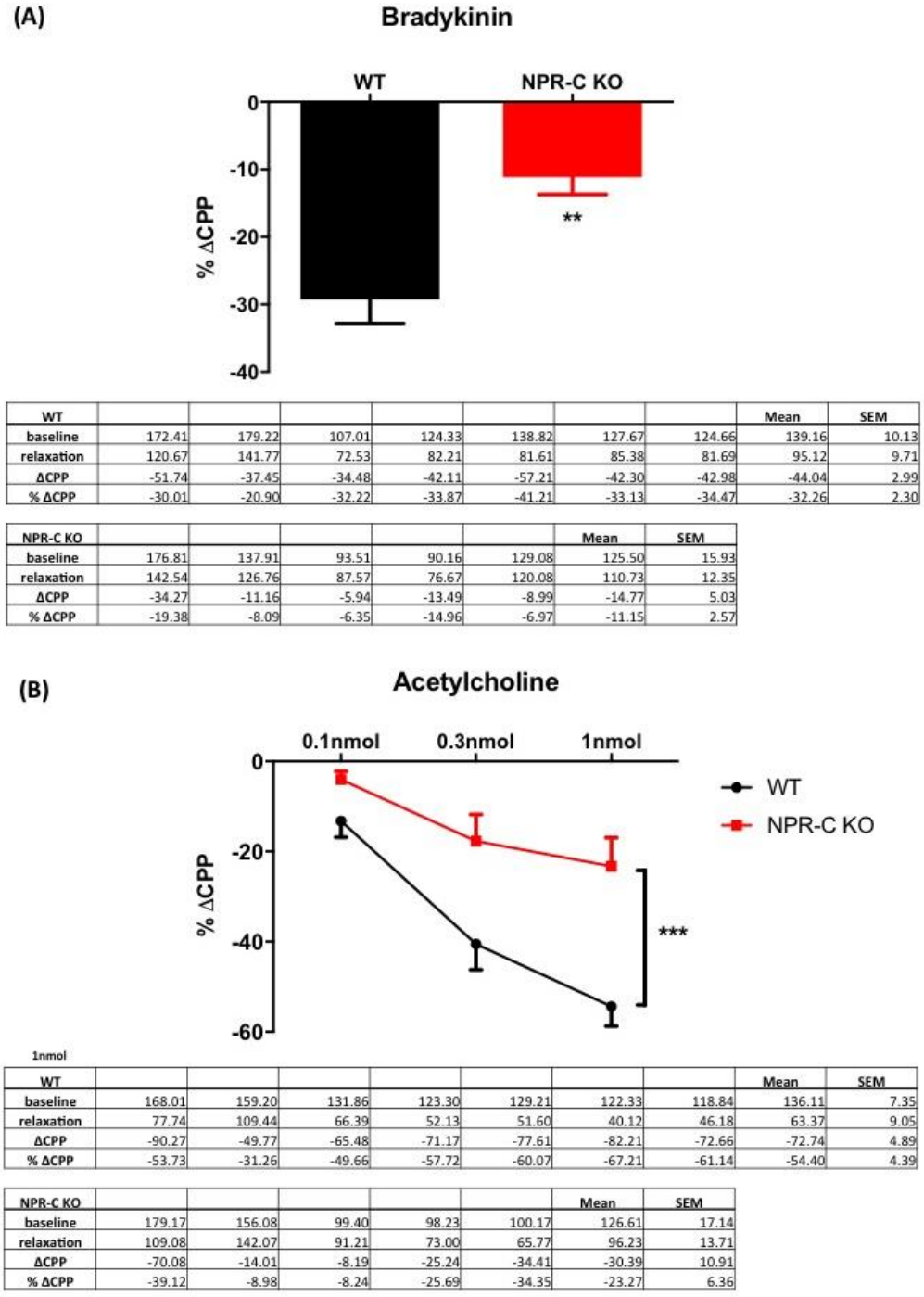

WT								Mean	SEM
baseline	172.41	179.22	107.01	124.33	138.82	127.67	124.66	139.16	10.13
relaxation	120.67	141.77	72.53	82.21	81.61	85.38	81.69	95.12	9.71
ΔCPP	-51.74	-37.45	-34.48	-42.11	-57.21	-42.30	-42.98	-44.04	2.99
% ΔCPP	-30.01	-20.90	-32.22	-33.87	-41.21	-33.13	-34.47	-32.26	2.30

NPR-C KO						Mean	SEM
baseline	176.81	137.91	93.51	90.16	129.08	125.50	15.93
relaxation	142.54	126.76	87.57	76.67	120.08	110.73	12.35
ΔCPP	-34.27	-11.16	-5.94	-13.49	-8.99	-14.77	5.03
% ΔCPP	-19.38	-8.09	-6.35	-14.96	-6.97	-11.15	2.57

1nmol

WT								Mean	SEM
baseline	168.01	159.20	131.86	123.30	129.21	122.33	118.84	136.11	7.35
relaxation	77.74	109.44	66.39	52.13	51.60	40.12	46.18	63.37	9.05
ΔCPP	-90.27	-49.77	-65.48	-71.17	-77.61	-82.21	-72.66	-72.74	4.89
% ΔCPP	-53.73	-31.26	-49.66	-57.72	-60.07	-67.21	-61.14	-54.40	4.39

NPR-C KO						Mean	SEM
baseline	179.17	156.08	99.40	98.23	100.17	126.61	17.14
relaxation	109.08	142.07	91.21	73.00	65.77	96.23	13.71
ΔCPP	-70.08	-14.01	-8.19	-25.24	-34.41	-30.39	10.91
% ΔCPP	-39.12	-8.98	-8.24	-25.69	-34.35	-23.27	6.36

Figure 28. Coronary reactivity in hearts from male WT and NPR-C KO mice in response to endothelium-dependent vasodilators

Vasorelaxant responses to bradykinin (10nmol) (A) and acetylcholine (0.1 – 1nmol) (B), in the presence of L-NAME (300µM), in WT and NPR-C KO mice. Data are represented as the mean±SEM. n=5-8. Unpaired t-test and 2-way ANOVA with Bonferroni *post-hoc* test was used to analyse the response to bradykinin and acetylcholine, respectively. ***p*<0.01, ***p<0.001, significantly different from corresponding WT littermates.

Coronary reactivity in hearts from male WT and NPR-C KO mice in response to reactive hyperaemia

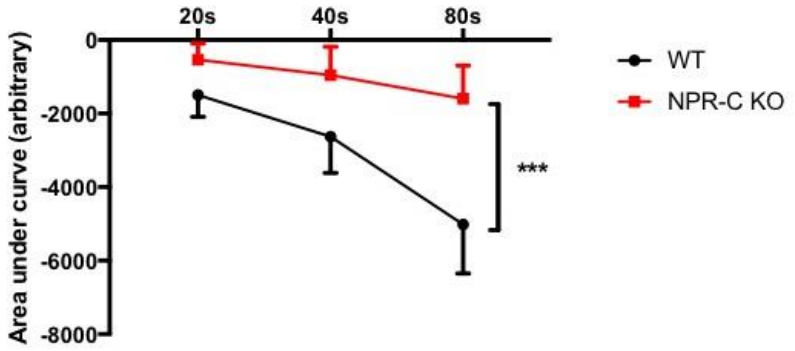

80s								Mean	SEM
WT	-5631.03	-2563.31	-6423.69	-4682.57	-4129.43	-5606.66	-6070.10	-5015.26	505.51
NPR-C KO	-668.34	-2355.29	-1673.52	-842.74	-1565.58	-2948.95	-1183.02	-1605.35	309.06

Figure 29. Coronary reactivity in hearts from WT and NPR-C KO mice in response to reactive hyperaemia.

Vasorelaxant responses to reactive hyperaemia (cessation of flow for 20, 40 and 80 seconds), in the presence of L-NAME (300µM), in WT and NPR-C KO mice. Data are represented as the mean±SEM. n=5-6. ***p<0.001 (2-way ANOVA with Bonferroni *post-hoc* test), significantly different from corresponding WT littermates.

Coronary reactivity in hearts from male WT and NPR-C KO mice in response to CNP

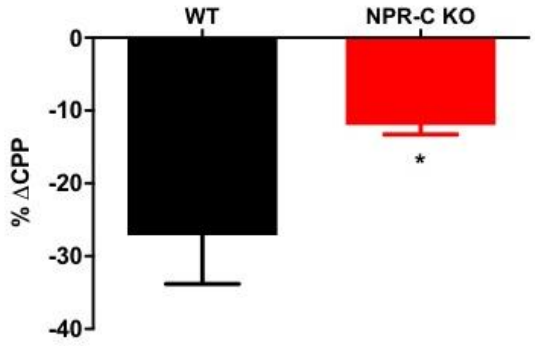

WT								Mean	SEM
baseline	173.09	168.38	129.42	117.47	115.42	94.16	74.82	124.68	13.65
relaxation	140.49	144.02	115.98	101.35	50.68	51.14	51.96	93.66	15.95
ΔCPP	-32.60	-24.35	-13.44	-16.12	-64.74	-43.01	-22.86	-31.02	6.77
% ΔCPP	-18.84	-14.46	-10.38	-13.72	-56.09	-45.68	-30.55	-27.10	6.70

NPR-C KO						Mean	SEM
baseline	163.71	161.53	143.79	99.80	93.75	132.52	15.02
relaxation	148.17	142.82	127.29	89.35	77.90	117.10	14.21
ΔCPP	-15.54	-18.71	-16.50	-10.46	-15.85	-15.41	1.36
% ΔCPP	-9.49	-11.59	-11.48	-10.48	-16.91	-11.99	1.29

Figure 30. Coronary reactivity in hearts from male WT and NPR-C KO mice in response to CNP.

Coronary endothelium-independent relaxation to CNP (10nmol), in the presence of L-NAME (300µM), in WT and NPR-C KO mice. Data are represented as the mean±SEM. n=5-7; *p<0.05 (unpaired t-test), significantly different compared to WT littermates.

IR injury in male WT and NPR-C KO mice

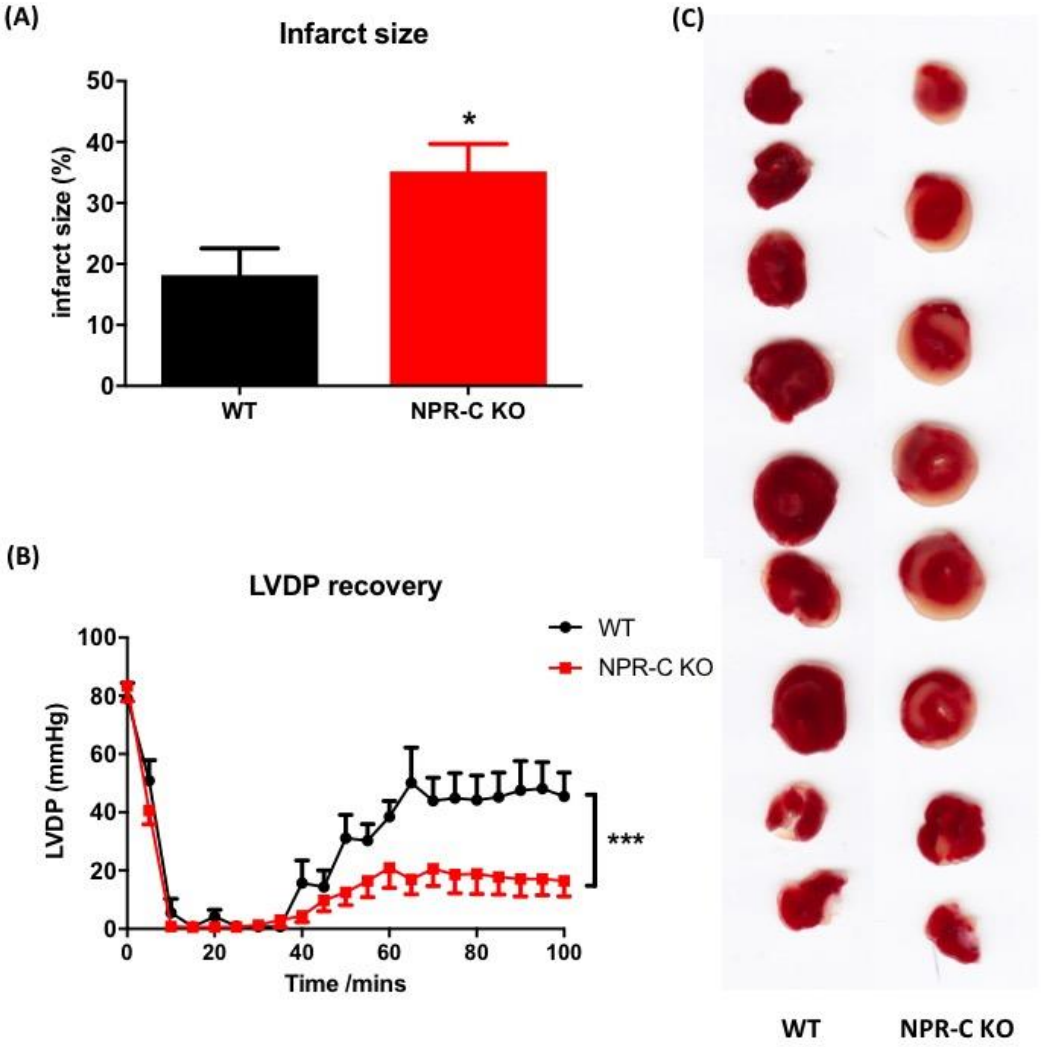

Figure 31. IR injury in male WT and NPR-C KO mice.

Infarct size (A) and left ventricular developed pressure (LVDP) (B) in isolated hearts from WT and NPR-C KO mice subjected to 35 minutes ischaemia followed by 60 minutes reperfusion. Representative images of TTC staining for infarcted areas (white regions) are illustrated (C). Data are represented as the mean±SEM. n=5-7. Unpaired t-test and 2-way ANOVA with Bonferroni *post-hoc* test was used to analyse infarct size and LVDP, respectively. **p*<0.05, ****p*<0.001, significantly different from corresponding WT littermates.

3.6 Summary of key findings

I have demonstrated that endothelium-derived CNP regulates coronary vascular function, at least in part, via NPR-C activation. In addition, production of CNP in the cardiomyocyte, rather than endothelium, protects the heart from IR injury via activation of NPR-C signalling. These data suggest CNP of endothelial and cardiomyocyte origins coordinate to govern coronary vascular function and cardioprotection following ischaemia. This intimates CNP may play an important role in ischaemic heart disease and represents a novel therapeutic target.

Chapter 4 – Results II

Chapter 4 – Results II

4 Results II

4.1 Introduction

The co-localisation of CNP and its cognate receptors in the heart (Del Ry et al., 2011b) suggests a possible role for CNP in regulating cardiac function in a physiological setting and in pathologies such as HF. Indeed, myocardial CNP production and plasma levels are increased in patients with HF (Cabiati et al., 2013, Del Ry et al., 2006a, Kalra et al., 2003). Moreover, pharmacological administration of CNP *in vivo* improves cardiac function and slows cardiac remodelling in pre-clinical MI and pressure-overload (i.e. HF) models (Soeki et al., 2005, Wang et al., 2007, Izumiya et al., 2012). This protective effect of exogenous CNP on cardiac remodelling is probably the result of its anti-hypertrophic and anti-fibrotic actions (Horio et al., 2003, Soeki et al., 2005). However, a role for endogenous CNP in cardiac function has not been demonstrated. Previous work has suggested that the protective effect of exogenous CNP can be attributed to activation of the NPR-B/cGMP cascade (Langenickel et al., 2006, Rosenkranz et al., 2003). Downregulation of NPR-B signalling contributes to cardiac hypertrophy but not fibrosis in preclinical models (Langenickel et al., 2006), suggesting NPR-B activation may not (solely) be the receptor responsible for the protection against maladaptive cardiac remodelling. On the other hand, NPR-C signalling appears to be involved in cardiac fibroblast and myocyte proliferation (Rose and Giles, 2008), suggesting NPR-C may play a part in preventing disease progression. In this chapter I have examined the patho/physiological role of CNP in cardiac function by using cmCNP KO mice subjected to two HF models; ISO-induced HF and pressure overload. Also, I have investigated the role of NPR-C in cardiac remodelling by using global NPR-C KO mice.

4.2 Isoprenaline-induced heart failure

4.2.1 Pilot studies in WT mice

Sustained β-adrenoceptor activation by chronic administration of ISO induces cardiac hypertrophy and fibrosis as well as myocardial necrosis, which leads to progressive HF (Grimm et al., 1998). This HF model mimics aspects of the sympathetic hyperactivation in

human HF (Packer, 1992). In my pilot studies, WT mice subjected to ISO (20 or 30 mg/kg/day, 14 days) via osmotic mini-pump elicited a trend towards an increase in left ventricular internal diameter (LVID) and left ventricular posterior wall diameter (LVPW), accompanied by a reduction in ejection fraction (EF) and fractional shortening (FS) (data not shown). In order to decide the optimum time course for ISO infusion in my studies (anticipating a deterioration in mice lacking cardiomyocyte-derived CNP), I conducted another set of pilot experiments utilising 20mg/kg/day ISO for 7 days and 14days. Both time courses exhibited a progressive cardiac dysfunction with a time-dependent increase in LVIDs (baseline, 1.75±0.12mm; 7 days ISO, 2.17±0.12mm; 14 days ISO, 2.39±0.17mm; $P<0.01$; n=5-9) and decrease in EF (baseline, 78.34±2.84%; 7 days ISO, 70.29±3.49%; 14 days ISO, 65.44±4.95%; $P<0.05$; n=5-9) (Figure 32). The heart and LV weights were also significantly increased after 14 days of ISO infusion (HW/BW: control, 0.50±0.02%, 14days ISO, 0.67±0.01%; $P<0.001$; LV/BW: control, 0.43±0.02%; 14days ISO 0.52±0.01%; $P<0.05$; n=5-9) (Figure 33). 14 day ISO administration induced a more severe cardiac dysfunction, so I decided to use the 7 day time period to study HF in cmCNP KO mice in order to be able to detect increased pathology.

4.2.2 Isoprenaline-induced heart failure in cmCNP KO mice

4.2.2.1 Effects of ISO-induced HF in WT and cmCNP KO mice on heart rate and blood pressure measured by radio-telemetry

The effects of ISO infusion (20mg/kg/day; 7 days) on HR, MABP and locomotor activity were measured by radio-telemetry over 24 hours (12 hours in light and 12 hours darkness). β-adrenoceptor hyperactivation by ISO infusion for 7 days increased HR by approximately 50bpm in both WT and cmCNP KO mice (WT: baseline, 590±5.50bpm, + ISO, 638±5.05bpm; cmCNP KO: baseline, 586±7.76bpm, + ISO, 640±4.80bpm; $P<0.01$; n=3) (Figure 34). There was no difference in the MABP and locomotor activity (Figure 35 and 36). In addition, the HF models were conducted in male animals because a sex difference is apparent in vascular reactivity (female mice are more reliant on CNP in the context of endothelial dysfunction; this study and Moyes *et al*. [2014]), and I wanted to investigate the direct effect of CNP deletion on the myocardium rather than potentially via indirectly altering endothelial signalling.

4.2.2.2 Effects of ISO-induced HF in WT and cmCNP KO mice on cardiac structure measured by echocardiography

Echocardiography was used to investigate cardiac function in a temporal fashion. Abrogation of cardiomyocyte-derived CNP did not affect cardiac function at baseline compared to WT controls, with no difference observed in chamber diameter (WT, 3.548±0.106mm; cmCNP KO, 3.545±0.080mm) (Figure 37), LVPW thickness (WT, 0.780±0.072mm; cmCNP KO, 0.816±0.058mm) (Figure 38), and EF (WT, 70.69±1.87%; cmCNP KO, 75.26±2.69%; all P>0.05; n=6) (Figure 39). After 7 days of ISO infusion, changes in cardiac structure and function were apparent in all animals but was more prominent in cmCNP KO mice with greater reduction in EF and FS (EF: cmCNP KO, Δ-23.87 ±8.61% vs. WT, Δ-3.90±6.09%; FS: cmCNP KO Δ-16.33±5.47% vs. WT, Δ-2.35±4.55%; p<0.05; n=6) (Figure 39). Mice lacking myocardial CNP also exhibited an enlargement of the LV chamber following ISO infusion, which was illustrated by a significant increase in LVID at both diastole and systole (LVID;d, Δ+0.47±0.16mm; LVID;s Δ+0.95±0.32mm; p< 0.05 compared to WT; n=6) (Figure 37). However, ISO did not expand the diameter of the LV chamber in WT controls.

4.2.2.3 Histology

Whole heart and LV weight were similar between WT and cmCNP KO following ISO infusion (HW/BW: WT, 0.57±0.02%; cmCNP KO, 0.57±0.01%; LV/BW: WT, 0.42±0.01%; cmCNP KO, 0.41±0.01%; p>0.05; n=6) (Figure 40). Consistent with these data, the increase in cardiomyocyte size in response to ISO also showed no genotypic difference (WT, 281.5±15.29μm^2 vs. cmCNP KO, 295.1±10.52μm^2; p>0.05; n=6) (Figure 42). These findings suggest that, despite changes in LVID, endogenous CNP might not play a significant role in ISO-induced cardiac hypertrophy. However, images obtained from MSB and picro-sirus red staining illustrated higher collagen deposition in cmCNP KO mice (WT, 9.41±1.54% vs. cmCNP KO, 13.86±1.49%; p<0.05; n=5-6) (Figure 41), suggesting cardiomyocyte-derived CNP may play a role in preventing the development of cardiac fibrosis.

Taken together, these observations imply that in chronic β-adrenergic stimulation cardiomyocyte-derived CNP prevents myocardial stiffening, preserves LV structure and maintains cardiac contractility, probably by limiting cardiac fibrosis, but has less of an impact on cardiac hypertrophy *per se*.

Effect of increasing the time period of isoprenaline infusion on cardiac structure and function in WT mice

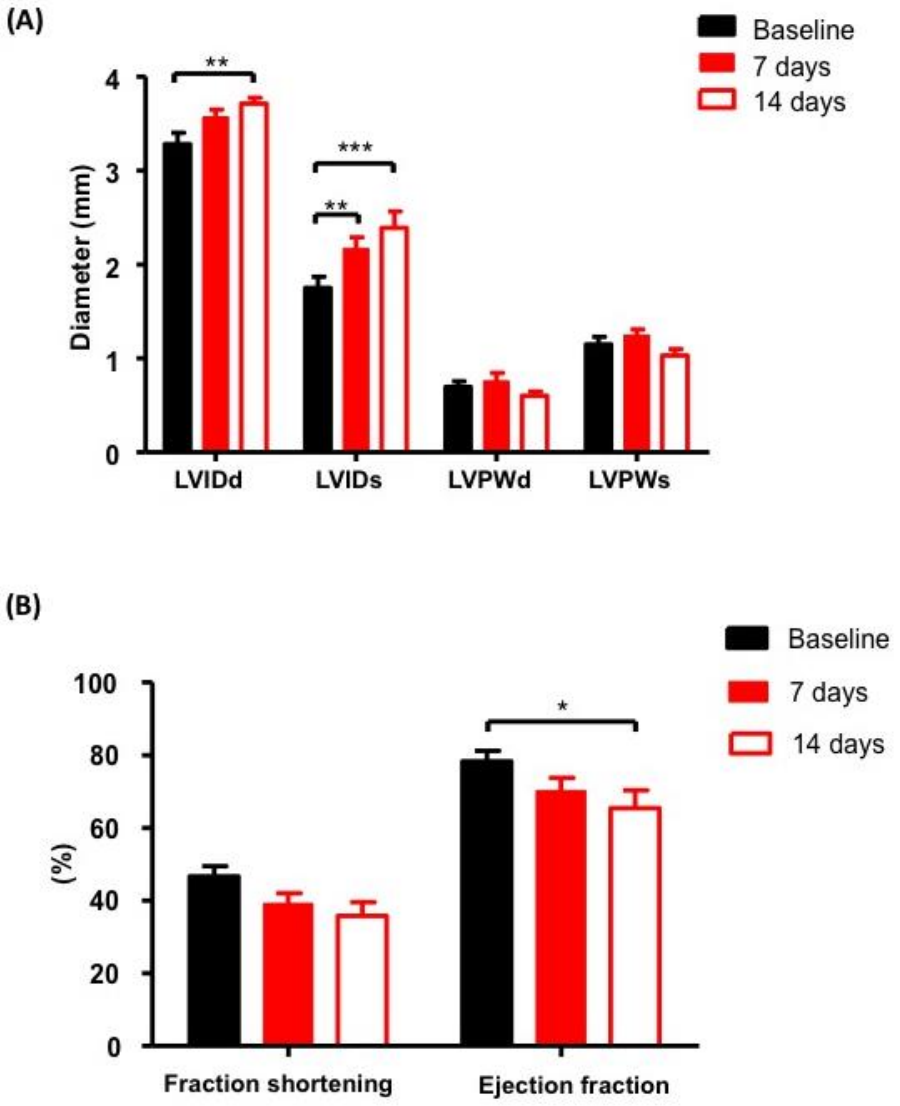

Figure 32. Effect of increasing the time period of isoprenaline infusion on cardiac structure and function in WT mice

Left ventricular structure (A) and contractile function (B) at baseline, 7 days and 14 days following 20mg/kg/day of isoprenaline infusion. Left ventricular internal diameter at end-diastole (LVID;d), and at end-systole (LVID;s), left ventricular posterior wall at end-diastole (LVPW;d) and at end-systole (LVPW;s). Data are represented as the mean±SEM. n=5-9. *p<0.05, **p<0.01, ***p<0.001, significantly different from corresponding WT littermates using 1-way ANOVA followed by Bonferroni *post-hoc* test.

Effect of isoprenaline infusion on the heart and left ventricular weight in WT mice

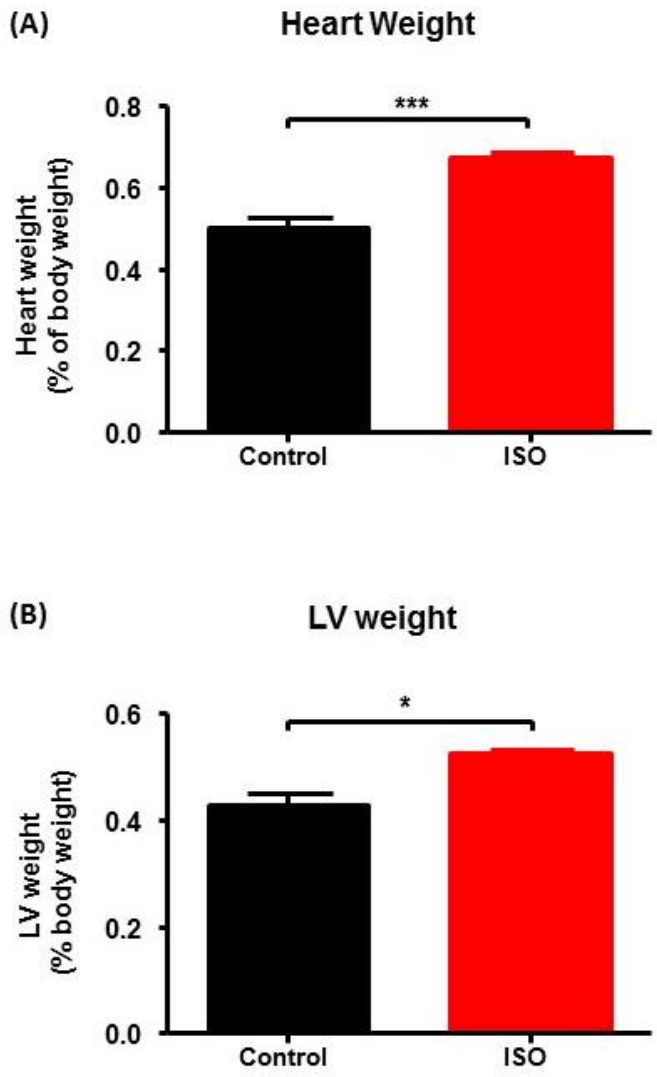

Figure 33. Effect of isoprenaline infusion on heart and left ventricular weight in WT mice.

Whole heart (A) and left ventricular (LV, [B]) weights are measured following 14 days of isoprenaline infusion (20mg/kg/day). Data are represented as the mean±SEM. n=5-9. *p<0.05, ***p<0.001 significantly different from control using unpaired t-test.

Effect of isoprenaline infusion on heart rate in WT and cmCNP KO mice

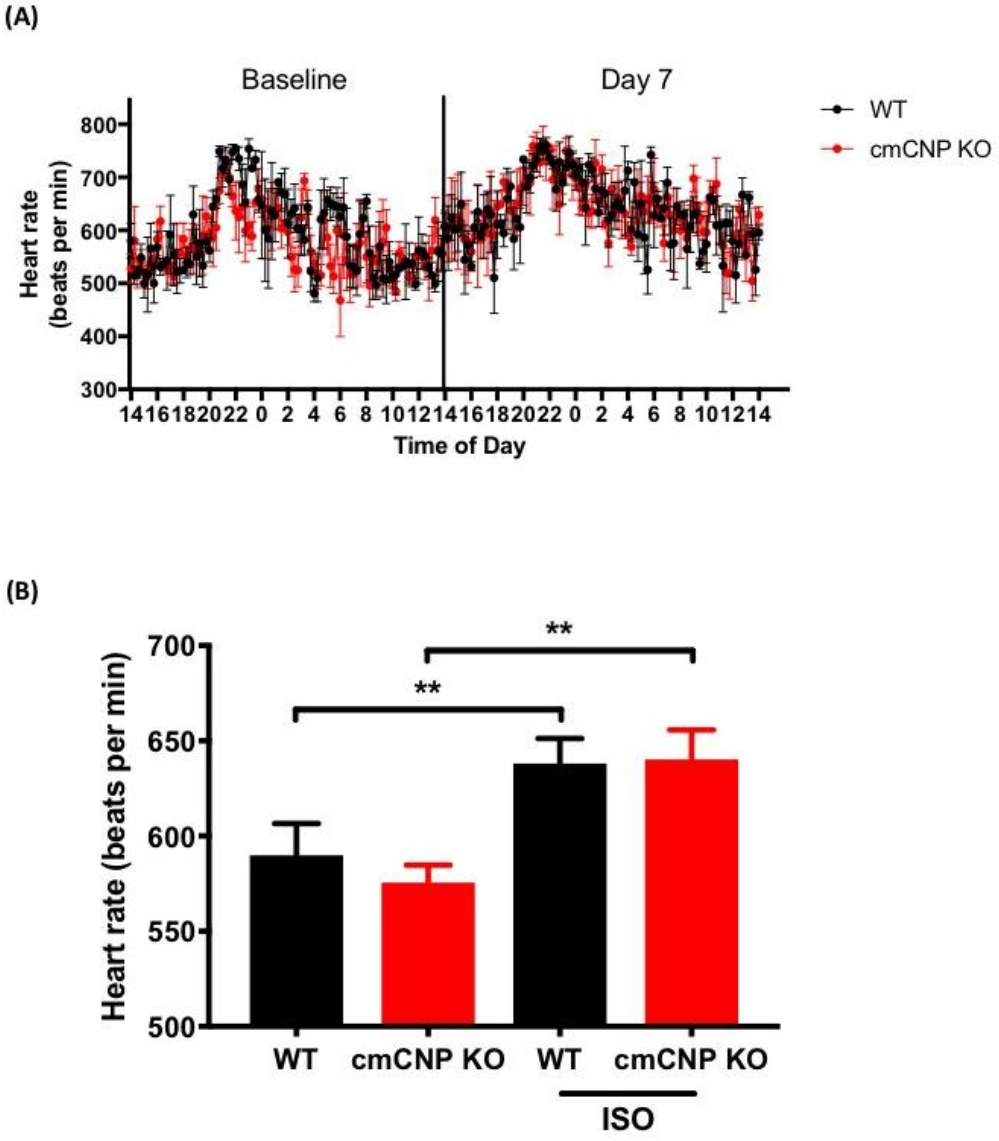

Figure 34. Effect of isoprenaline infusion on heart rate in WT and cmCNP KO mice.

Telemetry probe recording of the heart rate of WT and cmCNP KO mice at baseline and exposed to 7 days isoprenaline (20mg/kg/day) over a 24 hour period; (A) circadian cycle, (B) mean heart rate. Data are represented as the mean±SEM. n=3; $^{**}p<0.01$ using 2-way ANOVA followed by Bonferroni *post-hoc* test.

Effect of isoprenaline infusion on mean arterial blood pressure in WT and cmCNP KO mice

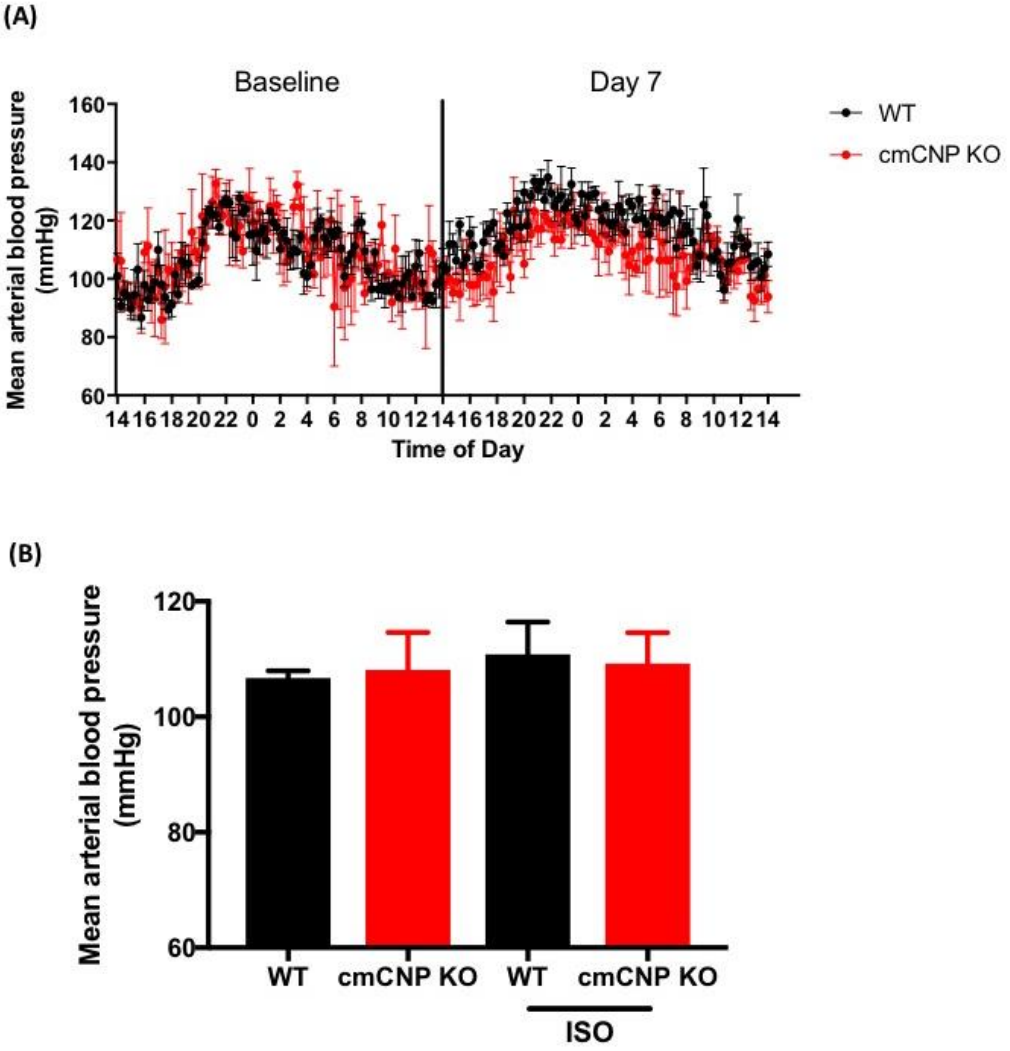

Figure 35. Effect of isoprenaline infusion on mean arterial blood pressure in WT and cmCNP KO mice.

Telemetry probe recording of the blood pressure of WT and cmCNP KO mice at baseline and exposed to 7 days isoprenaline (20mg/kg/day) over a 24 hour period; (A) circadian cycle, (B) mean arterial blood pressure. Data are represented as the mean±SEM. n=3.

Effect of isoprenaline infusion on activity in WT and cmCNP KO mice

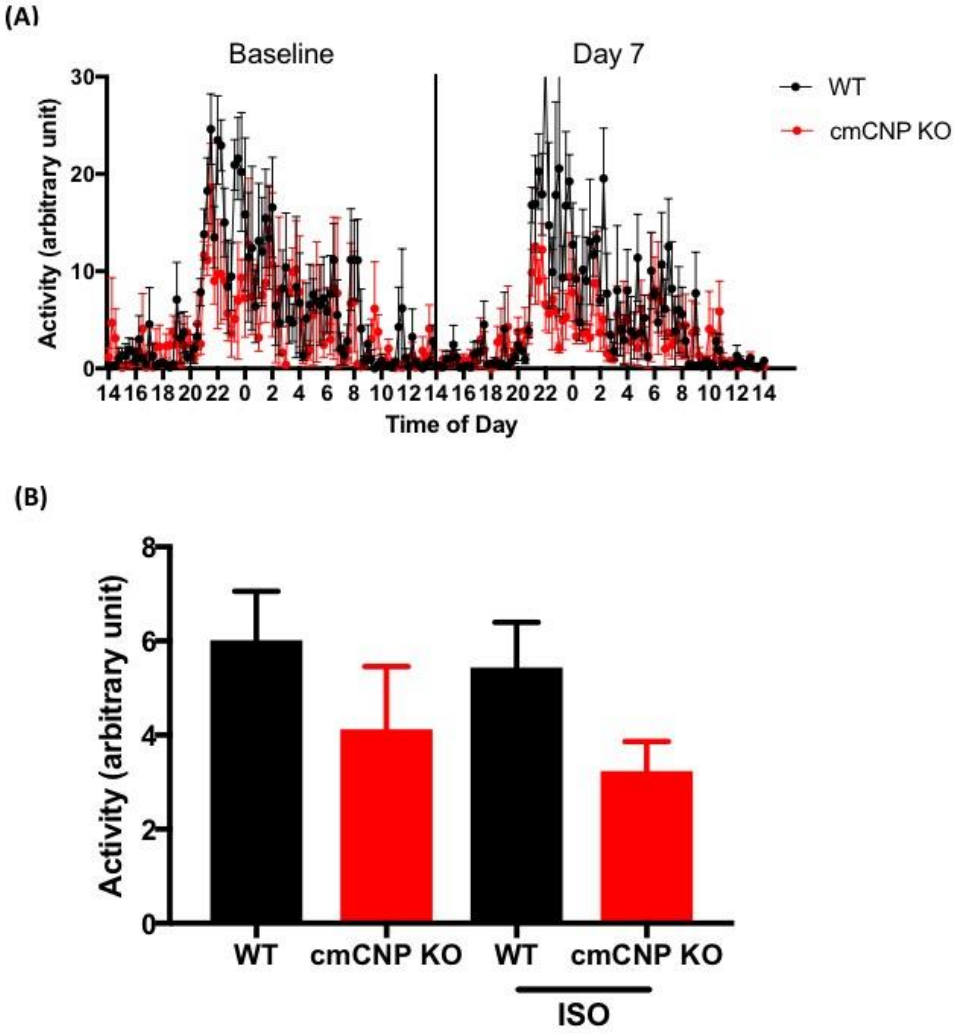

Figure 36. Effect of isoprenaline infusion on activity in WT and cmCNP KO mice.

Telemetry probe recording of the locomotor activity of WT and cmCNP KO mice at baseline and exposed to 7 days isoprenaline (20mg/kg/day) over a 24 hour period; (A) circadian cycle, (B) mean locomotor activity. Data are represented as the mean±SEM. n=3.

Effect of cardiomyocyte CNP deletion on cardiac structure in isoprenaline-induced heart failure

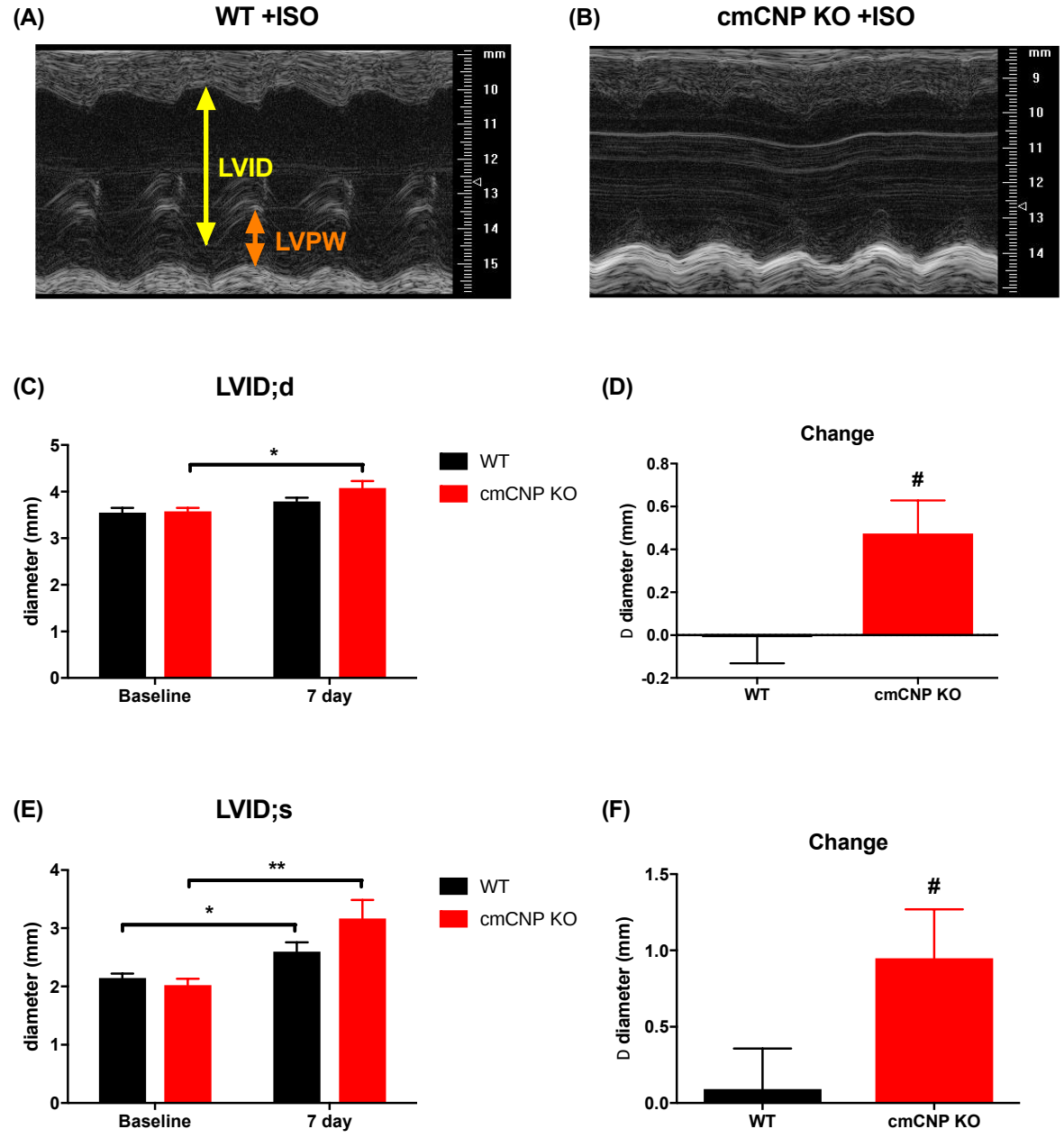

Figure 37. Effect of cardiomyocyte CNP deletion on cardiac structure in isoprenaline-induced heart failure.

Representative echocardiography images from WT (A) and cmCNP KO (B) mice exposed to 7 days isoprenaline (20mg/kg/day). Left ventricular internal diameter at end-diastole (LVID;d) (A, C) and at end-systole (LVID;s) (E, F). Data are represented as the mean±SEM. n=6. *p<0.05, **p<0.01, using 2-way ANOVA followed by Bonferroni post-hoc test. #p<0.05 significantly different compared to WT using unpaired t-test.

Effect of cardiomyocyte CNP deletion on cardiac structure in isoprenaline-induced heart failure

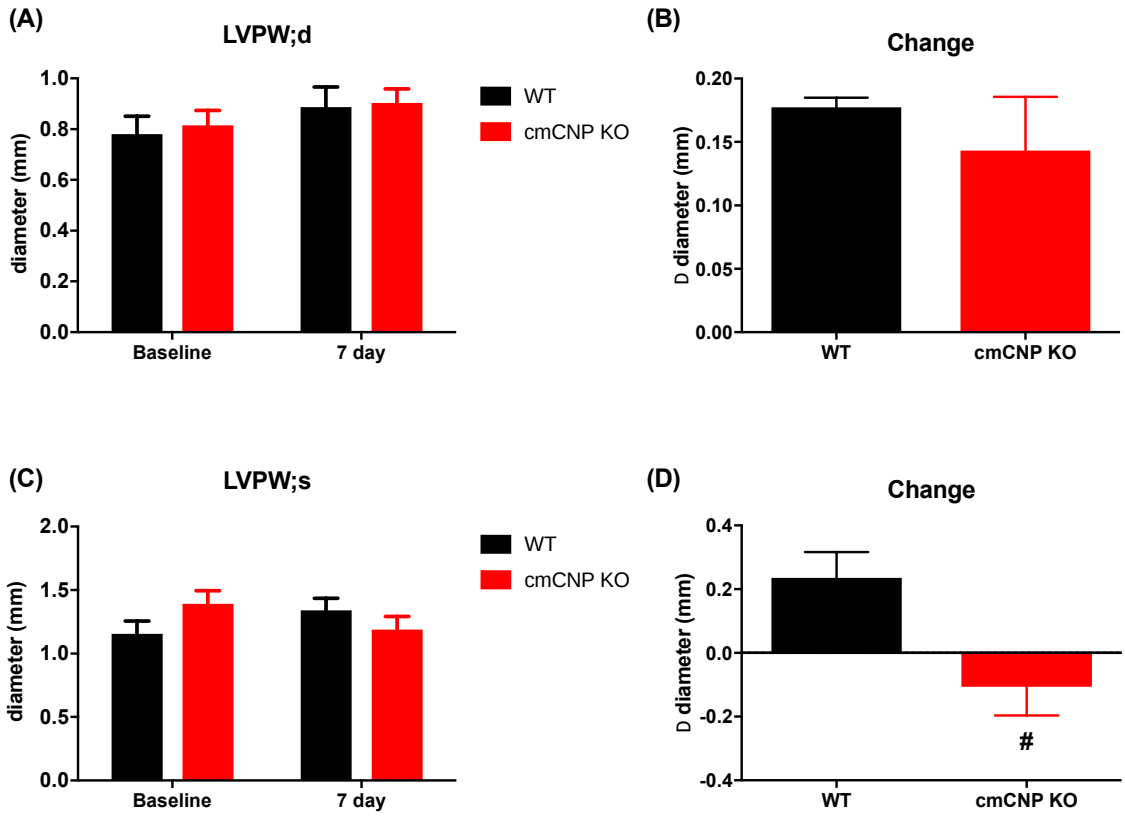

Figure 38. Effect of cardiomyocyte CNP deletion on left ventricular posterior wall diameter in isoprenaline-induced heart failure

Echocardiographic measurements of left ventricular posterior wall at end-diastole (LVPW;d) (A, B) and end-systole (LVPW;s) (C, D) in WT and cmCNP KO mice exposed to 7 days isoprenaline (20mg/kg/day). Data are represented as the mean±SEM. n=6. #p<0.05 significantly different compared to WT using unpaired t-test.

Effect of cardiomyocyte CNP deletion on systolic function in isoprenaline-induced heart failure

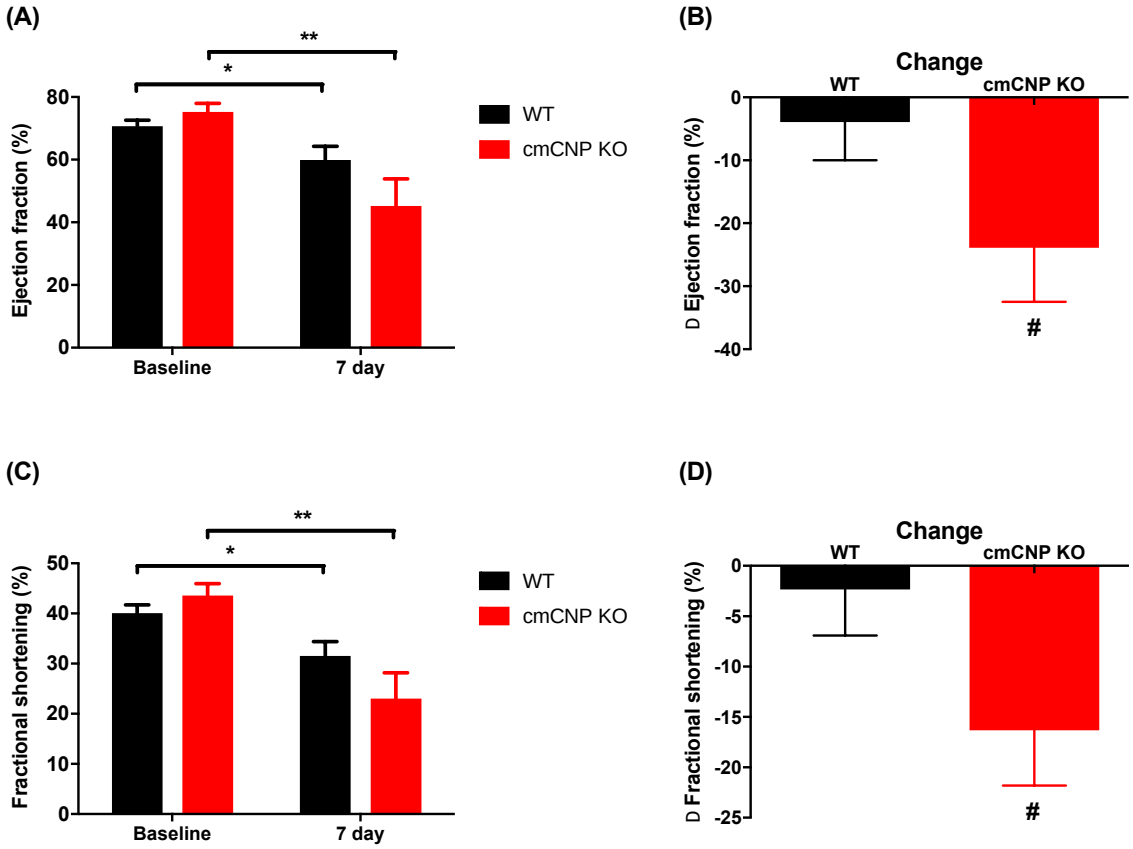

Figure 39. Effect of cardiomyocyte CNP deletion on systolic function in isoprenaline-induced heart failure.

Echocardiographic measurements of ejection fraction (EF) (A and B) and fractional shortening (FS) (C and D) in WT cmCNP KO mice exposed to 7 days of isoprenaline (ISO) infusion (20mg/kg/day). Data are represented as the mean±SEM. n=6. *p<0.05, **p<0.01 significantly different compared to baseline using 2-way ANOVA followed by Bonferroni *post-hoc* test. #p<0.05 significantly different compared to WT using unpaired t-test.

Effect of cardiomyocyte CNP deletion on the heart and left ventricular weight in isoprenaline-induced heart failure

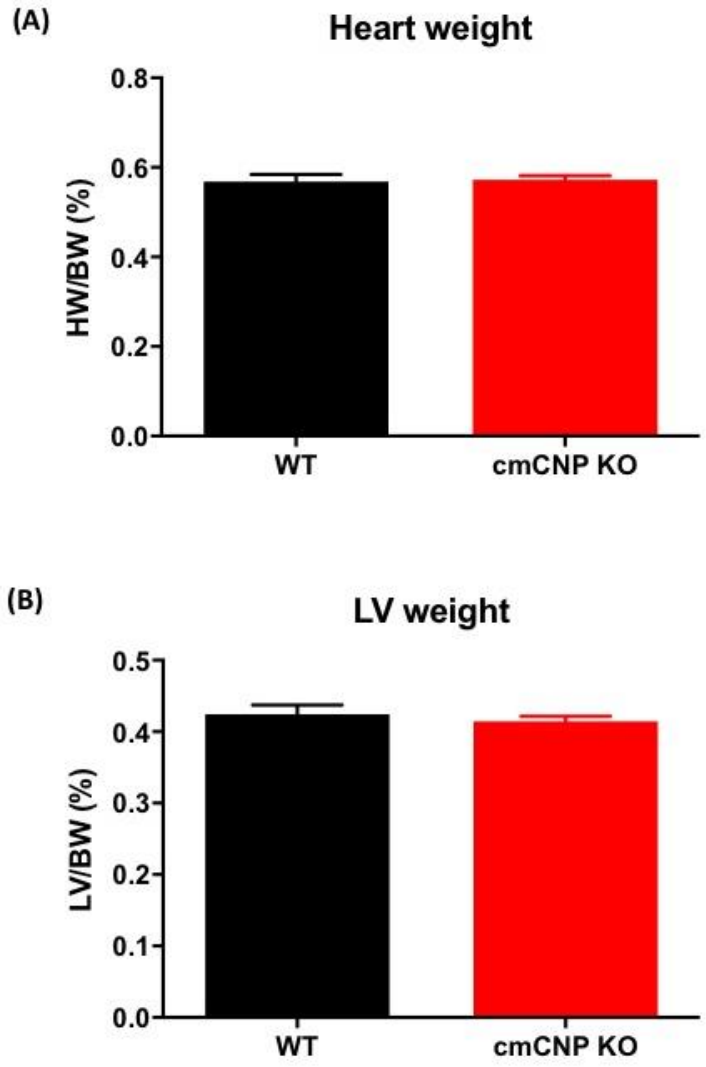

Figure 40. Effect of cardiomyocyte CNP deletion on the heart and left ventricular weight in isoprenaline-induced heart failure.

Whole heart (A) and left ventricular weight (B) in WT and cmCNP KO mice were measured following 7 days isoprenaline infusion (20mg/kg/day). Data are represented as the mean±SEM. n=6.

Effect of cardiomyocyte CNP deletion on cardiac fibrosis in isoprenaline-induced heart failure

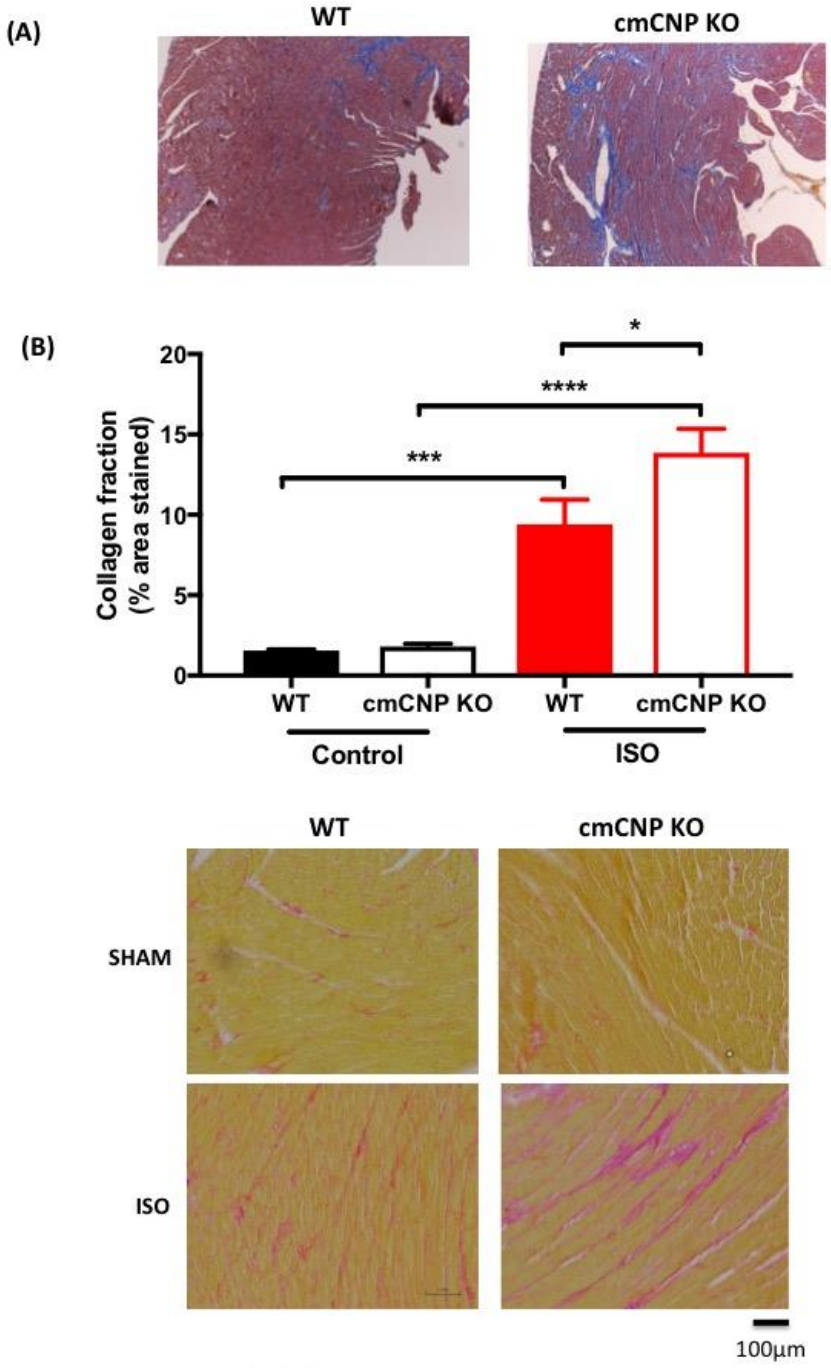

Figure 41. The effect of cardiomyocyte CNP deletion on cardiac fibrosis in isoprenaline-induced heart failure.

Martius Scarlet Blue staining (A): fibrin (red), erythrocytes (yellow) and connective tissue (blue), magnification 5X. Picro-sirus red staining (B): cytoplasm (yellow) and collagen (as an index of fibrosis) (red), magnification 20X. Data are represented as the mean±SEM. n=5-6. *p<0.05, ***p<0.001, ****p<0.0001 using 2-way ANOVA followed by Bonferroni *post-hoc* test.

Effect of cardiomyocyte CNP deletion on cardiomyocyte hypertrophy in isoprenaline-induced heart failure

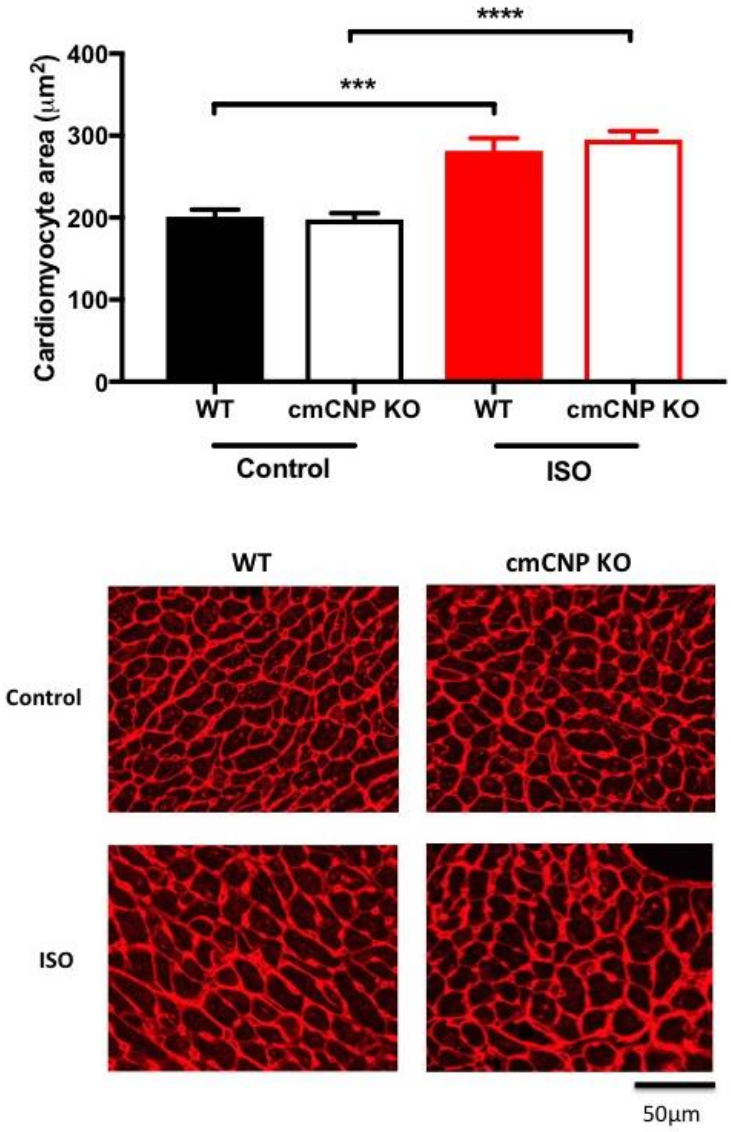

Figure 42. Effect of cardiomyocyte CNP deletion on cardiomyocyte hypertrophy in isoprenaline-induced heart failure.

Cardiomyocyte area (A) in WT and cmCNP KO mice exposed to 7 days isoprenaline (20mg/kg/day). (B) Representative wheat germ agglutinin (WGA) fluorescence stained images from each group, magnification 20X. Data are represented as the mean±SEM. n=6. ***p<0.001, ****p<0.0001 using 2-way ANOVA followed by Bonferroni *post-hoc* test.

4.3 Pressure overload-induced heart failure in cmCNP KO mice

4.3.1 Echocardiography

To determine whether cardiomyocyte-derived CNP had protective effects in a second, aetiologically distinct model of HF, I measured the development of cardiac dysfunction and remodelling in animals subjected to AAC-induced pressure-overload for 6 weeks. There was no genotypic difference in sham-operated animals (Figure 43 and Figure 44). AAC caused an increase in LVID in control mice (LVID;d, sham 3.46±0.10mm vs. AAC 3.84±0.09mm; LVID;s, sham 1.96±0.09mm vs. AAC 2.49±0.07mm; p<0.001; n=10) (Figure 43). Also, cardiac dysfunction was apparent with a significant reduction in EF and FS following AAC (EF, sham 75.20±1.55% vs. AAC 64.72±0.81%; FS, sham 43.54±1.60%, AAC 35.23±0.64%; p<0.001; n=10) (Figure 44). However, there were no significant changes in the diameter of the LVPW (Figure 43). In cmCNP KO mice, LVID increased to the same extent as WT in response to AAC (Figure 43). However, EF and FS were significantly lower than control animals following AAC (EF, WT 64.72±0.81% vs. cmCNP KO 56.35±2.32%; FS, WT 35.23±0.64% vs. cmCNP KO 28.70±1.49%; p<0.01; n=10) (Figure 44). Importantly, the increase in MABP following AAC was similar in both genotypes (WT, 108.6±1.319mmHg; cmCNP KO 108.0±1.795mmHg; n=7-10) (Figure 46), indicating the more severe phenotype observed in cmCNP KO mice was independent of afterload.

4.3.2 Histology

Whole heart and LV weight were significantly augmented in response to AAC in WT animals (HW/BW, sham 0.448±0.013% vs. AAC 0.557±0.014%; p<0.001; n=6-9) (Figure 45), indicating ventricular remodelling in response to haemodynamic stress. Similar measurements were obtained in cmCNP KO mice (HW/BW, sham 0.457±0.011% vs. AAC 0.567±0.018%; p<0.001; n=6-9) (Figure 45). Quantification of picro-sirus red staining illustrated a significant increase in collagen deposition following AAC in WT (sham 1.56±0.05% vs. AAC 2.94±0.35%; p<0.05; n=6) (Figure 47), indicating a maladaptive fibrosis. However, this structural deficit was significantly higher in cmCNP KO mice (WT AAC 2.94±0.35% vs. cmCNP KO AAC 4.14±0.35%; p<0.05; n=6) (Figure 47). Cardiomyocyte area was also increased in response to AAC in all animals, but a trend towards to a larger cell size was observed in cmCNP KO compared to WT (WT 260.0±3.76μm^2 vs. cmCNP KO 282.4±9.47μm^2; p=0.052; n=6) (Figure 48). Taken together, these findings indicate that cardiomyocyte-derived CNP protects against AAC-induced HF in a similar fashion and to a

similar extent as observed in the sympathetic hyperactivation model; this is primarily via an anti-fibrotic action.

Effect of cardiomyocyte CNP deletion on cardiac structure in pressure overload-induced heart failure

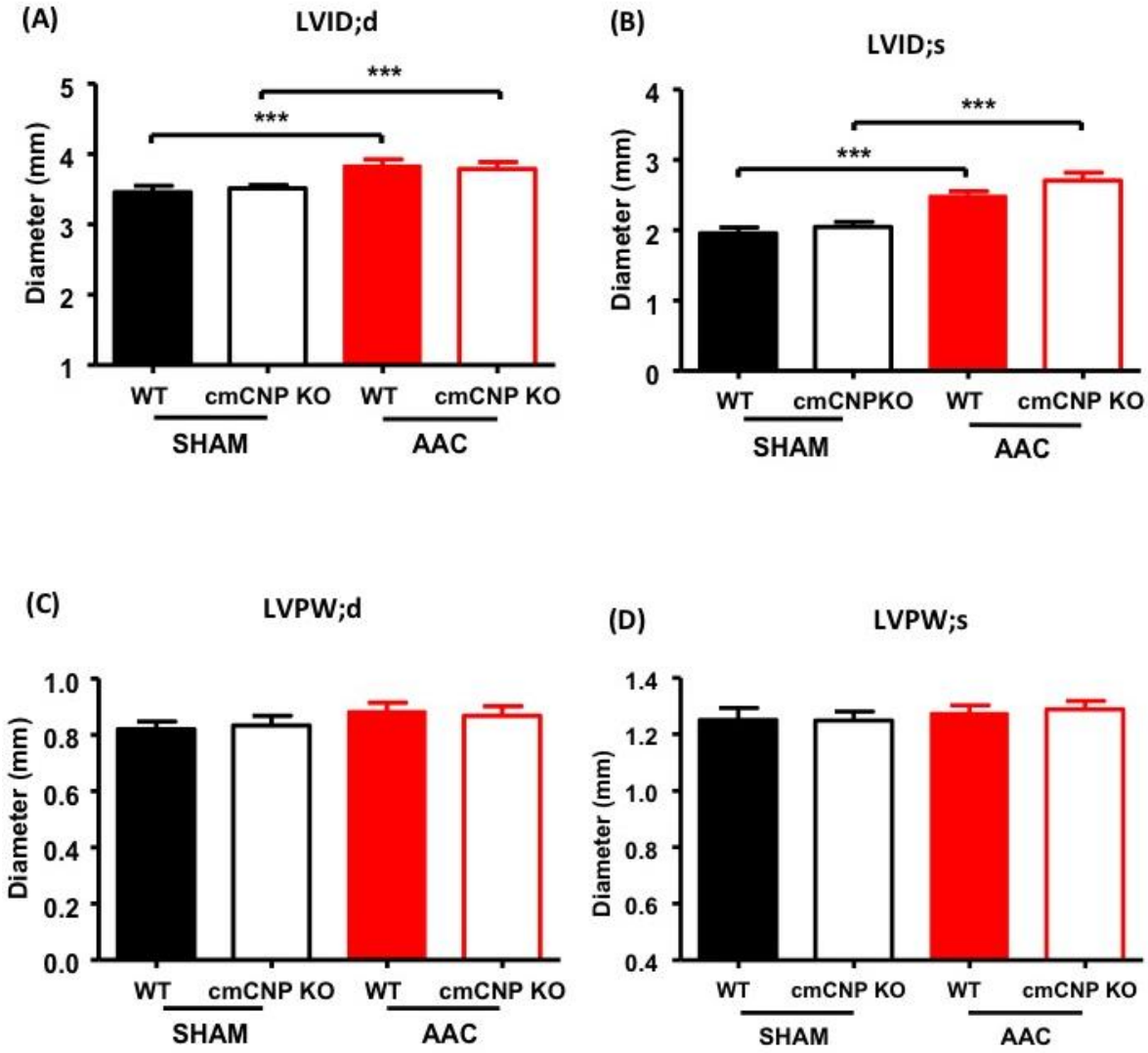

Figure 43. Effect of cardiomyocyte CNP deletion on left ventricular internal diameter and posterior wall in pressure overload-induced heart failure.

Left ventricular internal diameter at end-diastole (LVID;d) (A) and end-systole (LVID;s) (B), left ventricular posterior wall diameter at end-diastole (LVPW;d) and end-systole (LVPW;s) in WT and cmCNP KO mice subjected to sham or abdominal aortic constriction (AAC) for 6 weeks. Data are represented as the mean±SEM. n=10. ***p<0.001 using 2-way ANOVA followed by Bonferroni *post-hoc* test.

Effect of cardiomyocyte CNP deletion on systolic function in pressure overload-induced heart failure

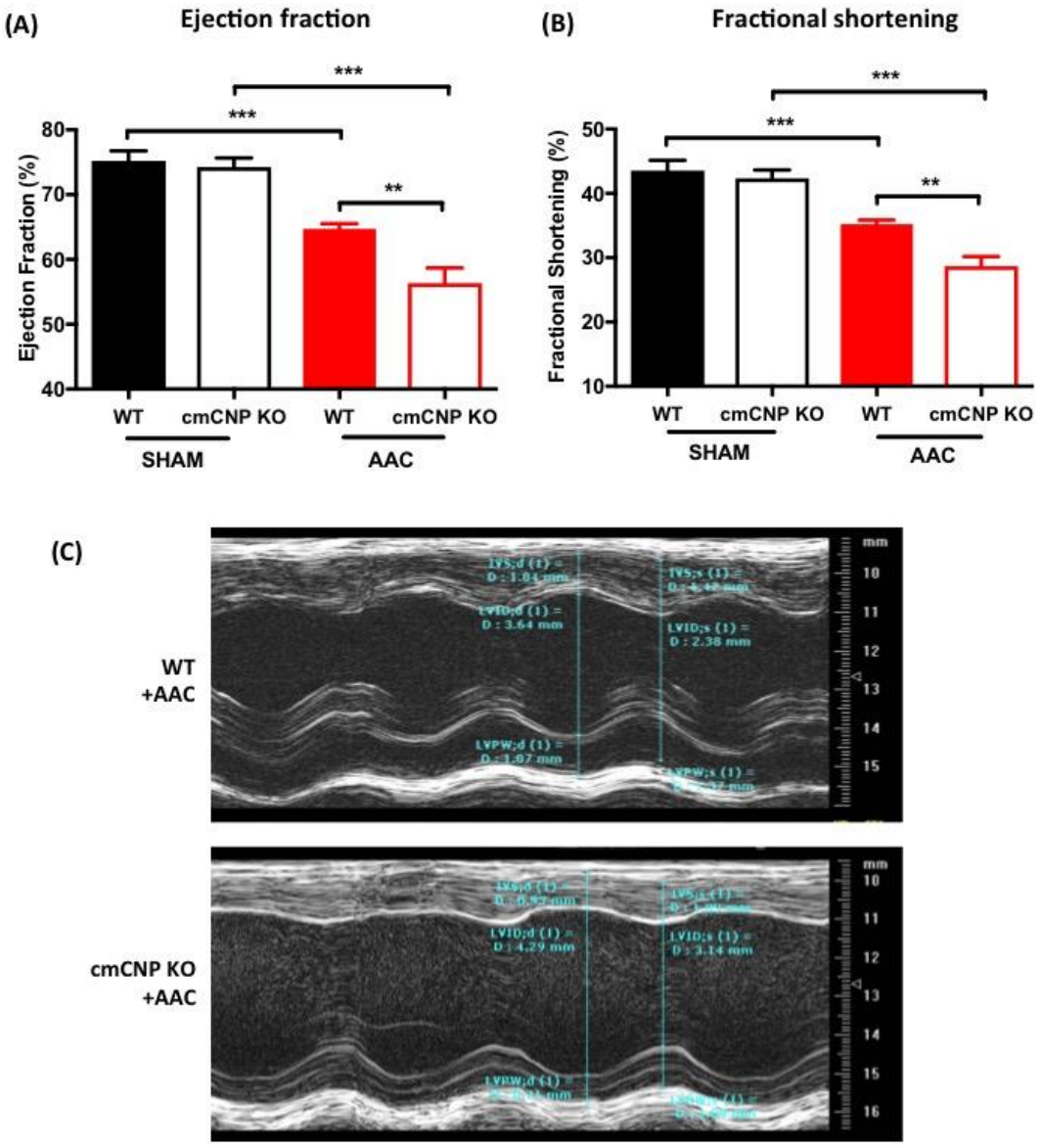

Figure 44. Effect of cardiomyocyte CNP deletion on systolic function in pressure overload-induced heart failure.

Ejection fraction (A) and fractional shortening (B) in WT and cmCNP KO mice subjected to sham or abdominal aortic constriction (AAC) for 6 weeks. (C) Representative echocardiography images from WT and cmCNP KO mice. Data are represented as the mean±SEM. n=10. ***p*<0.01, ****p*<0.001 using 2-way ANOVA followed by Bonferroni *post-hoc* test.

Effect of cardiomyocyte CNP deletion on the heart and left ventricular weight in pressure overload-induced heart failure

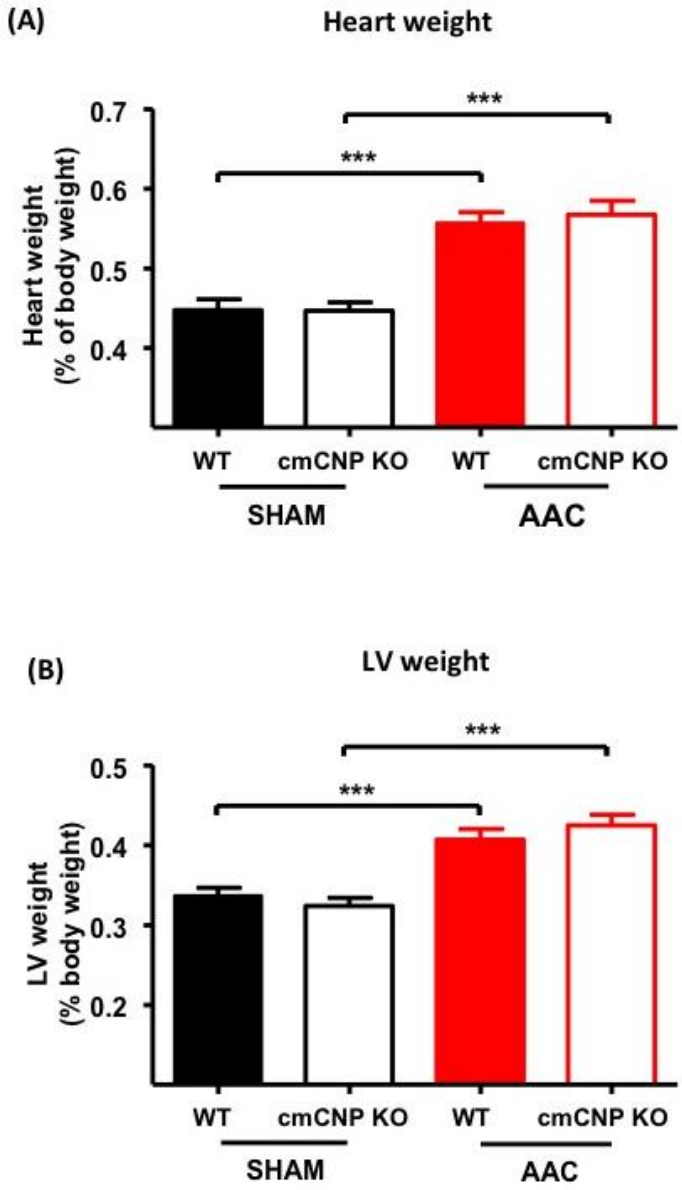

Figure 45. Effect of cardiomyocyte CNP deletion on the heart and left ventricular weight in pressure overload-induced heart failure.

Whole heart (A) and left ventricular (LV) (B) weight in WT and cmCNP KO mice subjected to sham or abdominal aortic constriction (AAC) for 6 weeks. Data are represented as the mean±SEM. n=6-9. ***p<0.001 using 2-way ANOVA followed by Bonferroni *post-hoc* test.

Effect of cardiomyocyte CNP deletion on mean arterial blood pressure in pressure overload-induced heart failure

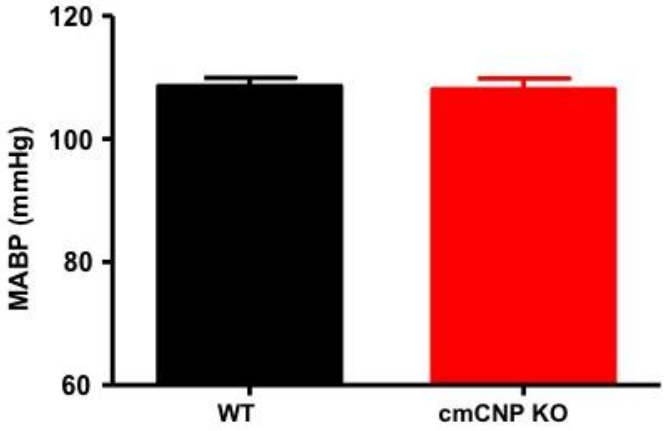

Figure 46. Effect of cardiomyocyte CNP deletion on mean arterial blood pressure in pressure overload-induced heart failure.

Left carotid mean arterial blood pressure (MABP) in WT and cmCNP KO mice subjected to abdominal aortic constriction (AAC) for 6 weeks. Data are represented as the mean±SEM. n=7-10.

Effect of cardiomyocyte CNP deletion on cardiac fibrosis in pressure overload-induced heart failure

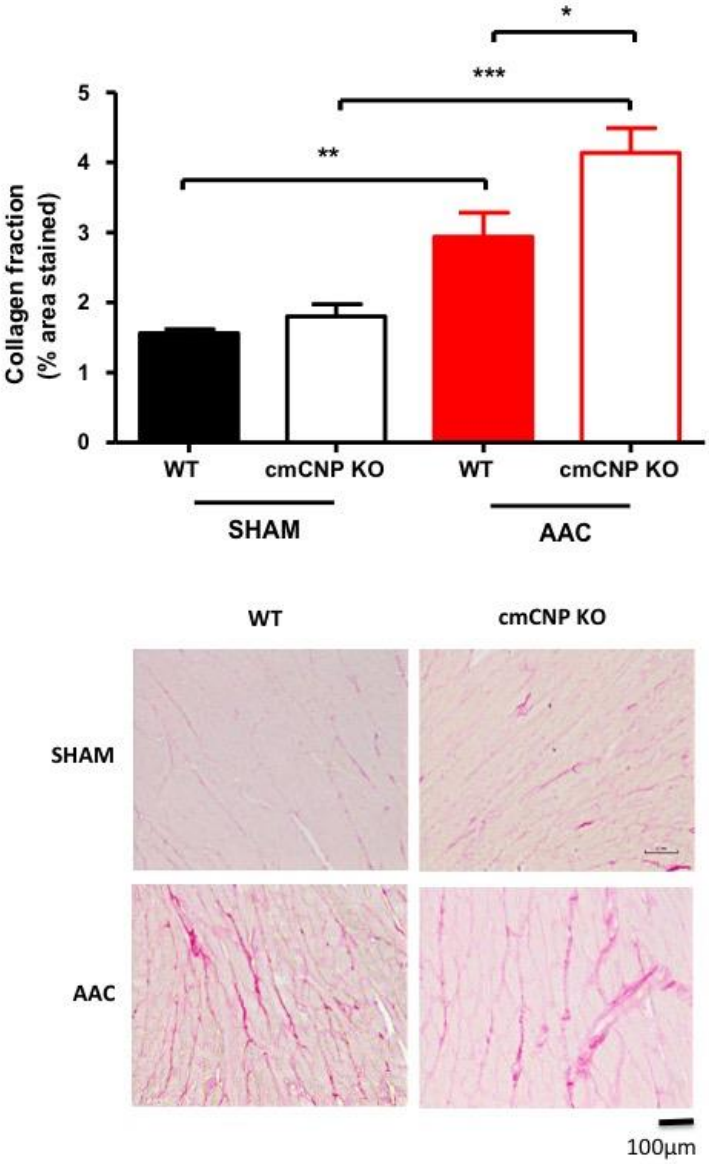

Figure 47. Effect of cardiomyocyte CNP deletion on cardiac fibrosis in pressure overload-induced heart failure.

Left ventricular collagen deposition in WT and cmCNP KO mice subjected to sham or abdominal aortic constriction (AAC) for 6 weeks. Representative piro-sirus red staining images (cytoplasm, yellow; collagen, red) from each group are shown on the lower panel, magnification 20X. Data are represented as the mean±SEM. n=6. *p<0.05, **p<0.01, ***p<0.001 using 2-way ANOVA followed by Bonferroni *post-hoc* test.

Effect of cardiomyocyte CNP deletion on cardiomyocyte hypertrophy in pressure overload-induced heart failure

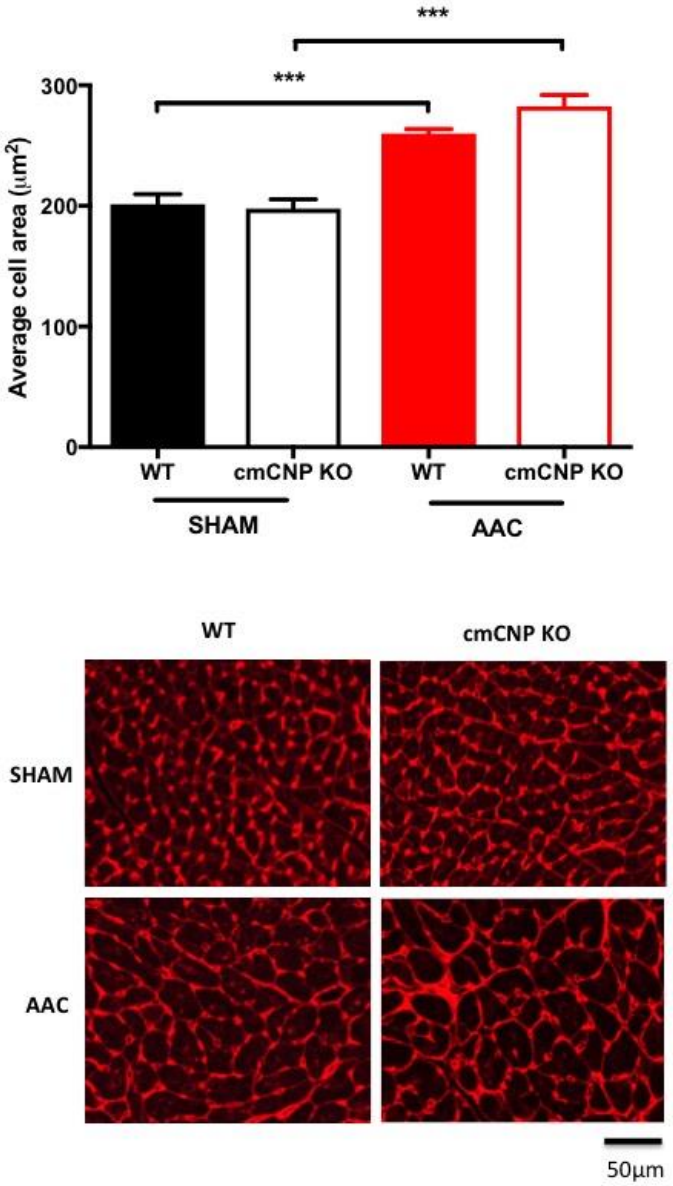

Figure 48. Effect of cardiomyocyte CNP deletion on cardiomyocyte hypertrophy in pressure overload-induced heart failure.

Cardiomyocyte area in WT and cmCNP KO mice subjected to sham or abdominal aortic constriction (AAC) for 6 weeks. Representative wheat germ agglutinin (WGA) fluorescence stained images from each group are shown on the lower panel, magnification 20X. Data are represented as the mean±SEM. n=6. ***p<0.001 using 2-way ANOVA followed by Bonferroni *post-hoc* test.

4.4 The role of CNP in cardiac hypertrophy *in vitro*

Neonatal cardiomyocytes from cmCNP KO mice and littermate controls were isolated and cultured to study the physiological role of CNP in cardiac hypertrophy in an isolated *in vitro* system. Cells with visible striations and that contracted spontaneously were regarded as cardiomyocytes. Cardiomyocyte area was similar at baseline between WT and cmCNP KO (WT, 2596±92.41μm^2; cmCNP KO 2598±61.57μm^2; p>0.05; n=18-23) (Figure 49). However, cardiomyocytes from cmCNP KO were markedly larger than from WT littermates following Ang II treatment (1μM; 48 hours; WT, 3453±96.10μm^2 vs. cmCNP KO, 3927±109.4μm^2; p<0.05; n=15-20) (Figure 49). Exogenous CNP addition (1μM) blunted the cardiomyocyte growth in cmCNP KO cells to a level similar to WT (cmCNP KO +CNP, 3171±106.7μm^2; WT 3372±171.3μm^2; p>0.05; n=8-11) (Figure 49), but did not have an additional effect in WT. This suggests cardiomyocyte-derived CNP has a physiological, autocrine role in preventing cardiac hypertrophy (here in response to Ang II), and can also achieve the same effect from a pharmacological perspective when CNP production is diminished.

Effect of cardiomyocyte CNP deletion and exogenous CNP on cardiomyocyte hypertrophy in response to angiotensin II

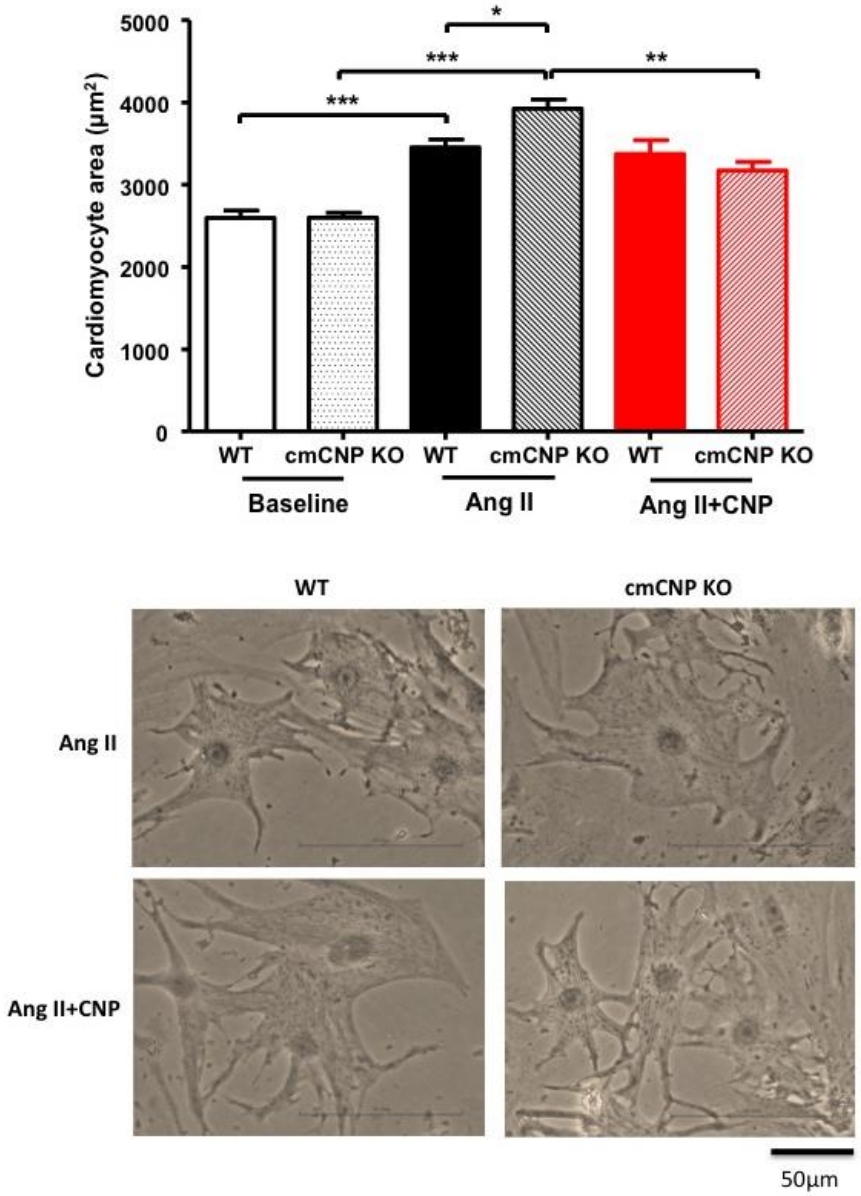

Figure 49. Effect of cardiomyocyte CNP deletion and exogenous CNP on cardiomyocyte hypertrophy in response to angiotensin II.

The cell area of isolated neonatal cardiomyocytes exposed to angiotensin II (Ang II; 1µM) alone or with CNP (1µM) for 48 hours. Representative images of isolated neonatal cardiomyocytes are shown in the lower panel. Data are represented as the mean±SEM. Ang II, n=15-20; Ang II +CNP, n=8-11. *p<0.05, **p<0.01, ***p<0.001 using 2-way ANOVA followed by Bonferroni *post-hoc* test.

4.5 Cardioprotective effects of CNP are mediated via NPR-C activation

In order to investigate which NPR(s) mediates the cardioprotective effects of CNP, the AAC-induced HF model was repeated in global NPR-C KO mice.

4.5.1 Cardiac function in NPR-C KO mice

Similar to cmCNP KO mice, a phenotype involving a significantly more dilated LV was observed in NPR-C KO mice compared to WT littermates subjected to AAC (LVID;d, WT AAC, 3.78±0.07mm vs. NPR-C KO AAC 4.47±0.11mm; LVID;s, WT AAC 2.47±0.05mm vs. cmCNP KO AAC 3.11±0.11mm; $p<0.01$; n=9) (Figure 50). EF and FS were also reduced to an overtly greater extent after AAC in NPR-C KO mice (EF, WT AAC 63.92±0.70% vs NPR-C KO AAC 57.78±2.22%; FS, WT AAC 34.76% vs. NPR-C KO AAC 30.40±1.45%; $p<0.05$; n=9) (Figure 51.). This more severe profile was accompanied by a marked increase in the heart and LV weight in NPR-C KO mice that was considerably higher than WT following AAC (WT, 0.542±0.009% vs. NPR-C KO, 0.636±0.048%; $p<0.05$; n=10-11) (Figure 52). Carotid MABP measurement confirmed that the differences observed were not due to an altered afterload (WT AAC, 110.1±2.09mmHg; NPR-C KO AAC, 105.2±3.85mmHg; $p>0.05$; n=5) (Figure 53).

4.5.2 Histology

A profound increase in fibrosis was observed in both WT and NPR-C KO mice in response to AAC, but the collagen deposition was significantly higher in NPR-C KO (WT, 3.38±0.39% vs. NPR-C KO 5.39±0.62%; $p<0.05$; n=6) (Figure 54). WGA fluorescence staining illustrated a marked increase in cardiomyocyte size after AAC in all animals. Again, the enlargement of the cells was significantly greater in NPR-C KO compared to WT littermates (WT, 265.60±4.26µm2 vs. NPR-C KO, 349.2±14.67µm2; $p<0.001$; n=6) (Figure 55). Taken together, these data suggest the loss of NPR-C signalling results in cardiac hypertrophy and fibrosis in response to pressure overload. Indeed, cardiac remodelling observed in NPR-C KO mice were even more striking than that observed in cmCNP KO (Figure 56), indicating a complete loss of NPR-C signalling is detrimental during cardiac stress.

Effect of global NPR-C deletion on cardiac structure in pressure overload-induced heart failure

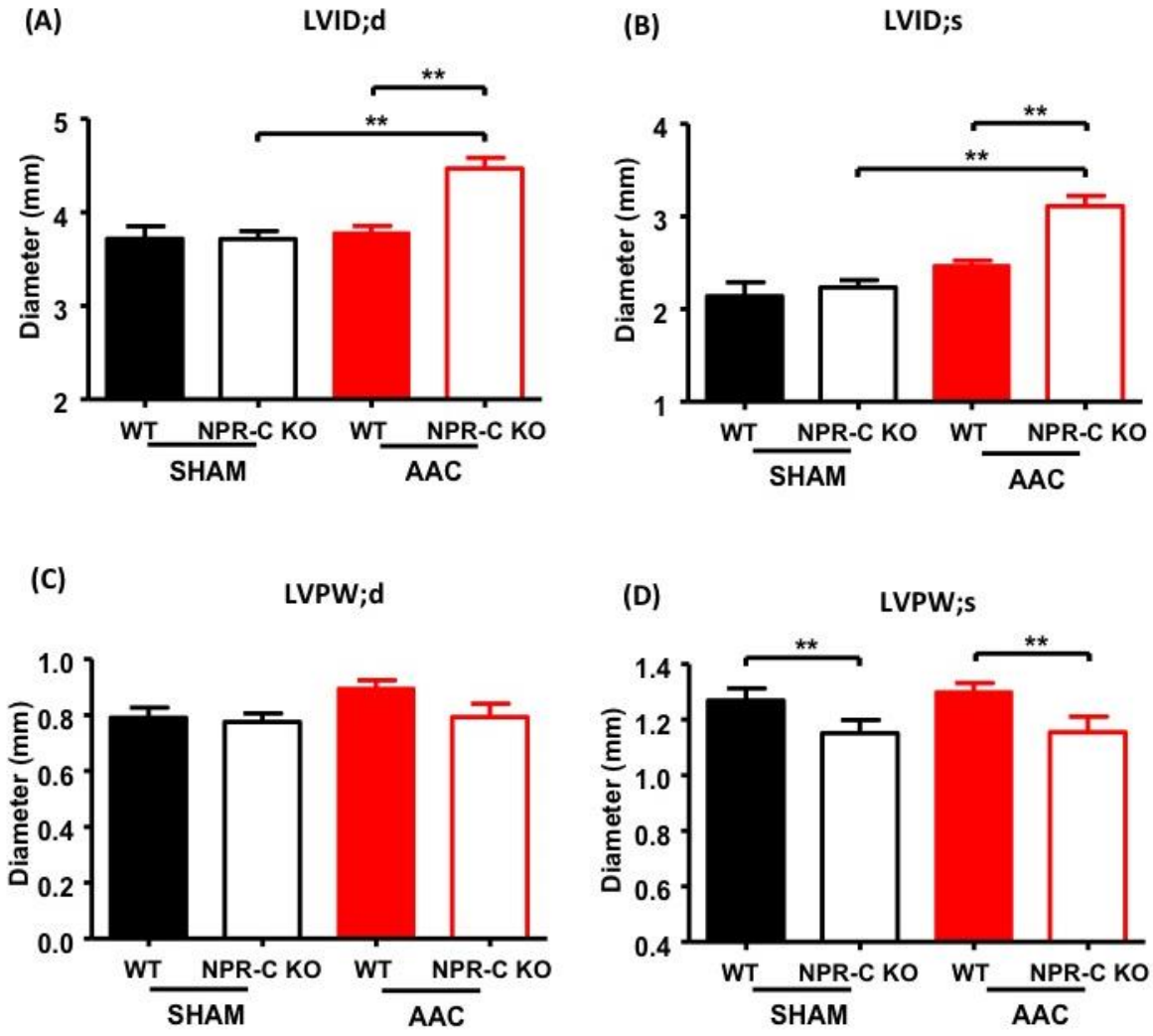

Figure 50. Effect of global NPR-C deletion on left ventricular internal diameter and posterior wall in pressure overload-induced heart failure.

Left ventricular internal diameter at end-diastole (LVID;d) (A) and end-systole (LVID;s) (B), left ventricular posterior wall diameter at end-diastole (LVPW;d) (C) and end-systole (LVPW;s) (D) in WT and NPR-C KO mice subjected to sham or abdominal aortic constriction (AAC) for 6 weeks. Data are represented as the mean±SEM. n=9. ***p*<0.01 using 2-way ANOVA followed by Bonferroni *post-hoc* test.

Effect of global NPR-C deletion on systolic function in pressure overload-induced heart failure

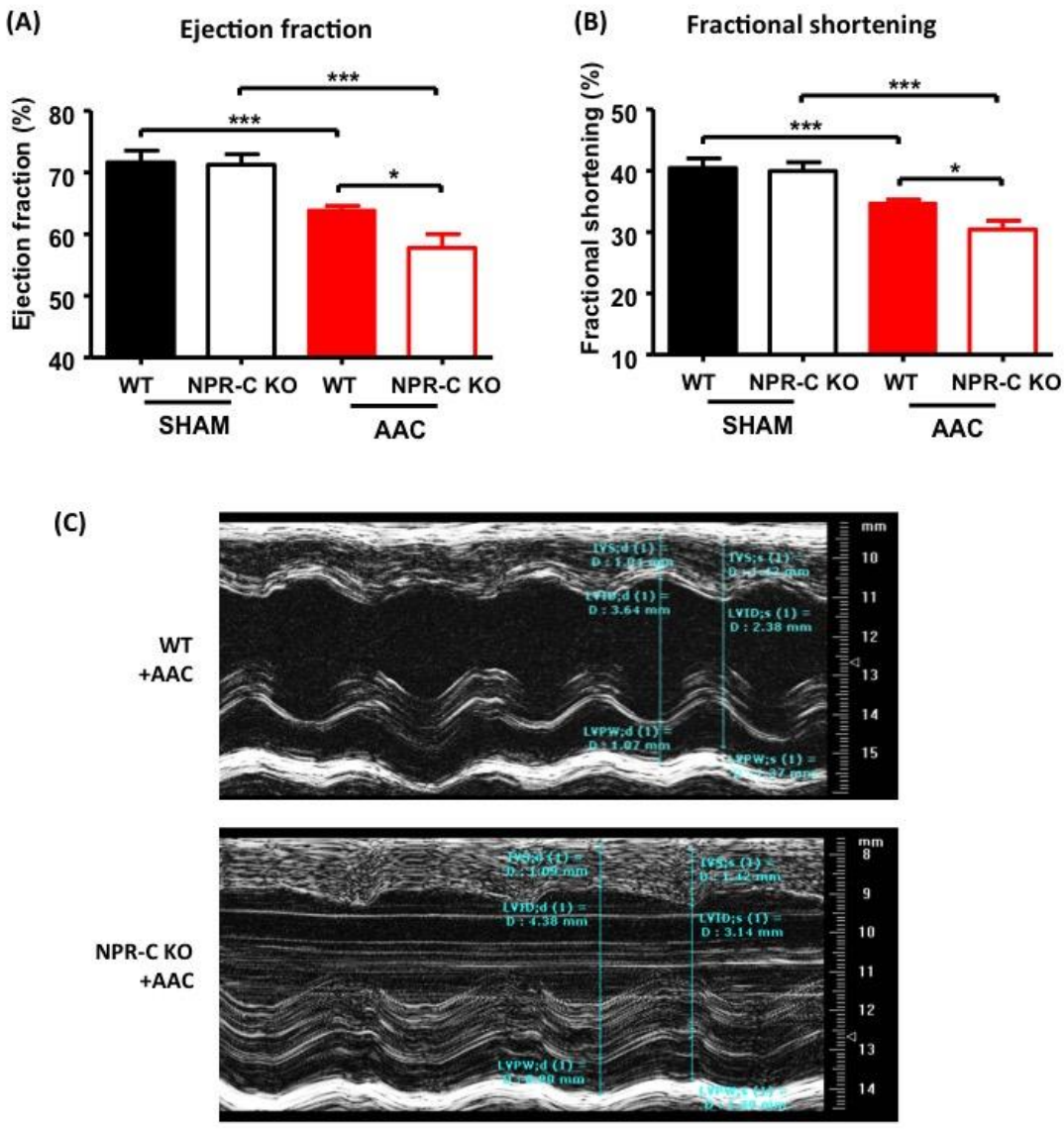

Figure 51. Effect of global NPR-C deletion on systolic function in pressure overload-induced heart failure

Ejection fraction (A) and fractional shortening (B) in WT and NPR-C KO mice subjected to sham or abdominal aortic constriction (AAC) for 6 weeks. (C) Representative echocardiography images from WT and NPR-C KO mice. Data are represented as the mean±SEM. n=9. **p*<0.05, ****p*<0.001 using 2-way ANOVA followed by Bonferroni *post-hoc* test.

Effect of global NPR-C deletion on the heart and left ventricular weight in pressure overload-induced heart failure

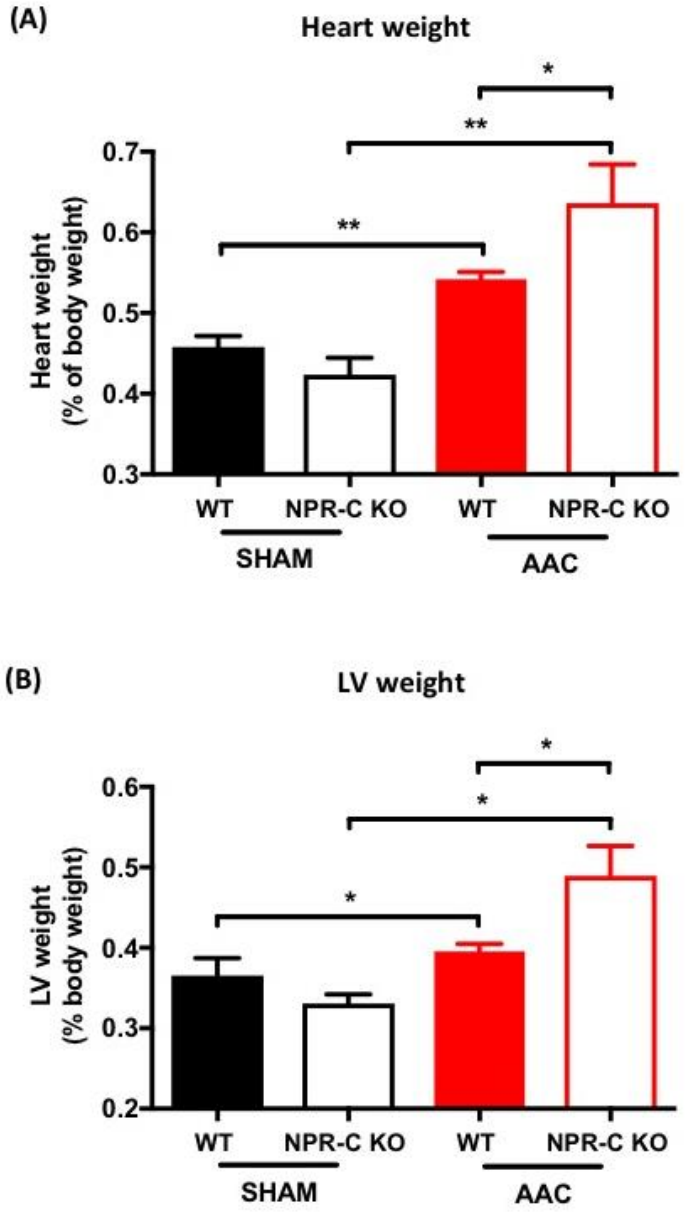

Figure 52. The effect of global NPR-C deletion on the heart and left ventricular weight in pressure overload-induced heart failure.

Whole heart (A) and left ventricular (LV) (B) weights were obtained from WT and NPR-C KO mice subjected to sham or abdominal aortic constriction (AAC) for 6 weeks. Data are represented as the mean±SEM. n=10-11. **p*<0.05, ***p*<0.01 using 2-way ANOVA followed by Bonferroni *post-hoc* test.

Effect of global NPR-C deletion on mean arterial blood pressure in pressure overload-induced heart failure

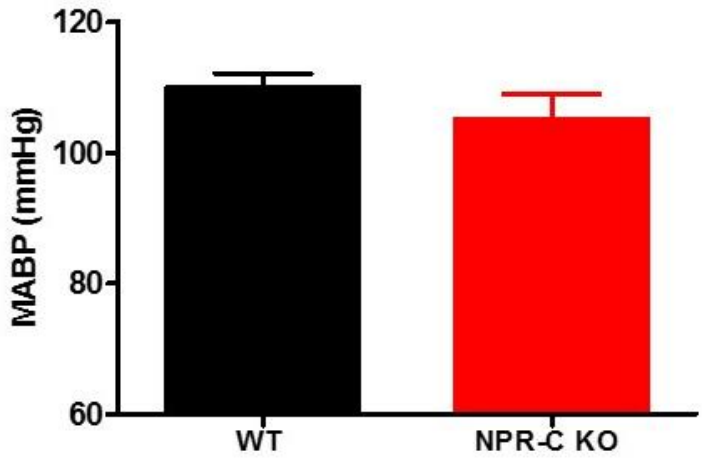

Figure 53. Effect of global NPR-C deletion on mean arterial blood pressure in pressure overload-induced heart failure.

Left carotid mean arterial blood pressure (MABP) in WT and NPR-C KO mice subjected to abdominal aortic constriction (AAC) for 6 weeks. Data are represented as the mean±SEM. n=5.

Effect of global NPR-C deletion on cardiac fibrosis in pressure overload-induced heart failure

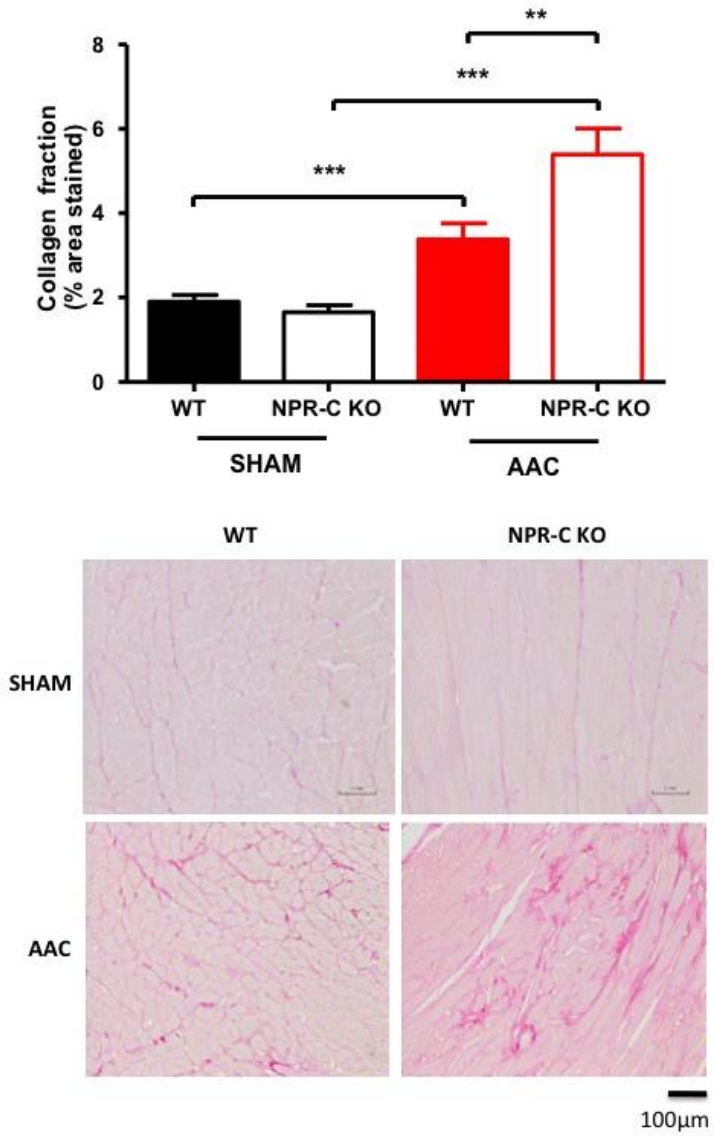

Figure 54. Effect of global NPR-C deletion on cardiac fibrosis in pressure overload-induced heart failure.

Collagen deposition in WT and NPR-C KO mice subjected to sham or abdominal aortic constriction (AAC) for 6 weeks. Representative picro-sirius red staining images (cytoplasm, yellow; collagen, red) from each group are shown on the lower panel, magnification 20X. Data are represented as the mean±SEM. n=6. ***p*<0.01, ****p*<0.001 using 2-way ANOVA followed by Bonferroni *post-hoc* test.

Effect of global NPR-C deletion on cardiomyocyte hypertrophy in pressure overload-induced heart failure

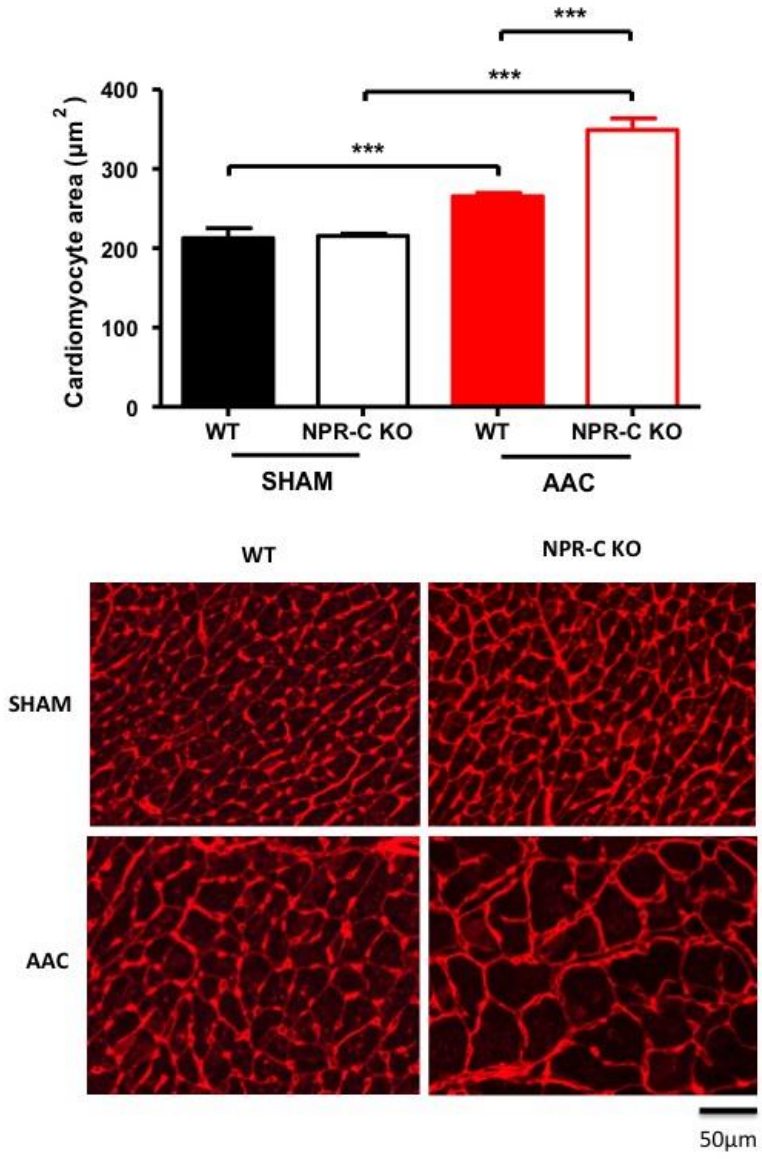

Figure 55. Effect of global NPR-C deletion on cardiomyocyte hypertrophy in pressure overload-induced heart failure.

Cardiomyocyte area in WT and NPR-C KO mice subjected to sham or abdominal aortic constriction (AAC) for 6 weeks. Representative wheat germ agglutinin (WGA) immunofluorescent staining images from each group are shown on the lower panel, magnification 20X. Data are represented as the mean±SEM. n=6. ***p<0.001 using 2-way ANOVA followed by Bonferroni *post-hoc* test.

Cardiac remodelling in cmCNP KO and NPR-C KO mice in response to abdominal aorta constriction

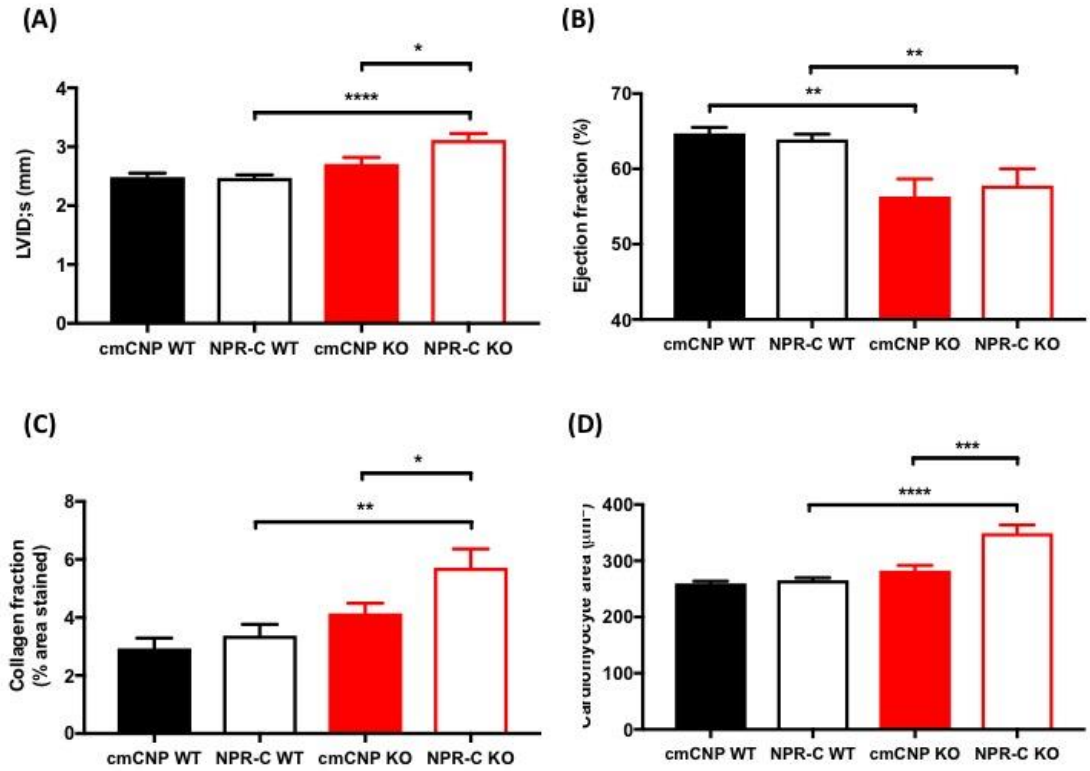

Figure 56. Cardiac remodelling in cmCNP KO and NPR-C KO mice in response to abdominal aorta constriction.

Comparison of left ventricular internal diameter at end-systole (LVID;s) (A), ejection fraction (EF) (B), picro-sirius red staining (collagen deposition) (C) and cardiomyocyte area (D) in cmCNP KO and NPR-C KO mice subjected to abdominal aortic constriction (AAC) for 6 weeks. Data are represented as the mean±SEM. n=6-9. *p<0.05, **p<0.01, ***p<0.001, ****p<0.0001 using one-way ANOVA followed by Bonferroni *post-hoc* test.

4.5.3 Exogenous CNP rescued cardiac dysfunction in WT but not in NPR-C KO mice

The findings above suggest that loss of CNP production by the myocardium accelerates the development of HF, and that NPR-C KO mice exhibited a similar, but exaggerated, phenotype. In order to demonstrate the importance of NPR-C signalling to the cardioprotective effect of cmCNP, and the therapeutic potential of targeting this pathway in HF, I investigated if administration of exogenous CNP provides a protective effect during cardiac stress in WT and NPR-C KO animals subjected to AAC. CNP (0.2mg/kg/day) was administrated via osmotic mini-pump, initiated at 3 week AAC to allow the HF phenotype to develop (to mimic a 'reversal' or therapeutic' administration). In WT mice, infusion of CNP was able to reverse the decline in EF and FS in response to AAC model (EF, AAC 62.72±1.09%, AAC+CNP 69.76±0.81%, $p<0.05$; FS, AAC 34.28±1.08%, AAC+CNP 38.67±0.66%, $p<0.01$; n=6-7) (Figure 57), without affecting MABP (AAC, 111.4±2.14mmHg; AAC+CNP, 109.9±5.43) (Figure 58). Collagen deposition in WT mice receiving CNP was also decreased to a level equivalent to sham animals (sham 1.903±0.0161%; AAC+CNP 1.082±0.132%; $p>0.05$; n=5-6) (Figure 59). Intriguingly, however, these protective effects were abolished in NPR-C KO mice (i.e. EF, NPR-C KO AAC 57.78±2.22% vs. NPR-C KO AAC+CNP 59.77±1.65%; $p>0.05$; n=5-9) (Figure 57), confirming the cardioprotective actions of CNP are mediated via NPR-C signalling. This result also illustrates a therapeutic window of cardioprotective effects of CNP via NPR-C without altering BP – which is key in HF patients due to potential detrimental effects of hypotension and inadequate renal perfusion.

Effect of CNP infusion on cardiac function in pressure overload-induced heart failure in WT and NPR-C KO mice

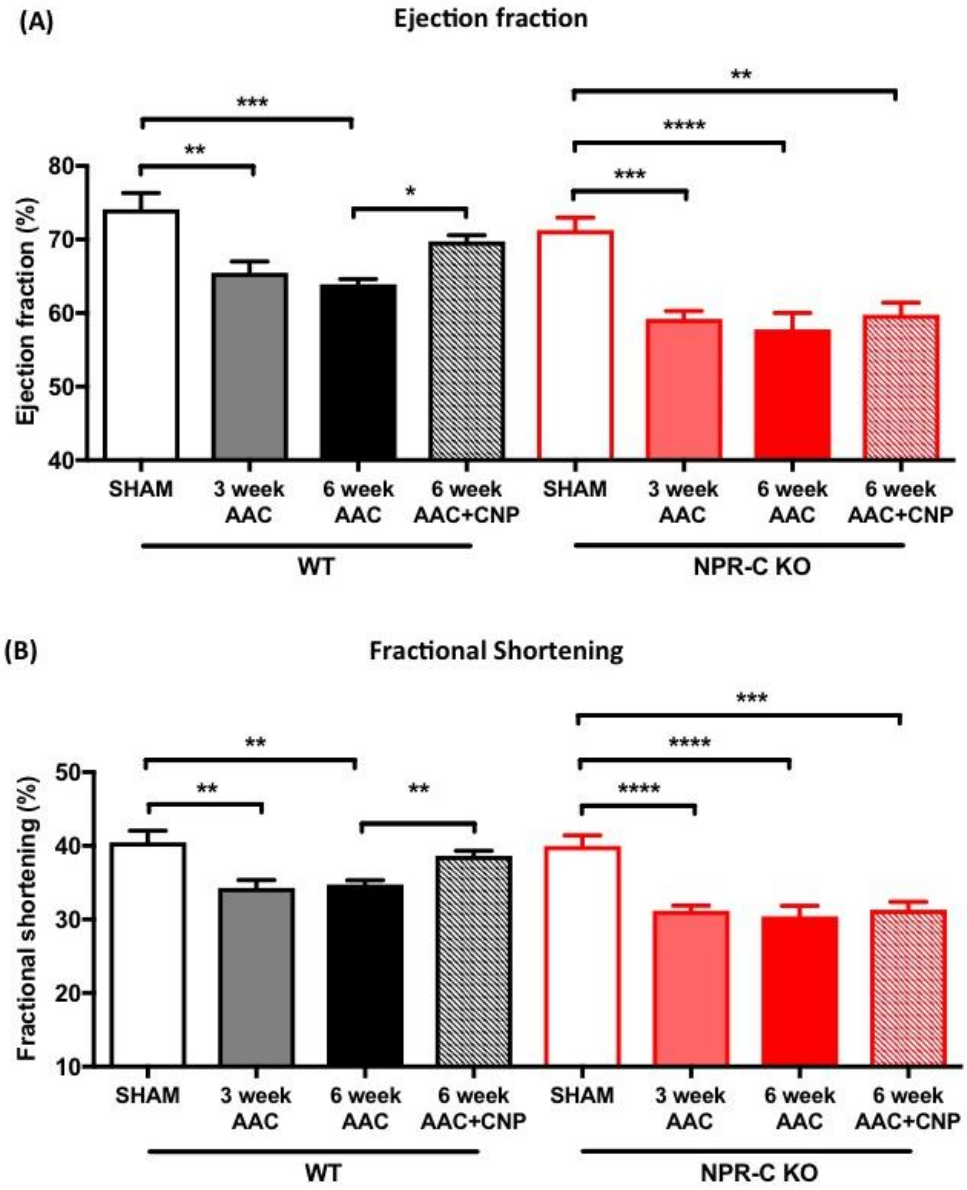

Figure 57. Effect of CNP infusion on cardiac function in pressure overload-induced heart failure in WT and NPR-C KO mice.

Ejection fraction (A) and fractional shortening (B) in WT and NPR-C KO mice subjected to sham, abdominal aortic constriction (AAC) alone or AAC with CNP (0.2mg/kg/day). Data are represented as the mean±SEM. n=6-7. **p*<0.05, ***p*<0.01, ****p*<0.001 using 2-way ANOVA followed by Bonferroni *post-hoc* test.

Effect of CNP infusion on mean arterial blood pressure in pressure overload-induced heart failure in WT mice

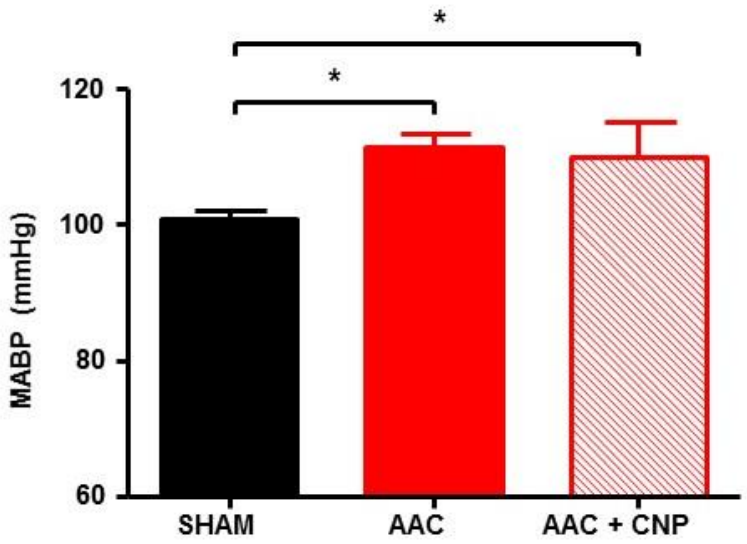

Figure 58. Effect of CNP infusion on mean arterial blood pressure in pressure overload-induced heart failure in WT mice.

Left carotid mean arterial blood pressure (MABP) from WT mice subjected to sham, abdominal aortic constriction (AAC) or AAC with CNP (0.2mg/kg/day). Data are represented as the mean±SEM. n=6-7. *p<0.05 using 1-way ANOVA followed by Bonferroni *post-hoc* test.

Effect of CNP infusion on cardiac fibrosis in pressure overload-induced heart failure in WT and NPR-C KO mice

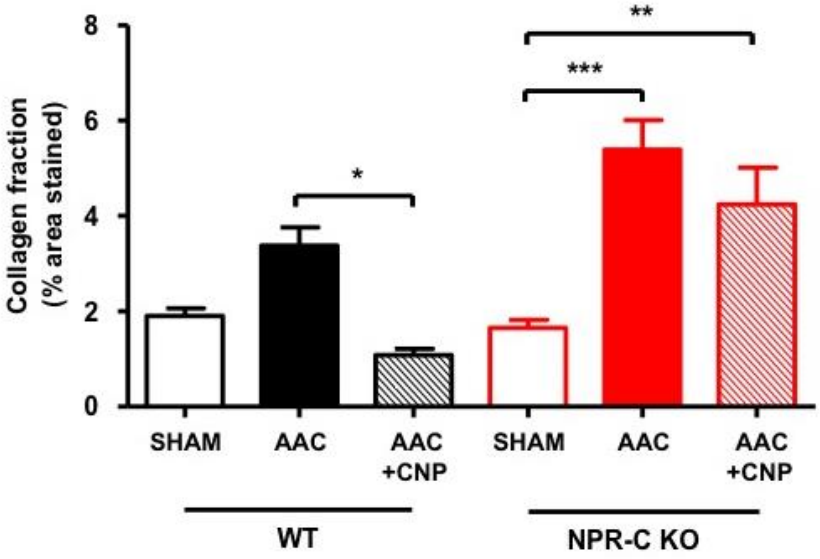

Figure 59. Effect of CNP infusion on cardiac fibrosis in pressure overload-induced heart failure in WT and NPR-C KO mice.

Left ventricular collagen deposition from picro-sirius red staining in WT and NPR-C KO mice subjected to sham, abdominal aortic constriction (AAC) or AAC with CNP (0.2mg/kg/day). Data are represented as the mean±SEM. n=5-6. *p<0.05, **p<0.01, ***p<0.001 using 2-way ANOVA followed by Bonferroni *post-hoc* test.

4.6 The role of cardiofibroblast-derived CNP in cardiac function

Earlier findings in this chapter hinted that NPR-C KO mice exhibit a more severe pathology compared to cmCNP KO animals when exposed to pressure-overload (e.g. bigger increase in LVID, higher collagen deposition and larger cardiomyocyte size) (Figure 56). One explanation for this exacerbated deterioration in cardiac structure and function is the incomplete deletion of CNP from the cardiomyocyte (approximately 83%) compared to the 100% (i.e. global) ablation of NPR-C. Another reason could be activation of NPR-C by another natriuretic peptide (i.e. ANP or BNP). However, an alternative plausible hypothesis is that an additional cellular source of CNP may contribute to triggering NPR-C to bring about a cardioprotective effect. Previous studies have demonstrated that CNP is synthesised and secreted from cardiac fibroblasts and may play an autocrine regulatory role in supressing collagen synthase (Horio et al., 2003). Hence, I developed a fibroblast-specific CNP KO mouse line (fbCNP KO) to investigate a potential role for cardiac fibroblast-derived CNP in cardiac remodelling and HF.

4.6.1 Characterisation of fbCNP KO mice

Tamoxifen-induced Cre-Lox technology was used to abrogate CNP expression in fibroblasts. Mice expressing Col1α2-Cre-ERT was crossed with floxed CNP animals to generate fbCNP KO mice. *CNP*$^{+/+}$ Cre mice were used as littermate (WT) controls. All animals received tamoxifen (TAM; 40mg/kg/day) intra-peritoneally for 5 consecutive days at age 4-5 weeks. CNP expression was significantly reduced (approximately 60%) in cardiac fibroblasts isolated from fbCNP KO mice compared to WT littermates (Figure 60). In contrast, the expression of CNP mRNA was equivalent in all other tissues examined from WT and fbCNP KO animals (Figure 60). Interestingly, CNP mRNA expression in the whole heart was not significantly different between fbCNP KO and WT. This may be due to the fact that fibroblasts are not the major cell population expressing CNP in the heart (including endothelium and cardiomyocytes); this fits with the observed 80% reduction in CNP mRNA expression I reported in cardiomyocytes (Figure 16).

4.6.2 Tamoxifen-induced cardiac toxicity

Previous studies have reported tamoxifen can induce transient cardiac dysfunction (Koitabashi et al., 2009). Therefore, both WT and fbCNP KO mice were given equal doses of TAM to ensure any cardiac effect(s) are due to the genetic deletion of CNP and not the potential adverse effects of the drug. A trend towards a reduced EF and FS was observed

following 1 week tamoxifen injection regardless of genotypes (EF: WT, pre-TAM 71.06±3.00%, post-TAM 65.55±2.91%; fbCNP KO, pre-TAM 70.56±1.63%, post-TAM 66.41±1.70%; FS: WT, pre-TAM 39.69±2.56%, post-TAM 35.55±2.25%, fbCNP KO, pre-TAM 38.99±1.33, post-TAM 35.85±1.31%; $p>0.05$; $n\geq5$) (Figure 61). However, the cardiac function fully recovered after 2 weeks, again regardless of whether the mice were WT or fbCNP KO (EF, WT 71.82±2.72%, fbCNP KO 70.77±2.25%; $p>0.05$) (Figure 61). Thus, TAM was given to mice aged 4-5 weeks (16-18g) to allow time for cardiac function to recover fully before being subjected to sham or AAC at 6-7 weeks of age (23-24g).

4.6.3 Echocardiography

Akin to cmCNP KO and NPR-C KO animals, mice with loss of fibroblast-derived CNP exhibited a dilated cardiomyopathy in response to AAC characterised by an increase in LVID compared with littermate controls (LVID;d, WT 3.70±0.07% vs. fbCNP KO 4.02±0.12%, $p<0.05$; LVID;s, WT 2.44±0.06% vs. fbCNP KO 2.84±0.15%, $p<0.01$; n= 10-12) (Figure 62). Correspondingly, EF and FS were significantly reduced in fbCNP KO mice compared to WT (EF, WT 64.92±1.15% vs. fbCNP KO 56.33±2.54%, $p<0.001$; FS, WT 34.96±0.88% vs. fbCNP KO 29.22±1.56%, $p<0.01$; n=10-12) (Figure 63). There was no difference in MABP between the genotypes following AAC (WT 111.7±1.49mmHg; fbCNP KO 108.7±2.12mmHg; n=10-12) (Figure 64), indicating that the deterioration seen in fbCNP KO mice was due to a loss of direct protective actions of fibroblast-derived CNP on cardiac structure and function.

4.6.4 Histology

Whole heart and LV weight in fbCNP KO animals following AAC were significantly higher than WT (HW/BW, WT 0.53±0.01% vs. fbCNP KO 0.60±0.02%, $p<0.05$; LV/BW, WT 0.42±0.01% vs. 0.47±0.02%, $p<0.01$; n=10-12) (Figure 65). Collagen deposition was significantly increased in response to AAC in both genotypes but it was more profound in fbCNP KO than WT mice (WT, 6.20±0.65% vs. fbCNP KO 8.23±0.56%; $p<0.05$; n=5-6) (Figure 66). Cardiomyocyte size was increased significantly in fbCNP KO mice following AAC (sham 230.7±7.04µm2, AAC 288.5±6.77µm2; $p<0.01$; n=5-6) (Figure 67), whilst there was no significant increase in cell size in WT animals.

Taken together, these data highlight loss of fibroblast-derived CNP results in a more hypertrophic and fibrotic phenotype in response to pressure-overload compared to WT animals.

Characterisation of CNP expression in WT and fbCNP KO mice

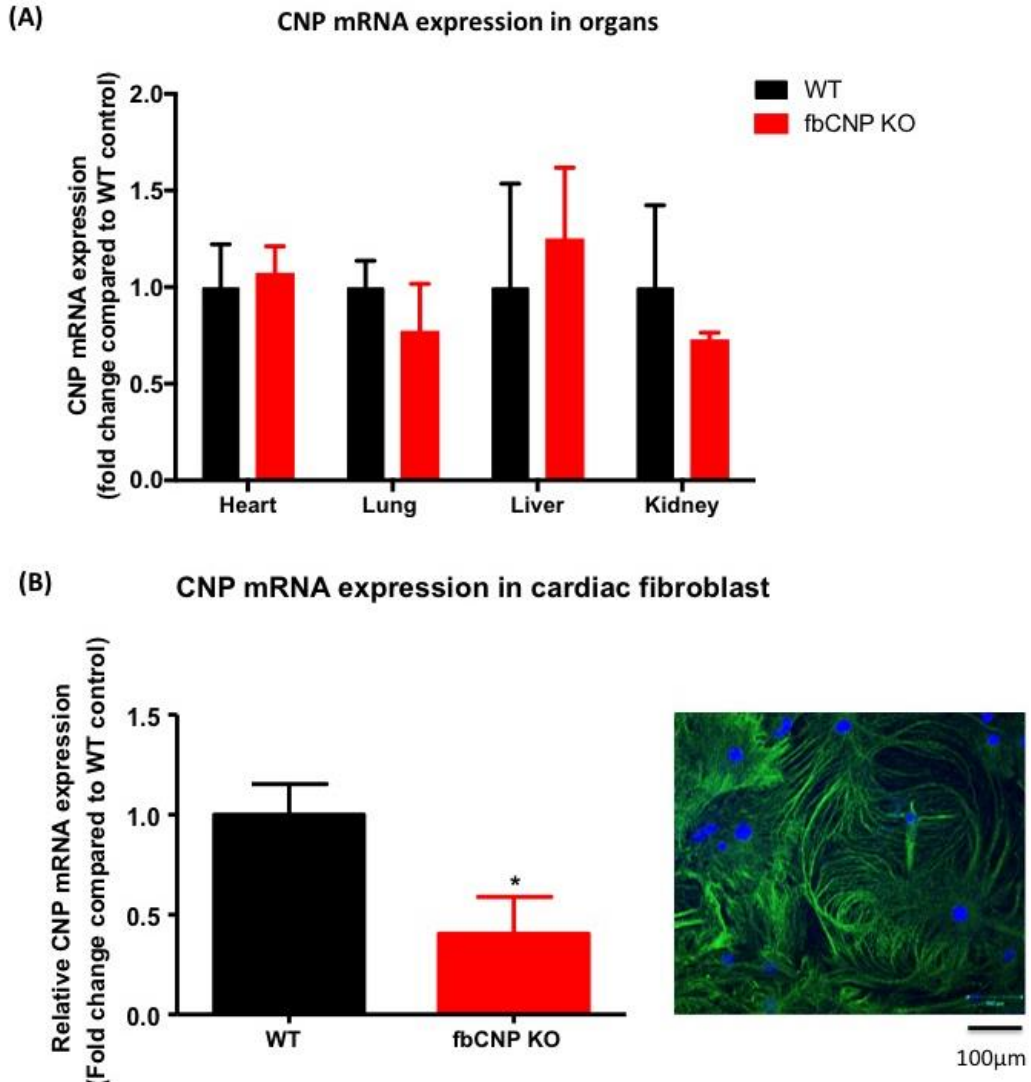

Figure 60. Characterisation of CNP expression in WT and fbCNP KO mice.

qPCR analysis of CNP mRNA from the heart and different tissues (A), and isolated cardiac fibroblasts (B) in WT and fbCNP KO animals. A representative confocal image (vimentin, green; nuclei, blue) of cardiac fibroblast is shown on the right panel. Data are represented as the mean±SEM. n=5-6. *p<0.05 significantly different from WT littermates using unpaired student t-test.

Effect of tamoxifen on cardiac function in WT and fbCNP KO mice

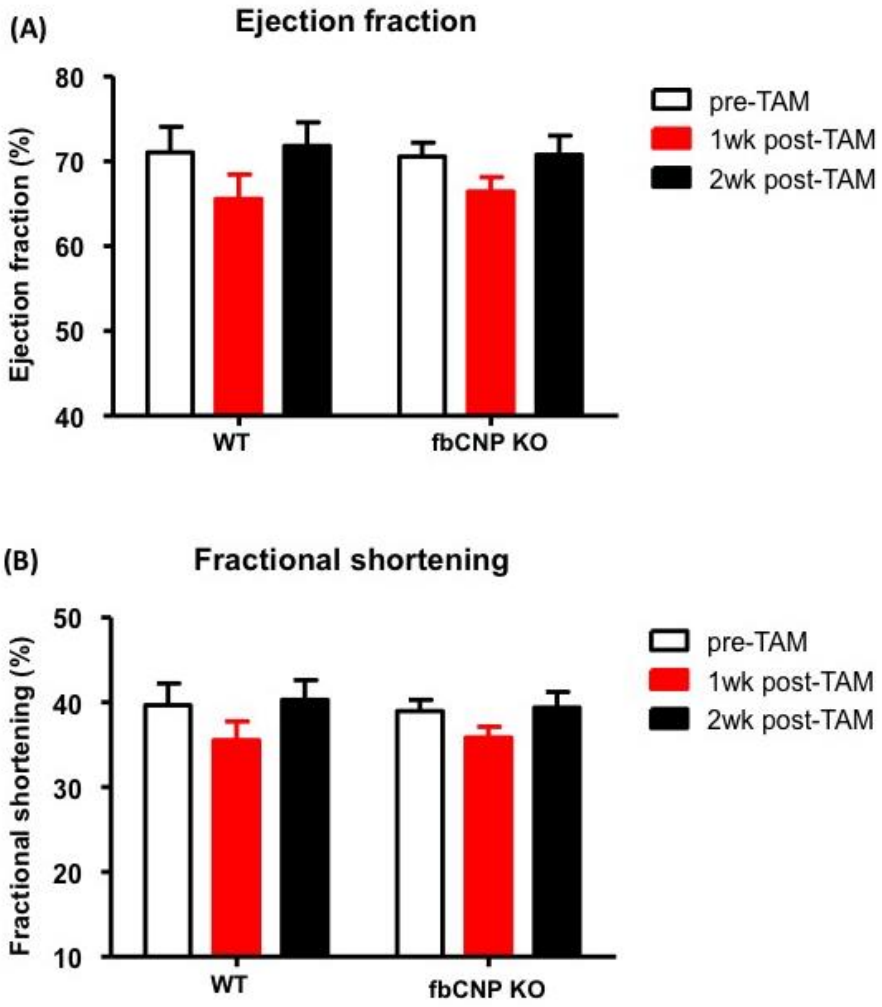

Figure 61. Effect of tamoxifen on cardiac function in WT and fbCNP KO mice.

Ejection fraction (A) and fractional shortening (B) in WT and fbCNP KO mice exposed to tamoxifen (TAM; 40mg/kg/day) for 5 consecutive days. Data are represented as the mean±SEM. n≥5.

Effect of fibroblast CNP deletion on cardiac structure in pressure overload-induced heart failure

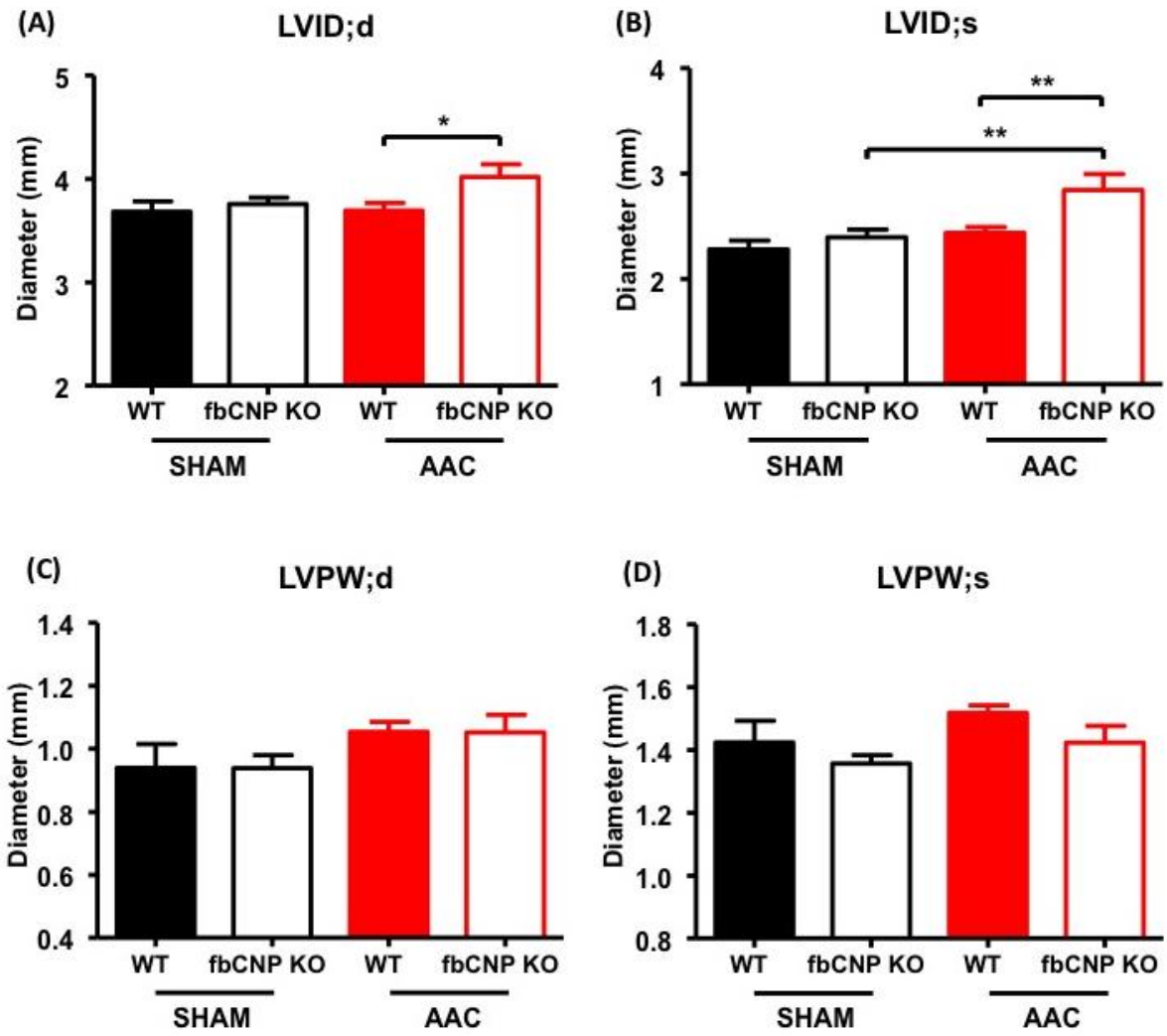

Figure 62. Effect of fibroblast CNP deletion on cardiac structure in pressure overload-induced heart failure.

Left ventricular internal diameter at end-diastole (LVID;d) (A) and end-systole (LVID;s) (B), left ventricular posterior wall diameter at both end-diastole (LVPW;d) (C) and end-systole (LVPW;s) (D) in WT and fbCNP KO mice subjected to sham or abdominal aortic constriction (AAC) for 6 weeks. Data are represented as the mean±SEM. n=10-12. *p<0.05, **p<0.01 using 2-way ANOVA followed by Bonferroni *post-hoc* test.

Effect of fibroblast CNP deletion on systolic function in pressure overload-induced heart failure

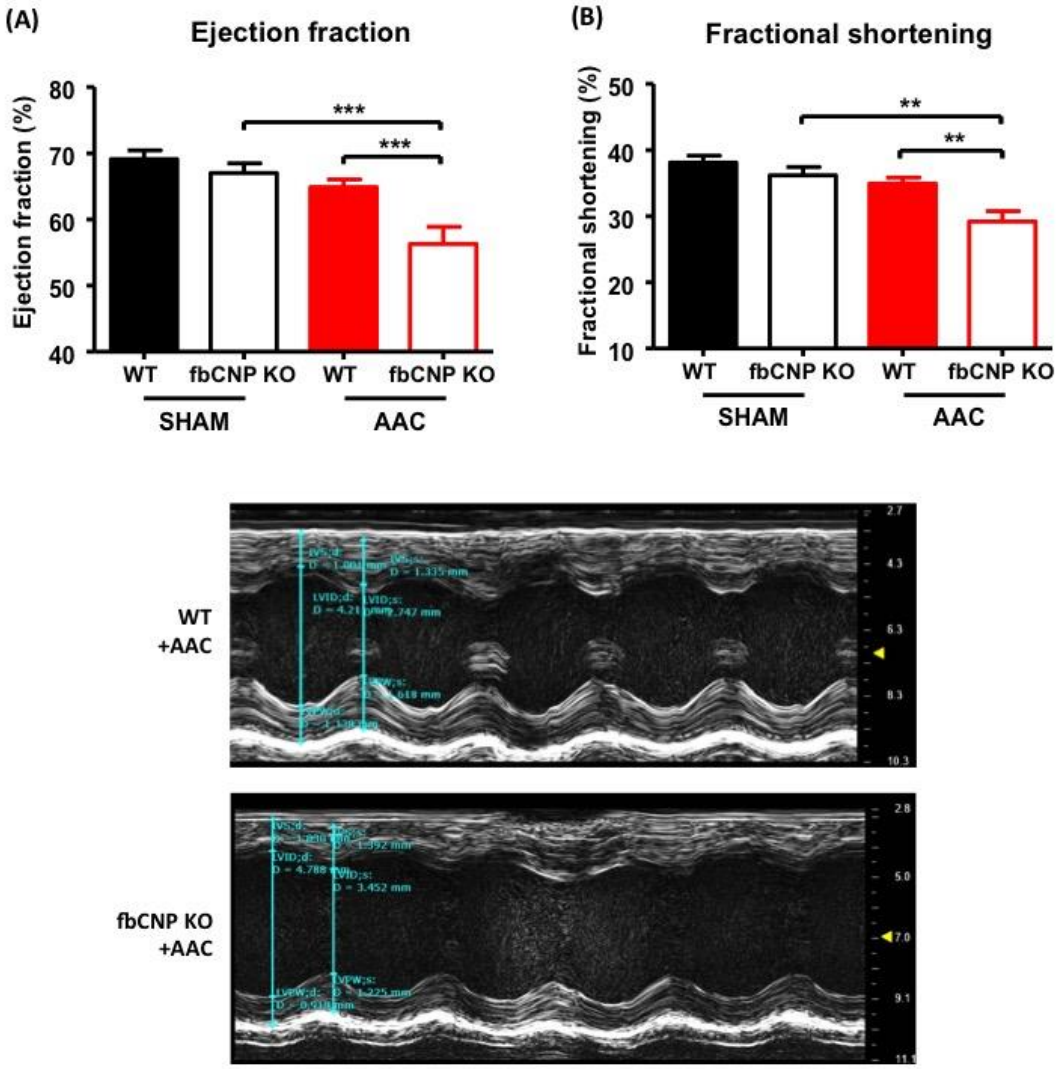

Figure 63. The effect of fibroblast CNP deletion on systolic function in pressure overload-induced heart failure.

Ejection fraction (A) and fractional shortening (B) in WT and fbCNP KO mice subjected to sham or abdominal aortic constriction (AAC) for 6 weeks. (C) Representative echocardiography images from WT and fbCNP KO mice after AAC. Data are represented as the mean±SEM. n=10-12. ***p*<0.01, ****p*<0.001 using 2-way ANOVA followed by Bonferroni *post-hoc* test.

Effect of fibroblast CNP deletion on mean arterial blood pressure in pressure overload-induced heart failure

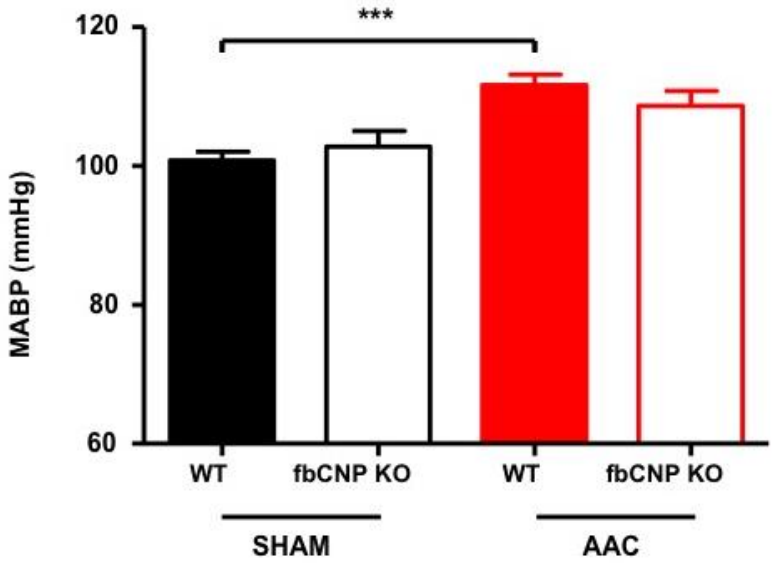

Figure 64. Effect of fibroblast CNP deletion on mean arterial blood pressure in pressure overload-induced heart failure.

Left carotid mean arterial blood pressure (MABP) in WT and fbCNP KO mice subjected to sham or abdominal aortic constriction (AAC) for 6 weeks. Data are represented as the mean±SEM. n=10-12. ***p<0.001 using 2-way ANOVA followed by Bonferroni *post-hoc* test.

Effect of fibroblast CNP deletion on the heart and left ventricular weight in pressure overload-induced heart failure

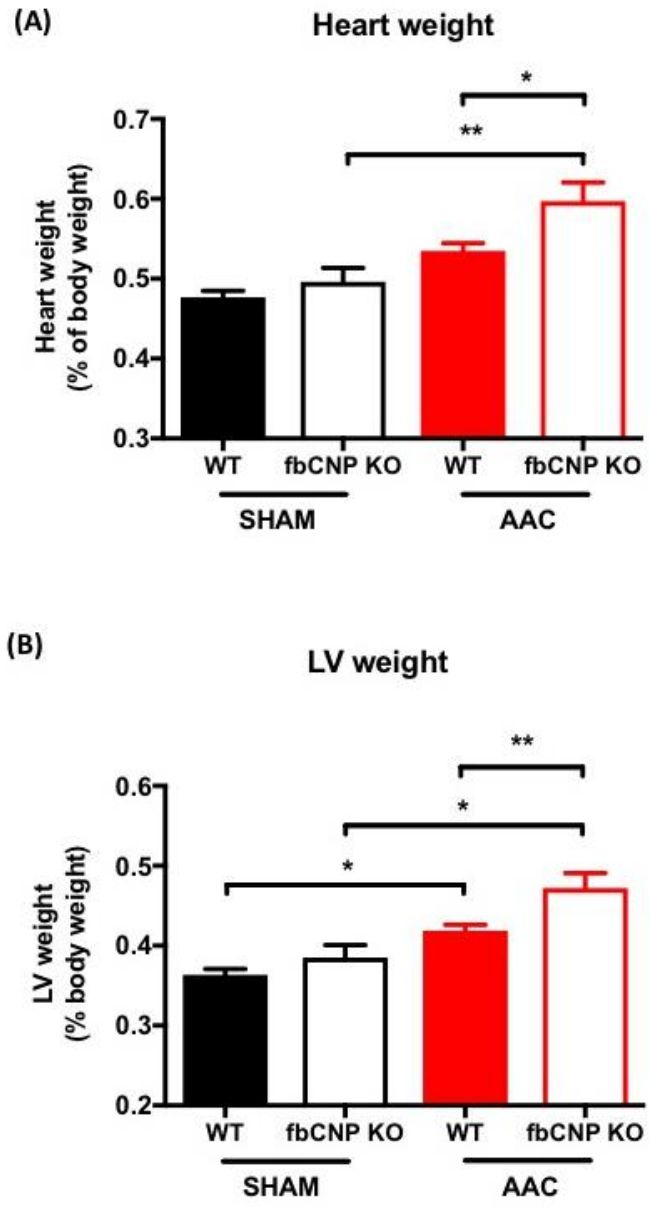

Figure 65. Effect of fibroblast CNP deletion on the heart and left ventricular weight in pressure overload-induced heart failure.

Whole heart (A) and left ventricular (LV) (B) weight obtained from WT and fbCNP KO mice subjected to sham or abdominal aortic constriction (AAC) for 6 weeks. Data are represented as the mean±SEM. n=10-12. *p<0.05, **p<0.01 using 2-way ANOVA followed by Bonferroni *post-hoc* test.

Effect of fibroblast CNP deletion on cardiac fibrosis in pressure overload-induced heart failure

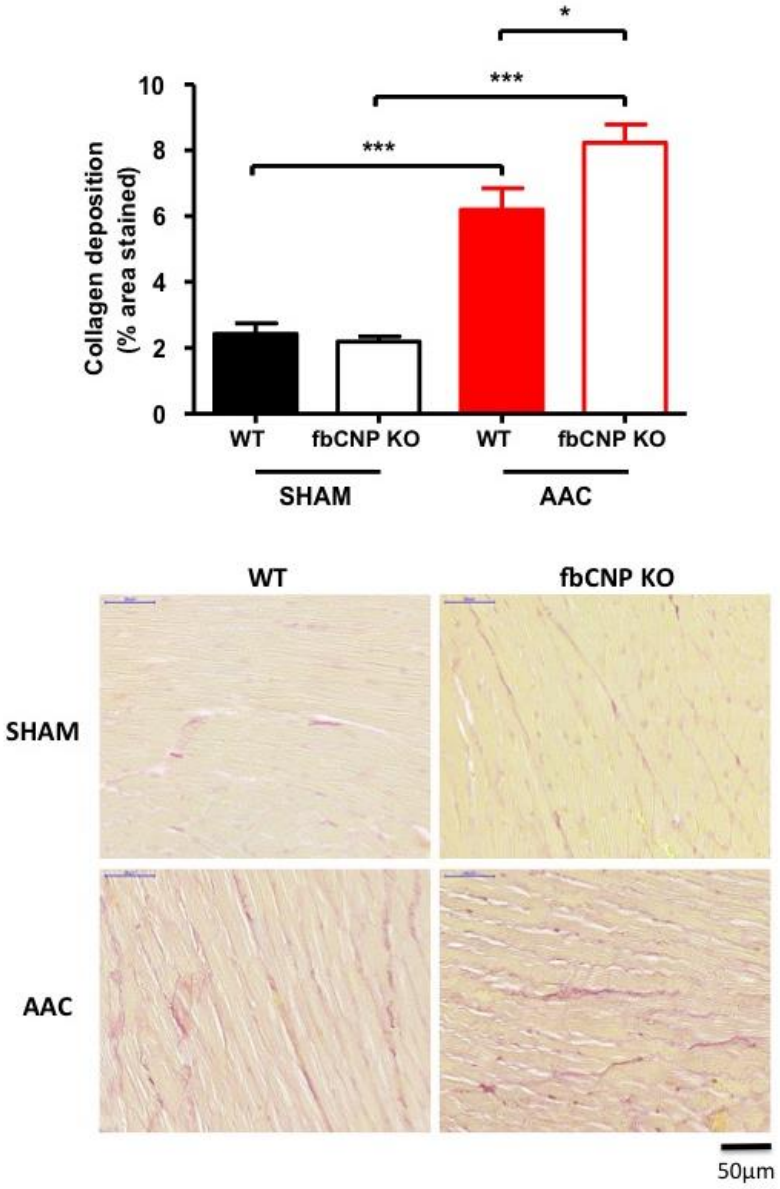

Figure 66. Effect of fibroblast CNP deletion on cardiac fibrosis in pressure overload-induced heart failure.

Left ventricular collagen deposition in WT and fbCNP KO mice subjected to sham or abdominal aortic constriction (AAC) for 6 weeks. Representative picro-sirius red staining images (cytoplasm, yellow; collagen, red) from each group are shown on the lower panel, magnification 20X. Data are represented as the mean±SEM. n=5-6. *p<0.05, ***p<0.001 using 2-way ANOVA followed by Bonferroni *post-hoc* test.

Effect of fibroblast CNP deletion on cardiac hypertrophy in pressure overload-induced heart failure

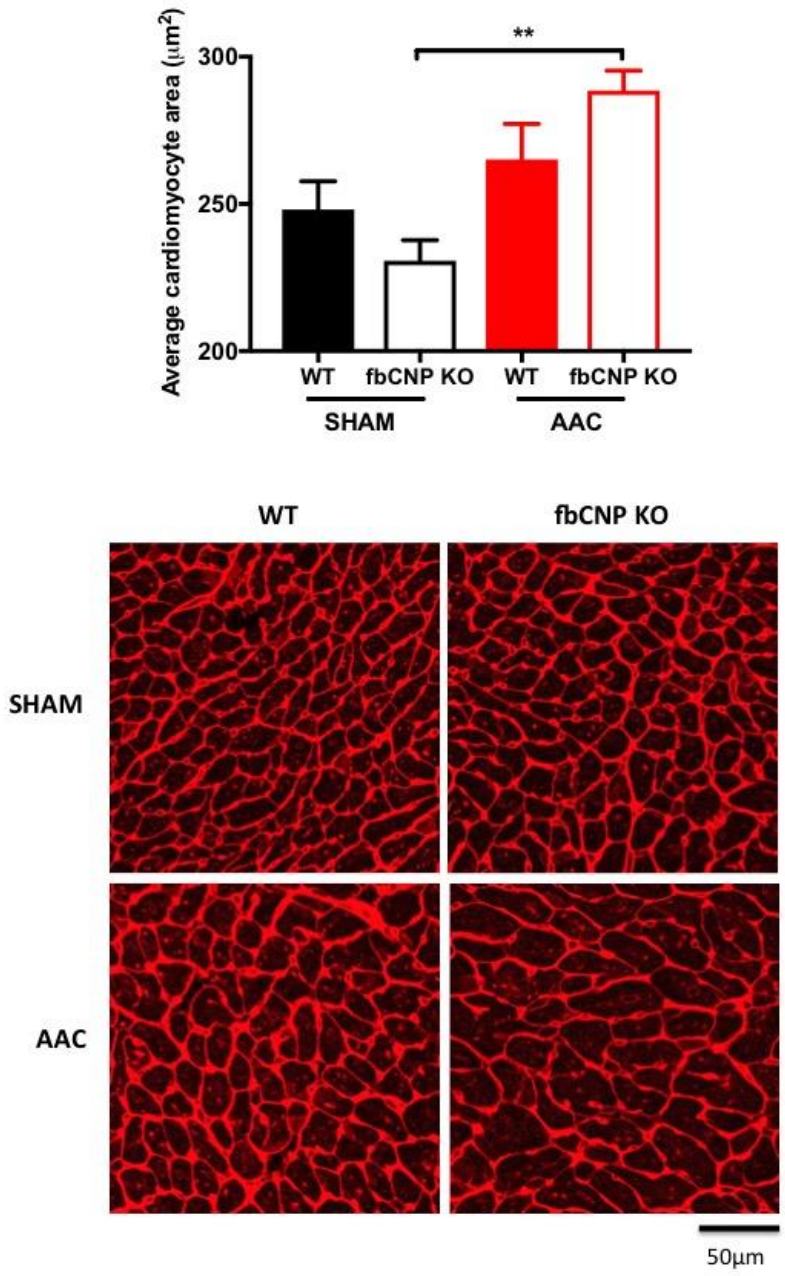

Figure 67. Effect of fibroblast CNP deletion on cardiac hypertrophy in pressure overload-induced heart failure.

Cardiomyocyte area in WT and fbCNP KO mice subjected to sham or abdominal aortic constriction (AAC) for 6 weeks. Representative wheat germ agglutinin (WGA) fluorescence stained images from each group are shown on the lower panel, magnification 20X. Data are represented as the mean±SEM. n=6. ** p<0.01 using 2-way ANOVA followed by Bonferroni *post-hoc* test.

4.7 Changes in mRNA expression in response to AAC

To understand how the loss of CNP drives cardiac remodelling, I investigated relative expression of an array of hypertrophic and fibrotic mediators and markers. Gene expression was normalised to two housekeeping genes, β-actin and RPL-19 (Bustin et al., 2009), and the expression of these genes was confirmed not to be altered in response to AAC (Figure 68).

4.7.1 Changes in ANP mRNA expression

ANP is a well-established HF biomarker the expression of which correlates with disease severity and the risk of cardiovascular events and death (Wang et al., 2004, Volpe et al., 2014). Surprisingly, ANP mRNA levels were higher in cmCNP KO mice at baseline (i.e. without cardiac stress) compared to WT (WT, 1.054±0.143; cmCNP KO, 1.548±0.076; $p<0.05$; n=5)(Figure 69), indicating deletion of cardiomyocyte CNP may predispose to cardiac dysfunction although that is not yet apparent from a functional standpoint at the age the mice were studied. ANP mRNA expression in cmCNP KO was increased further in response to AAC (WT, 1.063±0.238; cmCNP KO, 1.932±0.556; $p<0.05$; n=6) (Figure 69). In NPR-C KO mice, the ANP mRNA expression was comparable with its littermate control in sham, but markedly increased following AAC (WT, 0.582±0.108; NPR-C KO, 1.633±0.157; $p<0.001$; n=6) (Figure 69). Since ANP expression correlates with the severity of HF, these data substantiate the functional data (above) that the loss of cardiac CNP aggravates cardiac dysfunction and this was more pronounced in NPR-C null mice.

4.7.2 Changes in α- and β-MHC mRNA expression

Two isoforms of myosin heavy chain (MHC), α and β, exist in the mammalian myocardium (Nakao et al., 1997). It has been reported that pathological stimuli can cause a shift in MHC composition from α- to β-MHC (Depre et al., 1998, Nakao et al., 1997). Thus, a decrease in α-MHC/β-MHC ratio or upregulation of β-MHC expression is associated with cardiac hypertrophy and HF (Cox and Marsh, 2014). Expression of β-MHC was significantly higher in cmCNP KO mice in both sham and following AAC compared to WT (WT sham, 1.000±0.154 vs. cmCNP KO sham, 3.880±0.593; WT AAC 2.444±0.477 vs. cmCNP KO AAC, 4.101±0.935; $p<0.01$; n=4-6)(Figure 71). An enhanced expression of β-MHC was also found in NPR-C KO mice compared to WT following AAC (WT AAC, 1.135±0.231 vs. NPR-C KO, 1.917±0.399; $p<0.01$; n=4-5)(Figure 71). Moreover, no significant changes were observed in α-MHC expression in all mice following AAC (Figure 70). This is probably because α-MHC comprises

>90% of the MHC composition in rodents (Nakao et al., 1997), thus, subtle changes in the expression are difficult to detect.

4.7.3 Changes in SERCA2a mRNA expression

Myocyte Ca2+ cycling is primarily governed by SERCA2a, which mediates Ca2+ sequestration into the SR and regulates cardiac contractility (Frank et al., 2002). This is routinely reduced in failing hearts (Zima et al., 2014). A trend towards to a reduction of SERCA2a was observed following AAC in cmCNP KO (sham 1.097±0.118; AAC 0.728±0.16; n=6) and fbCNP KO (sham 0.721±0.174; AAC 0.474±0.143; n=4-5) (Figure 72). Unexpectedly, SERCA2a mRNA expression was significantly increased in NPR-C WT mice following AAC (sham 1.000±0.081, AAC 1.320±0.096; $p<0.05$; n=5-6), but this change was not apparent in NPR-C KO mice (Figure 72).

4.7.4 Changes in TGF-β1 mRNA expression and its linked extracellular matrix genes

TGF-β1 plays a key role in regulating many aspect of cardiac remodelling process including the upregulation of ECM genes, e.g. collagen I, collagen III, MMP-2 and fibronectin (Lijnen et al., 2000). TGF-β1 mRNA expression was significantly increased in cmCNP WT mice following AAC (sham 1.000±0.063, AAC 1.580±0.137; $p<0.05$; n=5-6) (Figure 73). There is a trend towards to an increased TGF-β1 mRNA expression in cmCNP KO sham mice compared to WT sham (WT sham, 1.000±0.063; cmCNP KO, 1.356±0.137; $p>0.05$; n=6), but this did not elevate further in response to AAC (Figure 73). Again, these observations suggest cmCNP KO mice have intrinsic upregulation of pro-fibrotic gene expression that underlies the accentuated fibrotic burden in pre-clinical models I demonstrated earlier.

Upregulation of MMP-2 mRNA expression was also observed in cmCNP KO mice in both sham and AAC compared to WT (sham: WT 1.000±0.074 vs. cmCNP KO 1.415±0.083; AAC: WT 1.268±0.174 vs. cmCNP KO 1.525±0.169; $p<0.05$; n=6) (Figure 74). A trend towards to an increased Col1a1 mRNA expression was also observed in cmCNP KO compared to WT following AAC (WT, 1.034±0.134; cmCNP KO, 1.463±0.215; $p>0.05$; n=6) (Figure 75). Furthermore, Col1a1 mRNA expression was equivalently increased in WT and NPR-C KO mice following AAC (WT: sham 1.000±108 vs. AAC 1.606±0.155; NPR-C KO: sham 1.046±0.114 vs.± 1.788±0.160; $p<0.05$; n=5-6) (Figure 75). Whereas, fibronectin expression was not altered in response to AAC in all animals (Figure 76).

Comparison of the expression of the reference genes in response to abdominal aorta constriction

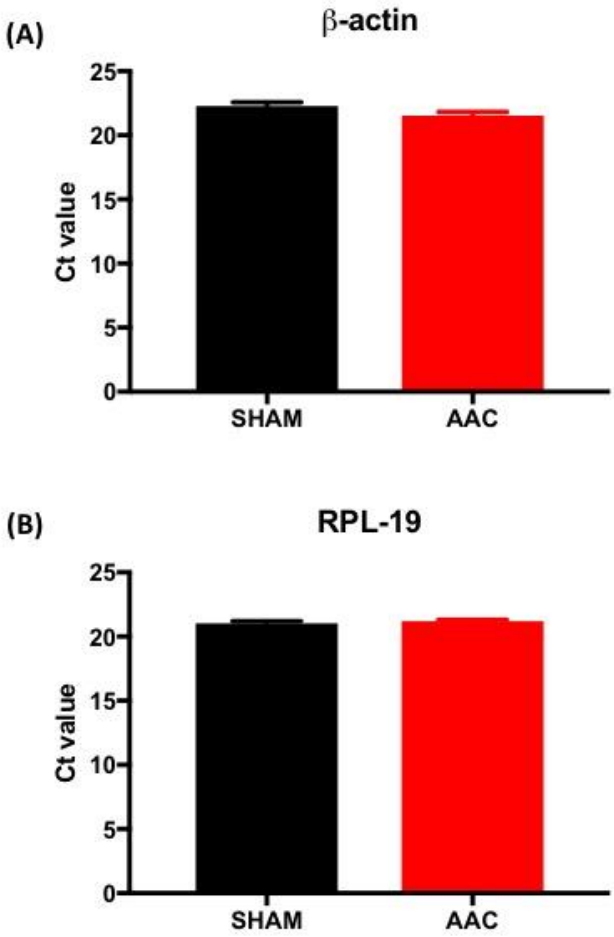

Figure 68. Comparison of the expression of the reference genes in response to abdominal aorta constriction.

Left ventricular mRNA expression of the two reference/housekeeping genes, β-actin (A) and RPL-19 (B) in WT mice subjected to sham or abdominal aortic constriction (AAC) for 6 weeks. Data are represented as the mean±SEM. n=10-12. *p*>0.05 using unpaired t-test.

Effect of cmCNP, fbCNP and NPR-C deletion on cardiac hypertrophic gene profile in pressure overload-induced heart failure

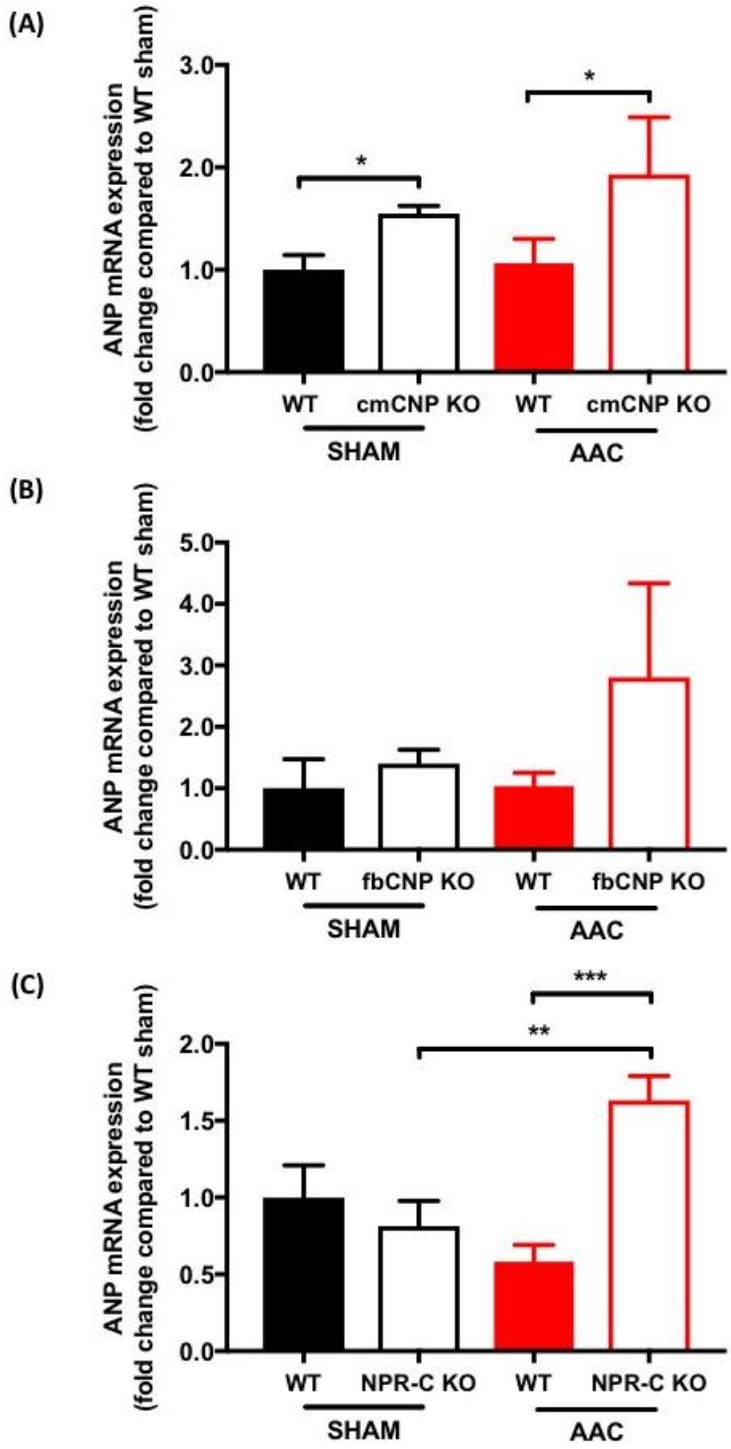

Figure 69. Effect of cmCNP, fbCNP and NPR-C deletion on ANP mRNA expression in pressure overload-induced heart failure.

ANP mRNA expression from left ventricles isolated from littermate WT, cmCNP KO, fbCNP KO and NPR-C KO mice subjected to sham or abdominal aortic constriction (AAC) for 6 weeks. Data are represented as the mean±SEM. n=3-6. *p<0.05, **p<0.01, ***p<0.001 using 2-way ANOVA followed by Bonferroni *post-hoc* test.

Effect of cmCNP, fbCNP and NPR-C deletion on cardiac hypertrophic gene profile in pressure overload-induced heart failure

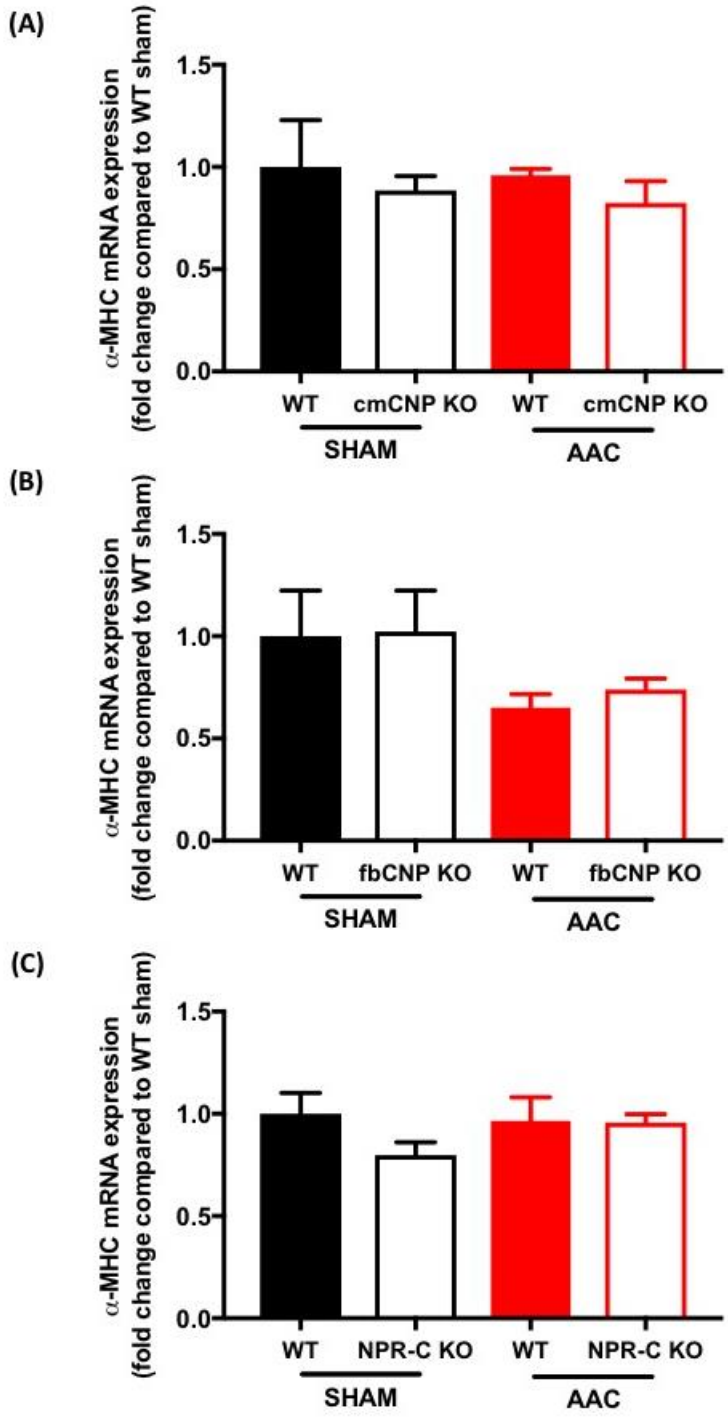

Figure 70. Effect of cmCNP, fbCNP and NPR-C deletion on α-MHC mRNA expression in pressure overload-induced heart failure.

α-MHC mRNA expression from left ventricles isolated from littermate WT, cmCNP KO (A), fbCNP KO (B) and NPR-C KO (C) mice subjected to sham or abdominal aortic constriction (AAC) for 6 weeks. Data are represented as the mean±SEM. n=4-6.

Effect of cmCNP, fbCNP and NPR-C deletion on cardiac hypertrophic gene profile in pressure overload-induced heart failure

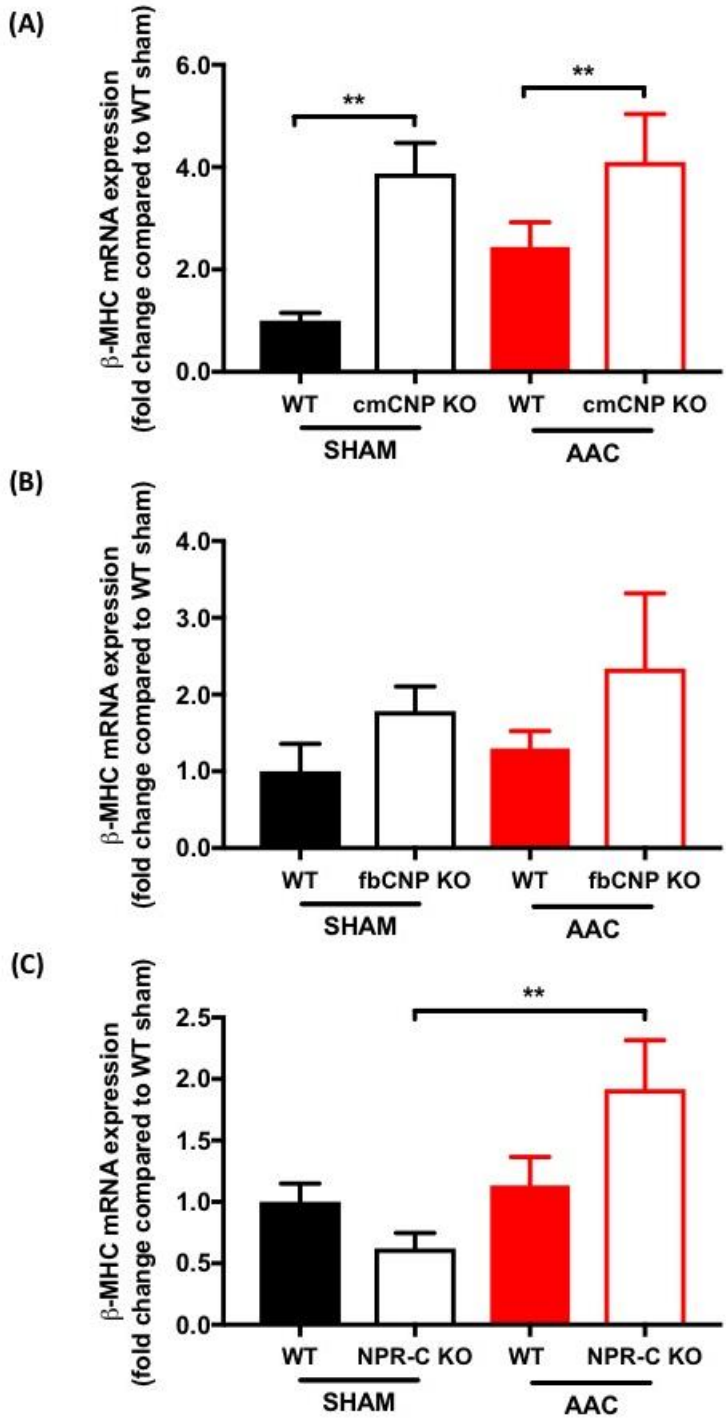

Figure 71. Effect of cmCNP, fbCNP and NPR-C deletion on β-MHC mRNA expression in pressure overload-induced heart failure.

β-MHC mRNA expression from left ventricles isolated from littermate WT, cmCNP KO, fbCNP KO and NPR-C KO mice subjected to sham or abdominal aortic constriction (AAC) for 6 weeks. Data are represented as the mean±SEM. n=3-6. ** $p<0.01$ using 2-way ANOVA followed by Bonferroni *post-hoc* test.

Effect of cmCNP, fbCNP and NPR-C deletion on cardiac hypertrophic gene profile in pressure overload-induced heart failure

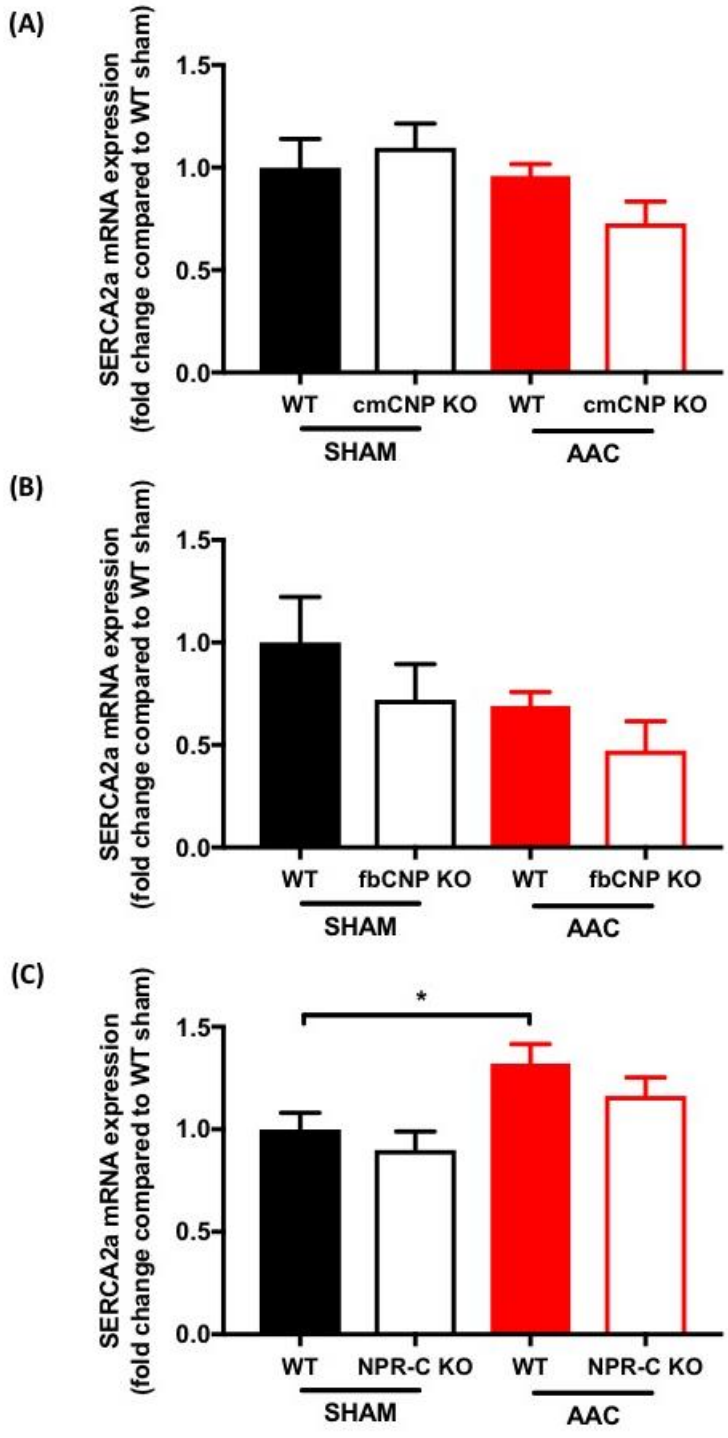

Figure 72. Effect of cmCNP, fbCNP and NPR-C deletion on SERCA2a mRNA expression in pressure overload-induced heart failure.

SERCA2a mRNA expression from left ventricles isolated from littermate WT, cmCNP KO, fbCNP KO and NPR-C KO mice subjected to sham or abdominal aortic constriction (AAC) for 6 weeks. Data are represented as the mean±SEM. n=4-6. *p<0.05 using 2-way ANOVA followed by Bonferroni *post-hoc* test.

Effect of cmCNP, fbCNP and NPR-C deletion on cardiac hypertrophic gene profile in pressure overload-induced heart failure

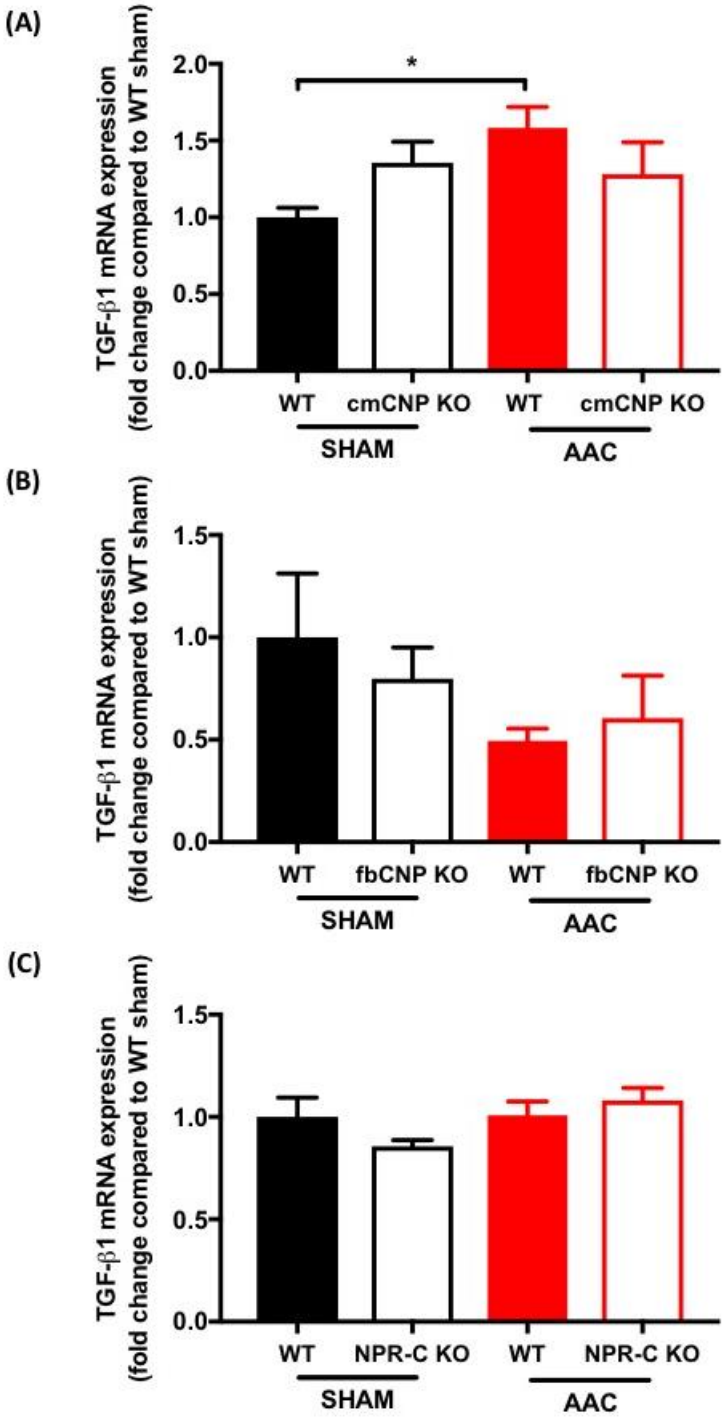

Figure 73. Effect of cmCNP, fbCNP and NPR-C deletion on TGF-β1 mRNA expression in pressure overload-induced heart failure.

TGF-β1 mRNA expression from left ventricles isolated from littermate WT, cmCNP KO, fbCNP KO and NPR-C KO mice subjected to sham or abdominal aortic constriction (AAC) for 6 weeks. Data are represented as the mean±SEM. n=4-6. *p<0.05 using 2-way ANOVA followed by Bonferroni *post-hoc* test.

Effect of cmCNP, fbCNP and NPR-C deletion on cardiac hypertrophic gene profile in pressure overload-induced heart failure

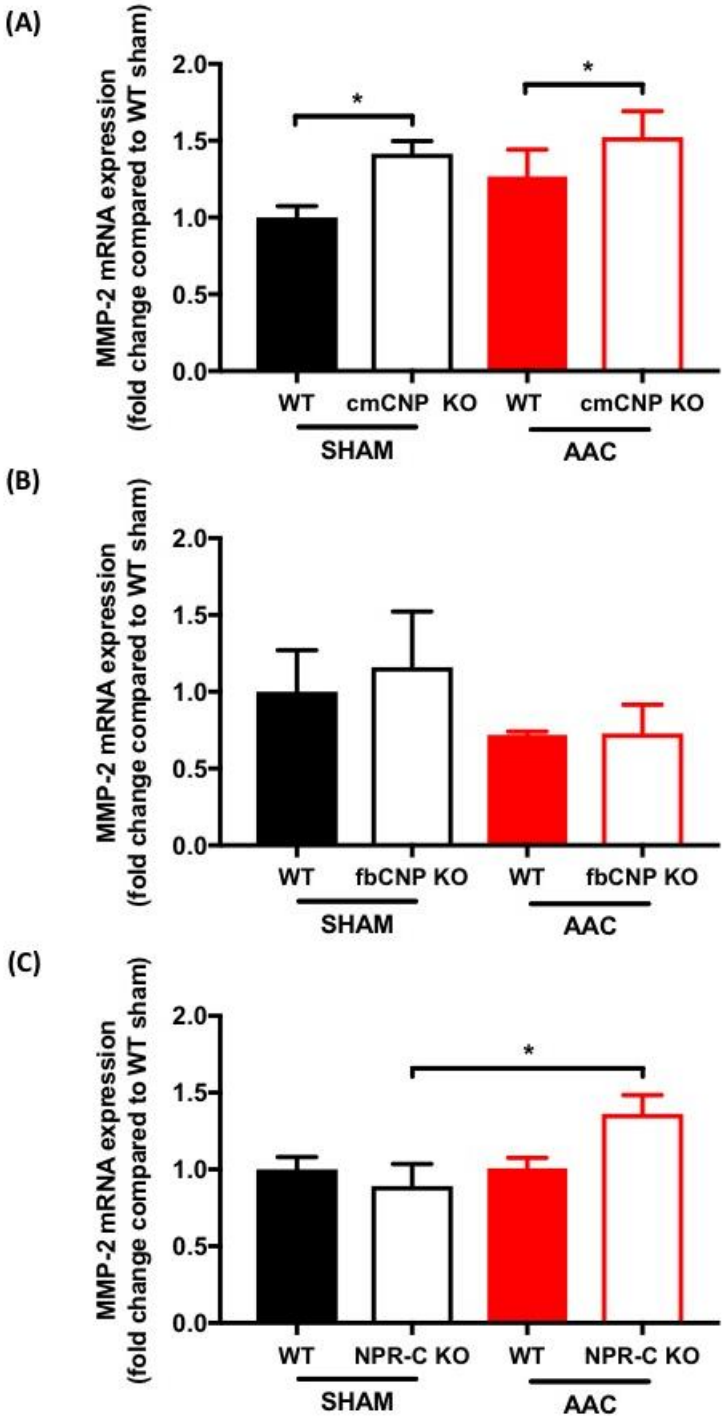

Figure 74. Effect of cmCNP, fbCNP and NPR-C deletion on MMP-2 mRNA expression in pressure overload-induced heart failure.

MMP-2 mRNA expression from left ventricles isolated from littermate WT, cmCNP KO, fbCNP KO and NPR-C KO mice subjected to sham or abdominal aortic constriction (AAC) for 6 weeks. Data are represented as the mean±SEM. n=4-6. *p<0.05 using 2-way ANOVA followed by Bonferroni *post-hoc* test.

Effect of cmCNP, fbCNP and NPR-C deletion on cardiac hypertrophic gene profile in pressure overload-induced heart failure

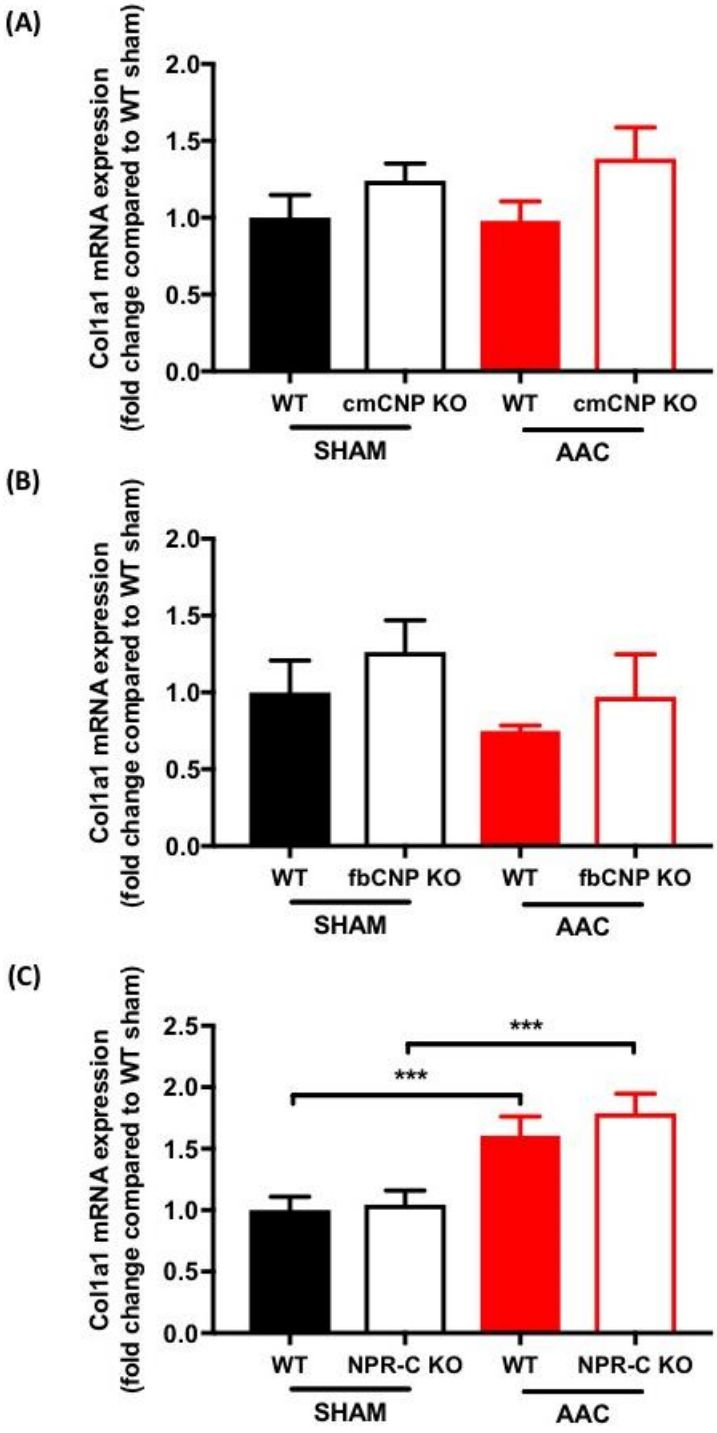

Figure 75. Effect of cmCNP, fbCNP and NPR-C deletion on Col1a1 mRNA expression in pressure overload-induced heart failure.

Col1a1 mRNA expression from left ventricles isolated from littermate WT, cmCNP KO, fbCNP KO and NPR-C KO mice subjected to sham or abdominal aortic constriction (AAC) for 6 weeks. Data are represented as the mean±SEM. n=4-6. ***p<0.001 using 2-way ANOVA followed by Bonferroni *post-hoc* test.

Effect of cmCNP, fbCNP and NPR-C deletion on cardiac hypertrophic gene profile in pressure overload-induced heart failure

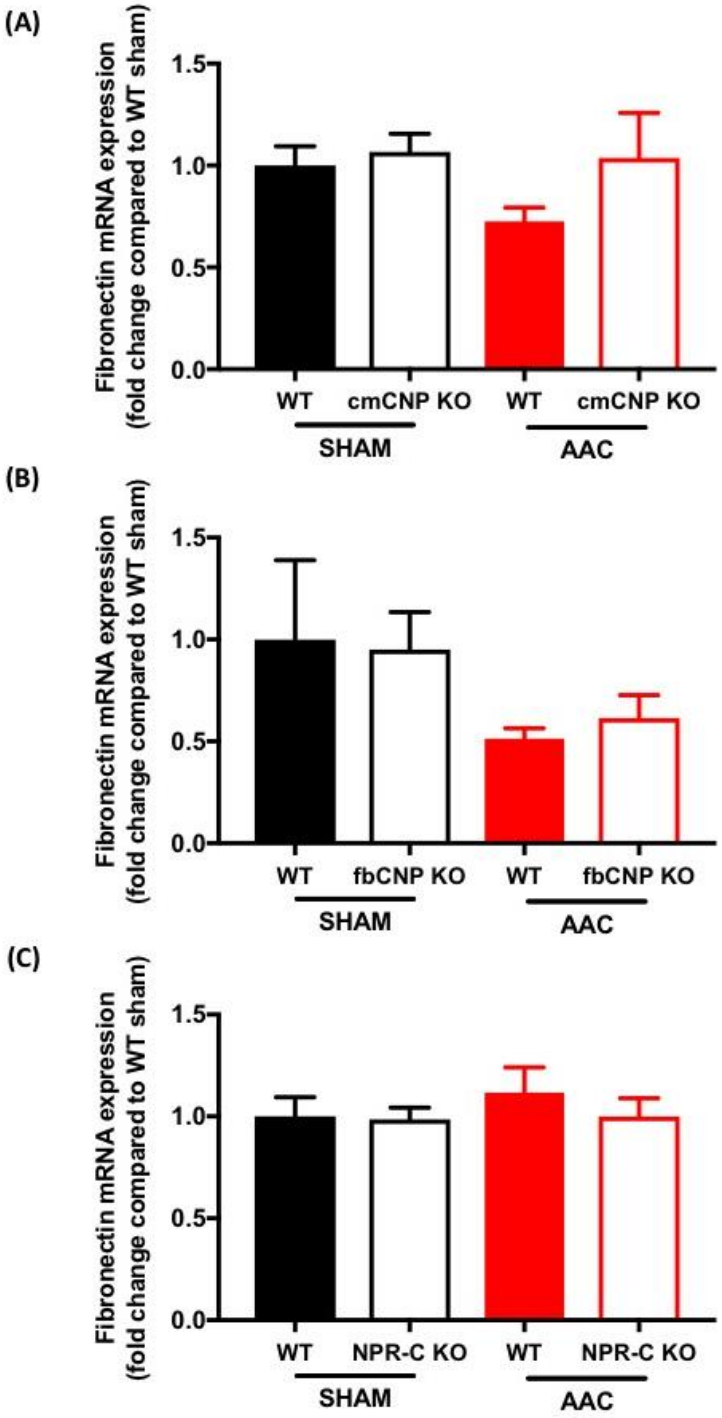

Figure 76. Effect of cmCNP, fbCNP and NPR-C deletion on fibronectin mRNA expression in pressure overload-induced heart failure.

Fibronectin mRNA expression from left ventricles isolated from littermate WT, cmCNP KO, fbCNP KO and NPR-C KO mice subjected to sham or abdominal aortic constriction (AAC) for 6 weeks. Data are represented as the mean±SEM. n=4-6.

4.8 Summary of key findings

The production of CNP from cardiomyocytes and cardiac fibroblasts in unison contributes to cardiac protection during HF. The cardiac dysfunction and morphology observed in cmCNP KO and fbCNP KO were replicated by the loss of NPR-C signalling, which was worse, *per se*, than each individual cell-specific CNP deletion. More importantly, administration of CNP rescued the deterioration of cardiac function and structure in WT mice, but this protective effect was absent in NPR-C KO mice. This indicates the importance of NPR-C signalling in CNP-mediated cardiac protection.

Chapter 5 – Discussion

Chapter 5 – Discussion

5 Discussion

5.1 Summary of key findings

In the first part of my thesis, I investigated the role of endogenous CNP in the coronary vasculature. My data showed the coronary reactivity is attenuated in ecCNP KO mice in response to endothelium-dependent vasodilators and reperfusion-induced vasodilatation compared to WT animals. This indicates endothelium-derived CNP is involved in the regulation of coronary vascular function. However, the production of CNP in the endothelium did not protect against IR injury, whilst cardiomyocyte-derived CNP displayed cardioprotective effects. These data suggest CNP has dual functions in the heart, i.e. regulates coronary vascular reactivity and protects against ischaemic myocardial damage. The reduced vascular responses and aggravated IR injury observed in ecCNP KO and cmCNP KO mice, respectively, were replicated in NPR-C KO mice, indicating endogenous CNP mediates its biological activity, at least in part, via NPR-C activation.

In the second part of this thesis, I explored the role of endogenous CNP in cardiac function, with focus on cardiac stress. I have demonstrated that mice lacking cardiomyocyte CNP exhibit worse cardiac dysfunction, accompanied by greater cardiac hypertrophy and fibrosis in both ISO- and pressure overload-induced HF models. This indicates that cardiomyocyte-derived CNP regulates cardiac function during cardiac stress via anti-remodelling and anti-fibrotic actions. This exacerbated response to cardiac stress was replicated in NPR-C KO mice. However, the phenotype observed in NPR-C KO was worse than cmCNP KO. This may stem from incomplete deletion of CNP (my data suggest an approximate 80% reduction in CNP mRNA expression in cardiomyocytes), activation of NPR-C by another natriuretic peptide (i.e. ANP or BNP), or that another cellular course of CNP is important. To investigate the latter hypothesis, I generated mice with fibroblast-restricted CNP deletion. This genetic alteration resulted in similar cardiac dysfunction to that observed in cmCNP KO mice following AAC. This indicates the production of CNP from both cardiomyocytes and cardiac fibroblasts in concert contributes to the cardioprotective effects during the development of HF. In addition, exogenous CNP attenuated the increase of hypertrophy in response to Ang II in isolated neonatal cardiomyocytes. In line with this finding, infusion of CNP normalised cardiac dysfunction following AAC in WT mice.

However, this protective effect was lost in mice lacking NPR-C. Taken together, the data suggest endogenous CNP has cardioprotective effects in the setting of HF and these are mediated via NPR-C activation.

5.2 CNP as a regulator of coronary vascular function

5.2.1 Endothelial derived CNP regulates coronary vascular reactivity

EDHF activity is of critical importance to cardiovascular physiology especially when production of NO/PGI_2 are compromised in CVDs (Luksha et al., 2009). This is illustrated in female eNOS/COX-1 double KO mice in which no alteration in resistance vascular reactivity and BP remains at basal levels (Scotland et al., 2005). Chauhan *et al*. 2003 showed that CNP is indistinguishable from EDHF, suggesting CNP plays a prominent role in endothelial function. In fact, recent studies have demonstrated that CNP is essential for multiple aspects of vascular regulation by influencing peripheral vascular resistance and systemic BP, vascular integrity, leukocyte infiltration and platelet aggregation (Moyes et al., 2014, Nakao et al., 2017). Indeed, CNP relaxes coronary arteries *in vitro* (Wei et al., 1994, Wright et al., 1996) and *ex vivo* (Hobbs et al., 2004). These observations provide support for the role of CNP in the coronary vasculature and, potentially, as a therapeutic target for CAD and MI.

In this study, I have demonstrated that ACh evokes the release of CNP from endothelial cells into the coronary circulation and induces vasodilatation. This corresponds with previous research in mesenteric arteries (Chauhan et al., 2003) and isolated hearts (Hobbs et al., 2004). The response to BK in male ecCNP KO was similar to its WT littermates but significantly reduced in female ecCNP KO, indicating a sex difference for the role of CNP in coronary vascular function. However, the response to ACh is equally blunted in both male and female ecCNP KO, suggesting CNP contributes to coronary endothelial function in both sexes. The reason why responses to BK were not altered in male ecCNP KO mice remains unclear, but previous work has shown that mesenteric artery responses to BK in male eNOS/COX-1 double KO are abolished, but 55% relaxation is preserved in female animals (Scotland et al., 2005). This suggests that male rodents predominantly release NO and/or PGI_2 in response to BK.

Shear-stress upregulates CNP expression in human endothelial cells (Chun et al., 1997, Okahara et al., 1995). Reperfusion following a transient cessation of flow creates shear force that can induce vasodilatation. In the isolated heart model, vasodilatation in response

to rapid reperfusion in female ecCNP KO mice was significantly blunted, indicating CNP is involved in shear-induced vasodilatation. This observation is particularly important in the context of MI as CNP could be released in response to shear force during the initial reperfusion of the ischaemic heart. The release of CNP potentially can provide a protective mechanism to offset IR injury (investigated in the later chapter of this thesis). The multi-faceted role of CNP, including vasodilatation, preventing leukocyte infiltration and platelet-aggregation, and inhibiting VSMC proliferation (Scotland et al., 2005, Khambata et al., 2011, Moyes et al., 2014) would undoubtedly be beneficial in preventing progression of CAD and/or as a secondary prevention after MI. Taking together, these data suggest endothelial release of CNP plays a role in regulating blood flow in the coronary vasculature and could be protective in ischaemic heart disease.

5.2.2 NPR-C as the cognate receptor that coveys CNP-mediated coronary reactivity

CNP binds to and activates both NPR-B and NPR-C. Early studies showed that CNP-induced relaxation of vascular smooth muscle is mediated via NPR-B activation in aorta (Drewett et al., 1995). However, ACh-induced vasodilatation in the mesenteric arteries is preserved in mice lacking NPR-B and such animals are normotensive (Nakao et al., 2017, Tamura et al., 2004). This suggests NPR-B is not the predominant receptor mediating the vascular/hypotensive actions of CNP. In contrast, endothelium-dependent dilatation to ACh is diminished in the resistance arteries of NPR-C KO mice and these animals display a hypertensive phenotype that is similar to ecCNP KO mice (Moyes et al., 2014). These observations indicate NPR-C is involved in conveying CNP biological signalling in the resistance vasculature. The distinct receptor responsible for the vasodilator actions of CNP is therefore likely to be specific to the vascular bed investigated, i.e. conduit (NPR-B) vs. resistance vessels (NPR-C).

In the present study, the coronary reactivity in NPR-C KO mice was markedly blunted in response to endothelium-dependent vasodilators and the response to reperfusion-induced vasodilatation compared to WT littermates, suggesting NPR-C activation is involved in coronary reactivity. These data are in line with previous studies that have demonstrated CNP bioactivity is mimicked by a selective NPR-C agonist, $cANF^{4-23}$, whilst the selective NPR-C inhibitor, M372049, attenuated the activity of both CNP and $cANF^{4-23}$ (Villar et al., 2007). However, my work has shown that the coronary response to exogenous CNP was not completely abolished in NPR-C KO mice, suggesting there is a NPR-B component in mediating CNP-induced vasodilatation. In addition, the reduced coronary reactivity in NPR-

C KO mice is more pronounced compared to ecCNP KO. This may due to incomplete deletion of endothelial production of CNP (~80%; (Moyes et al., 2014)) or that an additional natriuretic peptide could be secreted from the endothelium (although there is little or no precedence for this in the literature).

5.3 CNP protects against ischaemia-reperfusion injury

5.3.1 Endogenous CNP attenuates ischaemia-reperfusion injury

IR injury is the combination of cell damage caused by the initial ischaemic period and the process of reperfusion. This is characterised by endothelial dysfunction that leads to the loss of protective NO and PGI_2 signalling, resulting in vasoconstriction and infiltration of inflammatory cells. Experimental and clinical studies have demonstrated that short or long periods of myocardial ischaemia are associated with the rapid release of natriuretic peptides and induction of *de novo* peptide synthesis (Baxter, 2004). These responses possibly act as an innate cardioprotective mechanism to cardiac stress. Previous studies have shown that pharmacological administration of CNP or other natriuretic peptides including ANP, BNP and urodilatin, provides a protective effect against IR injury across different species (Hobbs et al., 2004, Jin et al., 2014, D'Souza et al., 2003, Padilla et al., 2001, Rastegar et al., 2000). A randomised clinical trial (J-WIND) has also demonstrated that infusion of ANP in patients with acute MI reduces infarct size, fewer reperfusion injuries and better cardiac function at 6-12 months follow-up compared to the placebo group (Kitakaze et al., 2007). However, some patients experience severe hypotension with ANP treatment. CNP is known to have less haemodynamic effects compared to ANP and BNP. Herein, I investigated the pathophysiological role of CNP in IR injury to examine if it has similar injury-limiting action. My findings have revealed that deletion of endothelial-derived CNP does not affect infarct size and recovery of LVDP, indicating endothelial CNP does not have a direct cardioprotective effect against acute IR injury. This is at odds with the protective effect observed following exogenous infusion of CNP in a previous study (Hobbs et al., 2004). This discrepancy could be due to the amount of endogenous CNP released that produced by shear stress at the beginning of reperfusion may not be sufficient to have a protective effect compared to exogenous CNP administration. The latter might be argued would have promoted greater vasorelaxations and/or able to penetrate into the myocardium, exerting direct protective effects on cardiomyocytes. Nevertheless, the importance of endothelial CNP in the maintenance of endothelium function, for example, reducing platelet aggregation, leukocyte adhesion and infiltration

(such cells are well established to exacerbate IR injury (Bonaventura et al., 2016) but are not present in isolated heart preparations perfused with Krebs-Henseleit buffer), may have a long-term cardioprotective mechanism in patients that experience an MI. Further studies with *in vivo* models of MI would be needed to confirm this hypothesis.

Although endothelium-derived CNP does not appear to protect against acute IR injury, I have demonstrated that mice with cardiomyocyte CNP deletion have significantly exacerbated infarct size and a reduction in LVDP recovery following IR injury in both female and male animals. These findings suggest cardiomyocyte-derived CNP acts in an autocrine fashion and protects myocytes from injury, possibly against necrosis/apoptosis. The mechanism of this cardioprotective effect exerted by CNP is unclear. Previous studies have demonstrated that BNP limits infarct size in isolated hearts (D'Souza et al., 2003, Burley and Baxter, 2007). This protective effect is abolished by K_{ATP} channel blockers, implying BNP/cGMP/K_{ATP} channel signalling may be responsible for the injury-limiting mechanism mediated by natriuretic peptides (D'Souza et al., 2003, Burley and Baxter, 2007).

5.3.2 NPR-C activation is involved in the cardioprotective effects of CNP against IR injury

In ischaemic conditions, the low intracellular pH induces a profound depressant effect on pGC in cultures of cardiomyocytes and endothelial cells (Agullo et al., 2003), suggesting NPR-A/B activity may not be the main contributor to IR protection. Hence, there may be a role for NPR-C signalling in IR injury. The present study has shown that NPR-C KO mice exhibit worse IR injury compared to WT controls; an observation that is equivalent to cmCNP KO animals. This indicates CNP/NPR-C signalling protect against acute IR injury, which is in agreement with previous study that reported blockade of NPR-C abolishes CNP-mediated cardiac protection in IR injury (Hobbs et al., 2004). This cardioprotective effect may be the results of increased coronary dilation, inhibition of L-type Ca^{2+} current and reduction of HR, which significantly increases myocardial perfusion (Rose et al., 2004, Hobbs et al., 2004).

Furthermore, it is well established that K_{ATP} channel opening on either cytoplasmic or mitochondrial membrane is protective in IR injury (Loukogeorgakis et al., 2007, Tinker et al., 2014, Suzuki et al., 2002). In fact, most neural, autocrine or paracrine mediators of ischaemic preconditioning signal via a transduction pathway involving putative mitochondrial K_{ATP} channel opening (Baxter, 2004). K_{ATP} channels can be modulated by CNP in the vasculature and cardiomyocytes (Umaru et al., 2015, Burley et al., 2014) that is likely

via activation of NPR-C receptor as its signalling is required for hyperpolarisation, vasorelaxation and endothelial proliferation (Villar et al., 2007, Khambata et al., 2011, Kun et al., 2008). Thus, K_{ATP} channel opening a plausible mechanism for the protective effects of cardiomyocyte-derived CNP demonstrated in this thesis. The opening of GIRK channels induces similar changes in K^+ influx as K_{ATP} channel activation and thus, CNP-induced opening of GIRK channel via NPR-C activation may be able to mediate a similar cardioprotective effect. In fact, there is evidence demonstrating that reduced K_{ir} channel activity exacerbates IR injury (Aziz et al., 2017). Furthermore, CNP signalling contributes to the activity of K_{ATP} channel in isolated myocardium (Burley et al., 2014) and K_{ATP} channel belongs to the K_{ir} channel superfamily. This suggests the beneficial effect of CNP against IR injury can be mediated via activating K_{ATP} channels directly or by opening of K_{ir} channel through NPR-C signalling. Interestingly, heart samples from patients with ischaemic cardiomyopathy have elevated levels of *Nppc* and *Npr3* mRNA expression, supporting the role of CNP/NPR-C in ischaemic CVD (Tarazon et al., 2014).

Nevertheless, one cannot exclude the possibility that NPR-B/cGMP transduction signalling may also contributes to the protective mechanism exerted by CNP. Previous studies have shown that elevations of cGMP by NPR-A activation or over-expression of eNOS attenuate IR injury (D'Souza et al., 2003, Okawa et al., 2003, Brunner et al., 2003). In addition, the protective action of BNP is blocked by NPR-A/B antagonism, K_{ATP} channel inhibitors and L-NAME (Burley and Baxter, 2007), indicating a cross-talk between NPRs/eNOS/K_{ATP} channel opening. However, in the same model, the NO donor SNP is not protective, illustrating the cardioprotective effect is result of a more complex mechanism that is not solely due to a general increase in intracellular cGMP. In fact, cGMP compartmentation is well documented and the generation of specific pools of cGMP "in the right place, and at the right time" could account for the differential responses to sGC and pGC stimulation triggered by NO and natriuretic peptides, respectively. CNP is the sole intrinsic agonist for NPR-B, so it would be interesting to investigate if NPR-B transduction participates in the cardioprotective mechanism of CNP. However, a selective NPR-B antagonist or agonist is not available, thus, generation of a cell-specific NPR-B KO mouse is merited as global NPR-B deletion results in dwarfism (Tamura et al., 2004), making evaluation of cardiovascular homeostasis difficult.

5.3.3 CNP has potential therapeutic benefits in MI

Microvascular dysfunction occurs post-MI and ultimately leads to CHF. It has been reported that microvascular dysfunction is found in the infarcted territory as well as the non-infarcted regions (Yong and Fearon, 2013). The presence of more widespread microvascular dysfunction in the injured heart is an independent predictor of long-term cardiac mortality in STEMI patients (van de Hoef et al., 2013). The loss of CNP signalling may contribute to microvascular dysfunction observed in patients with MI. In fact, diminished CNP-dependent signalling induced by a dominant negative NPR-B mutant exhibits cardiac hypertrophy at basal level (Langenickel et al., 2006). CNP mRNA expression in infarcted hearts is elevated (Soeki et al., 2005) and animals with over-expression of CNP are resistant to ventricular hypertrophy induced by MI (Wang et al., 2007). This chronic elevation of CNP expression in infarcted myocardium probably counteracts the pro-hypertrophic and pro-fibrotic signalling activated by other mediators such as Ang II, catecholamines and cytokines during cardiovascular pathology. Moreover, increase of plasma CNP levels by osterin, an endogenous peptide that competitively bound to NPR-C with natriuretic peptides, suppresses the progression of congestive heart failure after MI in mice (Miyazaki et al., 2018). Furthermore, the ability of CNP to promote endothelial growth while inhibiting VSMC proliferation undoubtedly can protects the heart from atherosclerosis and restenosis in MI patients who have undergone PCI. The acute and chronic actions of CNP in myocardial ischaemia suggest a profile of activity that may be therapeutically beneficial in the management of patients with acute coronary syndromes and in preventing post-infarction remodelling that leads to CHF.

In summary of my data from the isolated heart model, I have identified that endogenous CNP modulates coronary perfusion and has cardioprotective effects against acute IR injury. These biological activities of CNP are, at least in part, via NPR-C signalling.

5.4 CNP in chronic heart failure

5.4.1 CNP maintains cardiac structure and function in pathological conditions

Although ANP and BNP act on the same receptor, NPR-A, their role in the regulation of myocardial structure is not straightforward. Mice lacking ANP or NPR-A display salt-resistant arterial hypertension, with a disproportionate ventricular hypertrophy and cardiac fibrosis (John et al., 1995, Kuhn et al., 2002, Lopez et al., 1995). Whereas, BNP null mice do not exhibit cardiomyocyte hypertrophy, despite BNP being the predominant ventricular

natriuretic peptide; but they do exhibit a marked cardiac fibrosis (Tamura et al., 2000). Therefore, a better understanding of the complex signalling pathways underlying the natriuretic peptides in the regulation of myocardial architecture and cardiac function is required. Earlier studies have reported that ANP prevents ventricular remodelling via inhibition of the RAAS since cardiac hypertrophy induced by deletion of NPR-A is blocked by Ang II receptor deficiency (Li et al., 2009). Moreover, clinical studies also have shown that infusion of ANP supresses Ang II and ET-1, which could be responsible for the cardioprotective effects (Hayashi et al., 2001). In Japan, a recombinant ANP analogue, carperitide, has been approved for intravenous administration in patients with HF (Saito, 2010). While BNP (nesiritide), which has similar cardioprotective effects by acting on the same receptor (NPR-A), has been approved in the US (Burnett, 2005). In addition, BNP administration to isolated perfused rat hearts prior to and during an ischaemic insult reduces infarct size in a concentration-dependent fashion (D'Souza et al., 2003).

The role of CNP in cardiac function had been overlooked due to a failure to detect its presence in the heart and in the plasma of patients with CHF in early studies (Takahashi et al., 1992, Cargill et al., 1994). Only in recent years has it been confirmed that CNP and NPR-B are co-localised in the heart, and the plasma levels of CNP are increased in relation to the severity of CHF (Kalra et al., 2003, Del Ry et al., 2005, Del Ry et al., 2008a). It is well established that pharmacological administration of CNP has anti-hypertrophic and anti-fibrotic actions, and prevents cardiac remodelling in *in vivo* HF models (Soeki et al., 2005, Wang et al., 2007, Izumiya et al., 2012). In fact, studies showed that CNP has more potent anti-fibrotic and anti-hypertrophic effects than ANP (Tokudome et al., 2004, Horio et al., 2003). These findings might be due to the relative abundance of NPR-B over NPR-A in cardiac fibroblasts and in cardiomyocytes (Tokudome et al., 2004, Horio et al., 2003). Such evidence intimates a pathophysiological role of CNP in CHF and thus, suggests a novel therapeutic target. The present study demonstrated for the first time that cardiomyocyte-derived CNP exerts cardioprotective effects during cardiac stress, including aetiologically distinct models of HF.

Regardless of the pathological stimulus (AAC or ISO infusion), cmCNP KO mice exhibited a worse cardiac phenotype than littermate controls, i.e. LV dilatation, greater reduction in EF and FS, accompanied by higher collagen deposition (and a more modest effect on LV hypertrophy and cardiomyocyte size). Yet, isolated cardiomyocytes from cmCNP KO mice exhibited greater hypertrophic response to Ang II *in vitro*, which was reversed with

pharmacological administration of CNP. These observations in concert with previous work (Rosenkranz et al., 2003, Tokudome et al., 2004) imply CNP can play a fundamental, autocrine role in the regulation of cardiomyocyte hypertrophy.

More importantly, pharmacological infusion of CNP reverses the decline of cardiac function and fibrosis following AAC without affecting haemodynamics. This illustrates a critical role for CNP in maintaining cardiac structure and performance during cardiac stress. This corroborates early studies demonstrating CNP has positive inotropic, lusitropic, chronotropic and dromotropic effects in intact animals, isolated hearts, cardiac muscle preparations and isolated cardiomyocytes from different species (Beaulieu et al., 1997, Hirose et al., 1998, Brusq et al., 1999, Pierkes et al., 2002). In accord, the plasma levels of CNP in patients with chronic HF correlate with LV dp/dt and EF (Del Ry et al., 2008b), indicating CNP production is associated with cardiac contractility. Correspondingly, CNP infusion at pharmacological dose significantly increases maximum dP/dt, LV end-diastolic pressure and cardiac output (Obata et al., 2007, Soeki et al., 2005). These data illustrate that CNP is involved in the regulation of cardiovascular homeostasis and the fact that CNP concentrations increase with clinical severity support a compensatory effect to maintain cardiac function. Whereas, a loss/reduction of CNP production i.e. cmCNP KO mice, is more susceptible to the development of HF.

5.4.2 Different sources of CNP contribute to cardiac function

It has been reported that CNP is produced and secreted from cardiac fibroblasts in the failing heart and has a suppressive effect on fibroblast proliferation and ECM production (Kalra et al., 2003, Horio et al., 2003). Thus, one of the possible sources of increased CNP levels in patients with HF could be the cardiac fibroblast. In this regard, I have developed fbCNP KO mice and subjected them to pressure-overload to investigate the role of cardiac fibroblast-derived CNP in cardiac function. At baseline, the ablation of CNP from fibroblast has no adverse effect. But when exposing to AAC, those mice developed enhanced maladaptive cardiac hypertrophy and fibrosis with greater decline in cardiac function similar to cmCNP KO mice. This indicates cardiac fibroblast-derived CNP, likewise, prevents pathological cardiac remodelling. These observations are unsurprising. Previous *in vitro* studies have demonstrated that CNP is synthesised and secreted from cardiac fibroblast and act as an autocrine regulator, inhibiting excess collagen production (Horio et al., 2003). In addition, CNP prevents cardiac fibroblast differentiation and migration (Li et al., 2014b). These imply endogenous CNP might participate in fibroblast-myocyte communication

during cardiac remodelling and in concert, negatively regulate hypertrophy and fibrosis. Since different sources of CNP are playing a part in cardiovascular homeostasis, perhaps cm/fbCNP double KO mouse would be permitted to examine a wider effect of endogenous CNP in cardiovascular (patho)physiology?

5.5 Mechanistic delineation of CNP-mediated cardioprotection

5.5.1 NPR-B vs. NPR-C activation

Elevations in cGMP, for example following PDE5 inhibition (Takimoto et al., 2005) or NOS activation (Janssens et al., 2004), have shown to be cardioprotective and hence NPR-B/cGMP transduction signalling has been thought to play a key role in CNP-mediated beneficial effects. Previous studies have shown that CNP modulates the growth, proliferation, and hypertrophy of VSMCs, cardiomyocytes and fibroblasts via NPR-B activation (Rosenkranz et al., 2003, Horio et al., 2003, Furuya et al., 1991). Furthermore, transgenic rats expressing a dominant-negative mutant of NPR-B develop progressive, BP-independent cardiac hypertrophy (Langenickel et al., 2006). However, those mice did not exhibit an increased interstitial or perivascular fibrosis, while infusion of CNP attenuates cardiac fibrosis (Soeki et al., 2005). This discrepancy in CNP biology suggests a non NPR-B signalling pathway maybe involved. Moreover, the protective effect of ANP and CNP is thought to mediate via cGKI (or PKG). However, chronic ISO administration has no adverse effect in cardiac-specific PKG KO mice (Frantz et al., 2013). This suggests the cardiac dysfunction induced by ISO infusion in cmCNP KO mice is not due to the loss of cGMP/PKG signalling.

BNP has been shown to inhibit human fibroblast growth that is not affected by the application of the NPR-A/B blocker, HS-142-1, but surprisingly antagonised by a NPR-C ligand, $cANF^{4-23}$, suggesting BNP acts on NPR-C and regulates fibroblast proliferation. In addition, NPR-C has also been implicated in anti-hypertrophic effects in VSMCs (Cahill and Hassid, 1994, Khambata et al., 2011) and protects against cardiomyocyte apoptosis (Lin et al., 2016). These findings suggest NPR-C signalling may counteract cardiac remodelling and prevent ventricular wall thinning.

5.5.2 NPR-C activation is involved in CNP-mediated cardioprotective effects

In the present study, I have demonstrated that the cardiac dysfunction in cm/fbCNP KO mice is recapitulated in NPR-C KO animals, suggesting NPR-C signal transduction is

responsible for the cardioprotective mechanism of CNP. A recent study has demonstrated that an endogenous NPR-C ligand, osteocrin, suppresses infiltration of M1 macrophages and prevents cardiac remodelling following MI (Miyazaki et al., 2018). Such protective effects are thought to be attributed to the inhibition of ANP clearance when osteocrin binds to NPR-C. However, my thesis suggests NPR-C transduction pathway has a positive protective role in cardiovascular pathology as the NPR-C null mice exhibit an adverse response to cardiac stress, despite the removal of a clearance system for natriuretic peptides. Thus, osteocrin may exert cardioprotective effect directly via NPR-C activation. Indeed, the cardiac phenotype was worse following global deletion of NPR-C compared to individual cell-specific CNP KO (demonstrated by an additional increased in LV chamber, collagen deposition and cardiomyocyte size). Hence, activation of NPR-C offers more than just a clearance role; its signalling can be critical in mediating anti-remodelling mechanism(s). This notion is further supported by my study evaluating phenotypic rescue using pharmacological administration of CNP. A sub-pressor dose of CNP was able to prevent LV remodelling and preserve cardiac performance in WT mice subjected to pressure overload. However, the protective effect was lost in NPR-C KO mice, confirming the requirement of NPR-C activation in CNP-mediated cardiac protection. These data suggests that although CNP production is elevated in patients with HF (Del Ry et al., 2005) (likely as an endogenous protective mechanism), it is possible to further increase NPR-C-dependent signalling for therapeutic gain. Therefore, the development of NPR-C agonists may represent a novel approach for HF treatment.

5.5.3 Pro-hypertrophic and pro-fibrotic pathways inhibited by CNP/NPR-C signalling

Mechanistic delineation of CNP-mediated cardioprotection in response to cardiac stress was investigated by study of the pro-hypertrophic and pro-fibrotic markers in the hearts from cmCNP, fbCNP and NPR-C KO mice. The depressed cardiac performance in cmCNP KO and NPR-C KO animals in response to AAC was accompanied by up-regulation of ANP and β-MHC mRNA expressions, confirming an enhanced hypertrophic response. These hypertrophic genes are also correlate with the severity of HF (Koentges et al., 2017). It is possible that the loss of clearance function in NPR-C KO mice is partly responsible for the increase in ANP mRNA expression. However, studies in NPR-C KO mice detected no change in steady levels of plasma ANP although the ANP half-life was increased (Matsukawa et al., 1999). This indicates that ANP production (i.e. ANP mRNA level) in NPR-C KO mice is, if anything, decreased to match the reduced clearance rate. Hence, the increased ANP mRNA

expression in NPR-C KO mice in this study reflects the pathological severity. Mice with deletion of CNP or NPR-C also have a trend towards to a reduction in the expression of SERCA2a mRNA that encodes for SERCA. Myocyte Ca^{2+} cycling is primarily governed by SERCA, which mediates Ca^{2+} sequestration into the SR and regulates cardiac contractility. Alternated levels in SERCA is associated with human HF (Schwinger et al., 1999, Frank et al., 2002, Hayward et al., 2015), and observed in murine pressure-overload models (Zolk et al., 1998, Nagayama et al., 2009). The downregulation of SERCA2a expression in the KO mice subjected to AAC indicates impaired myocyte Ca^{2+} handling and accounts for diminished cardiac contractility. This hypothesis is supported by studies that showed CNP improves Ca^{2+} handling and contractile function in isolated adult myocytes (Wollert et al., 2003), and that plasma levels of CNP in patients with HF correlates with cardiac contractility (Del Ry et al., 2008b).

The worse cardiac fibrosis observed in cm CNP KO mice was explained by upregulation of fibrotic gene expression including Col1a1, fibronectin and MMP-2. This observation corresponds with previous studies that showed CNP directly inhibits both DNA and collagen synthesis in cardiac fibroblasts (Horio et al., 2003). Indeed, CNP expression tends to decrease as cardiac fibrosis increases (Sangaralingham et al., 2011, Ichiki et al., 2014). Furthermore, CNP mRNA expression is elevated in the fibrotic area of the infarct region following MI. Taken together, the findings indicate the release of CNP from cardiomyocytes may exert inhibitory action(s) on the adjacent cardiac fibroblasts and reduce the production of collagen/ECM.

In addition, cmCNP KO mice displayed increases in hypertrophic gene expression such as ANP, β-MHC and MMP-2 at basal level, suggesting that the deletion of cardiac CNP is prone to cardiac remodelling and dysfunction innately, and may potentially develop progressive HF with age. Indeed, natural aging hearts have progressive decline in CNP levels and associate with increase in LV fibrosis that leads to impairment of diastolic and systolic function.

5.6 The possible mechanisms of NPR-C-mediated cardioprotection

5.6.1 NPR-C couples with G_i-protein

NPR-C is traditionally known as a clearance receptor. However, the cytoplasmic domain of NPR-C comprises several PTx-sensitive G_i activator sequences implying it can elicit

physiological functions via inhibition of AC/cAMP signal transduction and/or through activation of PLC (Pagano and Anand-Srivastava, 2001, Anand-Srivastava et al., 1996). Consistent with this notion, Anand-Srivastava *et al*. (1991) have shown that ANP and the NPR-C agonist, $cANF^{4-23}$, inhibit AC activity in platelets that express only NPR-C. The group also demonstrated that NPR-C activation is sufficient for the inhibition of AC signalling by using an antibody raised against the NPR-C cytoplasmic domain (Anand-Srivastava et al., 1996). Furthermore, studies reported that NPR-C-mediated decreases in cAMP contribute to the activation of PLC signalling (Mouawad et al., 2004), which promotes cell proliferation (Schmidt et al., 1999, Hayashi et al., 2000) that suggests NPR-C activation may not attributes to the anti-hypertrophic effects. On the other hand, cAMP activity promotes cardiac hypertrophy and inotropy, explaining the contraindication of PDE3 inhibitors and β-agonists in HF. Thus, inhibitory action of NPR-C/G_i on cAMP may be cardioprotective. Moreover, dys-regulation of the autonomic nervous system has been implicated in both animal model of CVD and in human HF (van Bilsen et al., 2017). Buttgereit *et al.* 2016 has demonstrated that CNP via NPR-B signalling reduces sympathetic activation that could have beneficial effects. However, inhibition of cAMP via NPR-C/G_i-protein signalling may also be involved in sympatho-inhibition that could also be cardioprotective.

$G_i\alpha$ activation is implicated in hypertrophic cardiomyopathy (Ruan et al., 2007). *In vivo* treatment of $cANF^{4-23}$ attenuates high BP in SHR through inhibition of enhanced $G_i\alpha$ level and oxidative stress (Li et al., 2014a, Rahali et al., 2018). Similarly, $cANF^{4-23}$ attenuates Ang II-induced enhanced overexpression of $G_i\alpha$ protein, which leads to inhibition of MAPK signalling and attenuates hyper-proliferation (El Andalousi et al., 2013, Rahali et al., 2018, Madiraju et al., 2018). These data suggest NPR-C-mediated cardioprotective effects might be via inhibition of oxidative stress, suppression of $G_i\alpha$ protein expression and the associated pathways.

5.6.2 NPR-C and NOS cross-talk

It is well established that NO production by NOS activation increases cGMP levels and maintains cardiovascular homeostasis. Several studies have supported the importance of the cross-talk between NO and the natriuretic peptide system. Costa *et al*. (2006) have demonstrated that ANP and $cANF^{4-23}$ increase NOS activity, which is blunted by G_i inhibition, L-type Ca^{2+} channel blockers and calmodulin antagonists, indicating NPR-C/G_i-coupling mediates the activation of Ca^{2+}-dependent NOS (Costa et al., 2006). Moreover, NPR-A/B blockade induces no change in NOS stimulation via CNP (Caniffi et al., 2010),

confirming that CNP interacts with NPR-C, activating Ca^{2+}–calmodulin and eNOS via G_i proteins. Other mechanisms of cross-talk between NPR-C and eNOS have been proposed. Activation of NPR-C induces the release of $G_{\beta\gamma}$ -subunits that leads to PLC stimulation and subsequent PKC activation (Sabbatini et al., 2007). This leads to the generation of IP_3 and DAG from PIP_2 that results in intracellular Ca^{2+} mobilisation and activation of calmodulin (Murthy et al., 2000). G_i coupling also activates PI3 kinase, which triggers Akt and in turn phosphorylates NOS. In a parallel study in the Hobbs lab, mice with infusion of CNP subjected to AAC were administrated L-NAME in the drinking water to investigate whether CNP/NOS cross-talk is involved in the cardioprotective mechanism exerted by CNP. The rescue of cardiac function by CNP was unaffected by inhibition of NOS (data not shown), demonstrating CNP/NPR-C/NOS transduction is not responsible for the cardioprotective effects of CNP seen in this thesis. This corresponds to a recent study that demonstrated NPR-C activation by $cANF^{4-23}$ attenuates high BP in spontaneous hypertensive rat (SHR) but concomitantly decreases levels of eNOS and NO, suggesting NPR-C acts through an eNOS/cGMP independent pathway (Li et al., 2014a).

5.6.3 NPR-C and $G_q\alpha$ interaction

Activation of $G_q\alpha$ contributes to cardiomyocyte hypertrophy in cell culture and *in vivo* models (Akhter et al., 1998, Dorn et al., 2000, Filtz et al., 2009, Mende et al., 1998). Hormones such as Ang II, ET-1, and phenylephrine can activate G_q-coupled receptors, and have been implicated in the development and progression of cardiac hypertrophy and HF (Wettschureck et al., 2001, Dorn et al., 2000, Atef and Anand-Srivastava, 2014). Transgenic mice with cardiac overexpression of G_q have an intrinsic hypertrophic gene expression profile and develop a maladaptive form of eccentric hypertrophy in response to pressure-overload (Sakata et al., 1998). Consistent with this observation, cardiac-specific overexpression of a G_q dominant negative mini-gene causes resistance to cardiac hypertrophy following TAC (Akhter et al., 1998). These studies demonstrated G_q signalling is critical in triggering cardiac hypertrophy after the hemodynamic stress of pressure overload.

G_q signalling is implicated in MAPK/PI3K signalling upon NPR-C activation (Li et al., 2006, Jain and Anand-Srivastava, 2018). Also, alternation of $G_i\alpha$ protein levels has been implicated in MAPK/PI3K signalling (Bou Daou et al., 2016). These suggest NPR-C-mediated anti-proliferation could be achieved via attenuating $G_i\alpha$ activity that in turns suppress G_q and MAPK transduction signalling (El Andalousi et al., 2013, Hashim et al., 2006). Taken

together, it is likely that NPR-C activation exerts a critical brake against the upregulated G_q/PLC-β/MAPK pathway in response to AAC, and this cascade is worth to be investigated further in cmCNP and NPR-C KO hearts.

5.6.4 Regulator of G-protein signalling

Previous work has shown that activation of regulator of G-protein signalling (RGS) inhibits G_q/PLC-β signalling and mediates cardiac compensation to pressure-overload (Takimoto et al., 2009). RGS proteins are a set of negative controllers of GPCR activity that work by accelerating G_α-dependent GTP hydrolysis to reconstitute the heterotrimeric G protein complex, and hence inactivate the G-protein. RGS proteins can also directly antagonise the activity of G protein subunits by competing for the binding site of the effectors and inhibiting the downstream signalling. Among more than 30 RGS proteins, RGS2 and RGS4 have been implicated in cardiovascular pathophysiology and suppress G_q-mediated cardiac hypertrophy (Zhang et al., 2006, Takimoto et al., 2009, Tokudome et al., 2008, Rogers et al., 1999, Rogers et al., 2001). In addition, it has been reported RGS4 enhances anti-hypertrophic effects of natriuretic peptides by stimulating the translocation of RGS4 to the cell membrane, and enhance their association with G_α subunit leading to inactivation of G_q transduction signalling (Tokudome et al., 2008). This mechanism is proposed to be via the activation of cGMP/PKG cascade. In addition, G protein activation is also negatively modulated by phosphorylation of G_i (Pfeifer et al., 1995). Hence, it could be speculated that inactivation of G_q and stimulation of G_i contributes to the overall effect of CNP.

5.6.5 Sodium-hydrogen exchanger

Na^+/H^+ exchanger activation has been associated with Ca^{2+}-dependent activation of calcineurin, which leads to hypertrophic responses (Nakamura et al., 2008). Natriuretic peptides can inhibit Na^+/H^+ exchanger activity via a cGMP-dependent cascade, possibly involving PKG-dependent phosphorylation (Kilic et al., 2005, Tajima et al., 1998). The potency of CNP compared to ANP or BNP for blocking the exchanger is greater (Fidzinski et al., 2004). CU-NP, a chimeric peptide consisting of the ring structure and disulfide bond of CNP in combination with the N-terminus and the C-terminus of Urodilatin (Lisy et al., 2008), has been demonstrated to have direct anti-hypertrophic effects via Na^+/H^+ exchanger inhibition and prevents calcineurin activation and NFAT nuclear import (Kilic et al., 2010). This effect was mimicked by CNP (Kilic et al., 2010).

5.6.6 Transforming growth factor-β1/SMAD signalling

TGF-β1 is secreted by both cardiomyocytes and myofibroblasts. It also stimulates the transformation of cardiac fibroblasts into myofibroblasts that elevate the production of ECM. Hence, TGF-β1 plays a fundamental role in fibrotic remodelling of the heart. TGF-β1 expression is upregulated in patients with idiopathic hypertrophic, dilated cardiomyopathy and HF (Li et al., 1997, Sanderson et al., 2001, Lim and Zhu, 2006). Functional blockade of TGF-β1 signalling by neutralising antibodies or by inducible dominant-negative mutation prevents myocardial fibrosis in pressure overload model (Kuwahara et al., 2002, Hein et al., 2003, Chen et al., 2006, Teekakirikul et al., 2010). Binding of TGF-β1 to its receptor, TGFβR1 and TGFβR2, causes phosphorylation of Smad2 and Smad3 which forms homomeric and heteromeric complex with Smad4. The activated Smad complex subsequently translocates into the nucleus and activates the pro-fibrogenic genes. Studies have shown that the ANP/cGMP/PKG pathway inhibits cardiac fibrosis by counteracting the TGF-β1 signalling by blocking nuclear translocation of Smad (Li et al., 2008, Li et al., 2007). In addition, TGF-β1 significantly stimulates CNP secretion (Horio et al., 2003). This feedback mechanism suggests endogenous CNP may provide a brake on TGF-β1 signalling and suppress fibrosis.

5.7 CNP/NPR-C as a therapeutic target

GWAS in the general population have shown polymorphisms in the CNP (*nppc*) and NPR-C (*npr3*) gene are associated with hypertension and prone to CVDs (Ono et al., 2002, Ren et al., 2017). In addition, mutations in furin, an enzyme that is involved in pro-CNP cleavage, also associate with higher BP, indicating CNP production is important in human cardiovascular haemostasis (Ehret et al., 2011). Furthermore, both ecCNP KO and NPR-C KO mice have impaired endothelium functions in the mesenteric and coronary vasculature, and display a hypertensive phenotype (Moyes et al., 2014). These data hinting CNP/NPR-C transduction pathway could be a novel intervention for vascular diseases, including CAD.

CAD is caused by the development of atherosclerosis and can lead to MI, HF and death. Although many more patients survive the initial ischaemic insult, the reperfusion procedure itself (revascularisation) causes additional damage to the vasculature and myocardium that results in poorer prognosis and predisposes to the development of CHF. In addition, IR injury is not limited to MI, it also arises in stroke or organ transplantations. Thus, strategies to minimise IR injuries are critical in terms of longer-term morbidity and mortality. IR injury is characterised by micro-vascular dysfunction, leading to an inflammatory response, including increased leukocyte activation, cellular and fluid

extravasation, capillary constriction and decreased perfusion (Carden and Granger, 2000). The ability of CNP to inhibit leukocyte infiltration and induce vasodilatation seems promising in terms of improving IR injury. This thesis has shown that lack of either cardiac CNP production or NPR-C exacerbates the final infarct size and recovery of LV contractility. In concert with another study that demonstrated administration of CNP during the reperfusion period reduces IR injury (Hobbs et al., 2004), these observations suggest CNP/NPR-C transduction signalling may be beneficial in patients experiencing an ischaemia insult. Perhaps, CNP or CNP-mimicking molecules can be administrated to patients at the time of reperfusion, e.g. coating on the stent or intravenously, to improve perfusion and limit IR injury?

There is increasing evidence to suggest CNP has therapeutic potential post MI. In experimental models of MI, genetic knockdown of CNP aggravates myocardial damage (Wu et al., 2017a), whereas cardiac specific overexpression of CNP prevents cardiac hypertrophy, preserves cardiac contractility, reduces necrosis and inflammation following MI (Wang et al., 2007). Consistent with these findings, CNP infusion also reduces cardiac hypertrophy and fibrosis caused by MI without affecting BP (Soeki et al., 2005). Furthermore, administration of CNP also attenuates cardiac remodelling induced by other pathological stimuli, such as volume overload, Ang-II and ET-1 (Rosenkranz et al., 2003, Langenickel et al., 2006, Izumiya et al., 2012). These observations collectively support the beneficial effects of CNP treatment in HF. However, whether CNP mediates cardioprotective effects via NPR-B or/and NPR-C is still in question. Numerous studies have shown that the CNP-induced anti-hypertrophic effect is associated with elevation of cGMP level (Rosenkranz et al., 2003, Kilic et al., 2010), and dominant-negative mutant of NPR-B in rat displays progressive BP-independent cardiac hypertrophy (Langenickel et al., 2006). However, CNP/NPR-B signalling is involved in bone growth so targeting this directly may bring unwanted skeletal side effects.

I have demonstrated that CNP infusion in WT mice prevented the development of HF following AAC. This reversal study demonstrated a therapeutic potential of pharmacological administration of CNP or CNP mimicking molecules. In addition, the protective effects of CNP were lost in NPR-C KO mice, suggesting NPR-C mediates the biological activity of CNP in cardiac function and this merits the development of NPR-C activating agents. Furthermore, interaction of such NPR-C agonists might be expected to compete with endogenous natriuretic peptides for clearance and could lead to a moderate increase in the circulating native natriuretic peptide concentration that would provide an

additional beneficial effect to the CVS. Furthermore, long-term natriuretic peptide treatment may lead to changes in other endogenous natriuretic peptides. For example, a clinical study showed infusion of BNP causes a rise in CNP and NT-proCNP levels but fall in ANP and pro-ANP levels (Hillock et al., 2008). Therefore, CNP infusion in the pressure-overload HF model should be investigated further to examine how CNP treatment could affect other peptide responses; regardless, the overall effect of CNP is positive.

In sum, NPR-C is widely distributed in the CVS and its density in tissues is higher than other NPRs. Indeed, NPR-C contributes to 95% of all NPRs expression (Rose and Giles, 2008), suggesting NPR-C could be an effective pharmacological target. Nonetheless, the development of protein/peptides as therapeutic agents is challenging due to technical and compliance issues. Innovative bioencapsulation and nanotechnology can be used to effectively deliver physiologically active peptides orally to increase patient compliance and therapeutic efficacy and reduce cost (Kwon and Daniell, 2015, Crombez et al., 2008). Adapting these techniques to deliver NPR-C agonists, e.g. $cANF^{3-24}$, orally could be the next step in providing conceptual support for the therapeutic potential of CNP/NPR-C signalling. Alternatively, small non-peptide molecules can be developed to activate NPR-C for cardiac protection.

5.8 Limitations and future work

The Langendorff isolated heart system represents a quick and reproducible model that is widely used for cardiovascular physiological and pharmacological studies. However, it is described as a 'dying preparation' as the contractile and chronotropic function deteriorates at rates of 5-10% per hour (Sutherland and Hearse, 2000). Thus, the length of experiment is limited to approximately 2 hours and the time from heart excision to cannulation has to be fast (2-3 minutes) to avoid the potential effect of ischaemic preconditioning and injury. In addition, normoxic myocardium preferentially uses free fatty acid as the energy source (Bing, 2001), but glucose in the Krebs-Henseleit buffer is the main metabolite substrate. A further limitation of the buffer solution is the low oxygen carrying capacity and a low oncotic pressure that can induce tissue oedema and damage, especially following ischaemia reperfusion injury (Walters et al., 1992, Qiu and Hearse, 1992). This can be resolved by using whole blood perfusion or by adding red blood cell mixed with dextran/albumin into the buffer to obtain a near normal osmolality and oncotic pressure (Bell et al., 2011). However, haemolysis, technical complexity and expense of such preparations are huge drawbacks and thus, Krebs-Henseleit buffer remains a practical and

useful method of maintaining an isolated perfused heart for several hours. In addition, coronary flow with blood-free perfusion is much higher than blood flow *in vivo* due to lower viscosity of the fluid. This can be modified with a constant flow mode i.e. flow rate of 2ml/min is used in this thesis to match the coronary flow with whole blood perfusion (Bell et al., 2011). However, constant flow over-rides the vascular auto-regulatory mechanisms and does not inherently alter the amount of perfusate delivered to the heart when there are changes in heart rate or work, or when regional ischaemia is imposed (Sutherland and Hearse, 2000). Nevertheless, global ischaemia is applied in this thesis and constant flow provides an element of constancy and permits straightforward measurements of vascular tone/resistance. Yet, constant flow limits the investigation of reactive hyperaemia, which is the transient increase in flow that occurs following a brief period of ischaemia. Although, a similar protocol is used to study human forearm vasodilatation in which reactive hyperaemia is induced by blood pressure cuff inflation and deflation (Linder et al., 1990). Increased flow was not achievable in the constant flow mode, yet, I have observed prolonged delays of CPP returning to the baseline when flow was re-started following 80 seconds of ischaemia. This indicates a transient reduction of vascular resistance in response to the initial reperfusion after ischaemia. More importantly, this protocol potentially mimics the clinical setting when patients undergo reperfusion after MI. Furthermore, the Langendorff isolated heart model omits the confounding effect from other organ systems, autonomic regulation and peripheral neurohormonal factors thereby, enabling direct study of cardiac responses. This may be considered as an investigational advantage but it makes the model less representative of the *in vivo* setting. Nonetheless, it provides an essential bridge between *in vitro* and *in vivo* experiments. To validate the observed beneficial effects of CNP in IR injury, an *in vivo* model of MI will be the next step, i.e. by reversibly ligating the LADCA.

Infusion of CNP protects against IR injury in rats (Hobbs et al., 2004). It would be interesting to examine if exogenous CNP can rescue the IR injury in hearts lacking CNP production. It will also be plausible to infuse CNP in NPR-C KO mice to confirm if the protective effects of CNP require NPR-C transduction. Likewise, the NPR-C agonist, c-ANF$^{4-23}$ could be employed.

In the CVS, CNP is predominantly produced and secreted in endothelial cells, but also in cardiomyocytes and cardiac fibroblasts. In this thesis, I have demonstrated that CNP derived from each cell type has a distinct role but collectively protects cardiac function. How the secretion of CNP from one cell type affecting its neighbouring cell type is unclear. To investigate this intercellular interaction, a co-culture preparation of cardiomyocyte and

cardiac fibroblast could be employed (i.e. cardiomyocyte from cmCNP KO culturing with cardiac fibroblast from WT, or vice versa).

In order to investigate the overall role of CNP in cardiovascular function, generating a global CNP KO mouse is merited. In addition, a recent study has demonstrated that CNP contributes to metabolism, inflammation and diabetes (Bae et al., 2017). This suggests CNP has a widespread systemic role that is worth investigating. However, global CNP KO is detrimental during development. Hence, a timed CNP deletion is required, e.g. by using tamoxifen-induced activation of Cre, to bypass the early developmental defects.

The global NPR-C KO strain used in this study exhibits bone malformation due to reduced clearance of CNP. This can be avoided by generating cell-specific NPR-C KO (i.e. in endothelial cells, cardiomyocyte and fibroblasts). The undesired bone malformation phenotype will be avoided in these mouse lines and allow investigation of which cell type(s) CNP is acting on to produce the most favourable effects.

5.9 Conclusion

First, I have demonstrated that endothelium-derived CNP regulates coronary vascular function and is released in response to shear stress. Secondly, cardiomyocyte-derived CNP protects the heart against acute IR injury, and ameliorates cardiac dysfunction caused by β-adrenergic over-stimulation or pressure-overload. In addition, cardiac fibroblast-derived CNP also contributes to the cardioprotective effects. Taken together, endogenous CNP from different cell sources has distinct, complementary roles in the heart, modulating cardiac function by influencing coronary vascular tone, protecting against IR injury and HF.

This thesis also demonstrated pharmacological administration of CNP is proven to be beneficial in response to hemodynamic stress, which could potentially translate to patients with chronic hypertension to prevent the development of HF. The anti-ischaemic, anti-hypertrophic and anti-fibrotic profile of CNP make it an attractive therapeutic target for further investigation as a potential treatment in acute coronary syndromes, MI and HF.

Finally, the present study has shown that the protective effects of CNP are mediated, at least in part, via NPR-C activation. Thus, developing specific NPR-C agonists would be a promising therapeutic intervention in CVDs.

Chapter 6 – References

6 References

1987a. Effects of enalapril on mortality in severe congestive heart failure. Results of the Cooperative North Scandinavian Enalapril Survival Study (CONSENSUS). *N Engl J Med,* 316**,** 1429-35.

1987b. Effects of enalapril on mortality in severe congestive heart failure. Results of the Cooperative North Scandinavian Enalapril Survival Study (CONSENSUS). The CONSENSUS Trial Study Group. *N Engl J Med,* 316**,** 1429-35.

1991. Effect of enalapril on survival in patients with reduced left ventricular ejection fractions and congestive heart failure. The SOLVD Investigators. *N Engl J Med,* 325**,** 293-302.

1999a. The Cardiac Insufficiency Bisoprolol Study II (CIBIS-II): a randomised trial. *Lancet,* 353**,** 9-13.

1999b. Effect of metoprolol CR/XL in chronic heart failure: Metoprolol CR/XL Randomised Intervention Trial in Congestive Heart Failure (MERIT-HF). *Lancet,* 353**,** 2001-7.

ABDALLAH, Y., GKATZOFLIA, A., PIEPER, H., ZOGA, E., WALTHER, S., KASSECKERT, S., SCHAFER, M., SCHLUTER, K. D., PIPER, H. M. & SCHAFER, C. 2005. Mechanism of cGMP-mediated protection in a cellular model of myocardial reperfusion injury. *Cardiovasc Res,* 66**,** 123-31.

ABE, J. & BERK, B. C. 2014. Novel mechanisms of endothelial mechanotransduction. *Arterioscler Thromb Vasc Biol,* 34**,** 2378-86.

ABEYRATHNA, P. & SU, Y. 2015. The critical role of Akt in cardiovascular function. *Vascul Pharmacol,* 74**,** 38-48.

AGAH, R., FRENKEL, P. A., FRENCH, B. A., MICHAEL, L. H., OVERBEEK, P. A. & SCHNEIDER, M. D. 1997. Gene recombination in postmitotic cells. Targeted expression of Cre recombinase provokes cardiac-restricted, site-specific rearrangement in adult ventricular muscle in vivo. *J Clin Invest,* 100**,** 169-79.

AGARWAL, R., SIVA, S., DUNN, S. R. & SHARMA, K. 2002. Add-on angiotensin II receptor blockade lowers urinary transforming growth factor-beta levels. *Am J Kidney Dis,* 39**,** 486-92.

AGULLO, L., GARCIA-DORADO, D., ESCALONA, N., RUIZ-MEANA, M., INSERTE, J. & SOLER-SOLER, J. 2003. Effect of ischemia on soluble and particulate guanylyl cyclase-mediated cGMP synthesis in cardiomyocytes. *Am J Physiol Heart Circ Physiol,* 284**,** H2170-6.

AHLUWALIA, A. & HOBBS, A. J. 2005. Endothelium-derived C-type natriuretic peptide: more than just a hyperpolarizing factor. *Trends Pharmacol Sci,* 26**,** 162-7.

AHMETAJ-SHALA, B., KIRKBY, N. S., KNOWLES, R., AL'YAMANI, M., MAZI, S., WANG, Z., TUCKER, A. T., MACKENZIE, L., ARMSTRONG, P. C., NUSING, R. M., TOMLINSON, J. A., WARNER, T. D., LEIPER, J. & MITCHELL, J. A. 2015. Evidence that links loss of cyclooxygenase-2 with increased asymmetric dimethylarginine: novel explanation of cardiovascular side effects associated with anti-inflammatory drugs. *Circulation,* 131**,** 633-42.

AKHTER, S. A., LUTTRELL, L. M., ROCKMAN, H. A., IACCARINO, G., LEFKOWITZ, R. J. & KOCH, W. J. 1998. Targeting the receptor-Gq interface to inhibit in vivo pressure overload myocardial hypertrophy. *Science,* 280**,** 574-7.

ANAND-SRIVASTAVA, M. B. 2005. Natriuretic peptide receptor-C signaling and regulation. *Peptides,* 26**,** 1044-59.

ANAND-SRIVASTAVA, M. B., SEHL, P. D. & LOWE, D. G. 1996. Cytoplasmic domain of natriuretic peptide receptor-C inhibits adenylyl cyclase. Involvement of a pertussis toxin-sensitive G protein. *J Biol Chem,* 271**,** 19324-9.

ANDERSON, M. E. 2005. Calmodulin kinase signaling in heart: an intriguing candidate target for therapy of myocardial dysfunction and arrhythmias. *Pharmacol Ther,* 106**,** 39-55.

APPENZELLER, S., PINEAU, C. A. & CLARKE, A. E. 2011. Acute lupus myocarditis: Clinical features and outcome. *Lupus,* 20**,** 981-8.

ARAI, M., LEFER, D. J., SO, T., DIPAULA, A., AVERSANO, T. & BECKER, L. C. 1996. An anti-CD18 antibody limits infarct size and preserves left ventricular function in dogs with ischemia and 48-hour reperfusion. *J Am Coll Cardiol,* 27**,** 1278-85.

ARMSTRONG, P. W., ROESSIG, L., PATEL, M. J., ANSTROM, K. J., BUTLER, J., VOORS, A. A., LAM, C. S. P., PONIKOWSKI, P., TEMPLE, T., PIESKE, B., EZEKOWITZ, J., HERNANDEZ, A. F., KOGLIN, J. & O'CONNOR, C. M. 2018. A Multicenter, Randomized, Double-Blind, Placebo-Controlled Trial of the Efficacy and

Safety of the Oral Soluble Guanylate Cyclase Stimulator: The VICTORIA Trial. *JACC Heart Fail,* 6**,** 96-104.

ARORA, R. R., VENKATESH, P. K. & MOLNAR, J. 2006. Short and long-term mortality with nesiritide. *Am Heart J,* 152**,** 1084-90.

ASPROMONTE, N., GULIZIA, M. M., CLERICO, A., DI TANO, G., EMDIN, M., FEOLA, M., IACOVIELLO, M., LATINI, R., MORTARA, A., VALLE, R., MISURACA, G., PASSINO, C., MASSON, S., AIMO, A., CIACCIO, M. & MIGLIARDI, M. 2017. ANMCO/ELAS/SIBioC Consensus Document: biomarkers in heart failure. *Eur Heart J Suppl,* 19**,** D102-d112.

ATEF, M. E. & ANAND-SRIVASTAVA, M. B. 2014. Enhanced expression of Gqalpha and PLC-beta1 proteins contributes to vascular smooth muscle cell hypertrophy in SHR: role of endogenous angiotensin II and endothelin-1. *Am J Physiol Cell Physiol,* 307**,** C97-106.

AVERSANO, T., ZHOU, W., NEDELMAN, M., NAKADA, M. & WEISMAN, H. 1995. A chimeric IgG4 monoclonal antibody directed against CD18 reduces infarct size in a primate model of myocardial ischemia and reperfusion. *J Am Coll Cardiol,* 25**,** 781-8.

AZER, J., HUA, R., KRISHNASWAMY, P. S. & ROSE, R. A. 2014. Effects of natriuretic peptides on electrical conduction in the sinoatrial node and atrial myocardium of the heart. *J Physiol,* 592**,** 1025-45.

AZER, J., HUA, R., VELLA, K. & ROSE, R. A. 2012. Natriuretic peptides regulate heart rate and sinoatrial node function by activating multiple natriuretic peptide receptors. *J Mol Cell Cardiol,* 53**,** 715-24.

AZIZ, Q., LI, Y., ANDERSON, N., OJAKE, L., TSISANOVA, E. & TINKER, A. 2017. Molecular and functional characterization of the endothelial ATP-sensitive potassium channel. *J Biol Chem,* 292**,** 17587-17597.

BACKS, J., BACKS, T., NEEF, S., KREUSSER, M. M., LEHMANN, L. H., PATRICK, D. M., GRUETER, C. E., QI, X., RICHARDSON, J. A., HILL, J. A., KATUS, H. A., BASSEL-DUBY, R., MAIER, L. S. & OLSON, E. N. 2009. The delta isoform of CaM kinase II is required for pathological cardiac hypertrophy and remodeling after pressure overload. *Proc Natl Acad Sci U S A,* 106**,** 2342-7.

BACKS, J. & OLSON, E. N. 2006. Control of cardiac growth by histone acetylation/deacetylation. *Circ Res,* 98**,** 15-24.

BADORFF, C., RUETTEN, H., MUELLER, S., STAHMER, M., GEHRING, D., JUNG, F., IHLING, C., ZEIHER, A. M. & DIMMELER, S. 2002. Fas receptor signaling inhibits glycogen synthase kinase 3 beta and induces cardiac hypertrophy following pressure overload. *J Clin Invest,* 109**,** 373-81.

BAE, C. R., HINO, J., HOSODA, H., ARAI, Y., SON, C., MAKINO, H., TOKUDOME, T., TOMITA, T., KIMURA, T., NOJIRI, T., HOSODA, K., MIYAZATO, M. & KANGAWA, K. 2017. Overexpression of C-type Natriuretic Peptide in Endothelial Cells Protects against Insulin Resistance and Inflammation during Diet-induced Obesity. *Sci Rep,* 7**,** 9807.

BAGHERI, F., KHORI, V., ALIZADEH, A. M., KHALIGHFARD, S., KHODAYARI, S. & KHODAYARI, H. 2016. Reactive oxygen species-mediated cardiac-reperfusion injury: Mechanisms and therapies. *Life Sci,* 165**,** 43-55.

BARAN, K. W., NGUYEN, M., MCKENDALL, G. R., LAMBREW, C. T., DYKSTRA, G., PALMERI, S. T., GIBBONS, R. J., BORZAK, S., SOBEL, B. E., GOURLAY, S. G., RUNDLE, A. C., GIBSON, C. M. & BARRON, H. V. 2001. Double-blind, randomized trial of an anti-CD18 antibody in conjunction with recombinant tissue plasminogen activator for acute myocardial infarction: limitation of myocardial infarction following thrombolysis in acute myocardial infarction (LIMIT AMI) study. *Circulation,* 104**,** 2778-83.

BARATCHI, S., KHOSHMANESH, K., WOODMAN, O. L., POTOCNIK, S., PETER, K. & MCINTYRE, P. 2017. Molecular Sensors of Blood Flow in Endothelial Cells. *Trends Mol Med,* 23**,** 850-868.

BARBER, D. A., BURNETT, J. C., JR., FITZPATRICK, L. A., SIECK, G. C. & MILLER, V. M. 1998. Gender and relaxation to C-type natriuretic peptide in porcine coronary arteries. *J Cardiovasc Pharmacol,* 32**,** 5-11.

BARTELS, C. F., BUKULMEZ, H., PADAYATTI, P., RHEE, D. K., VAN RAVENSWAAIJ-ARTS, C., PAULI, R. M., MUNDLOS, S., CHITAYAT, D., SHIH, L. Y., AL-GAZALI, L. I., KANT, S., COLE, T., MORTON, J., CORMIER-DAIRE, V., FAIVRE, L., LEES, M., KIRK, J., MORTIER, G. R., LEROY, J., ZABEL, B., KIM, C. A., CROW, Y., BRAVERMAN, N. E., VAN DEN AKKER, F. & WARMAN, M. L. 2004. Mutations in the transmembrane natriuretic peptide receptor NPR-B impair skeletal growth and cause acromesomelic dysplasia, type Maroteaux. *Am J Hum Genet,* 75**,** 27-34.

BARTON, M., BENY, J. L., D'USCIO, L. V., WYSS, T., NOLL, G. & LUSCHER, T. F. 1998. Endothelium-independent relaxation and hyperpolarization to C-type natriuretic peptide in porcine coronary arteries. *J Cardiovasc Pharmacol,* 31**,** 377-83.

BASSI, R., BURGOYNE, J. R., DENICOLA, G. F., RUDYK, O., DESANTIS, V., CHARLES, R. L., EATON, P. & MARBER, M. S. 2017. Redox-dependent dimerization of p38alpha mitogen-activated protein kinase with mitogen-activated protein kinase kinase 3. *J Biol Chem,* 292**,** 16161-16173.

BAXTER, G. F. 2004. Natriuretic peptides and myocardial ischaemia. *Basic Res Cardiol,* 99**,** 90-3.

BEAULIEU, P., CARDINAL, R., PAGE, P., FRANCOEUR, F., TREMBLAY, J. & LAMBERT, C. 1997. Positive chronotropic and inotropic effects of C-type natriuretic peptide in dogs. *Am J Physiol,* 273**,** H1933-40.

BELL, R. M., MOCANU, M. M. & YELLON, D. M. 2011. Retrograde heart perfusion: the Langendorff technique of isolated heart perfusion. *J Mol Cell Cardiol,* 50**,** 940-50.

BELLAHCENE, M., JACQUET, S., CAO, X. B., TANNO, M., HAWORTH, R. S., LAYLAND, J., KABIR, A. M., GAESTEL, M., DAVIS, R. J., FLAVELL, R. A., SHAH, A. M., AVKIRAN, M. & MARBER, M. S. 2006. Activation of p38 mitogen-activated protein kinase contributes to the early cardiodepressant action of tumor necrosis factor. *J Am Coll Cardiol,* 48**,** 545-55.

BENDALL, J. K., DOUGLAS, G., MCNEILL, E., CHANNON, K. M. & CRABTREE, M. J. 2014. Tetrahydrobiopterin in cardiovascular health and disease. *Antioxid Redox Signal,* 20**,** 3040-77.

BERNARDO, B. C., WEEKS, K. L., PRETORIUS, L. & MCMULLEN, J. R. 2010. Molecular distinction between physiological and pathological cardiac hypertrophy: experimental findings and therapeutic strategies. *Pharmacol Ther,* 128**,** 191-227.

BING, R. J. 2001. Some aspects of biochemistry of myocardial infarction. *Cell Mol Life Sci,* 58**,** 351-5.

BISHOP, J. E. & LINDAHL, G. 1999. Regulation of cardiovascular collagen synthesis by mechanical load. *Cardiovasc Res,* 42**,** 27-44.

BISHU, K., DESWAL, A., CHEN, H. H., LEWINTER, M. M., LEWIS, G. D., SEMIGRAN, M. J., BORLAUG, B. A., MCNULTY, S., HERNANDEZ, A. F., BRAUNWALD, E. & REDFIELD, M. M. 2012. Biomarkers in acutely decompensated heart failure with preserved or reduced ejection fraction. *Am Heart J,* 164**,** 763-770.e3.

BOAG, S. E., ANDREANO, E. & SPYRIDOPOULOS, I. 2017. Lymphocyte Communication in Myocardial Ischemia/Reperfusion Injury. *Antioxid Redox Signal,* 26**,** 660-675.

BOBIN, P., BELACEL-OUARI, M., BEDIOUNE, I., ZHANG, L., LEROY, J., LEBLAIS, V., FISCHMEISTER, R. & VANDECASTEELE, G. 2016. Cyclic nucleotide phosphodiesterases in heart and vessels: A therapeutic perspective. *Arch Cardiovasc Dis,* 109**,** 431-43.

BOLUYT, M. O. & BING, O. H. 2000. Matrix gene expression and decompensated heart failure: the aged SHR model. *Cardiovasc Res,* 46**,** 239-49.

BONAVENTURA, A., MONTECUCCO, F. & DALLEGRI, F. 2016. Cellular recruitment in myocardial ischaemia/reperfusion injury. *Eur J Clin Invest,* 46**,** 590-601.

BOND, J. M., HERMAN, B. & LEMASTERS, J. J. 1991. Protection by acidotic pH against anoxia/reoxygenation injury to rat neonatal cardiac myocytes. *Biochem Biophys Res Commun,* 179**,** 798-803.

BOU DAOU, G., LI, Y. & ANAND-SRIVASTAVA, M. B. 2016. Enhanced expression of Gialpha proteins contributes to the hyperproliferation of vascular smooth muscle cells from spontaneously hypertensive rats via MAP kinase- and PI3 kinase-independent pathways. *Can J Physiol Pharmacol,* 94**,** 49-58.

BRAND, T. & SCHNEIDER, M. D. 1995. The TGF beta superfamily in myocardium: ligands, receptors, transduction, and function. *J Mol Cell Cardiol,* 27**,** 5-18.

BRAZ, J. C., BUENO, O. F., LIANG, Q., WILKINS, B. J., DAI, Y. S., PARSONS, S., BRAUNWART, J., GLASCOCK, B. J., KLEVITSKY, R., KIMBALL, T. F., HEWETT, T. E. & MOLKENTIN, J. D. 2003. Targeted inhibition of p38 MAPK promotes hypertrophic cardiomyopathy through upregulation of calcineurin-NFAT signaling. *J Clin Invest,* 111**,** 1475-86.

BRAZ, J. C., GREGORY, K., PATHAK, A., ZHAO, W., SAHIN, B., KLEVITSKY, R., KIMBALL, T. F., LORENZ, J. N., NAIRN, A. C., LIGGETT, S. B., BODI, I., WANG, S., SCHWARTZ, A., LAKATTA, E. G., DEPAOLI-ROACH, A. A., ROBBINS, J., HEWETT, T. E., BIBB, J. A., WESTFALL, M. V., KRANIAS, E. G. & MOLKENTIN, J. D. 2004. PKC-alpha regulates cardiac contractility and propensity toward heart failure. *Nat Med,* 10**,** 248-54.

BRECKENRIDGE, R. 2010. Heart failure and mouse models. *Dis Model Mech,* 3**,** 138-43.

BREDEMEIER, M., LOPES, L. M., EISENREICH, M. A., HICKMANN, S., BONGIORNO, G. K., D'AVILA, R., MORSCH, A. L. B., DA SILVA STEIN, F. & CAMPOS, G. G. D. 2018. Xanthine oxidase inhibitors for prevention of

cardiovascular events: a systematic review and meta-analysis of randomized controlled trials. *BMC Cardiovasc Disord,* 18**,** 24.

BROOKS, W. W. & CONRAD, C. H. 2000. Myocardial fibrosis in transforming growth factor beta(1)heterozygous mice. *J Mol Cell Cardiol,* 32**,** 187-95.

BRUNNER, F., MAIER, R., ANDREW, P., WOLKART, G., ZECHNER, R. & MAYER, B. 2003. Attenuation of myocardial ischemia/reperfusion injury in mice with myocyte-specific overexpression of endothelial nitric oxide synthase. *Cardiovasc Res,* 57**,** 55-62.

BRUSQ, J. M., MAYOUX, E., GUIGUI, L. & KIRILOVSKY, J. 1999. Effects of C-type natriuretic peptide on rat cardiac contractility. *Br J Pharmacol,* 128**,** 206-12.

BUBIKAT, A., DE WINDT, L. J., ZETSCHE, B., FABRITZ, L., SICKLER, H., ECKARDT, D., GODECKE, A., BABA, H. A. & KUHN, M. 2005. Local atrial natriuretic peptide signaling prevents hypertensive cardiac hypertrophy in endothelial nitric-oxide synthase-deficient mice. *J Biol Chem,* 280**,** 21594-9.

BUENO, O. F., DE WINDT, L. J., TYMITZ, K. M., WITT, S. A., KIMBALL, T. R., KLEVITSKY, R., HEWETT, T. E., JONES, S. P., LEFER, D. J., PENG, C. F., KITSIS, R. N. & MOLKENTIN, J. D. 2000. The MEK1-ERK1/2 signaling pathway promotes compensated cardiac hypertrophy in transgenic mice. *Embo j,* 19**,** 6341-50.

BURCHFIELD, J. S., XIE, M. & HILL, J. A. 2013. Pathological ventricular remodeling: mechanisms: part 1 of 2. *Circulation,* 128**,** 388-400.

BURGER, A. J., HORTON, D. P., LEJEMTEL, T., GHALI, J. K., TORRE, G., DENNISH, G., KOREN, M., DINERMAN, J., SILVER, M., CHENG, M. L., ELKAYAM, U. & PROSPECTIVE RANDOMIZED EVALUATION OF CARDIAC ECTOPY WITH DOBUTAMINE OR NATRECOR, T. 2002. Effect of nesiritide (B-type natriuretic peptide) and dobutamine on ventricular arrhythmias in the treatment of patients with acutely decompensated congestive heart failure: the PRECEDENT study. *Am Heart J,* 144**,** 1102-8.

BURLEY, D. S. & BAXTER, G. F. 2007. B-type natriuretic peptide at early reperfusion limits infarct size in the rat isolated heart. *Basic Res Cardiol,* 102**,** 529-41.

BURLEY, D. S., COX, C. D., ZHANG, J., WANN, K. T. & BAXTER, G. F. 2014. Natriuretic peptides modulate ATP-sensitive K(+) channels in rat ventricular cardiomyocytes. *Basic Res Cardiol,* 109**,** 402.

BURLEY, D. S., FERDINANDY, P. & BAXTER, G. F. 2007. Cyclic GMP and protein kinase-G in myocardial ischaemia-reperfusion: opportunities and obstacles for survival signaling. *Br J Pharmacol,* 152**,** 855-69.

BURNETT, J. C. 2005. Nesiritide: new hope for acute heart failure syndromes? *European Heart Journal Supplements,* 7**,** B25-B30.

BUSSE, R., EDWARDS, G., FELETOU, M., FLEMING, I., VANHOUTTE, P. M. & WESTON, A. H. 2002. EDHF: bringing the concepts together. *Trends Pharmacol Sci,* 23**,** 374-80.

BUSTIN, S. A., BENES, V., GARSON, J. A., HELLEMANS, J., HUGGETT, J., KUBISTA, M., MUELLER, R., NOLAN, T., PFAFFL, M. W., SHIPLEY, G. L., VANDESOMPELE, J. & WITTWER, C. T. 2009. The MIQE guidelines: minimum information for publication of quantitative real-time PCR experiments. *Clin Chem,* 55**,** 611-22.

BUTLER, J., YOUNG, J. B., ABRAHAM, W. T., BOURGE, R. C., ADAMS, K. F., JR., CLARE, R. & O'CONNOR, C. 2006. Beta-blocker use and outcomes among hospitalized heart failure patients. *J Am Coll Cardiol,* 47**,** 2462-9.

BUTTGEREIT, J., SHANKS, J., LI, D., HAO, G., ATHWAL, A., LANGENICKEL, T. H., WRIGHT, H., DA COSTA GONCALVES, A. C., MONTI, J., PLEHM, R., POPOVA, E., QADRI, F., LAPIDUS, I., RYAN, B., OZCELIK, C., PATERSON, D. J., BADER, M. & HERRING, N. 2016. C-type natriuretic peptide and natriuretic peptide receptor B signalling inhibits cardiac sympathetic neurotransmission and autonomic function. *Cardiovasc Res,* 112**,** 637-644.

CABIATI, M., SABATINO, L., CARUSO, R., VERDE, A., CASELLI, C., PRESCIMONE, T., GIANNESSI, D. & DEL RY, S. 2013. C-type natriuretic peptide transcriptomic profiling increases in human leukocytes of patients with chronic heart failure as a function of clinical severity. *Peptides,* 47**,** 110-4.

CAHILL, P. A. & HASSID, A. 1994. ANF-C-receptor-mediated inhibition of aortic smooth muscle cell proliferation and thymidine kinase activity. *Am J Physiol,* 266**,** R194-203.

CANIFFI, C., ELESGARAY, R., GIRONACCI, M., ARRANZ, C. & COSTA, M. A. 2010. C-type natriuretic peptide effects on cardiovascular nitric oxide system in spontaneously hypertensive rats. *Peptides,* 31**,** 1309-18.

CARGILL, R. I., BARR, C. S., COUTIE, W. J., STRUTHERS, A. D. & LIPWORTH, B. J. 1994. C-type natriuretic peptide levels in cor pulmonale and in congestive heart failure. *Thorax,* 49**,** 1247-9.

CASCO, V. H., VEINOT, J. P., KUROSKI DE BOLD, M. L., MASTERS, R. G., STEVENSON, M. M. & DE BOLD, A. J. 2002. Natriuretic peptide system gene expression in human coronary arteries. *J Histochem Cytochem,* 50**,** 799-809.

CHAN, E. C. & WOODMAN, O. L. 1999. Enhanced role for the opening of potassium channels in relaxant responses to acetylcholine after myocardial ischaemia and reperfusion in dog coronary arteries. *Br J Pharmacol,* 126**,** 925-32.

CHARRON, F., PARADIS, P., BRONCHAIN, O., NEMER, G. & NEMER, M. 1999. Cooperative interaction between GATA-4 and GATA-6 regulates myocardial gene expression. *Mol Cell Biol,* 19**,** 4355-65.

CHAUHAN, S. D., NILSSON, H., AHLUWALIA, A. & HOBBS, A. J. 2003. Release of C-type natriuretic peptide accounts for the biological activity of endothelium-derived hyperpolarizing factor. *Proc Natl Acad Sci U S A,* 100**,** 1426-31.

CHEN, H. H. 2014. *Nesiritide Therapy to Preserve Function of the Left Ventricle After Myocardial Infarction (Believe II)* [Online]. ClinicalTrials.gov. Available: https://clinicaltrials.gov/ct2/show/results/NCT00573144?sect=X4301256 - othr [Accessed 18 August 2018].

CHEN, H. H., ANSTROM, K. J., GIVERTZ, M. M., STEVENSON, L. W., SEMIGRAN, M. J., GOLDSMITH, S. R., BART, B. A., BULL, D. A., STEHLIK, J., LEWINTER, M. M., KONSTAM, M. A., HUGGINS, G. S., ROULEAU, J. L., O'MEARA, E., TANG, W. H., STARLING, R. C., BUTLER, J., DESWAL, A., FELKER, G. M., O'CONNOR, C. M., BONITA, R. E., MARGULIES, K. B., CAPPOLA, T. P., OFILI, E. O., MANN, D. L., DAVILA-ROMAN, V. G., MCNULTY, S. E., BORLAUG, B. A., VELAZQUEZ, E. J., LEE, K. L., SHAH, M. R., HERNANDEZ, A. F., BRAUNWALD, E., REDFIELD, M. M. & NETWORK, N. H. F. C. R. 2013. Low-dose dopamine or low-dose nesiritide in acute heart failure with renal dysfunction: the ROSE acute heart failure randomized trial. *JAMA,* 310**,** 2533-43.

CHEN, H. H. & BURNETT, J. C., JR. 1998. C-type natriuretic peptide: the endothelial component of the natriuretic peptide system. *J Cardiovasc Pharmacol,* 32 Suppl 3**,** S22-8.

CHEN, H. H., GLOCKNER, J. F., SCHIRGER, J. A., CATALIOTTI, A., REDFIELD, M. M. & BURNETT, J. C., JR. 2012. Novel protein therapeutics for systolic heart failure: chronic subcutaneous B-type natriuretic peptide. *J Am Coll Cardiol,* 60**,** 2305-12.

CHEN, H. H., MARTIN, F. L., GIBBONS, R. J., SCHIRGER, J. A., WRIGHT, R. S., SCHEARS, R. M., REDFIELD, M. M., SIMARI, R. D., LERMAN, A., CATALIOTTI, A. & BURNETT, J. C., JR. 2009. Low-dose nesiritide in human anterior myocardial infarction suppresses aldosterone and preserves ventricular function and structure: a proof of concept study. *Heart,* 95**,** 1315-9.

CHEN, J. Y., YE, Z. X., WANG, X. F., CHANG, J., YANG, M. W., ZHONG, H. H., HONG, F. F. & YANG, S. L. 2017. Nitric oxide bioavailability dysfunction involves in atherosclerosis. *Biomed Pharmacother,* 97**,** 423-428.

CHEN, Y. F., FENG, J. A., LI, P., XING, D., AMBALAVANAN, N. & OPARIL, S. 2006. Atrial natriuretic peptide-dependent modulation of hypoxia-induced pulmonary vascular remodeling. *Life Sci,* 79**,** 1357-65.

CHENG, H., WOODGETT, J., MAAMARI, M. & FORCE, T. 2011. Targeting GSK-3 family members in the heart: a very sharp double-edged sword. *J Mol Cell Cardiol,* 51**,** 607-13.

CHUN, T. H., ITOH, H., OGAWA, Y., TAMURA, N., TAKAYA, K., IGAKI, T., YAMASHITA, J., DOI, K., INOUE, M., MASATSUGU, K., KORENAGA, R., ANDO, J. & NAKAO, K. 1997. Shear stress augments expression of C-type natriuretic peptide and adrenomedullin. *Hypertension,* 29**,** 1296-302.

CHUN, T. H., ITOH, H., SAITO, T., YAMAHARA, K., DOI, K., MORI, Y., OGAWA, Y., YAMASHITA, J., TANAKA, T., INOUE, M., MASATSUGU, K., SAWADA, N., FUKUNAGA, Y. & NAKAO, K. 2000. Oxidative stress augments secretion of endothelium-derived relaxing peptides, C-type natriuretic peptide and adrenomedullin. *J Hypertens,* 18**,** 575-80.

CHUSHO, H., TAMURA, N., OGAWA, Y., YASODA, A., SUDA, M., MIYAZAWA, T., NAKAMURA, K., NAKAO, K., KURIHARA, T., KOMATSU, Y., ITOH, H., TANAKA, K., SAITO, Y., KATSUKI, M. & NAKAO, K. 2001. Dwarfism and early death in mice lacking C-type natriuretic peptide. *Proc Natl Acad Sci U S A,* 98**,** 4016-21.

CLARK, J., LOONAT, A. A., MARTIN, E. D., SARAFRAZ SHEKARY, N., TILGNER, K. D., T HERTZ, N., ... MARBER, M. S. 2018. p38 MAPK contributes to left ventricular remodeling following pathological stress and disinhibits calpain through phosphorylation of calpastatin. *Faseb journal*.

CLARK, J. E., SARAFRAZ, N. & MARBER, M. S. 2007. Potential of p38-MAPK inhibitors in the treatment of ischaemic heart disease. *Pharmacol Ther,* 116**,** 192-206.

CLAVELL, A. L., STINGO, A. J., WEI, C. M., HEUBLEIN, D. M. & BURNETT, J. C., JR. 1993. C-type natriuretic peptide: a selective cardiovascular peptide. *Am J Physiol,* 264**,** R290-5.

COHEN, D., KOH, G. Y., NIKONOVA, L. N., PORTER, J. G. & MAACK, T. 1996. Molecular determinants of the clearance function of type C receptors of natriuretic peptides. *J Biol Chem,* 271**,** 9863-9.

COLUCCI, W. S., ELKAYAM, U., HORTON, D. P., ABRAHAM, W. T., BOURGE, R. C., JOHNSON, A. D., WAGONER, L. E., GIVERTZ, M. M., LIANG, C. S., NEIBAUR, M., HAUGHT, W. H. & LEJEMTEL, T. H. 2000. Intravenous nesiritide, a natriuretic peptide, in the treatment of decompensated congestive heart failure. Nesiritide Study Group. *N Engl J Med,* 343**,** 246-53.

CONDORELLI, G., DRUSCO, A., STASSI, G., BELLACOSA, A., RONCARATI, R., IACCARINO, G., RUSSO, M. A., GU, Y., DALTON, N., CHUNG, C., LATRONICO, M. V., NAPOLI, C., SADOSHIMA, J., CROCE, C. M. & ROSS, J., JR. 2002. Akt induces enhanced myocardial contractility and cell size in vivo in transgenic mice. *Proc Natl Acad Sci U S A,* 99**,** 12333-8.

COOK, S. A., SUGDEN, P. H. & CLERK, A. 1999. Activation of c-Jun N-terminal kinases and p38-mitogen-activated protein kinases in human heart failure secondary to ischaemic heart disease. *J Mol Cell Cardiol,* 31**,** 1429-34.

COSTA, M. A., ELESGARAY, R., BALASZCZUK, A. M. & ARRANZ, C. 2006. Role of NPR-C natriuretic receptor in nitric oxide system activation induced by atrial natriuretic peptide. *Regul Pept,* 135**,** 63-8.

COX, E. J. & MARSH, S. A. 2014. A systematic review of fetal genes as biomarkers of cardiac hypertrophy in rodent models of diabetes. *PLoS One,* 9**,** e92903.

CREEMERS, E. E. & PINTO, Y. M. 2011. Molecular mechanisms that control interstitial fibrosis in the pressure-overloaded heart. *Cardiovasc Res,* 89**,** 265-72.

CROMBEZ, L., MORRIS, M. C., DESHAYES, S., HEITZ, F. & DIVITA, G. 2008. Peptide-based nanoparticle for ex vivo and in vivo drug delivery. *Curr Pharm Des,* 14**,** 3656-65.

CUNNINGTON, C., VAN ASSCHE, T., SHIRODARIA, C., KYLINTIREAS, I., LINDSAY, A. C., LEE, J. M., ANTONIADES, C., MARGARITIS, M., LEE, R., CERRATO, R., CRABTREE, M. J., FRANCIS, J. M., SAYEED, R., RATNATUNGA, C., PILLAI, R., CHOUDHURY, R. P., NEUBAUER, S. & CHANNON, K. M. 2012. Systemic and vascular oxidation limits the efficacy of oral tetrahydrobiopterin treatment in patients with coronary artery disease. *Circulation,* 125**,** 1356-66.

D'SOUZA, S. P., DAVIS, M. & BAXTER, G. F. 2004. Autocrine and paracrine actions of natriuretic peptides in the heart. *Pharmacol Ther,* 101**,** 113-29.

D'SOUZA, S. P., YELLON, D. M., MARTIN, C., SCHULZ, R., HEUSCH, G., ONODY, A., FERDINANDY, P. & BAXTER, G. F. 2003. B-type natriuretic peptide limits infarct size in rat isolated hearts via KATP channel opening. *Am J Physiol Heart Circ Physiol,* 284**,** H1592-600.

DARGIE, H. 2005. Heart failure post-myocardial infarction: a review of the issues. *Heart,* 91 Suppl 2**,** ii3-6; discussion ii31, ii43-8.

DAVID C. DUGDALE, M. A. C. 2012. *Hypertensive heart disease* [Online]. U.S. National Library of Medicine. Available: http://www.nlm.nih.gov/medlineplus/ency/article/000163.htm [Accessed 16/07/2014].

DAVIDSON, N. C., BARR, C. S. & STRUTHERS, A. D. 1996. C-type natriuretic peptide. An endogenous inhibitor of vascular angiotensin-converting enzyme activity. *Circulation,* 93**,** 1155-9.

DE BOLD, A. J., BORENSTEIN, H. B., VERESS, A. T. & SONNENBERG, H. 1981. A rapid and potent natriuretic response to intravenous injection of atrial myocardial extract in rats. *Life Sci,* 28**,** 89-94.

DEANFIELD, J. E., HALCOX, J. P. & RABELINK, T. J. 2007. Endothelial function and dysfunction: testing and clinical relevance. *Circulation,* 115**,** 1285-95.

DEBOSCH, B., TRESKOV, I., LUPU, T. S., WEINHEIMER, C., KOVACS, A., COURTOIS, M. & MUSLIN, A. J. 2006. Akt1 is required for physiological cardiac growth. *Circulation,* 113**,** 2097-104.

DEL RY, S., CABIATI, M. & CLERICO, A. 2013. Recent advances on natriuretic peptide system: new promising therapeutic targets for the treatment of heart failure. *Pharmacol Res,* 76**,** 190-8.

DEL RY, S., CABIATI, M., LIONETTI, V., EMDIN, M., RECCHIA, F. A. & GIANNESSI, D. 2008a. Expression of C-type natriuretic peptide and of its receptor NPR-B in normal and failing heart. *Peptides,* 29**,** 2208-15.

DEL RY, S., CABIATI, M., STEFANO, T., CATAPANO, G., CASELLI, C., PRESCIMONE, T., PASSINO, C., EMDIN, M. & GIANNESSI, D. 2011a. Comparison of NT-proCNP and CNP plasma levels in heart failure, diabetes and cirrhosis patients. *Regul Pept,* 166**,** 15-20.

DEL RY, S., CABIATI, M., VOZZI, F., BATTOLLA, B., CASELLI, C., FORINI, F., SEGNANI, C., PRESCIMONE, T., GIANNESSI, D. & MATTII, L. 2011b. Expression of C-type natriuretic peptide and its receptor NPR-B in cardiomyocytes. *Peptides,* 32**,** 1713-8.

DEL RY, S., MALTINTI, M., CABIATI, M., EMDIN, M., GIANNESSI, D. & MORALES, M. A. 2008b. C-type natriuretic peptide and its relation to non-invasive indices of left ventricular function in patients with chronic heart failure. *Peptides,* 29**,** 79-82.

DEL RY, S., MALTINTI, M., PIACENTI, M., PASSINO, C., EMDIN, M. & GIANNESSI, D. 2006a. Cardiac production of C-type natriuretic peptide in heart failure. *J Cardiovasc Med (Hagerstown),* 7**,** 397-9.

DEL RY, S., PASSINO, C., EMDIN, M. & GIANNESSI, D. 2006b. C-type natriuretic peptide and heart failure. *Pharmacol Res,* 54**,** 326-33.

DEL RY, S., PASSINO, C., MALTINTI, M., EMDIN, M. & GIANNESSI, D. 2005. C-type natriuretic peptide plasma levels increase in patients with chronic heart failure as a function of clinical severity. *Eur J Heart Fail,* 7**,** 1145-8.

DEPRE, C., SHIPLEY, G. L., CHEN, W., HAN, Q., DOENST, T., MOORE, M. L., STEPKOWSKI, S., DAVIES, P. J. & TAEGTMEYER, H. 1998. Unloaded heart in vivo replicates fetal gene expression of cardiac hypertrophy. *Nat Med,* 4**,** 1269-75.

DICKEY, D. M., DRIES, D. L., MARGULIES, K. B. & POTTER, L. R. 2012. Guanylyl cyclase (GC)-A and GC-B activities in ventricles and cardiomyocytes from failed and non-failed human hearts: GC-A is inactive in the failed cardiomyocyte. *J Mol Cell Cardiol,* 52**,** 727-32.

DICKEY, D. M., FLORA, D. R., BRYAN, P. M., XU, X., CHEN, Y. & POTTER, L. R. 2007. Differential regulation of membrane guanylyl cyclases in congestive heart failure: natriuretic peptide receptor (NPR)-B, Not NPR-A, is the predominant natriuretic peptide receptor in the failing heart. *Endocrinology,* 148**,** 3518-22.

DOEVENDANS, P. A., DAEMEN, M. J., DE MUINCK, E. D. & SMITS, J. F. 1998. Cardiovascular phenotyping in mice. *Cardiovasc Res,* 39**,** 34-49.

DOI, K., IKEDA, T., ITOH, H., UEYAMA, K., HOSODA, K., OGAWA, Y., YAMASHITA, J., CHUN, T. H., INOUE, M., MASATSUGU, K., SAWADA, N., FUKUNAGA, Y., SAITO, T., SONE, M., YAMAHARA, K., KOOK, H., KOMEDA, M., UEDA, M. & NAKAO, K. 2001. C-type natriuretic peptide induces redifferentiation of vascular smooth muscle cells with accelerated reendothelialization. *Arterioscler Thromb Vasc Biol,* 21**,** 930-6.

DORN, G. W., 2ND & FORCE, T. 2005. Protein kinase cascades in the regulation of cardiac hypertrophy. *J Clin Invest,* 115**,** 527-37.

DORN, G. W., 2ND, TEPE, N. M., WU, G., YATANI, A. & LIGGETT, S. B. 2000. Mechanisms of impaired beta-adrenergic receptor signaling in G(alphaq)-mediated cardiac hypertrophy and ventricular dysfunction. *Mol Pharmacol,* 57**,** 278-87.

DOWNEY, J. M. 1990. Free radicals and their involvement during long-term myocardial ischemia and reperfusion. *Annu Rev Physiol,* 52**,** 487-504.

DREWETT, J. G., FENDLY, B. M., GARBERS, D. L. & LOWE, D. G. 1995. Natriuretic peptide receptor-B (guanylyl cyclase-B) mediates C-type natriuretic peptide relaxation of precontracted rat aorta. *J Biol Chem,* 270**,** 4668-74.

DUMITRESCU, C., BIONDI, R., XIA, Y., CARDOUNEL, A. J., DRUHAN, L. J., AMBROSIO, G. & ZWEIER, J. L. 2007. Myocardial ischemia results in tetrahydrobiopterin (BH4) oxidation with impaired endothelial function ameliorated by BH4. *Proc Natl Acad Sci U S A,* 104**,** 15081-6.

DURANSKI, M. R., GREER, J. J., DEJAM, A., JAGANMOHAN, S., HOGG, N., LANGSTON, W., PATEL, R. P., YET, S. F., WANG, X., KEVIL, C. G., GLADWIN, M. T. & LEFER, D. J. 2005. Cytoprotective effects of nitrite during in vivo ischemia-reperfusion of the heart and liver. *J Clin Invest,* 115**,** 1232-40.

EGOM, E. E., VELLA, K., HUA, R., JANSEN, H. J., MOGHTADAEI, M., POLINA, I., BOGACHEV, O., HURNIK, R., MACKASEY, M., RAFFERTY, S., RAY, G. & ROSE, R. A. 2014. Impaired sinoatrial node function and increased susceptibility to atrial fibrillation in mice lacking natriuretic peptide receptor C. *J Physiol*.

EHRET, G. B., MUNROE, P. B., RICE, K. M., BOCHUD, M., JOHNSON, A. D., CHASMAN, D. I., SMITH, A. V., TOBIN, M. D., VERWOERT, G. C., HWANG, S. J., PIHUR, V., VOLLENWEIDER, P., O'REILLY, P. F., AMIN, N., BRAGG-GRESHAM, J. L., TEUMER, A., GLAZER, N. L., LAUNER, L., ZHAO, J. H., AULCHENKO, Y., HEATH, S., SOBER, S., PARSA, A., LUAN, J., ARORA, P., DEHGHAN, A., ZHANG, F., LUCAS, G., HICKS, A. A., JACKSON, A. U., PEDEN, J. F., TANAKA, T., WILD, S. H., RUDAN, I., IGL, W., MILANESCHI, Y., PARKER, A. N., FAVA, C., CHAMBERS, J. C., FOX, E. R., KUMARI, M., GO, M. J., VAN DER HARST, P., KAO, W. H., SJOGREN, M., VINAY, D. G., ALEXANDER, M., TABARA, Y., SHAW-HAWKINS, S., WHINCUP, P. H., LIU, Y., SHI, G., KUUSISTO, J., TAYO, B., SEIELSTAD, M., SIM, X., NGUYEN, K. D., LEHTIMAKI, T., MATULLO, G., WU, Y., GAUNT, T. R., ONLAND-MORET, N. C., COOPER, M. N., PLATOU, C. G., ORG, E., HARDY, R., DAHGAM, S., PALMEN, J., VITART, V., BRAUND, P. S., KUZNETSOVA, T., UITERWAAL, C. S., ADEYEMO, A., PALMAS, W., CAMPBELL, H., LUDWIG, B., TOMASZEWSKI, M., TZOULAKI, I., PALMER, N. D., ASPELUND, T., GARCIA, M., CHANG, Y. P., O'CONNELL, J. R., STEINLE, N. I., GROBBEE, D. E., ARKING, D. E., KARDIA, S. L., MORRISON, A. C., HERNANDEZ, D., NAJJAR, S., MCARDLE, W. L., HADLEY, D., BROWN, M. J., CONNELL, J. M., HINGORANI, A. D., DAY, I. N., LAWLOR, D. A., BEILBY, J. P., LAWRENCE, R. W., CLARKE, R., et al. 2011. Genetic variants in novel pathways influence blood pressure and cardiovascular disease risk. *Nature,* 478**,** 103-9.

EL ANDALOUSI, J., LI, Y. & ANAND-SRIVASTAVA, M. B. 2013. Natriuretic peptide receptor-C agonist attenuates the expression of cell cycle proteins and proliferation of vascular smooth muscle cells from spontaneously hypertensive rats: role of Gi proteins and MAPkinase/PI3kinase signaling. *PLoS One,* 8**,** e76183.

ELSNER, D., MUDERS, F., MUNTZE, A., KROMER, E. P., FORSSMANN, W. G. & RIEGGER, G. A. 1995. Efficacy of prolonged infusion of urodilatin [ANP-(95-126)] in patients with congestive heart failure. *Am Heart J,* 129**,** 766-73.

ESPOSITO, G., PRASAD, S. V., RAPACCIUOLO, A., MAO, L., KOCH, W. J. & ROCKMAN, H. A. 2001. Cardiac overexpression of a G(q) inhibitor blocks induction of extracellular signal-regulated kinase and c-Jun NH(2)-terminal kinase activity in in vivo pressure overload. *Circulation,* 103**,** 1453-8.

ESTRADA, K., KRAWCZAK, M., SCHREIBER, S., VAN DUIJN, K., STOLK, L., VAN MEURS, J. B., LIU, F., PENNINX, B. W., SMIT, J. H., VOGELZANGS, N., HOTTENGA, J. J., WILLEMSEN, G., DE GEUS, E. J., LORENTZON, M., VON ELLER-EBERSTEIN, H., LIPS, P., SCHOOR, N., POP, V., DE KEIJZER, J., HOFMAN, A., AULCHENKO, Y. S., OOSTRA, B. A., OHLSSON, C., BOOMSMA, D. I., UITTERLINDEN, A. G., VAN DUIJN, C. M., RIVADENEIRA, F. & KAYSER, M. 2009. A genome-wide association study of northwestern Europeans involves the C-type natriuretic peptide signaling pathway in the etiology of human height variation. *Hum Mol Genet,* 18**,** 3516-24.

FAXON, D. P., GIBBONS, R. J., CHRONOS, N. A., GURBEL, P. A. & SHEEHAN, F. 2002. The effect of blockade of the CD11/CD18 integrin receptor on infarct size in patients with acute myocardial infarction treated with direct angioplasty: the results of the HALT-MI study. *J Am Coll Cardiol,* 40**,** 1199-204.

FIDZINSKI, P., SALVADOR-SILVA, M., CHORITZ, L., GEIBEL, J. & COCA-PRADOS, M. 2004. Inhibition of NHE-1 Na+/H+ exchanger by natriuretic peptides in ocular nonpigmented ciliary epithelium. *Am J Physiol Cell Physiol,* 287**,** C655-63.

FIELITZ, J., HEIN, S., MITROVIC, V., PREGLA, R., ZURBRUGG, H. R., WARNECKE, C., SCHAPER, J., FLECK, E. & REGITZ-ZAGROSEK, V. 2001. Activation of the cardiac renin-angiotensin system and increased myocardial collagen expression in human aortic valve disease. *J Am Coll Cardiol,* 37**,** 1443-9.

FILTZ, T. M., GRUBB, D. R., MCLEOD-DRYDEN, T. J., LUO, J. & WOODCOCK, E. A. 2009. Gq-initiated cardiomyocyte hypertrophy is mediated by phospholipase Cbeta1b. *Faseb j,* 23**,** 3564-70.

FLAHERTY, M. P., BROWN, M., GRUPP, I. L., SCHULTZ, J. E., MURPHREE, S. S. & JONES, W. K. 2007. eNOS deficient mice develop progressive cardiac hypertrophy with altered cytokine and calcium handling protein expression. *Cardiovasc Toxicol,* 7**,** 165-77.

FRANGOGIANNIS, N. G. 2012. Regulation of the inflammatory response in cardiac repair. *Circ Res,* 110**,** 159-73.

FRANK, A., BONNEY, M., BONNEY, S., WEITZEL, L., KOEPPEN, M. & ECKLE, T. 2012. Myocardial ischemia reperfusion injury: from basic science to clinical bedside. *Semin Cardiothorac Vasc Anesth,* 16**,** 123-32.

FRANK, K. F., BOLCK, B., BRIXIUS, K., KRANIAS, E. G. & SCHWINGER, R. H. 2002. Modulation of SERCA: implications for the failing human heart. *Basic Res Cardiol,* 97 Suppl 1**,** I72-8.

FRANTZ, S., KLAIBER, M., BABA, H. A., OBERWINKLER, H., VOLKER, K., GABETANER, B., BAYER, B., ABEBETAER, M., SCHUH, K., FEIL, R., HOFMANN, F. & KUHN, M. 2013. Stress-dependent dilated cardiomyopathy in mice with cardiomyocyte-restricted inactivation of cyclic GMP-dependent protein kinase I. *Eur Heart J,* 34**,** 1233-44.

FUJII, K., OHMORI, S., TOMINAGA, M., ABE, I., TAKATA, Y., OHYA, Y., KOBAYASHI, K. & FUJISHIMA, M. 1993. Age-related changes in endothelium-dependent hyperpolarization in the rat mesenteric artery. *Am J Physiol,* 265**,** H509-16.

FURUYA, M., AISAKA, K., MIYAZAKI, T., HONBOU, N., KAWASHIMA, K., OHNO, T., TANAKA, S., MINAMINO, N., KANGAWA, K. & MATSUO, H. 1993. C-type natriuretic peptide inhibits intimal thickening after vascular injury. *Biochem Biophys Res Commun,* 193**,** 248-53.

FURUYA, M., YOSHIDA, M., HAYASHI, Y., OHNUMA, N., MINAMINO, N., KANGAWA, K. & MATSUO, H. 1991. C-type natriuretic peptide is a growth inhibitor of rat vascular smooth muscle cells. *Biochem Biophys Res Commun,* 177**,** 927-31.

GARLAND, C. J., PLANE, F., KEMP, B. K. & COCKS, T. M. 1995. Endothelium-dependent hyperpolarization: a role in the control of vascular tone. *Trends Pharmacol Sci,* 16**,** 23-30.

GASPARI, T. A., BARBER, M. N., WOODS, R. L. & DUSTING, G. J. 2000. Type-C natriuretic peptide prevents development of experimental atherosclerosis in rabbits. *Clin Exp Pharmacol Physiol,* 27**,** 653-5.

GERDES, A. M. 1997. A reliable, efficient, and comprehensive approach to assess myocyte remodeling in cardiac hypertrophy and failure. *J Card Fail,* 3**,** 63-8.

GEWALTIG, M. T. & KOJDA, G. 2002. Vasoprotection by nitric oxide: mechanisms and therapeutic potential. *Cardiovasc Res,* 55**,** 250-60.

GHEORGHIADE, M., COLUCCI, W. S. & SWEDBERG, K. 2003. Beta-blockers in chronic heart failure. *Circulation,* 107**,** 1570-5.

GHOSH, S. M., KAPIL, V., FUENTES-CALVO, I., BUBB, K. J., PEARL, V., MILSOM, A. B., KHAMBATA, R., MALEKI-TOYSERKANI, S., YOUSUF, M., BENJAMIN, N., WEBB, A. J., CAULFIELD, M. J., HOBBS, A. J. & AHLUWALIA, A. 2013. Enhanced vasodilator activity of nitrite in hypertension: critical role for erythrocytic xanthine oxidoreductase and translational potential. *Hypertension,* 61**,** 1091-102.

GILLIAN POCOCK, C. D. R. 2006. *Human Physiology: The basis of medicine*, Oxford.

GOBEIL, F., JR., HALLE, S., BLAIS, P. A. & REGOLI, D. 2002. Studies on the angiotensin-converting enzyme and the kinin B2 receptor in the rabbit jugular vein: modulation of contractile response to bradykinin. *Can J Physiol Pharmacol,* 80**,** 153-63.

GODO, S. & SHIMOKAWA, H. 2017. Endothelial Functions. *Arterioscler Thromb Vasc Biol,* 37**,** e108-e114.

GOTO, K., FUJII, K., ONAKA, U., ABE, I. & FUJISHIMA, M. 2000. Renin-angiotensin system blockade improves endothelial dysfunction in hypertension. *Hypertension,* 36**,** 575-80.

GRANGER, D. N. & KVIETYS, P. R. 2015. Reperfusion injury and reactive oxygen species: The evolution of a concept. *Redox Biol,* 6**,** 524-51.

GRIFFITHS, E. J. & HALESTRAP, A. P. 1995. Mitochondrial non-specific pores remain closed during cardiac ischaemia, but open upon reperfusion. *Biochem J,* 307 (Pt 1)**,** 93-8.

GRIMM, D., ELSNER, D., SCHUNKERT, H., PFEIFER, M., GRIESE, D., BRUCKSCHLEGEL, G., MUDERS, F., RIEGGER, G. A. & KROMER, E. P. 1998. Development of heart failure following isoproterenol administration in the rat: role of the renin-angiotensin system. *Cardiovasc Res,* 37**,** 91-100.

GROSSER, T., FRIES, S. & FITZGERALD, G. A. 2006. Biological basis for the cardiovascular consequences of COX-2 inhibition: therapeutic challenges and opportunities. *J Clin Invest,* 116**,** 4-15.

GROSSMAN, W., JONES, D. & MCLAURIN, L. P. 1975. Wall stress and patterns of hypertrophy in the human left ventricle. *J Clin Invest,* 56**,** 56-64.

GUTKOWSKA, J., JANKOWSKI, M., SAIRAM, M. R., FUJIO, N., REIS, A. M., MUKADDAM-DAHER, S. & TREMBLAY, J. 1999. Hormonal regulation of natriuretic peptide system during induced ovarian follicular development in the rat. *Biol Reprod,* 61**,** 162-70.

HAGA, Y., OHTSUBO, T., MURAKAMI, N., NOGUCHI, H., KANSUI, Y., GOTO, K., MATSUMURA, K. & KITAZONO, T. 2017. Disruption of xanthine oxidoreductase gene attenuates renal ischemia reperfusion injury in mice. *Life Sci,* 182**,** 73-79.

HAHN, H. S., MARREEZ, Y., ODLEY, A., STERBLING, A., YUSSMAN, M. G., HILTY, K. C., BODI, I., LIGGETT, S. B., SCHWARTZ, A. & DORN, G. W., 2ND 2003. Protein kinase Calpha negatively regulates systolic and diastolic function in pathological hypertrophy. *Circ Res,* 93**,** 1111-9.

HALL, B., LIMAYE, A. & KULKARNI, A. B. 2009. Overview: Generation of Gene Knockout Mice. *Current protocols in cell biology / editorial board, Juan S. Bonifacino ... [et al.],* CHAPTER**,** Unit-19.1217.

HAMA, N., ITOH, H., SHIRAKAMI, G., SUGA, S., KOMATSU, Y., YOSHIMASA, T., TANAKA, I., MORI, K. & NAKAO, K. 1994. Detection of C-type natriuretic peptide in human circulation and marked increase of plasma CNP level in septic shock patients. *Biochem Biophys Res Commun,* 198**,** 1177-82.

HANSSON, G. K. 2005. Inflammation, atherosclerosis, and coronary artery disease. *N Engl J Med,* 352**,** 1685-95.

HAQ, S., CHOUKROUN, G., KANG, Z. B., RANU, H., MATSUI, T., ROSENZWEIG, A., MOLKENTIN, J. D., ALESSANDRINI, A., WOODGETT, J., HAJJAR, R., MICHAEL, A. & FORCE, T. 2000. Glycogen synthase kinase-3beta is a negative regulator of cardiomyocyte hypertrophy. *J Cell Biol,* 151**,** 117-30.

HAQ, S., CHOUKROUN, G., LIM, H., TYMITZ, K. M., DEL MONTE, F., GWATHMEY, J., GRAZETTE, L., MICHAEL, A., HAJJAR, R., FORCE, T. & MOLKENTIN, J. D. 2001. Differential activation of signal transduction pathways in human hearts with hypertrophy versus advanced heart failure. *Circulation,* 103**,** 670-7.

HARADA, K., KOMURO, I., SHIOJIMA, I., HAYASHI, D., KUDOH, S., MIZUNO, T., KIJIMA, K., MATSUBARA, H., SUGAYA, T., MURAKAMI, K. & YAZAKI, Y. 1998. Pressure overload induces cardiac hypertrophy in angiotensin II type 1A receptor knockout mice. *Circulation,* 97**,** 1952-9.

HARDT, S. E. & SADOSHIMA, J. 2002. Glycogen synthase kinase-3beta: a novel regulator of cardiac hypertrophy and development. *Circ Res,* 90**,** 1055-63.

HASHIM, S., LI, Y. & ANAND-SRIVASTAVA, M. B. 2006. Small cytoplasmic domain peptides of natriuretic peptide receptor-C attenuate cell proliferation through Gialpha protein/MAP kinase/PI3-kinase/AKT pathways. *Am J Physiol Heart Circ Physiol,* 291**,** H3144-53.

HASHIMOTO, Y., NAKAO, K., HAMA, N., IMURA, H., MORI, S., YAMAGUCHI, M., YASUHARA, M. & HORI, R. 1994. Clearance mechanisms of atrial and brain natriuretic peptides in rats. *Pharm Res,* 11**,** 60-4.

HAUSENLOY, D. J. & YELLON, D. M. 2013. Myocardial ischemia-reperfusion injury: a neglected therapeutic target. *J Clin Invest,* 123**,** 92-100.

HAYASHI, M., TSUTAMOTO, T., WADA, A., MAEDA, K., MABUCHI, N., TSUTSUI, T., HORIE, H., OHNISHI, M. & KINOSHITA, M. 2001. Intravenous atrial natriuretic peptide prevents left ventricular remodeling in patients with first anterior acute myocardial infarction. *J Am Coll Cardiol,* 37**,** 1820-6.

HAYASHI, S., MORISHITA, R., MATSUSHITA, H., NAKAGAMI, H., TANIYAMA, Y., NAKAMURA, T., AOKI, M., YAMAMOTO, K., HIGAKI, J. & OGIHARA, T. 2000. Cyclic AMP inhibited proliferation of human aortic vascular smooth muscle cells, accompanied by induction of p53 and p21. *Hypertension,* 35**,** 237-43.

HAYWARD, C., BANNER, N. R., MORLEY-SMITH, A., LYON, A. R. & HARDING, S. E. 2015. The Current and Future Landscape of SERCA Gene Therapy for Heart Failure: A Clinical Perspective. *Hum Gene Ther,* 26**,** 293-304.

HEGER, J., SCHULZ, R. & EULER, G. 2016. Molecular switches under TGFbeta signalling during progression from cardiac hypertrophy to heart failure. *Br J Pharmacol,* 173**,** 3-14.

HEIN, S., ARNON, E., KOSTIN, S., SCHONBURG, M., ELSASSER, A., POLYAKOVA, V., BAUER, E. P., KLOVEKORN, W. P. & SCHAPER, J. 2003. Progression from compensated hypertrophy to failure in the pressure-overloaded human heart: structural deterioration and compensatory mechanisms. *Circulation,* 107**,** 984-91.

HEINEKE, J. & MOLKENTIN, J. D. 2006. Regulation of cardiac hypertrophy by intracellular signalling pathways. *Nat Rev Mol Cell Biol,* 7**,** 589-600.

HENRY, S. P. & KILLILEA, S. D. 1994. Purification and characterization of bovine heart glycogen synthase kinase-3. *Prep Biochem,* 24**,** 263-77.

HERRING, N., ZAMAN, J. A. & PATERSON, D. J. 2001. Natriuretic peptides like NO facilitate cardiac vagal neurotransmission and bradycardia via a cGMP pathway. *Am J Physiol Heart Circ Physiol,* 281**,** H2318-27.

HILLOCK, R. J., FRAMPTON, C. M., YANDLE, T. G., TROUGHTON, R. W., LAINCHBURY, J. G. & RICHARDS, A. M. 2008. B-type natriuretic peptide infusions in acute myocardial infarction. *Heart,* 94**,** 617-22.

HIROOKA, Y., TAKESHITA, A., IMAIZUMI, T., SUZUKI, S., YOSHIDA, M., ANDO, S. & NAKAMURA, M. 1990. Attenuated forearm vasodilative response to intra-arterial atrial natriuretic peptide in patients with heart failure. *Circulation,* 82**,** 147-53.

HIROSE, M., FURUKAWA, Y., KUROGOUCHI, F., NAKAJIMA, K., MIYASHITA, Y. & CHIBA, S. 1998. C-type natriuretic peptide increases myocardial contractility and sinus rate mediated by guanylyl cyclase-linked natriuretic peptide receptors in isolated, blood-perfused dog heart preparations. *J Pharmacol Exp Ther,* 286**,** 70-6.

HIRSCH, J. R., MEYER, M. & FORSSMANN, W. G. 2006. ANP and urodilatin: who is who in the kidney. *Eur J Med Res,* 11**,** 447-54.

HISADO-OLIVA, A., RUZAFA-MARTIN, A., SENTCHORDI, L., FUNARI, M. F. A., BEZANILLA-LOPEZ, C., ALONSO-BERNALDEZ, M., BARRAZA-GARCIA, J., RODRIGUEZ-ZABALA, M., LERARIO, A. M., BENITO-SANZ, S., AZA-CARMONA, M., CAMPOS-BARROS, A., JORGE, A. A. L. & HEATH, K. E. 2018. Mutations in C-natriuretic peptide (NPPC): a novel cause of autosomal dominant short stature. *Genet Med,* 20**,** 91-97.

HOBBS, A., FOSTER, P., PRESCOTT, C., SCOTLAND, R. & AHLUWALIA, A. 2004. Natriuretic peptide receptor-C regulates coronary blood flow and prevents myocardial ischemia/reperfusion injury: novel cardioprotective role for endothelium-derived C-type natriuretic peptide. *Circulation,* 110**,** 1231-5.

HOBBS, R. E., MILLER, L. W., BOTT-SILVERMAN, C., JAMES, K. B., RINCON, G. & GROSSBARD, E. B. 1996. Hemodynamic effects of a single intravenous injection of synthetic human brain natriuretic peptide in patients with heart failure secondary to ischemic or idiopathic dilated cardiomyopathy. *Am J Cardiol,* 78**,** 896-901.

HOLMES, S. J., ESPINER, E. A., RICHARDS, A. M., YANDLE, T. G. & FRAMPTON, C. 1993. Renal, endocrine, and hemodynamic effects of human brain natriuretic peptide in normal man. *J Clin Endocrinol Metab,* 76**,** 91-6.

HOLTWICK, R., VAN EICKELS, M., SKRYABIN, B. V., BABA, H. A., BUBIKAT, A., BEGROW, F., SCHNEIDER, M. D., GARBERS, D. L. & KUHN, M. 2003. Pressure-independent cardiac hypertrophy in mice with cardiomyocyte-restricted inactivation of the atrial natriuretic peptide receptor guanylyl cyclase-A. *J Clin Invest,* 111**,** 1399-407.

HONDA, H. M., KORGE, P. & WEISS, J. N. 2005. Mitochondria and ischemia/reperfusion injury. *Ann N Y Acad Sci,* 1047**,** 248-58.

HORCKMANS, M., RING, L., DUCHENE, J., SANTOVITO, D., SCHLOSS, M. J., DRECHSLER, M., WEBER, C., SOEHNLEIN, O. & STEFFENS, S. 2017. Neutrophils orchestrate post-myocardial infarction healing by polarizing macrophages towards a reparative phenotype. *Eur Heart J,* 38**,** 187-197.

HORIO, T., TOKUDOME, T., MAKI, T., YOSHIHARA, F., SUGA, S., NISHIKIMI, T., KOJIMA, M., KAWANO, Y. & KANGAWA, K. 2003. Gene expression, secretion, and autocrine action of C-type natriuretic peptide in cultured adult rat cardiac fibroblasts. *Endocrinology,* 144**,** 2279-84.

HUEBERT, R. C., LI, Q., ADHIKARI, N., CHARLES, N. J., HAN, X., EZZAT, M. K., GRINDLE, S., PARK, S., ORMAZA, S., FERMIN, D., MILLER, L. W. & HALL, J. L. 2004. Identification and regulation of Sprouty1, a negative inhibitor of the ERK cascade, in the human heart. *Physiol Genomics,* 18**,** 284-9.

HULSMANS, M., SAM, F. & NAHRENDORF, M. 2016. Monocyte and macrophage contributions to cardiac remodeling. *J Mol Cell Cardiol,* 93**,** 149-55.

HUNT, P. J., RICHARDS, A. M., ESPINER, E. A., NICHOLLS, M. G. & YANDLE, T. G. 1994. Bioactivity and metabolism of C-type natriuretic peptide in normal man. *J Clin Endocrinol Metab,* 78**,** 1428-35.

ICHIKI, T., SCHIRGER, J. A., HUNTLEY, B. K., BROZOVICH, F. V., MALESZEWSKI, J. J., SANDBERG, S. M., SANGARALINGHAM, S. J., PARK, S. J. & BURNETT, J. C., JR. 2014. Cardiac fibrosis in end-stage human heart failure and the cardiac natriuretic peptide guanylyl cyclase system: Regulation and therapeutic implications. *J Mol Cell Cardiol,* 75c**,** 199-205.

IGAKI, T., ITOH, H., SUGA, S., HAMA, N., OGAWA, Y., KOMATSU, Y., MUKOYAMA, M., SUGAWARA, A., YOSHIMASA, T., TANAKA, I. & NAKAO, K. 1996. C-type natriuretic peptide in chronic renal failure and its action in humans. *Kidney Int Suppl,* 55**,** S144-7.

IGNARRO, L. J., BUGA, G. M., WOOD, K. S., BYRNS, R. E. & CHAUDHURI, G. 1987. Endothelium-derived relaxing factor produced and released from artery and vein is nitric oxide. *Proc Natl Acad Sci U S A,* 84**,** 9265-9.

INOUE, K., NARUSE, K., YAMAGAMI, S., MITANI, H., SUZUKI, N. & TAKEI, Y. 2003. Four functionally distinct C-type natriuretic peptides found in fish reveal evolutionary history of the natriuretic peptide system. *Proc Natl Acad Sci U S A,* 100**,** 10079-84.

INSERTE, J., GARCIA-DORADO, D., AGULLO, L., PANIAGUA, A. & SOLER-SOLER, J. 2000. Urodilatin limits acute reperfusion injury in the isolated rat heart. *Cardiovasc Res,* 45**,** 351-9.

INSERTE, J., GARCIA-DORADO, D., RUIZ-MEANA, M., PADILLA, F., BARRABES, J. A., PINA, P., AGULLO, L., PIPER, H. M. & SOLER-SOLER, J. 2002. Effect of inhibition of Na(+)/Ca(2+) exchanger at the time of myocardial reperfusion on hypercontracture and cell death. *Cardiovasc Res,* 55**,** 739-48.

IZUMIYA, Y., ARAKI, S., USUKU, H., ROKUTANDA, T., HANATANI, S. & OGAWA, H. 2012. Chronic C-Type Natriuretic Peptide Infusion Attenuates Angiotensin II-Induced Myocardial Superoxide Production and Cardiac Remodeling. *Int J Vasc Med,* 2012**,** 246058.

JACKSON, G., GIBBS, C. R., DAVIES, M. K. & LIP, G. Y. 2000. ABC of heart failure. Pathophysiology. *Bmj,* 320**,** 167-70.

JAIN, A. & ANAND-SRIVASTAVA, M. B. 2018. Natriuretic peptide receptor-C-mediated attenuation of vascular smooth muscle cell hypertrophy involves Gqalpha/PLCbeta1 proteins and ROS-associated signaling. *Pharmacol Res Perspect,* 6.

JALIL, J. E., DOERING, C. W., JANICKI, J. S., PICK, R., CLARK, W. A., ABRAHAMS, C. & WEBER, K. T. 1988. Structural vs. contractile protein remodeling and myocardial stiffness in hypertrophied rat left ventricle. *J Mol Cell Cardiol,* 20**,** 1179-87.

JANSSENS, S., POKREISZ, P., SCHOONJANS, L., PELLENS, M., VERMEERSCH, P., TJWA, M., JANS, P., SCHERRER-CROSBIE, M., PICARD, M. H., SZELID, Z., GILLIJNS, H., VAN DE WERF, F., COLLEN, D. & BLOCH, K. D. 2004. Cardiomyocyte-specific overexpression of nitric oxide synthase 3 improves left ventricular performance and reduces compensatory hypertrophy after myocardial infarction. *Circ Res,* 94**,** 1256-62.

JAUBERT, J., JAUBERT, F., MARTIN, N., WASHBURN, L. L., LEE, B. K., EICHER, E. M. & GUENET, J. L. 1999. Three new allelic mouse mutations that cause skeletal overgrowth involve the natriuretic peptide receptor C gene (Npr3). *Proc Natl Acad Sci U S A,* 96**,** 10278-83.

JIN, X., ZHANG, Y., LI, X., ZHANG, J. & XU, D. 2014. C-type natriuretic peptide ameliorates ischemia/reperfusion-induced acute kidney injury by inhibiting apoptosis and oxidative stress in rats. *Life Sci,* 117**,** 40-5.

JOHN, S. W., KREGE, J. H., OLIVER, P. M., HAGAMAN, J. R., HODGIN, J. B., PANG, S. C., FLYNN, T. G. & SMITHIES, O. 1995. Genetic decreases in atrial natriuretic peptide and salt-sensitive hypertension. *Science,* 267**,** 679-81.

JONG, P., YUSUF, S., ROUSSEAU, M. F., AHN, S. A. & BANGDIWALA, S. I. 2003. Effect of enalapril on 12-year survival and life expectancy in patients with left ventricular systolic dysfunction: a follow-up study. *Lancet,* 361**,** 1843-8.

KAGIYAMA, S., MATSUMURA, K., GOTO, K., OTSUBO, T. & IIDA, M. 2010. Role of Rho kinase and oxidative stress in cardiac fibrosis induced by aldosterone and salt in angiotensin type 1a receptor knockout mice. *Regul Pept,* 160**,** 133-9.

KAI, H., MURAISHI, A., SUGIU, Y., NISHI, H., SEKI, Y., KUWAHARA, F., KIMURA, A., KATO, H. & IMAIZUMI, T. 1998. Expression of proto-oncogenes and gene mutation of sarcomeric proteins in patients with hypertrophic cardiomyopathy. *Circ Res,* 83**,** 594-601.

KALRA, P. R., ANKER, S. D., STRUTHERS, A. D. & COATS, A. J. 2001. The role of C-type natriuretic peptide in cardiovascular medicine. *Eur Heart J,* 22**,** 997-1007.

KALRA, P. R., CLAGUE, J. R., BOLGER, A. P., ANKER, S. D., POOLE-WILSON, P. A., STRUTHERS, A. D. & COATS, A. J. 2003. Myocardial production of C-type natriuretic peptide in chronic heart failure. *Circulation,* 107**,** 571-3.

KEHAT, I., DAVIS, J., TIBURCY, M., ACCORNERO, F., SABA-EL-LEIL, M. K., MAILLET, M., YORK, A. J., LORENZ, J. N., ZIMMERMANN, W. H., MELOCHE, S. & MOLKENTIN, J. D. 2011. Extracellular signal-regulated kinases 1 and 2 regulate the balance between eccentric and concentric cardiac growth. *Circ Res,* 108**,** 176-83.

KENNY, A. J., BOURNE, A. & INGRAM, J. 1993. Hydrolysis of human and pig brain natriuretic peptides, urodilatin, C-type natriuretic peptide and some C-receptor ligands by endopeptidase-24.11. *Biochem J,* 291 (Pt 1)**,** 83-8.

KENTSCH, M., LUDWIG, D., DRUMMER, C., GERZER, R. & MULLER-ESCH, G. 1992a. Haemodynamic and renal effects of urodilatin bolus injections in patients with congestive heart failure. *Eur J Clin Invest,* 22**,** 662-9.

KENTSCH, M., LUDWIG, D., DRUMMER, C., GERZER, R. & MULLER-ESCH, G. 1992b. Haemodynamic and renal effects of urodilatin in healthy volunteers. *Eur J Clin Invest,* 22**,** 319-25.

KERR, M. A. & KENNY, A. J. 1974. The purification and specificity of a neutral endopeptidase from rabbit kidney brush border. *Biochem J,* 137**,** 477-88.

KHAMBATA, R. S., PANAYIOTOU, C. M. & HOBBS, A. J. 2011. Natriuretic peptide receptor-3 underpins the disparate regulation of endothelial and vascular smooth muscle cell proliferation by C-type natriuretic peptide. *Br J Pharmacol,* 164**,** 584-97.

KHAN, K. N., PAULSON, S. K., VERBURG, K. M., LEFKOWITH, J. B. & MAZIASZ, T. J. 2002. Pharmacology of cyclooxygenase-2 inhibition in the kidney. *Kidney Int,* 61**,** 1210-9.

KILIC, A., RAJAPUROHITAM, V., SANDBERG, S. M., ZEIDAN, A., HUNTER, J. C., SAID FARUQ, N., LEE, C. Y., BURNETT, J. C., JR. & KARMAZYN, M. 2010. A novel chimeric natriuretic peptide reduces cardiomyocyte hypertrophy through the NHE-1-calcineurin pathway. *Cardiovasc Res,* 88**,** 434-42.

KILIC, A., VELIC, A., DE WINDT, L. J., FABRITZ, L., VOSS, M., MITKO, D., ZWIENER, M., BABA, H. A., VAN EICKELS, M., SCHLATTER, E. & KUHN, M. 2005. Enhanced activity of the myocardial Na+/H+ exchanger NHE-1 contributes to cardiac remodeling in atrial natriuretic peptide receptor-deficient mice. *Circulation,* 112**,** 2307-17.

KIM, J. C., SON, M. J., WANG, J. & WOO, S. H. 2017. Regulation of cardiac Ca2+ and ion channels by shear mechanotransduction. *Arch Pharm Res,* 40**,** 783-795.

KIM, J. S., JIN, Y. & LEMASTERS, J. J. 2006a. Reactive oxygen species, but not Ca2+ overloading, trigger pH- and mitochondrial permeability transition-dependent death of adult rat myocytes after ischemia-reperfusion. *Am J Physiol Heart Circ Physiol,* 290**,** H2024-34.

KIM, K. H., KIM, H. K., HWANG, I. C., CHO, H. J., JE, N., KWON, O. M., CHOI, S. J., LEE, S. P., KIM, Y. J. & SOHN, D. W. 2015. PDE 5 inhibition with udenafil improves left ventricular systolic/diastolic functions and exercise capacity in patients with chronic heart failure with reduced ejection fraction; A 12-week, randomized, double-blind, placebo-controlled trial. *Am Heart J,* 169**,** 813-822.e3.

KIM, N., KIM, H., YOUM, J. B., PARK, W. S., WARDA, M., KO, J. H. & HAN, J. 2006b. Site specific differential activation of ras/raf/ERK signaling in rabbit isoproterenol-induced left ventricular hypertrophy. *Biochim Biophys Acta,* 1763**,** 1067-75.

KIM, S., OHTA, K., HAMAGUCHI, A., YUKIMURA, T., MIURA, K. & IWAO, H. 1995. Angiotensin II induces cardiac phenotypic modulation and remodeling in vivo in rats. *Hypertension,* 25**,** 1252-9.

KIM, Y., PHAN, D., VAN ROOIJ, E., WANG, D. Z., MCANALLY, J., QI, X., RICHARDSON, J. A., HILL, J. A., BASSEL-DUBY, R. & OLSON, E. N. 2008. The MEF2D transcription factor mediates stress-dependent cardiac remodeling in mice. *J Clin Invest,* 118**,** 124-32.

KIPSHIDZE, N., DANGAS, G., TSAPENKO, M., MOSES, J., LEON, M. B., KUTRYK, M. & SERRUYS, P. 2004. Role of the endothelium in modulating neointimal formation: vasculoprotective approaches to attenuate restenosis after percutaneous coronary interventions. *J Am Coll Cardiol,* 44**,** 733-9.

KIRKBY, N. S., LUNDBERG, M. H., HARRINGTON, L. S., LEADBEATER, P. D., MILNE, G. L., POTTER, C. M., AL-YAMANI, M., ADEYEMI, O., WARNER, T. D. & MITCHELL, J. A. 2012. Cyclooxygenase-1, not cyclooxygenase-2, is responsible for physiological production of prostacyclin in the cardiovascular system. *Proc Natl Acad Sci U S A,* 109**,** 17597-602.

KISANUKI, Y. Y., HAMMER, R. E., MIYAZAKI, J., WILLIAMS, S. C., RICHARDSON, J. A. & YANAGISAWA, M. 2001. Tie2-Cre transgenic mice: a new model for endothelial cell-lineage analysis in vivo. *Dev Biol,* 230**,** 230-42.

KITAKAZE, M., ASAKURA, M., KIM, J., SHINTANI, Y., ASANUMA, H., HAMASAKI, T., SEGUCHI, O., MYOISHI, M., MINAMINO, T., OHARA, T., NAGAI, Y., NANTO, S., WATANABE, K., FUKUZAWA, S., HIRAYAMA, A., NAKAMURA, N., KIMURA, K., FUJII, K., ISHIHARA, M., SAITO, Y., TOMOIKE, H. & KITAMURA, S. 2007. Human atrial natriuretic peptide and nicorandil as adjuncts to reperfusion treatment for acute myocardial infarction (J-WIND): two randomised trials. *Lancet,* 370**,** 1483-93.

KOENTGES, C., PEPIN, M. E., MUSSE, C., PFEIL, K., ALVAREZ, S. V. V., HOPPE, N., HOFFMANN, M. M., ODENING, K. E., SOSSALLA, S., ZIRLIK, A., HEIN, L., BODE, C., WENDE, A. R. & BUGGER, H. 2017. Gene expression analysis to identify mechanisms underlying heart failure susceptibility in mice and humans. *Basic Res Cardiol,* 113**,** 8.

KOHNO, M., HORIO, T., YOKOKAWA, K., KURIHARA, N. & TAKEDA, T. 1992. C-type natriuretic peptide inhibits thrombin- and angiotensin II-stimulated endothelin release via cyclic guanosine 3',5'-monophosphate. *Hypertension,* 19**,** 320-5.

KOITABASHI, N., BEDJA, D., ZAIMAN, A. L., PINTO, Y. M., ZHANG, M., GABRIELSON, K. L., TAKIMOTO, E. & KASS, D. A. 2009. Avoidance of transient cardiomyopathy in cardiomyocyte-targeted tamoxifen-induced MerCreMer gene deletion models. *Circ Res,* 105**,** 12-5.

KOLLER, K. J., DE SAUVAGE, F. J., LOWE, D. G. & GOEDDEL, D. V. 1992. Conservation of the kinaselike regulatory domain is essential for activation of the natriuretic peptide receptor guanylyl cyclases. *Mol Cell Biol,* 12**,** 2581-90.

KOMATSU, Y., CHUSHO, H., TAMURA, N., YASODA, A., MIYAZAWA, T., SUDA, M., MIURA, M., OGAWA, Y. & NAKAO, K. 2002. Significance of C-type natriuretic peptide (CNP) in endochondral ossification: analysis of CNP knockout mice. *J Bone Miner Metab,* 20**,** 331-6.

KUHN, M., HOLTWICK, R., BABA, H. A., PERRIARD, J. C., SCHMITZ, W. & EHLER, E. 2002. Progressive cardiac hypertrophy and dysfunction in atrial natriuretic peptide receptor (GC-A) deficient mice. *Heart,* 87**,** 368-74.

KUHN, M., VOSS, M., MITKO, D., STYPMANN, J., SCHMID, C., KAWAGUCHI, N., GRABELLUS, F. & BABA, H. A. 2004. Left ventricular assist device support reverses altered cardiac expression and function of natriuretic peptides and receptors in end-stage heart failure. *Cardiovasc Res,* 64**,** 308-14.

KUN, A., KIRALY, I., PATARICZA, J., MARTON, Z., KRASSOI, I., VARRO, A., SIMONSEN, U., PAPP, J. G. & PAJOR, L. 2008. C-type natriuretic peptide hyperpolarizes and relaxes human penile resistance arteries. *J Sex Med,* 5**,** 1114-1125.

KUWAHARA, F., KAI, H., TOKUDA, K., KAI, M., TAKESHITA, A., EGASHIRA, K. & IMAIZUMI, T. 2002. Transforming growth factor-beta function blocking prevents myocardial fibrosis and diastolic dysfunction in pressure-overloaded rats. *Circulation,* 106**,** 130-5.

KWON, K. C. & DANIELL, H. 2015. Low-cost oral delivery of protein drugs bioencapsulated in plant cells. *Plant Biotechnol J,* 13**,** 1017-22.

LANGENICKEL, T. H., BUTTGEREIT, J., PAGEL-LANGENICKEL, I., LINDNER, M., MONTI, J., BEUERLEIN, K., AL-SAADI, N., PLEHM, R., POPOVA, E., TANK, J., DIETZ, R., WILLENBROCK, R. & BADER, M. 2006. Cardiac hypertrophy in transgenic rats expressing a dominant-negative mutant of the natriuretic peptide receptor B. *Proc Natl Acad Sci U S A,* 103**,** 4735-40.

LARSEN, H. E., LEFKIMMIATIS, K. & PATERSON, D. J. 2016. Sympathetic neurons are a powerful driver of myocyte function in cardiovascular disease. *Sci Rep,* 6**,** 38898.

LEE, C. Y. & BURNETT, J. C., JR. 2007. Natriuretic peptides and therapeutic applications. *Heart Fail Rev,* 12**,** 131-42.

LEENEN, F. H., WHITE, R. & YUAN, B. 2001. Isoproterenol-induced cardiac hypertrophy: role of circulatory versus cardiac renin-angiotensin system. *Am J Physiol Heart Circ Physiol,* 281**,** H2410-6.

LEFER, D. J., SHANDELYA, S. M., SERRANO, C. V., JR., BECKER, L. C., KUPPUSAMY, P. & ZWEIER, J. L. 1993. Cardioprotective actions of a monoclonal antibody against CD-18 in myocardial ischemia-reperfusion injury. *Circulation,* 88**,** 1779-87.

LEITMAN, D. C., ANDRESEN, J. W., KUNO, T., KAMISAKI, Y., CHANG, J. K. & MURAD, F. 1986. Identification of multiple binding sites for atrial natriuretic factor by affinity cross-linking in cultured endothelial cells. *J Biol Chem,* 261**,** 11650-5.

LEVY, F. O. 2013. Cardiac PDEs and crosstalk between cAMP and cGMP signalling pathways in the regulation of contractility. *Naunyn Schmiedebergs Arch Pharmacol,* 386**,** 665-70.

LEWIS, G. D., SHAH, R., SHAHZAD, K., CAMUSO, J. M., PAPPAGIANOPOULOS, P. P., HUNG, J., TAWAKOL, A., GERSZTEN, R. E., SYSTROM, D. M., BLOCH, K. D. & SEMIGRAN, M. J. 2007. Sildenafil improves exercise capacity and quality of life in patients with systolic heart failure and secondary pulmonary hypertension. *Circulation,* 116**,** 1555-62.

LI, J., WANG, J., RUSSELL, F. D. & MOLENAAR, P. 2005. Activation of calcineurin in human failing heart ventricle by endothelin-1, angiotensin II and urotensin II. *Br J Pharmacol,* 145**,** 432-40.

LI, J. M. & BROOKS, G. 1997. Differential protein expression and subcellular distribution of TGFbeta1, beta2 and beta3 in cardiomyocytes during pressure overload-induced hypertrophy. *J Mol Cell Cardiol,* 29**,** 2213-24.

LI, P., OPARIL, S., NOVAK, L., CAO, X., SHI, W., LUCAS, J. & CHEN, Y. F. 2007. ANP signaling inhibits TGF-beta-induced Smad2 and Smad3 nuclear translocation and extracellular matrix expression in rat pulmonary arterial smooth muscle cells. *J Appl Physiol (1985),* 102**,** 390-8.

LI, P., WANG, D., LUCAS, J., OPARIL, S., XING, D., CAO, X., NOVAK, L., RENFROW, M. B. & CHEN, Y. F. 2008. Atrial natriuretic peptide inhibits transforming growth factor beta-induced Smad signaling and myofibroblast transformation in mouse cardiac fibroblasts. *Circ Res,* 102**,** 185-92.

LI, R. K., LI, G., MICKLE, D. A., WEISEL, R. D., MERANTE, F., LUSS, H., RAO, V., CHRISTAKIS, G. T. & WILLIAMS, W. G. 1997. Overexpression of transforming growth factor-beta1 and insulin-like growth factor-I in patients with idiopathic hypertrophic cardiomyopathy. *Circulation,* 96**,** 874-81.

LI, W., MITAL, S., OJAIMI, C., CSISZAR, A., KALEY, G. & HINTZE, T. H. 2004a. Premature death and age-related cardiac dysfunction in male eNOS-knockout mice. *J Mol Cell Cardiol,* 37**,** 671-80.

LI, Y., HASHIM, S. & ANAND-SRIVASTAVA, M. B. 2006. Intracellular peptides of natriuretic peptide receptor-C inhibit vascular hypertrophy via Gqalpha/MAP kinase signaling pathways. *Cardiovasc Res,* 72**,** 464-72.

LI, Y., SAITO, Y., KUWAHARA, K., RONG, X., KISHIMOTO, I., HARADA, M., ADACHI, Y., NAKANISHI, M., KINOSHITA, H., HORIUCHI, M., MURRAY, M. & NAKAO, K. 2009. Guanylyl cyclase-A inhibits angiotensin II type 2 receptor-mediated pro-hypertrophic signaling in the heart. *Endocrinology,* 150**,** 3759-65.

LI, Y., SARKAR, O., BROCHU, M. & ANAND-SRIVASTAVA, M. B. 2014a. Natriuretic peptide receptor-C attenuates hypertension in spontaneously hypertensive rats: role of nitroxidative stress and Gi proteins. *Hypertension,* 63**,** 846-55.

LI, Z., TRAN, T. T., MA, J. Y., O'YOUNG, G., KAPOUN, A. M., CHAKRAVARTY, S., DUGAR, S., SCHREINER, G. & PROTTER, A. A. 2004b. p38 alpha mitogen-activated protein kinase inhibition improves cardiac function and reduces myocardial damage in isoproterenol-induced acute myocardial injury in rats. *J Cardiovasc Pharmacol,* 44**,** 486-92.

LI, Z. Q., LIU, Y. L., LI, G., LI, B., LIU, Y., LI, X. F. & LIU, A. J. 2014b. Inhibitory effects of Ctype natriuretic peptide on the differentiation of cardiac fibroblasts, and secretion of monocyte chemoattractant protein1 and plasminogen activator inhibitor1. *Mol Med Rep*.

LIAO, P., GEORGAKOPOULOS, D., KOVACS, A., ZHENG, M., LERNER, D., PU, H., SAFFITZ, J., CHIEN, K., XIAO, R. P., KASS, D. A. & WANG, Y. 2001. The in vivo role of p38 MAP kinases in cardiac remodeling and restrictive cardiomyopathy. *Proc Natl Acad Sci U S A,* 98**,** 12283-8.

LIBBY, P. 2002. Inflammation and Atherosclerosis. *Circulation,* 105**,** 1135-1143.

LIM, H. & ZHU, Y. Z. 2006. Role of transforming growth factor-beta in the progression of heart failure. *Cell Mol Life Sci,* 63**,** 2584-96.

LIMBIRD, L. E. & VAUGHAN, D. E. 1999. Augmenting beta receptors in the heart: short-term gains offset by long-term pains? *Proc Natl Acad Sci U S A,* 96**,** 7125-7.

LIN, D., CHAI, Y., IZADPANAH, R., BRAUN, S. E. & ALT, E. 2016. NPR3 protects cardiomyocytes from apoptosis through inhibition of cytosolic BRCA1 and TNF-alpha. *Cell Cycle,* 15**,** 2414-9.

LINDER, L., KIOWSKI, W., BUHLER, F. R. & LUSCHER, T. F. 1990. Indirect evidence for release of endothelium-derived relaxing factor in human forearm circulation in vivo. Blunted response in essential hypertension. *Circulation,* 81**,** 1762-7.

LISY, O., HUNTLEY, B. K., MCCORMICK, D. J., KURLANSKY, P. A. & BURNETT, J. C., JR. 2008. Design, synthesis, and actions of a novel chimeric natriuretic peptide: CD-NP. *J Am Coll Cardiol,* 52**,** 60-8.

LIU, W., ZI, M., JIN, J., PREHAR, S., OCEANDY, D., KIMURA, T. E., LEI, M., NEYSES, L., WESTON, A. H., CARTWRIGHT, E. J. & WANG, X. 2009. Cardiac-specific deletion of mkk4 reveals its role in pathological hypertrophic remodeling but not in physiological cardiac growth. *Circ Res,* 104**,** 905-14.

LIVAK, K. J. & SCHMITTGEN, T. D. 2001. Analysis of relative gene expression data using real-time quantitative PCR and the 2(-Delta Delta C(T)) Method. *Methods,* 25**,** 402-8.

LOHMEIER, T. E., MIZELLE, H. L. & REINHART, G. A. 1995. Role of atrial natriuretic peptide in long-term volume homeostasis. *Clin Exp Pharmacol Physiol,* 22**,** 55-61.

LOPEZ, M. J., WONG, S. K., KISHIMOTO, I., DUBOIS, S., MACH, V., FRIESEN, J., GARBERS, D. L. & BEUVE, A. 1995. Salt-resistant hypertension in mice lacking the guanylyl cyclase-A receptor for atrial natriuretic peptide. *Nature,* 378**,** 65-8.

LOSORDO, D. W., ISNER, J. M. & DIAZ-SANDOVAL, L. J. 2003. Endothelial recovery: the next target in restenosis prevention. *Circulation,* 107**,** 2635-7.

LOUKOGEORGAKIS, S. P., WILLIAMS, R., PANAGIOTIDOU, A. T., KOLVEKAR, S. K., DONALD, A., COLE, T. J., YELLON, D. M., DEANFIELD, J. E. & MACALLISTER, R. J. 2007. Transient limb ischemia induces remote preconditioning and remote postconditioning in humans by a K(ATP)-channel dependent mechanism. *Circulation,* 116**,** 1386-95.

LUKSHA, L., AGEWALL, S. & KUBLICKIENE, K. 2009. Endothelium-derived hyperpolarizing factor in vascular physiology and cardiovascular disease. *Atherosclerosis,* 202**,** 330-44.

LUO, J. D., XIE, F., ZHANG, W. W., MA, X. D., GUAN, J. X. & CHEN, X. 2001. Simvastatin inhibits noradrenaline-induced hypertrophy of cultured neonatal rat cardiomyocytes. *Br J Pharmacol,* 132**,** 159-64.

MA, X. L., TSAO, P. S. & LEFER, A. M. 1991. Antibody to CD-18 exerts endothelial and cardiac protective effects in myocardial ischemia and reperfusion. *J Clin Invest,* 88**,** 1237-43.

MADHANI, M., SCOTLAND, R. S., MACALLISTER, R. J. & HOBBS, A. J. 2003. Vascular natriuretic peptide receptor-linked particulate guanylate cyclases are modulated by nitric oxide-cyclic GMP signalling. *Br J Pharmacol,* 139**,** 1289-96.

MADIRAJU, P., HOSSAIN, E. & ANAND-SRIVASTAVA, M. B. 2018. Natriuretic peptide receptor-C activation attenuates angiotensin II-induced enhanced oxidative stress and hyperproliferation of aortic vascular smooth muscle cells. *Mol Cell Biochem*.

MAHJOUB, H., RUSINARU, D., SOULIERE, V., DURIER, C., PELTIER, M. & TRIBOUILLOY, C. 2008. Long-term survival in patients older than 80 years hospitalised for heart failure. A 5-year prospective study. *Eur J Heart Fail,* 10**,** 78-84.

MAISEL, A. S., PHILLIPS, C., MICHEL, M. C., ZIEGLER, M. G. & CARTER, S. M. 1989. Regulation of cardiac beta-adrenergic receptors by captopril. Implications for congestive heart failure. *Circulation,* 80**,** 669-75.

MALMSJO, M., BERGDAHL, A., ZHAO, X. H., SUN, X. Y., HEDNER, T., EDVINSSON, L. & ERLINGE, D. 1999. Enhanced acetylcholine and P2Y-receptor stimulated vascular EDHF-dilatation in congestive heart failure. *Cardiovasc Res,* 43**,** 200-9.

MANABE, I., SHINDO, T. & NAGAI, R. 2002. Gene expression in fibroblasts and fibrosis: involvement in cardiac hypertrophy. *Circ Res,* 91**,** 1103-13.

MARTIN, E. D., BASSI, R. & MARBER, M. S. 2015. p38 MAPK in cardioprotection - are we there yet? *Br J Pharmacol,* 172**,** 2101-13.

MARTINDALE, J. J., WALL, J. A., MARTINEZ-LONGORIA, D. M., ARYAL, P., ROCKMAN, H. A., GUO, Y., BOLLI, R. & GLEMBOTSKI, C. C. 2005. Overexpression of mitogen-activated protein kinase kinase 6 in the heart improves functional recovery from ischemia in vitro and protects against myocardial infarction in vivo. *J Biol Chem,* 280**,** 669-76.

MATSUI, T., LI, L., WU, J. C., COOK, S. A., NAGOSHI, T., PICARD, M. H., LIAO, R. & ROSENZWEIG, A. 2002. Phenotypic spectrum caused by transgenic overexpression of activated Akt in the heart. *J Biol Chem,* 277**,** 22896-901.

MATSUI, T. & ROSENZWEIG, A. 2005. Convergent signal transduction pathways controlling cardiomyocyte survival and function: the role of PI 3-kinase and Akt. *J Mol Cell Cardiol,* 38**,** 63-71.

MATSUKAWA, N., GRZESIK, W. J., TAKAHASHI, N., PANDEY, K. N., PANG, S., YAMAUCHI, M. & SMITHIES, O. 1999. The natriuretic peptide clearance receptor locally modulates the physiological effects of the natriuretic peptide system. *Proc Natl Acad Sci U S A,* 96**,** 7403-8.

MATSUMOTO, T., WADA, A., TSUTAMOTO, T., OMURA, T., YOKOHAMA, H., OHNISHI, M., NAKAE, I., TAKAHASHI, M. & KINOSHITA, M. 1999. Vasorelaxing effects of atrial and brain natriuretic peptides on coronary circulation in heart failure. *Am J Physiol,* 276**,** H1935-42.

MAZZOLAI, L., PEDRAZZINI, T., NICOUD, F., GABBIANI, G., BRUNNER, H. R. & NUSSBERGER, J. 2000. Increased cardiac angiotensin II levels induce right and left ventricular hypertrophy in normotensive mice. *Hypertension,* 35**,** 985-91.

MCCULLOCH, A. I. & RANDALL, M. D. 1998. Sex differences in the relative contributions of nitric oxide and EDHF to agonist-stimulated endothelium-dependent relaxations in the rat isolated mesenteric arterial bed. *Br J Pharmacol,* 123**,** 1700-6.

MCDONALD, K. S. 2011. The interdependence of Ca2+ activation, sarcomere length, and power output in the heart. *Pflugers Arch,* 462**,** 61-7.

MCGETTIGAN, P. & HENRY, D. 2011. Cardiovascular risk with non-steroidal anti-inflammatory drugs: systematic review of population-based controlled observational studies. *PLoS Med,* 8**,** e1001098.

MCGUIRE, J. J., HOLLENBERG, M. D., BENNETT, B. M. & TRIGGLE, C. R. 2004. Hyperpolarization of murine small caliber mesenteric arteries by activation of endothelial proteinase-activated receptor 2. *Can J Physiol Pharmacol,* 82**,** 1103-12.

MCMULLEN, J. R., AMIRAHMADI, F., WOODCOCK, E. A., SCHINKE-BRAUN, M., BOUWMAN, R. D., HEWITT, K. A., MOLLICA, J. P., ZHANG, L., ZHANG, Y., SHIOI, T., BUERGER, A., IZUMO, S., JAY, P. Y. & JENNINGS, G. L. 2007. Protective effects of exercise and phosphoinositide 3-kinase(p110alpha) signaling in dilated and hypertrophic cardiomyopathy. *Proc Natl Acad Sci U S A,* 104**,** 612-7.

MCMULLEN, J. R., SHIOI, T., HUANG, W. Y., ZHANG, L., TARNAVSKI, O., BISPING, E., SCHINKE, M., KONG, S., SHERWOOD, M. C., BROWN, J., RIGGI, L., KANG, P. M. & IZUMO, S. 2004. The insulin-like growth factor 1 receptor induces physiological heart growth via the phosphoinositide 3-kinase(p110alpha) pathway. *J Biol Chem,* 279**,** 4782-93.

MCMULLEN, J. R., SHIOI, T., ZHANG, L., TARNAVSKI, O., SHERWOOD, M. C., KANG, P. M. & IZUMO, S. 2003. Phosphoinositide 3-kinase(p110alpha) plays a critical role for the induction of physiological, but not pathological, cardiac hypertrophy. *Proc Natl Acad Sci U S A,* 100**,** 12355-60.

MCMURRAY, J. J., PACKER, M., DESAI, A. S., GONG, J., LEFKOWITZ, M. P., RIZKALA, A. R., ROULEAU, J. L., SHI, V. C., SOLOMON, S. D., SWEDBERG, K. & ZILE, M. R. 2014. Angiotensin-neprilysin inhibition versus enalapril in heart failure. *N Engl J Med,* 371**,** 993-1004.

MEHEL, H., EMONS, J., VETTEL, C., WITTKOPPER, K., SEPPELT, D., DEWENTER, M., LUTZ, S., SOSSALLA, S., MAIER, L. S., LECHENE, P., LEROY, J., LEFEBVRE, F., VARIN, A., ESCHENHAGEN, T., NATTEL, S., DOBREV, D., ZIMMERMANN, W. H., NIKOLAEV, V. O., VANDECASTEELE, G., FISCHMEISTER, R. & EL-ARMOUCHE, A. 2013. Phosphodiesterase-2 is up-regulated in human failing hearts and blunts beta-adrenergic responses in cardiomyocytes. *J Am Coll Cardiol,* 62**,** 1596-606.

MEIER, S., ANDRESSEN, K. W., ARONSEN, J. M., SJAASTAD, I., HOUGEN, K., SKOMEDAL, T., OSNES, J. B., QVIGSTAD, E., LEVY, F. O. & MOLTZAU, L. R. 2017. PDE3 inhibition by C-type natriuretic peptide-induced cGMP enhances cAMP-mediated signaling in both non-failing and failing hearts. *Eur J Pharmacol*.

MENDE, U., KAGEN, A., COHEN, A., ARAMBURU, J., SCHOEN, F. J. & NEER, E. J. 1998. Transient cardiac expression of constitutively active Galphaq leads to hypertrophy and dilated cardiomyopathy by calcineurin-dependent and independent pathways. *Proc Natl Acad Sci U S A,* 95**,** 13893-8.

MENTZER, R. M., JR., OZ, M. C., SLADEN, R. N., GRAEVE, A. H., HEBELER, R. F., JR., LUBER, J. M., JR., SMEDIRA, N. G. & INVESTIGATORS, N. 2007. Effects of perioperative nesiritide in patients with left ventricular dysfunction undergoing cardiac surgery:the NAPA Trial. *J Am Coll Cardiol,* 49**,** 716-26.

MESSERLI, F. H. & KETELHUT, R. 1991. Left ventricular hypertrophy: an independent risk factor. *J Cardiovasc Pharmacol,* 17 Suppl 4**,** S59-66; discussion S66-7.

METRICH, M., LUCAS, A., GASTINEAU, M., SAMUEL, J. L., HEYMES, C., MOREL, E. & LEZOUALC'H, F. 2008. Epac mediates beta-adrenergic receptor-induced cardiomyocyte hypertrophy. *Circ Res,* 102**,** 959-65.

MEWTON, N., CROISILLE, P., GAHIDE, G., RIOUFOL, G., BONNEFOY, E., SANCHEZ, I., CUNG, T. T., SPORTOUCH, C., ANGOULVANT, D., FINET, G., ANDRE-FOUET, X., DERUMEAUX, G., PIOT, C., VERNHET, H., REVEL, D. & OVIZE, M. 2010. Effect of cyclosporine on left ventricular remodeling after reperfused myocardial infarction. *J Am Coll Cardiol,* 55**,** 1200-5.

MILLS, R. M., LEJEMTEL, T. H., HORTON, D. P., LIANG, C., LANG, R., SILVER, M. A., LUI, C. & CHATTERJEE, K. 1999. Sustained hemodynamic effects of an infusion of nesiritide (human b-type natriuretic peptide) in heart failure: a randomized, double-blind, placebo-controlled clinical trial. Natrecor Study Group. *J Am Coll Cardiol,* 34**,** 155-62.

MIYAZAKI, T., OTANI, K., CHIBA, A., NISHIMURA, H., TOKUDOME, T., WATANABE-TAKANO, H., MATSUO, A., ISHIKAWA, H., SHIMAMOTO, K., FUKUI, H., KANAI, Y., YASODA, A., OGATA, S., NISHIMURA, K., MINAMINO, N. & MOCHIZUKI, N. 2018. A New Secretory Peptide of Natriuretic Peptide Family, Osteocrin, Suppresses the Progression of Congestive Heart Failure After Myocardial Infarction. *Circ Res*.

MOENS, A. L., CHAMPION, H. C., CLAEYS, M. J., TAVAZZI, B., KAMINSKI, P. M., WOLIN, M. S., BORGONJON, D. J., VAN NASSAUW, L., HAILE, A., ZVIMAN, M., BEDJA, D., WUYTS, F. L., ELSAESSER, R. S., COS, P., GABRIELSON, K. L., LAZZARINO, G., PAOLOCCI, N., TIMMERMANS, J. P., VRINTS, C. J. & KASS, D. A. 2008. High-dose folic acid pretreatment blunts cardiac dysfunction during ischemia coupled to maintenance of high-energy phosphates and reduces postreperfusion injury. *Circulation,* 117**,** 1810-9.

MOGHTADAEI, M., LANGILLE, E., RAFFERTY, S. A., BOGACHEV, O. & ROSE, R. A. 2017. Altered heart rate regulation by the autonomic nervous system in mice lacking natriuretic peptide receptor C (NPR-C). *Sci Rep,* 7**,** 17564.

MOLKENTIN, J. D., LU, J. R., ANTOS, C. L., MARKHAM, B., RICHARDSON, J., ROBBINS, J., GRANT, S. R. & OLSON, E. N. 1998. A calcineurin-dependent transcriptional pathway for cardiac hypertrophy. *Cell,* 93**,** 215-28.

MORALES, A. & HERSHBERGER, R. 2017. Clinical Application of Genetic Testing in Heart Failure. *Curr Heart Fail Rep*.

MORGADO, M., CAIRRAO, E., SANTOS-SILVA, A. J. & VERDE, I. 2012. Cyclic nucleotide-dependent relaxation pathways in vascular smooth muscle. *Cell Mol Life Sci,* 69**,** 247-66.

MORI, T., CHEN, Y. F., FENG, J. A., HAYASHI, T., OPARIL, S. & PERRY, G. J. 2004. Volume overload results in exaggerated cardiac hypertrophy in the atrial natriuretic peptide knockout mouse. *Cardiovasc Res,* 61**,** 771-9.

MORIMOTO, H., KAJIKAWA, M., ODA, N., IDEI, N., HIRANO, H., HIDA, E., MARUHASHI, T., IWAMOTO, Y., KISHIMOTO, S., MATSUI, S., AIBARA, Y., HIDAKA, T., KIHARA, Y., CHAYAMA, K., GOTO, C., NOMA, K., NAKASHIMA, A., UKAWA, T., TSUJI, T. & HIGASHI, Y. 2016. Endothelial Function Assessed by Automatic Measurement of Enclosed Zone Flow-Mediated Vasodilation Using an Oscillometric Method Is an Independent Predictor of Cardiovascular Events. *J Am Heart Assoc,* 5.

MORISCO, C., ZEBROWSKI, D., CONDORELLI, G., TSICHLIS, P., VATNER, S. F. & SADOSHIMA, J. 2000. The Akt-glycogen synthase kinase 3beta pathway regulates transcription of atrial natriuretic factor induced by beta-adrenergic receptor stimulation in cardiac myocytes. *J Biol Chem,* 275**,** 14466-75.

MORISCO, C., ZEBROWSKI, D. C., VATNER, D. E., VATNER, S. F. & SADOSHIMA, J. 2001. Beta-adrenergic cardiac hypertrophy is mediated primarily by the beta(1)-subtype in the rat heart. *J Mol Cell Cardiol,* 33**,** 561-73.

MORISHIGE, K., SHIMOKAWA, H., YAMAWAKI, T., MIYATA, K., ETO, Y., KANDABASHI, T., YOGO, K., HIGO, T., EGASHIRA, K., UENO, H. & TAKESHITA, A. 2000. Local adenovirus-mediated transfer of C-type natriuretic peptide suppresses vascular remodeling in porcine coronary arteries in vivo. *J Am Coll Cardiol,* 35**,** 1040-7.

MOUAWAD, R., LI, Y. & ANAND-SRIVASTAVA, M. B. 2004. Atrial natriuretic peptide-C receptor-induced attenuation of adenylyl cyclase signaling activates phosphatidylinositol turnover in A10 vascular smooth muscle cells. *Mol Pharmacol,* 65**,** 917-24.

MOYES, A. J., KHAMBATA, R. S., VILLAR, I., BUBB, K. J., BALIGA, R. S., LUMSDEN, N. G., XIAO, F., GANE, P. J., REBSTOCK, A. S., WORTHINGTON, R. J., SIMONE, M. I., MOTA, F., RIVILLA, F., VALLEJO, S., PEIRO, C., SANCHEZ FERRER, C. F., DJORDJEVIC, S., CAULFIELD, M. J., MACALLISTER, R. J., SELWOOD, D. L., AHLUWALIA, A. & HOBBS, A. J. 2014. Endothelial C-type natriuretic peptide maintains vascular homeostasis. *J Clin Invest,* 124**,** 4039-51.

MUKHERJEE, D., NISSEN, S. E. & TOPOL, E. J. 2001. Risk of cardiovascular events associated with selective COX-2 inhibitors. *Jama,* 286**,** 954-9.

MURTHY, K. S., TENG, B. Q., ZHOU, H., JIN, J. G., GRIDER, J. R. & MAKHLOUF, G. M. 2000. G(i-1)/G(i-2)-dependent signaling by single-transmembrane natriuretic peptide clearance receptor. *Am J Physiol Gastrointest Liver Physiol,* 278**,** G974-80.

MUTHURAMU, I., LOX, M., JACOBS, F. & DE GEEST, B. 2014. Permanent ligation of the left anterior descending coronary artery in mice: a model of post-myocardial infarction remodelling and heart failure. *J Vis Exp*.

NAGAYAMA, T., HSU, S., ZHANG, M., KOITABASHI, N., BEDJA, D., GABRIELSON, K. L., TAKIMOTO, E. & KASS, D. A. 2009. Sildenafil stops progressive chamber, cellular, and molecular remodeling and improves calcium handling and function in hearts with pre-existing advanced hypertrophy caused by pressure overload. *J Am Coll Cardiol,* 53**,** 207-15.

NAHRENDORF, M. & SWIRSKI, F. K. 2013. Monocyte and macrophage heterogeneity in the heart. *Circ Res,* 112**,** 1624-33.

NAKAMURA, M., ARAKAWA, N., YOSHIDA, H., MAKITA, S. & HIRAMORI, K. 1994. Vasodilatory effects of C-type natriuretic peptide on forearm resistance vessels are distinct from those of atrial natriuretic peptide in chronic heart failure. *Circulation,* 90**,** 1210-4.

NAKAMURA, T. Y., IWATA, Y., ARAI, Y., KOMAMURA, K. & WAKABAYASHI, S. 2008. Activation of Na+/H+ exchanger 1 is sufficient to generate Ca2+ signals that induce cardiac hypertrophy and heart failure. *Circ Res,* 103**,** 891-9.

NAKAO, K., KUWAHARA, K., NISHIKIMI, T., NAKAGAWA, Y., KINOSHITA, H., MINAMI, T., KUWABARA, Y., YAMADA, C., YAMADA, Y., TOKUDOME, T., NAGAI-OKATANI, C., MINAMINO, N., NAKAO, Y. M., YASUNO, S., UESHIMA, K., SONE, M., KIMURA, T., KANGAWA, K. & NAKAO, K. 2017. Endothelium-

Derived C-Type Natriuretic Peptide Contributes to Blood Pressure Regulation by Maintaining Endothelial Integrity. *Hypertension*.

NAKAO, K., MINOBE, W., RODEN, R., BRISTOW, M. R. & LEINWAND, L. A. 1997. Myosin heavy chain gene expression in human heart failure. *J Clin Invest,* 100**,** 2362-70.

NAKAO, K., NAKAO, K., KUWAHARA, K. & KANGAWA, K. 2015. Implication of C-type natriuretic peptide derived from vascular endothelial cells on blood pressure regulation. *BMC Pharmacol Toxicol,* 16**,** A28.

NARUKO, T., UEDA, M., VAN DER WAL, A. C., VAN DER LOOS, C. M., ITOH, H., NAKAO, K. & BECKER, A. E. 1996. C-type natriuretic peptide in human coronary atherosclerotic lesions. *Circulation,* 94**,** 3103-8.

NAUMOVA, A. V., CHACKO, V. P., OUWERKERK, R., STULL, L., MARBAN, E. & WEISS, R. G. 2006. Xanthine oxidase inhibitors improve energetics and function after infarction in failing mouse hearts. *Am J Physiol Heart Circ Physiol,* 290**,** H837-43.

NAZARIO, B., HU, R. M., PEDRAM, A., PRINS, B. & LEVIN, E. R. 1995. Atrial and brain natriuretic peptides stimulate the production and secretion of C-type natriuretic peptide from bovine aortic endothelial cells. *J Clin Invest,* 95**,** 1151-7.

NEWBY, L. K., MARBER, M. S., MELLONI, C., SAROV-BLAT, L., ABERLE, L. H., AYLWARD, P. E., CAI, G., DE WINTER, R. J., HAMM, C. W., HEITNER, J. F., KIM, R., LERMAN, A., PATEL, M. R., TANGUAY, J. F., LEPORE, J. J., AL-KHALIDI, H. R., SPRECHER, D. L. & GRANGER, C. B. 2014. Losmapimod, a novel p38 mitogen-activated protein kinase inhibitor, in non-ST-segment elevation myocardial infarction: a randomised phase 2 trial. *Lancet,* 384**,** 1187-95.

NICHTOVA, Z., NOVOTOVA, M., KRALOVA, E. & STANKOVICOVA, T. 2012. Morphological and functional characteristics of models of experimental myocardial injury induced by isoproterenol. *Gen Physiol Biophys,* 31**,** 141-51.

NIR, A., ZHANG, D. F., FIXLER, R., BURNETT, J. C., JR., EILAM, Y. & HASIN, Y. 2001. C-type natriuretic peptide has a negative inotropic effect on cardiac myocytes. *Eur J Pharmacol,* 412**,** 195-201.

NISHIDA, K., YAMAGUCHI, O., HIROTANI, S., HIKOSO, S., HIGUCHI, Y., WATANABE, T., TAKEDA, T., OSUKA, S., MORITA, T., KONDOH, G., UNO, Y., KASHIWASE, K., TANIIKE, M., NAKAI, A., MATSUMURA, Y., MIYAZAKI, J., SUDO, T., HONGO, K., KUSAKARI, Y., KURIHARA, S., CHIEN, K. R., TAKEDA, J., HORI, M. & OTSU, K. 2004. p38alpha mitogen-activated protein kinase plays a critical role in cardiomyocyte survival but not in cardiac hypertrophic growth in response to pressure overload. *Mol Cell Biol,* 24**,** 10611-20.

NOORDALI, H., LOUDON, B. L., FRENNEAUX, M. P. & MADHANI, M. 2018. Cardiac metabolism - A promising therapeutic target for heart failure. *Pharmacol Ther,* 182**,** 95-114.

NUSSENZVEIG, D. R., LEWICKI, J. A. & MAACK, T. 1990. Cellular mechanisms of the clearance function of type C receptors of atrial natriuretic factor. *J Biol Chem,* 265**,** 20952-8.

O'CONNOR, C. M., STARLING, R. C., HERNANDEZ, A. F., ARMSTRONG, P. W., DICKSTEIN, K., HASSELBLAD, V., HEIZER, G. M., KOMAJDA, M., MASSIE, B. M., MCMURRAY, J. J., NIEMINEN, M. S., REIST, C. J., ROULEAU, J. L., SWEDBERG, K., ADAMS, K. F., JR., ANKER, S. D., ATAR, D., BATTLER, A., BOTERO, R., BOHIDAR, N. R., BUTLER, J., CLAUSELL, N., CORBALAN, R., COSTANZO, M. R., DAHLSTROM, U., DECKELBAUM, L. I., DIAZ, R., DUNLAP, M. E., EZEKOWITZ, J. A., FELDMAN, D., FELKER, G. M., FONAROW, G. C., GENNEVOIS, D., GOTTLIEB, S. S., HILL, J. A., HOLLANDER, J. E., HOWLETT, J. G., HUDSON, M. P., KOCIOL, R. D., KRUM, H., LAUCEVICIUS, A., LEVY, W. C., MENDEZ, G. F., METRA, M., MITTAL, S., OH, B. H., PEREIRA, N. L., PONIKOWSKI, P., TANG, W. H., TANOMSUP, S., TEERLINK, J. R., TRIPOSKIADIS, F., TROUGHTON, R. W., VOORS, A. A., WHELLAN, D. J., ZANNAD, F. & CALIFF, R. M. 2011. Effect of nesiritide in patients with acute decompensated heart failure. *N Engl J Med,* 365**,** 32-43.

OBATA, H., YANAGAWA, B., TANAKA, K., OHNISHI, S., KATAOKA, M., MIYAHARA, Y., ISHIBASHI-UEDA, H., KODAMA, M., AIZAWA, Y., KANGAWA, K. & NAGAYA, N. 2007. CNP infusion attenuates cardiac dysfunction and inflammation in myocarditis. *Biochem Biophys Res Commun,* 356**,** 60-6.

OCKAILI, R., SALLOUM, F., HAWKINS, J. & KUKREJA, R. C. 2002. Sildenafil (Viagra) induces powerful cardioprotective effect via opening of mitochondrial K(ATP) channels in rabbits. *Am J Physiol Heart Circ Physiol,* 283**,** H1263-9.

OGAWA, H., QIU, Y., OGATA, C. M. & MISONO, K. S. 2004. Crystal structure of hormone-bound atrial natriuretic peptide receptor extracellular domain: rotation mechanism for transmembrane signal transduction. *J Biol Chem,* 279**,** 28625-31.

OGAWA, Y., NAKAO, K., NAKAGAWA, O., KOMATSU, Y., HOSODA, K., SUGA, S., ARAI, H., NAGATA, K., YOSHIDA, N. & IMURA, H. 1992. Human C-type natriuretic peptide. Characterization of the gene and peptide. *Hypertension,* 19**,** 809-13.

OHNO, N., ITOH, H., IKEDA, T., UEYAMA, K., YAMAHARA, K., DOI, K., YAMASHITA, J., INOUE, M., MASATSUGU, K., SAWADA, N., FUKUNAGA, Y., SAKAGUCHI, S., SONE, M., YURUGI, T., KOOK, H., KOMEDA, M. & NAKAO, K. 2002. Accelerated reendothelialization with suppressed thrombogenic property and neointimal hyperplasia of rabbit jugular vein grafts by adenovirus-mediated gene transfer of C-type natriuretic peptide. *Circulation,* 105**,** 1623-6.

OKAHARA, K., KAMBAYASHI, J., OHNISHI, T., FUJIWARA, Y., KAWASAKI, T. & MONDEN, M. 1995. Shear stress induces expression of CNP gene in human endothelial cells. *FEBS Lett,* 373**,** 108-10.

OKAWA, H., HORIMOTO, H., MIENO, S., NOMURA, Y., YOSHIDA, M. & SHINJIRO, S. 2003. Preischemic infusion of alpha-human atrial natriuretic peptide elicits myoprotective effects against ischemia reperfusion in isolated rat hearts. *Mol Cell Biochem,* 248**,** 171-7.

OLIVER, P. M., FOX, J. E., KIM, R., ROCKMAN, H. A., KIM, H. S., REDDICK, R. L., PANDEY, K. N., MILGRAM, S. L., SMITHIES, O. & MAEDA, N. 1997. Hypertension, cardiac hypertrophy, and sudden death in mice lacking natriuretic peptide receptor A. *Proc Natl Acad Sci U S A,* 94**,** 14730-5.

ONO, K., MANNAMI, T., BABA, S., TOMOIKE, H., SUGA, S. & IWAI, N. 2002. A single-nucleotide polymorphism in C-type natriuretic peptide gene may be associated with hypertension. *Hypertens Res,* 25**,** 727-30.

OSADCHII, O. E. 2007. Cardiac hypertrophy induced by sustained beta-adrenoreceptor activation: pathophysiological aspects. *Heart Fail Rev,* 12**,** 66-86.

OTTANI, F., LATINI, R., STASZEWSKY, L., LA VECCHIA, L., LOCURATOLO, N., SICURO, M., MASSON, S., BARLERA, S., MILANI, V., LOMBARDI, M., COSTALUNGA, A., MOLLICHELLI, N., SANTARELLI, A., DE CESARE, N., SGANZERLA, P., BOI, A., MAGGIONI, A. P. & LIMBRUNO, U. 2016. Cyclosporine A in Reperfused Myocardial Infarction: The Multicenter, Controlled, Open-Label CYCLE Trial. *J Am Coll Cardiol,* 67**,** 365-374.

OUDIT, G. Y., CRACKOWER, M. A., ERIKSSON, U., SARAO, R., KOZIERADZKI, I., SASAKI, T., IRIE-SASAKI, J., GIDREWICZ, D., RYBIN, V. O., WADA, T., STEINBERG, S. F., BACKX, P. H. & PENNINGER, J. M. 2003. Phosphoinositide 3-kinase gamma-deficient mice are protected from isoproterenol-induced heart failure. *Circulation,* 108**,** 2147-52.

OZAKI, M., KAWASHIMA, S., YAMASHITA, T., HIRASE, T., OHASHI, Y., INOUE, N., HIRATA, K. & YOKOYAMA, M. 2002. Overexpression of endothelial nitric oxide synthase attenuates cardiac hypertrophy induced by chronic isoproterenol infusion. *Circ J,* 66**,** 851-6.

PACKER, M. 1992. The neurohormonal hypothesis: a theory to explain the mechanism of disease progression in heart failure. *J Am Coll Cardiol,* 20**,** 248-54.

PADILLA, F., GARCIA-DORADO, D., AGULLO, L., BARRABES, J. A., INSERTE, J., ESCALONA, N., MEYER, M., MIRABET, M., PINA, P. & SOLER-SOLER, J. 2001. Intravenous administration of the natriuretic peptide urodilatin at low doses during coronary reperfusion limits infarct size in anesthetized pigs. *Cardiovasc Res,* 51**,** 592-600.

PAGANO, M. & ANAND-SRIVASTAVA, M. B. 2001. Cytoplasmic domain of natriuretic peptide receptor C constitutes Gi activator sequences that inhibit adenylyl cyclase activity. *J Biol Chem,* 276**,** 22064-70.

PAGEL-LANGENICKEL, I., BUTTGEREIT, J., BADER, M. & LANGENICKEL, T. H. 2007. Natriuretic peptide receptor B signaling in the cardiovascular system: protection from cardiac hypertrophy. *J Mol Med (Berl),* 85**,** 797-810.

PALAZZO, A. J., JONES, S. P., ANDERSON, D. C., GRANGER, D. N. & LEFER, D. J. 1998. Coronary endothelial P-selectin in pathogenesis of myocardial ischemia-reperfusion injury. *Am J Physiol,* 275**,** H1865-72.

PALMER, R. M., FERRIGE, A. G. & MONCADA, S. 1987. Nitric oxide release accounts for the biological activity of endothelium-derived relaxing factor. *Nature,* 327**,** 524-6.

PANDEY, K. N. 2011. Guanylyl cyclase / atrial natriuretic peptide receptor-A: role in the pathophysiology of cardiovascular regulation. *Can J Physiol Pharmacol,* 89**,** 557-73.

PATTEN, R. D. & HALL-PORTER, M. R. 2009. Small Animal Models of Heart Failure: Development of Novel Therapies, Past and Present. *Circulation: Heart Failure,* 2**,** 138-144.

PELISEK, J., FUCHS, A. T., KUEHNL, A., TIAN, W., KUHLMANN, M. T., ROLLAND, P. H., MEKKAOUI, C., GAEDTKE, L. & NIKOL, S. 2006. C-type natriuretic peptide for reduction of restenosis: gene transfer is superior over single peptide administration. *J Gene Med,* 8**,** 835-44.

PETRICH, B. G., ELOFF, B. C., LERNER, D. L., KOVACS, A., SAFFITZ, J. E., ROSENBAUM, D. S. & WANG, Y. 2004. Targeted activation of c-Jun N-terminal kinase in vivo induces restrictive cardiomyopathy and conduction defects. *J Biol Chem,* 279**,** 15330-8.

PFEIFER, A., NURNBERG, B., KAMM, S., UHDE, M., SCHULTZ, G., RUTH, P. & HOFMANN, F. 1995. Cyclic GMP-dependent protein kinase blocks pertussis toxin-sensitive hormone receptor signaling pathways in Chinese hamster ovary cells. *J Biol Chem,* 270**,** 9052-9.

PHILLIPS, L., TOLEDO, A. H., LOPEZ-NEBLINA, F., ANAYA-PRADO, R. & TOLEDO-PEREYRA, L. H. 2009. Nitric oxide mechanism of protection in ischemia and reperfusion injury. *J Invest Surg,* 22**,** 46-55.

PIERKES, M., GAMBARYAN, S., BOKNIK, P., LOHMANN, S. M., SCHMITZ, W., POTTHAST, R., HOLTWICK, R. & KUHN, M. 2002. Increased effects of C-type natriuretic peptide on cardiac ventricular contractility and relaxation in guanylyl cyclase A-deficient mice. *Cardiovasc Res,* 53**,** 852-61.

PIOT, C., CROISILLE, P., STAAT, P., THIBAULT, H., RIOUFOL, G., MEWTON, N., ELBELGHITI, R., CUNG, T. T., BONNEFOY, E., ANGOULVANT, D., MACIA, C., RACZKA, F., SPORTOUCH, C., GAHIDE, G., FINET, G., ANDRE-FOUET, X., REVEL, D., KIRKORIAN, G., MONASSIER, J. P., DERUMEAUX, G. & OVIZE, M. 2008. Effect of cyclosporine on reperfusion injury in acute myocardial infarction. *N Engl J Med,* 359**,** 473-81.

PIPER, H. M., GARCIA-DORADO, D. & OVIZE, M. 1998. A fresh look at reperfusion injury. *Cardiovasc Res,* 38**,** 291-300.

PIPER, H. M., MEUTER, K. & SCHAFER, C. 2003. Cellular mechanisms of ischemia-reperfusion injury. *Ann Thorac Surg,* 75**,** S644-8.

PONCELET, A. C. & SCHNAPER, H. W. 2001. Sp1 and Smad proteins cooperate to mediate transforming growth factor-beta 1-induced alpha 2(I) collagen expression in human glomerular mesangial cells. *J Biol Chem,* 276**,** 6983-92.

POTTER, L. R. 2011a. Guanylyl cyclase structure, function and regulation. *Cell Signal,* 23**,** 1921-6.

POTTER, L. R. 2011b. Natriuretic peptide metabolism, clearance and degradation. *FEBS J,* 278**,** 1808-17.

POTTER, L. R., ABBEY-HOSCH, S. & DICKEY, D. M. 2006. Natriuretic peptides, their receptors, and cyclic guanosine monophosphate-dependent signaling functions. *Endocr Rev,* 27**,** 47-72.

POTTER, L. R., YODER, A. R., FLORA, D. R., ANTOS, L. K. & DICKEY, D. M. 2009. Natriuretic peptides: their structures, receptors, physiologic functions and therapeutic applications. *Handb Exp Pharmacol***,** 341-66.

POWERS, S. K., MURLASITS, Z., WU, M. & KAVAZIS, A. N. 2007. Ischemia-reperfusion-induced cardiac injury: a brief review. *Med Sci Sports Exerc,* 39**,** 1529-36.

PUETT, D. W., FORMAN, M. B., CATES, C. U., WILSON, B. H., HANDE, K. R., FRIESINGER, G. C. & VIRMANI, R. 1987. Oxypurinol limits myocardial stunning but does not reduce infarct size after reperfusion. *Circulation,* 76**,** 678-86.

QIU, Y. & HEARSE, D. J. 1992. Comparison of ischemic vulnerability and responsiveness to cardioplegic protection in crystalloid-perfused versus blood-perfused hearts. *J Thorac Cardiovasc Surg,* 103**,** 960-8.

QVIGSTAD, E., MOLTZAU, L. R., ARONSEN, J. M., NGUYEN, C. H., HOUGEN, K., SJAASTAD, I., LEVY, F. O., SKOMEDAL, T. & OSNES, J. B. 2010. Natriuretic peptides increase beta1-adrenoceptor signalling in failing hearts through phosphodiesterase 3 inhibition. *Cardiovasc Res,* 85**,** 763-72.

RAHALI, S., LI, Y. & ANAND-SRIVASTAVA, M. B. 2018. Contribution of oxidative stress and growth factor receptor transactivation in natriuretic peptide receptor C-mediated attenuation of hyperproliferation of vascular smooth muscle cells from SHR. *PLoS One,* 13**,** e0191743.

RAJENDRAN, P., RENGARAJAN, T., THANGAVEL, J., NISHIGAKI, Y., SAKTHISEKARAN, D., SETHI, G. & NISHIGAKI, I. 2013. The vascular endothelium and human diseases. *Int J Biol Sci,* 9**,** 1057-69.

RASTEGAR, M. A., VEGH, A., PAPP, J. G. & PARRATT, J. R. 2000. Atrial natriuretic peptide reduces the severe consequences of coronary artery occlusion in anaesthetized dogs. *Cardiovasc Drugs Ther,* 14**,** 471-9.

REDFIELD, M. M., CHEN, H. H., BORLAUG, B. A., SEMIGRAN, M. J., LEE, K. L., LEWIS, G., LEWINTER, M. M., ROULEAU, J. L., BULL, D. A., MANN, D. L., DESWAL, A., STEVENSON, L. W., GIVERTZ, M. M., OFILI, E. O., O'CONNOR, C. M., FELKER, G. M., GOLDSMITH, S. R., BART, B. A., MCNULTY, S. E., IBARRA, J. C., LIN,

G., OH, J. K., PATEL, M. R., KIM, R. J., TRACY, R. P., VELAZQUEZ, E. J., ANSTROM, K. J., HERNANDEZ, A. F., MASCETTE, A. M., BRAUNWALD, E. & TRIAL, R. 2013. Effect of phosphodiesterase-5 inhibition on exercise capacity and clinical status in heart failure with preserved ejection fraction: a randomized clinical trial. *JAMA,* 309**,** 1268-77.

REN, J., ZHANG, S., KOVACS, A., WANG, Y. & MUSLIN, A. J. 2005. Role of p38alpha MAPK in cardiac apoptosis and remodeling after myocardial infarction. *J Mol Cell Cardiol,* 38**,** 617-23.

REN, M., NG, F. L., WARREN, H., WITKOWSKA, K., BARON, M., JIA, Z., CABRERA, C., ZHANG, R., MIFSUD, B., MUNROE, P. B., XIAO, Q., TOWNSEND-NICHOLSON, A., HOBBS, A., YE, S. & CAULFIELD, M. 2017. The biological impact of blood pressure associated genetic variants in the natriuretic peptide receptor C gene on human vascular smooth muscle. *Hum Mol Genet*.

ROCKMAN, H. A., ROSS, R. S., HARRIS, A. N., KNOWLTON, K. U., STEINHELPER, M. E., FIELD, L. J., ROSS, J., JR. & CHIEN, K. R. 1991. Segregation of atrial-specific and inducible expression of an atrial natriuretic factor transgene in an in vivo murine model of cardiac hypertrophy. *Proc Natl Acad Sci U S A,* 88**,** 8277-81.

ROGERS, J. H., TAMIRISA, P., KOVACS, A., WEINHEIMER, C., COURTOIS, M., BLUMER, K. J., KELLY, D. P. & MUSLIN, A. J. 1999. RGS4 causes increased mortality and reduced cardiac hypertrophy in response to pressure overload. *J Clin Invest,* 104**,** 567-76.

ROGERS, J. H., TSIRKA, A., KOVACS, A., BLUMER, K. J., DORN, G. W., 2ND & MUSLIN, A. J. 2001. RGS4 reduces contractile dysfunction and hypertrophic gene induction in Galpha q overexpressing mice. *J Mol Cell Cardiol,* 33**,** 209-18.

ROMAN, B. B., GEENEN, D. L., LEITGES, M. & BUTTRICK, P. M. 2001. PKC-beta is not necessary for cardiac hypertrophy. *Am J Physiol Heart Circ Physiol,* 280**,** H2264-70.

RONA, G., CHAPPEL, C. I., BALAZS, T. & GAUDRY, R. 1959. An infarct-like myocardial lesion and other toxic manifestations produced by isoproterenol in the rat. *AMA Arch Pathol,* 67**,** 443-55.

ROSE, R. A. & GILES, W. R. 2008. Natriuretic peptide C receptor signalling in the heart and vasculature. *J Physiol,* 586**,** 353-66.

ROSE, R. A., LOMAX, A. E., KONDO, C. S., ANAND-SRIVASTAVA, M. B. & GILES, W. R. 2004. Effects of C-type natriuretic peptide on ionic currents in mouse sinoatrial node: a role for the NPR-C receptor. *Am J Physiol Heart Circ Physiol,* 286**,** H1970-7.

ROSENKRANZ, A. C., WOODS, R. L., DUSTING, G. J. & RITCHIE, R. H. 2003. Antihypertrophic actions of the natriuretic peptides in adult rat cardiomyocytes: importance of cyclic GMP. *Cardiovasc Res,* 57**,** 515-22.

ROSENKRANZ, S. 2004. TGF-beta1 and angiotensin networking in cardiac remodeling. *Cardiovasc Res,* 63**,** 423-32.

ROSENKRANZ, S., FLESCH, M., AMANN, K., HAEUSELER, C., KILTER, H., SEELAND, U., SCHLUTER, K. D. & BOHM, M. 2002. Alterations of beta-adrenergic signaling and cardiac hypertrophy in transgenic mice overexpressing TGF-beta(1). *Am J Physiol Heart Circ Physiol,* 283**,** H1253-62.

RUAN, H., MITCHELL, S., VAINORIENE, M., LOU, Q., XIE, L. H., REN, S., GOLDHABER, J. I. & WANG, Y. 2007. Gi alpha 1-mediated cardiac electrophysiological remodeling and arrhythmia in hypertrophic cardiomyopathy. *Circulation,* 116**,** 596-605.

RUBATTU, S., CALVIERI, C., PAGLIARO, B. & VOLPE, M. 2013. Atrial natriuretic peptide and regulation of vascular function in hypertension and heart failure: implications for novel therapeutic strategies. *J Hypertens,* 31**,** 1061-72.

RUSKOAHO, H. 1992. Atrial natriuretic peptide: synthesis, release, and metabolism. *Pharmacol Rev,* 44**,** 479-602.

RUSNAK, J. M., KOPECKY, S. L., CLEMENTS, I. P., GIBBONS, R. J., HOLLAND, A. E., PETERMAN, H. S., MARTIN, J. S., SAOUD, J. B., FELDMAN, R. L., BREISBLATT, W. M., SIMONS, M., GESSLER, C. J., JR. & YU, A. S. 2001. An anti-CD11/CD18 monoclonal antibody in patients with acute myocardial infarction having percutaneous transluminal coronary angioplasty (the FESTIVAL study). *Am J Cardiol,* 88**,** 482-7.

SABBAH, H. N., SHAROV, V. G., LESCH, M. & GOLDSTEIN, S. 1995. Progression of heart failure: a role for interstitial fibrosis. *Mol Cell Biochem,* 147**,** 29-34.

SABBATINI, M. E., VATTA, M. S., DAVIO, C. A. & BIANCIOTTI, L. G. 2007. Atrial natriuretic factor negatively modulates secretin intracellular signaling in the exocrine pancreas. *Am J Physiol Gastrointest Liver Physiol,* 292**,** G349-57.

SACKNER-BERNSTEIN, J. D., SKOPICKI, H. A. & AARONSON, K. D. 2005. Risk of worsening renal function with nesiritide in patients with acutely decompensated heart failure. *Circulation,* 111**,** 1487-91.

SADOSHIMA, J., MONTAGNE, O., WANG, Q., YANG, G., WARDEN, J., LIU, J., TAKAGI, G., KAROOR, V., HONG, C., JOHNSON, G. L., VATNER, D. E. & VATNER, S. F. 2002. The MEKK1-JNK pathway plays a protective role in pressure overload but does not mediate cardiac hypertrophy. *J Clin Invest,* 110**,** 271-9.

SAITO, T., FUKUZAWA, J., OSAKI, J., SAKURAGI, H., YAO, N., HANEDA, T., FUJINO, T., WAKAMIYA, N., KIKUCHI, K. & HASEBE, N. 2003. Roles of calcineurin and calcium/calmodulin-dependent protein kinase II in pressure overload-induced cardiac hypertrophy. *J Mol Cell Cardiol,* 35**,** 1153-60.

SAITO, Y. 2010. Roles of atrial natriuretic peptide and its therapeutic use. *J Cardiol,* 56**,** 262-70.

SAITO, Y., NAKAO, K., ITOH, H., YAMADA, T., MUKOYAMA, M., ARAI, H., HOSODA, K., SHIRAKAMI, G., SUGA, S., MINAMINO, N. & ET AL. 1989. Brain natriuretic peptide is a novel cardiac hormone. *Biochem Biophys Res Commun,* 158**,** 360-8.

SAKATA, Y., HOIT, B. D., LIGGETT, S. B., WALSH, R. A. & DORN, G. W., 2ND 1998. Decompensation of pressure-overload hypertrophy in G alpha q-overexpressing mice. *Circulation,* 97**,** 1488-95.

SANDERSON, J. E., LAI, K. B., SHUM, I. O., WEI, S. & CHOW, L. T. 2001. Transforming growth factor-beta(1) expression in dilated cardiomyopathy. *Heart,* 86**,** 701-8.

SANGARALINGHAM, S. J., BURNETT, J. C., JR., MCKIE, P. M., SCHIRGER, J. A. & CHEN, H. H. 2013. Rationale and design of a randomized, double-blind, placebo-controlled clinical trial to evaluate the efficacy of B-type natriuretic peptide for the preservation of left ventricular function after anterior myocardial infarction. *J Card Fail,* 19**,** 533-9.

SANGARALINGHAM, S. J., HUNTLEY, B. K., MARTIN, F. L., MCKIE, P. M., BELLAVIA, D., ICHIKI, T., HARDERS, G. E., CHEN, H. H. & BURNETT, J. C., JR. 2011. The aging heart, myocardial fibrosis, and its relationship to circulating C-type natriuretic Peptide. *Hypertension,* 57**,** 201-7.

SANO, Y., HARADA, J., TASHIRO, S., GOTOH-MANDEVILLE, R., MAEKAWA, T. & ISHII, S. 1999. ATF-2 is a common nuclear target of Smad and TAK1 pathways in transforming growth factor-beta signaling. *J Biol Chem,* 274**,** 8949-57.

SCHAFER, C., LADILOV, Y., INSERTE, J., SCHAFER, M., HAFFNER, S., GARCIA-DORADO, D. & PIPER, H. M. 2001. Role of the reverse mode of the Na+/Ca2+ exchanger in reoxygenation-induced cardiomyocyte injury. *Cardiovasc Res,* 51**,** 241-50.

SCHAFER, S., VISWANATHAN, S., WIDJAJA, A. A., LIM, W. W., MORENO-MORAL, A., DELAUGHTER, D. M., NG, B., PATONE, G., CHOW, K., KHIN, E., TAN, J., CHOTHANI, S. P., YE, L., RACKHAM, O. J. L., KO, N. S. J., SAHIB, N. E., PUA, C. J., ZHEN, N. T. G., XIE, C., WANG, M., MAATZ, H., LIM, S., SAAR, K., BLACHUT, S., PETRETTO, E., SCHMIDT, S., PUTOCZKI, T., GUIMARAES-CAMBOA, N., WAKIMOTO, H., VAN HEESCH, S., SIGMUNDSSON, K., LIM, S. L., SOON, J. L., CHAO, V. T. T., CHUA, Y. L., TAN, T. E., EVANS, S. M., LOH, Y. J., JAMAL, M. H., ONG, K. K., CHUA, K. C., ONG, B. H., CHAKARAMAKKIL, M. J., SEIDMAN, J. G., SEIDMAN, C. E., HUBNER, N., SIN, K. Y. K. & COOK, S. A. 2017. IL-11 is a crucial determinant of cardiovascular fibrosis. *Nature,* 552**,** 110-115.

SCHMEDTJE, J. F., JR., JI, Y. S., LIU, W. L., DUBOIS, R. N. & RUNGE, M. S. 1997. Hypoxia induces cyclooxygenase-2 via the NF-kappaB p65 transcription factor in human vascular endothelial cells. *J Biol Chem,* 272**,** 601-8.

SCHMIDT, C. M., MCKILLOP, I. H., CAHILL, P. A. & SITZMANN, J. V. 1999. The role of cAMP-MAPK signalling in the regulation of human hepatocellular carcinoma growth in vitro. *Eur J Gastroenterol Hepatol,* 11**,** 1393-9.

SCHNEIDER, S., CHEN, W., HOU, J., STEENBERGEN, C. & MURPHY, E. 2001. Inhibition of p38 MAPK alpha/beta reduces ischemic injury and does not block protective effects of preconditioning. *Am J Physiol Heart Circ Physiol,* 280**,** H499-508.

SCHULZ, R., KELM, M. & HEUSCH, G. 2004. Nitric oxide in myocardial ischemia/reperfusion injury. *Cardiovasc Res,* 61**,** 402-13.

SCHWINGER, R. H., MUNCH, G., BOLCK, B., KARCZEWSKI, P., KRAUSE, E. G. & ERDMANN, E. 1999. Reduced Ca(2+)-sensitivity of SERCA 2a in failing human myocardium due to reduced serin-16 phospholamban phosphorylation. *J Mol Cell Cardiol,* 31**,** 479-91.

SCOTLAND, R. S., MADHANI, M., CHAUHAN, S., MONCADA, S., ANDRESEN, J., NILSSON, H., HOBBS, A. J. & AHLUWALIA, A. 2005. Investigation of vascular responses in endothelial nitric oxide

synthase/cyclooxygenase-1 double-knockout mice: key role for endothelium-derived hyperpolarizing factor in the regulation of blood pressure in vivo. *Circulation,* 111**,** 796-803.

SEE, F., THOMAS, W., WAY, K., TZANIDIS, A., KOMPA, A., LEWIS, D., ITESCU, S. & KRUM, H. 2004. p38 mitogen-activated protein kinase inhibition improves cardiac function and attenuates left ventricular remodeling following myocardial infarction in the rat. *J Am Coll Cardiol,* 44**,** 1679-89.

SELEMIDIS, S. & COCKS, T. M. 2002. Endothelium-dependent hyperpolarization as a remote anti-atherogenic mechanism. *Trends Pharmacol Sci,* 23**,** 213-20.

SENZAKI, H., SMITH, C. J., JUANG, G. J., ISODA, T., MAYER, S. P., OHLER, A., PAOLOCCI, N., TOMASELLI, G. F., HARE, J. M. & KASS, D. A. 2001. Cardiac phosphodiesterase 5 (cGMP-specific) modulates beta-adrenergic signaling in vivo and is down-regulated in heart failure. *Faseb j,* 15**,** 1718-26.

SHIMOKAWA, H., YASUTAKE, H., FUJII, K., OWADA, M. K., NAKAIKE, R., FUKUMOTO, Y., TAKAYANAGI, T., NAGAO, T., EGASHIRA, K., FUJISHIMA, M. & TAKESHITA, A. 1996. The importance of the hyperpolarizing mechanism increases as the vessel size decreases in endothelium-dependent relaxations in rat mesenteric circulation. *J Cardiovasc Pharmacol,* 28**,** 703-11.

SHINOMIYA, M., TASHIRO, J., SAITO, Y., YOSHIDA, S., FURUYA, M., OKA, N., TANAKA, S., KANGAWA, K. & MATSUO, H. 1994. C-type natriuretic peptide inhibits intimal thickening of rabbit carotid artery after balloon catheter injury. *Biochem Biophys Res Commun,* 205**,** 1051-6.

SHIOI, T., KANG, P. M., DOUGLAS, P. S., HAMPE, J., YBALLE, C. M., LAWITTS, J., CANTLEY, L. C. & IZUMO, S. 2000. The conserved phosphoinositide 3-kinase pathway determines heart size in mice. *Embo j,* 19**,** 2537-48.

SIEGMUND, B., SCHLACK, W., LADILOV, Y. V., BALSER, C. & PIPER, H. M. 1997. Halothane protects cardiomyocytes against reoxygenation-induced hypercontracture. *Circulation,* 96**,** 4372-9.

SIMONIS, G., BRIEM, S. K., SCHOEN, S. P., BOCK, M., MARQUETANT, R. & STRASSER, R. H. 2007. Protein kinase C in the human heart: differential regulation of the isoforms in aortic stenosis or dilated cardiomyopathy. *Mol Cell Biochem,* 305**,** 103-11.

SINGH, R. M., CUMMINGS, E., PANTOS, C. & SINGH, J. 2017. Protein kinase C and cardiac dysfunction: a review. *Heart Fail Rev,* 22**,** 843-859.

SMALL, E. M., THATCHER, J. E., SUTHERLAND, L. B., KINOSHITA, H., GERARD, R. D., RICHARDSON, J. A., DIMAIO, J. M., SADEK, H., KUWAHARA, K. & OLSON, E. N. 2010. Myocardin-related transcription factor-a controls myofibroblast activation and fibrosis in response to myocardial infarction. *Circ Res,* 107**,** 294-304.

SOEKI, T., KISHIMOTO, I., OKUMURA, H., TOKUDOME, T., HORIO, T., MORI, K. & KANGAWA, K. 2005. C-type natriuretic peptide, a novel antifibrotic and antihypertrophic agent, prevents cardiac remodeling after myocardial infarction. *J Am Coll Cardiol,* 45**,** 608-16.

SOLOMON, D. H., SCHNEEWEISS, S., GLYNN, R. J., KIYOTA, Y., LEVIN, R., MOGUN, H. & AVORN, J. 2004. Relationship between selective cyclooxygenase-2 inhibitors and acute myocardial infarction in older adults. *Circulation,* 109**,** 2068-73.

SOLOMON, S. D., ZILE, M., PIESKE, B., VOORS, A., SHAH, A., KRAIGHER-KRAINER, E., SHI, V., BRANSFORD, T., TAKEUCHI, M., GONG, J., LEFKOWITZ, M., PACKER, M. & MCMURRAY, J. J. 2012. The angiotensin receptor neprilysin inhibitor LCZ696 in heart failure with preserved ejection fraction: a phase 2 double-blind randomised controlled trial. *Lancet,* 380**,** 1387-95.

SONG, W., WANG, H. & WU, Q. 2015. Atrial natriuretic peptide in cardiovascular biology and disease (NPPA). *Gene,* 569**,** 1-6.

SORENSSON, P., RYDEN, L., SALEH, N., TORNVALL, P., ARHEDEN, H. & PERNOW, J. 2013. Long-term impact of postconditioning on infarct size and left ventricular ejection fraction in patients with ST-elevation myocardial infarction. *BMC Cardiovasc Disord,* 13**,** 22.

SPINALE, F. G. 2007. Myocardial matrix remodeling and the matrix metalloproteinases: influence on cardiac form and function. *Physiol Rev,* 87**,** 1285-342.

SPIRANEC, K., CHEN, W., WERNER, F., NIKOLAEV, V. O., NARUKE, T., KOCH, F., WERNER, A., EDER-NEGRIN, P., DIEGUEZ-HURTADO, R., ADAMS, R. H., BABA, H. A., SCHMIDT, H., SCHUH, K., SKRYABIN, B. V., MOVAHEDI, K., SCHWEDA, F. & KUHN, M. 2018. Endothelial C-Type Natriuretic Peptide Acts on Pericytes to Regulate Microcirculatory Flow and Blood Pressure. *Circulation*.

SPRINGER, J., AZER, J., HUA, R., ROBBINS, C., ADAMCZYK, A., MCBOYLE, S., BISSELL, M. B. & ROSE, R. A. 2012. The natriuretic peptides BNP and CNP increase heart rate and electrical conduction by stimulating ionic currents in the sinoatrial node and atrial myocardium following activation of guanylyl cyclase-linked natriuretic peptide receptors. *J Mol Cell Cardiol,* 52**,** 1122-34.

STEPAN, H., LEITNER, E., BADER, M. & WALTHER, T. 2000. Organ-specific mRNA distribution of C-type natriuretic peptide in neonatal and adult mice. *Regul Pept,* 95**,** 81-5.

STINGO, A. J., CLAVELL, A. L., HEUBLEIN, D. M., WEI, C. M., PITTELKOW, M. R. & BURNETT, J. C., JR. 1992. Presence of C-type natriuretic peptide in cultured human endothelial cells and plasma. *Am J Physiol,* 263**,** H1318-21.

STRAND, A. H., GUDMUNDSDOTTIR, H., OS, I., SMITH, G., WESTHEIM, A. S., BJORNERHEIM, R. & KJELDSEN, S. E. 2006. Arterial plasma noradrenaline predicts left ventricular mass independently of blood pressure and body build in men who develop hypertension over 20 years. *J Hypertens,* 24**,** 905-13.

SUDOH, T., KANGAWA, K., MINAMINO, N. & MATSUO, H. 1988. A new natriuretic peptide in porcine brain. *Nature,* 332**,** 78-81.

SUDOH, T., MAEKAWA, K., KOJIMA, M., MINAMINO, N., KANGAWA, K. & MATSUO, H. 1989. Cloning and sequence analysis of cDNA encoding a precursor for human brain natriuretic peptide. *Biochem Biophys Res Commun,* 159**,** 1427-34.

SUGDEN, P. H. & CLERK, A. 1998. Cellular mechanisms of cardiac hypertrophy. *J Mol Med (Berl),* 76**,** 725-46.

SUTHERLAND, F. J. & HEARSE, D. J. 2000. The isolated blood and perfusion fluid perfused heart. *Pharmacol Res,* 41**,** 613-27.

SUTHERLAND, F. J., SHATTOCK, M. J., BAKER, K. E. & HEARSE, D. J. 2003. Mouse isolated perfused heart: characteristics and cautions. *Clin Exp Pharmacol Physiol,* 30**,** 867-78.

SUZUKI, M., SASAKI, N., MIKI, T., SAKAMOTO, N., OHMOTO-SEKINE, Y., TAMAGAWA, M., SEINO, S., MARBÁN, E. & NAKAYA, H. 2002. Role of sarcolemmal KATP channels in cardioprotection against ischemia/reperfusion injury in mice. *Journal of Clinical Investigation,* 109**,** 509-516.

TACHIBANA, H., PERRINO, C., TAKAOKA, H., DAVIS, R. J., NAGA PRASAD, S. V. & ROCKMAN, H. A. 2006. JNK1 is required to preserve cardiac function in the early response to pressure overload. *Biochem Biophys Res Commun,* 343**,** 1060-6.

TAJIMA, M., BARTUNEK, J., WEINBERG, E. O., ITO, N. & LORELL, B. H. 1998. Atrial natriuretic peptide has different effects on contractility and intracellular pH in normal and hypertrophied myocytes from pressure-overloaded hearts. *Circulation,* 98**,** 2760-4.

TAKAHASHI, T., ALLEN, P. D. & IZUMO, S. 1992. Expression of A-, B-, and C-type natriuretic peptide genes in failing and developing human ventricles. Correlation with expression of the Ca(2+)-ATPase gene. *Circ Res,* 71**,** 9-17.

TAKIMOTO, E., CHAMPION, H. C., LI, M., BELARDI, D., REN, S., RODRIGUEZ, E. R., BEDJA, D., GABRIELSON, K. L., WANG, Y. & KASS, D. A. 2005. Chronic inhibition of cyclic GMP phosphodiesterase 5A prevents and reverses cardiac hypertrophy. *Nat Med,* 11**,** 214-22.

TAKIMOTO, E., KOITABASHI, N., HSU, S., KETNER, E. A., ZHANG, M., NAGAYAMA, T., BEDJA, D., GABRIELSON, K. L., BLANTON, R., SIDEROVSKI, D. P., MENDELSOHN, M. E. & KASS, D. A. 2009. Regulator of G protein signaling 2 mediates cardiac compensation to pressure overload and antihypertrophic effects of PDE5 inhibition in mice. *J Clin Invest,* 119**,** 408-20.

TAMURA, N., DOOLITTLE, L. K., HAMMER, R. E., SHELTON, J. M., RICHARDSON, J. A. & GARBERS, D. L. 2004. Critical roles of the guanylyl cyclase B receptor in endochondral ossification and development of female reproductive organs. *Proc Natl Acad Sci U S A,* 101**,** 17300-5.

TAMURA, N., OGAWA, Y., CHUSHO, H., NAKAMURA, K., NAKAO, K., SUDA, M., KASAHARA, M., HASHIMOTO, R., KATSUURA, G., MUKOYAMA, M., ITOH, H., SAITO, Y., TANAKA, I., OTANI, H. & KATSUKI, M. 2000. Cardiac fibrosis in mice lacking brain natriuretic peptide. *Proc Natl Acad Sci U S A,* 97**,** 4239-44.

TARAZON, E., ROSELLO-LLETI, E., ORTEGA, A., MOLINA-NAVARRO, M. M., SANCHEZ-LAZARO, I., LAGO, F., GONZALEZ-JUANATEY, J. R., RIVERA, M. & PORTOLES, M. 2014. Differential gene expression of C-type natriuretic peptide and its related molecules in dilated and ischemic cardiomyopathy. A new option for the management of heart failure. *Int J Cardiol,* 174**,** e84-6.

TEEKAKIRIKUL, P., EMINAGA, S., TOKA, O., ALCALAI, R., WANG, L., WAKIMOTO, H., NAYOR, M., KONNO, T., GORHAM, J. M., WOLF, C. M., KIM, J. B., SCHMITT, J. P., MOLKENTIN, J. D., NORRIS, R. A., TAGER, A.

M., HOFFMAN, S. R., MARKWALD, R. R., SEIDMAN, C. E. & SEIDMAN, J. G. 2010. Cardiac fibrosis in mice with hypertrophic cardiomyopathy is mediated by non-myocyte proliferation and requires Tgf-beta. *J Clin Invest,* 120**,** 3520-9.

TEERLINK, J. R., PFEFFER, J. M. & PFEFFER, M. A. 1994. Progressive ventricular remodeling in response to diffuse isoproterenol-induced myocardial necrosis in rats. *Circ Res,* 75**,** 105-13.

TERKELSEN, C. J., CHRISTIANSEN, E. H., SORENSEN, J. T., KRISTENSEN, S. D., LASSEN, J. F., THUESEN, L., ANDERSEN, H. R., VACH, W. & NIELSEN, T. T. 2009. Primary PCI as the preferred reperfusion therapy in STEMI: it is a matter of time. *Heart,* 95**,** 362-9.

THOMAS, R., CHENG, Y., YAN, J., BETTINGER, T., BROILLET, A., RIOUFOL, G. & NUNN, A. D. 2010. Upregulation of coronary endothelial P-selectin in a monkey heart ischemia reperfusion model. *J Mol Histol,* 41**,** 277-87.

TIEFENBACHER, C. P., LEE, C. H., KAPITZA, J., DIETZ, V. & NIROOMAND, F. 2003. Sepiapterin reduces postischemic injury in the rat heart. *Pflugers Arch,* 447**,** 1-7.

TINKER, A., AZIZ, Q. & THOMAS, A. 2014. The role of ATP-sensitive potassium channels in cellular function and protection in the cardiovascular system. *Br J Pharmacol,* 171**,** 12-23.

TOJO, S. J., YOKOTA, S., KOIKE, H., SCHULTZ, J., HAMAZUME, Y., MISUGI, E., YAMADA, K., HAYASHI, M., PAULSON, J. C. & MOROOKA, S. 1996. Reduction of rat myocardial ischemia and reperfusion injury by sialyl Lewis x oligosaccharide and anti-rat P-selectin antibodies. *Glycobiology,* 6**,** 463-9.

TOKUDOME, T., HORIO, T., SOEKI, T., MORI, K., KISHIMOTO, I., SUGA, S., YOSHIHARA, F., KAWANO, Y., KOHNO, M. & KANGAWA, K. 2004. Inhibitory effect of C-type natriuretic peptide (CNP) on cultured cardiac myocyte hypertrophy: interference between CNP and endothelin-1 signaling pathways. *Endocrinology,* 145**,** 2131-40.

TOKUDOME, T., KISHIMOTO, I., HORIO, T., ARAI, Y., SCHWENKE, D. O., HINO, J., OKANO, I., KAWANO, Y., KOHNO, M., MIYAZATO, M., NAKAO, K. & KANGAWA, K. 2008. Regulator of G-protein signaling subtype 4 mediates antihypertrophic effect of locally secreted natriuretic peptides in the heart. *Circulation,* 117**,** 2329-39.

TOMITA, H., NAZMY, M., KAJIMOTO, K., YEHIA, G., MOLINA, C. A. & SADOSHIMA, J. 2003. Inducible cAMP early repressor (ICER) is a negative-feedback regulator of cardiac hypertrophy and an important mediator of cardiac myocyte apoptosis in response to beta-adrenergic receptor stimulation. *Circ Res,* 93**,** 12-22.

TSAI, E. J. & KASS, D. A. 2009. Cyclic GMP signaling in cardiovascular pathophysiology and therapeutics. *Pharmacol Ther,* 122**,** 216-38.

TSUTAMOTO, T., KANAMORI, T., MORIGAMI, N., SUGIMOTO, Y., YAMAOKA, O. & KINOSHITA, M. 1993. Possibility of downregulation of atrial natriuretic peptide receptor coupled to guanylate cyclase in peripheral vascular beds of patients with chronic severe heart failure. *Circulation,* 87**,** 70-5.

UKAI, T., CHENG, C. P., TACHIBANA, H., IGAWA, A., ZHANG, Z. S., CHENG, H. J. & LITTLE, W. C. 2001. Allopurinol enhances the contractile response to dobutamine and exercise in dogs with pacing-induced heart failure. *Circulation,* 103**,** 750-5.

UMARU, B., PYRIOCHOU, A., KOTSIKORIS, V., PAPAPETROPOULOS, A. & TOPOUZIS, S. 2015. ATP-sensitive potassium channel activation induces angiogenesis in vitro and in vivo. *J Pharmacol Exp Ther,* 354**,** 79-87.

VADUGANATHAN, M., GREENE, S. J., AMBROSY, A. P., GHEORGHIADE, M. & BUTLER, J. 2013. The disconnect between phase II and phase III trials of drugs for heart failure. *Nat Rev Cardiol,* 10**,** 85-97.

VAN BILSEN, M., PATEL, H. C., BAUERSACHS, J., BOHM, M., BORGGREFE, M., BRUTSAERT, D., COATS, A. J. S., DE BOER, R. A., DE KEULENAER, G. W., FILIPPATOS, G. S., FLORAS, J., GRASSI, G., JANKOWSKA, E. A., KORNET, L., LUNDE, I. G., MAACK, C., MAHFOUD, F., POLLESELLO, P., PONIKOWSKI, P., RUSCHITZKA, F., SABBAH, H. N., SCHULTZ, H. D., SEFEROVIC, P., SLART, R., TAGGART, P., TOCCHETTI, C. G., VAN LAAKE, L. W., ZANNAD, F., HEYMANS, S. & LYON, A. R. 2017. The autonomic nervous system as a therapeutic target in heart failure: a scientific position statement from the Translational Research Committee of the Heart Failure Association of the European Society of Cardiology. *Eur J Heart Fail,* 19**,** 1361-1378.

VAN DE HOEF, T. P., BAX, M., MEUWISSEN, M., DAMMAN, P., DELEWI, R., DE WINTER, R. J., KOCH, K. T., SCHOTBORGH, C., HENRIQUES, J. P., TIJSSEN, J. G. & PIEK, J. J. 2013. Impact of coronary microvascular function on long-term cardiac mortality in patients with acute ST-segment-elevation myocardial infarction. *Circ Cardiovasc Interv,* 6**,** 207-15.

VANDERHEYDEN, M., BARTUNEK, J. & GOETHALS, M. 2004. Brain and other natriuretic peptides: molecular aspects. *Eur J Heart Fail,* 6**,** 261-8.

VANE, J. R. & BOTTING, R. M. 1998. Mechanism of action of antiinflammatory drugs. *Int J Tissue React,* 20**,** 3-15.

VILLAR, I. C., PANAYIOTOU, C. M., SHERAZ, A., MADHANI, M., SCOTLAND, R. S., NOBLES, M., KEMP-HARPER, B., AHLUWALIA, A. & HOBBS, A. J. 2007. Definitive role for natriuretic peptide receptor-C in mediating the vasorelaxant activity of C-type natriuretic peptide and endothelium-derived hyperpolarising factor. *Cardiovasc Res,* 74**,** 515-25.

VINCENT, J. L. 2008. Understanding cardiac output. *Crit Care,* 12**,** 174.

VOLPE, M., RUBATTU, S. & BURNETT, J., JR. 2014. Natriuretic peptides in cardiovascular diseases: current use and perspectives. *Eur Heart J,* 35**,** 419-25.

WAKASAKI, H., KOYA, D., SCHOEN, F. J., JIROUSEK, M. R., WAYS, D. K., HOIT, B. D., WALSH, R. A. & KING, G. L. 1997. Targeted overexpression of protein kinase C beta2 isoform in myocardium causes cardiomyopathy. *Proc Natl Acad Sci U S A,* 94**,** 9320-5.

WALTERS, H. L., 3RD, DIGERNESS, S. B., NAFTEL, D. C., WAGGONER, J. R., 3RD, BLACKSTONE, E. H. & KIRKLIN, J. W. 1992. The response to ischemia in blood perfused vs. crystalloid perfused isolated rat heart preparations. *J Mol Cell Cardiol,* 24**,** 1063-77.

WALTHER, T., SCHUITHEISS, H. P. & TSCHOPE, C. 2001. Impaired angiotensin II regulation of renal C-type natriuretic peptide mRNA expression in experimental diabetes mellitus. *Cardiovasc Res,* 51**,** 562-6.

WANG, D., GLADYSHEVA, I. P., FAN, T. H., SULLIVAN, R., HOUNG, A. K. & REED, G. L. 2014. Atrial natriuretic peptide affects cardiac remodeling, function, heart failure, and survival in a mouse model of dilated cardiomyopathy. *Hypertension,* 63**,** 514-9.

WANG, T. J., LARSON, M. G., LEVY, D., BENJAMIN, E. J., LEIP, E. P., OMLAND, T., WOLF, P. A. & VASAN, R. S. 2004. Plasma natriuretic peptide levels and the risk of cardiovascular events and death. *N Engl J Med,* 350**,** 655-63.

WANG, Y. 2007. Mitogen-activated protein kinases in heart development and diseases. *Circulation,* 116**,** 1413-23.

WANG, Y., DE WAARD, M. C., STERNER-KOCK, A., STEPAN, H., SCHULTHEISS, H. P., DUNCKER, D. J. & WALTHER, T. 2007. Cardiomyocyte-restricted over-expression of C-type natriuretic peptide prevents cardiac hypertrophy induced by myocardial infarction in mice. *Eur J Heart Fail,* 9**,** 548-57.

WANG, Y., HUANG, S., SAH, V. P., ROSS, J., JR., BROWN, J. H., HAN, J. & CHIEN, K. R. 1998a. Cardiac muscle cell hypertrophy and apoptosis induced by distinct members of the p38 mitogen-activated protein kinase family. *J Biol Chem,* 273**,** 2161-8.

WANG, Y., SU, B., SAH, V. P., BROWN, J. H., HAN, J. & CHIEN, K. R. 1998b. Cardiac hypertrophy induced by mitogen-activated protein kinase kinase 7, a specific activator for c-Jun NH2-terminal kinase in ventricular muscle cells. *J Biol Chem,* 273**,** 5423-6.

WEGENER, J. W., NAWRATH, H., WOLFSGRUBER, W., KUHBANDNER, S., WERNER, C., HOFMANN, F. & FEIL, R. 2002. cGMP-dependent protein kinase I mediates the negative inotropic effect of cGMP in the murine myocardium. *Circ Res,* 90**,** 18-20.

WEI, C. M., HU, S., MILLER, V. M. & BURNETT, J. C., JR. 1994. Vascular actions of C-type natriuretic peptide in isolated porcine coronary arteries and coronary vascular smooth muscle cells. *Biochem Biophys Res Commun,* 205**,** 765-71.

WENZEL, S., ROHDE, C., WINGERNING, S., ROTH, J., KOJDA, G. & SCHLUTER, K. D. 2007. Lack of endothelial nitric oxide synthase-derived nitric oxide formation favors hypertrophy in adult ventricular cardiomyocytes. *Hypertension,* 49**,** 193-200.

WETTSCHURECK, N., RUTTEN, H., ZYWIETZ, A., GEHRING, D., WILKIE, T. M., CHEN, J., CHIEN, K. R. & OFFERMANNS, S. 2001. Absence of pressure overload induced myocardial hypertrophy after conditional inactivation of Galphaq/Galpha11 in cardiomyocytes. *Nat Med,* 7**,** 1236-40.

WILEY, K. E. & DAVENPORT, A. P. 2001. Physiological antagonism of endothelin-1 in human conductance and resistance coronary artery. *Br J Pharmacol,* 133**,** 568-74.

WILKINS, B. J., DAI, Y. S., BUENO, O. F., PARSONS, S. A., XU, J., PLANK, D. M., JONES, F., KIMBALL, T. R. & MOLKENTIN, J. D. 2004. Calcineurin/NFAT coupling participates in pathological, but not physiological, cardiac hypertrophy. *Circ Res,* 94**,** 110-8.

WILLIAMS, B. 2001. Angiotensin II and the pathophysiology of cardiovascular remodeling. *Am J Cardiol,* 87**,** 10C-17C.

WILLIAMS, B., COCKCROFT, J. R., KARIO, K., ZAPPE, D. H., BRUNEL, P. C., WANG, Q. & GUO, W. 2017. Effects of Sacubitril/Valsartan Versus Olmesartan on Central Hemodynamics in the Elderly With Systolic Hypertension: The PARAMETER Study. *Hypertension,* 69**,** 411-420.

WILLIAMS, F. M., KUS, M., TANDA, K. & WILLIAMS, T. J. 1994. Effect of duration of ischaemia on reduction of myocardial infarct size by inhibition of neutrophil accumulation using an anti-CD18 monoclonal antibody. *Br J Pharmacol,* 111**,** 1123-8.

WITTELES, R. M., KAO, D., CHRISTOPHERSON, D., MATSUDA, K., VAGELOS, R. H., SCHREIBER, D. & FOWLER, M. B. 2007. Impact of nesiritide on renal function in patients with acute decompensated heart failure and pre-existing renal dysfunction a randomized, double-blind, placebo-controlled clinical trial. *J Am Coll Cardiol,* 50**,** 1835-40.

WOLLERT, K. C., YURUKOVA, S., KILIC, A., BEGROW, F., FIEDLER, B., GAMBARYAN, S., WALTER, U., LOHMANN, S. M. & KUHN, M. 2003. Increased effects of C-type natriuretic peptide on contractility and calcium regulation in murine hearts overexpressing cyclic GMP-dependent protein kinase I. *Br J Pharmacol,* 140**,** 1227-36.

WOOD, A. R., ESKO, T., YANG, J., VEDANTAM, S., PERS, T. H., GUSTAFSSON, S., CHU, A. Y., ESTRADA, K., LUAN, J., KUTALIK, Z., AMIN, N., BUCHKOVICH, M. L., CROTEAU-CHONKA, D. C., DAY, F. R., DUAN, Y., FALL, T., FEHRMANN, R., FERREIRA, T., JACKSON, A. U., KARJALAINEN, J., LO, K. S., LOCKE, A. E., MAGI, R., MIHAILOV, E., PORCU, E., RANDALL, J. C., SCHERAG, A., VINKHUYZEN, A. A., WESTRA, H. J., WINKLER, T. W., WORKALEMAHU, T., ZHAO, J. H., ABSHER, D., ALBRECHT, E., ANDERSON, D., BARON, J., BEEKMAN, M., DEMIRKAN, A., EHRET, G. B., FEENSTRA, B., FEITOSA, M. F., FISCHER, K., FRASER, R. M., GOEL, A., GONG, J., JUSTICE, A. E., KANONI, S., KLEBER, M. E., KRISTIANSSON, K., LIM, U., LOTAY, V., LUI, J. C., MANGINO, M., MATEO LEACH, I., MEDINA-GOMEZ, C., NALLS, M. A., NYHOLT, D. R., PALMER, C. D., PASKO, D., PECHLIVANIS, S., PROKOPENKO, I., RIED, J. S., RIPKE, S., SHUNGIN, D., STANCAKOVA, A., STRAWBRIDGE, R. J., SUNG, Y. J., TANAKA, T., TEUMER, A., TROMPET, S., VAN DER LAAN, S. W., VAN SETTEN, J., VAN VLIET-OSTAPTCHOUK, J. V., WANG, Z., YENGO, L., ZHANG, W., AFZAL, U., ARNLOV, J., ARSCOTT, G. M., BANDINELLI, S., BARRETT, A., BELLIS, C., BENNETT, A. J., BERNE, C., BLUHER, M., BOLTON, J. L., BOTTCHER, Y., BOYD, H. A., BRUINENBERG, M., BUCKLEY, B. M., BUYSKE, S., CASPERSEN, I. H., CHINES, P. S., CLARKE, R., CLAUDI-BOEHM, S., COOPER, M., DAW, E. W., DE JONG, P. A., DEELEN, J., DELGADO, G., et al. 2014. Defining the role of common variation in the genomic and biological architecture of adult human height. *Nat Genet,* 46**,** 1173-86.

WRIGHT, R. S., WEI, C. M., KIM, C. H., KINOSHITA, M., MATSUDA, Y., AARHUS, L. L., BURNETT, J. C., JR. & MILLER, W. L. 1996. C-type natriuretic peptide-mediated coronary vasodilation: role of the coronary nitric oxide and particulate guanylate cyclase systems. *J Am Coll Cardiol,* 28**,** 1031-8.

WU, L. H., ZHANG, Q., ZHANG, S., MENG, L. Y., WANG, Y. C. & SHENG, C. J. 2017a. Effects of Gene Knockdown of CNP on Ventricular Remodeling after Myocardial Ischemia-Reperfusion Injury through NPRB/Cgmp Signaling Pathway in Rats. *J Cell Biochem*.

WU, Q. Q., XIAO, Y., YUAN, Y., MA, Z. G., LIAO, H. H., LIU, C., ZHU, J. X., YANG, Z., DENG, W. & TANG, Q. Z. 2017b. Mechanisms contributing to cardiac remodelling. *Clin Sci (Lond),* 131**,** 2319-2345.

YAMASHIRO, S., NOGUCHI, K., MATSUZAKI, T., MIYAGI, K., NAKASONE, J., SAKANASHI, M., KOJA, K. & SAKANASHI, M. 2002. Beneficial effect of tetrahydrobiopterin on ischemia-reperfusion injury in isolated perfused rat hearts. *J Thorac Cardiovasc Surg,* 124**,** 775-84.

YAMAZAKI, T., SEKO, Y., TAMATANI, T., MIYASAKA, M., YAGITA, H., OKUMURA, K., NAGAI, R. & YAZAKI, Y. 1993a. Expression of intercellular adhesion molecule-1 in rat heart with ischemia/reperfusion and limitation of infarct size by treatment with antibodies against cell adhesion molecules. *Am J Pathol,* 143**,** 410-8.

YAMAZAKI, T., TOBE, K., HOH, E., MAEMURA, K., KAIDA, T., KOMURO, I., TAMEMOTO, H., KADOWAKI, T., NAGAI, R. & YAZAKI, Y. 1993b. Mechanical loading activates mitogen-activated protein kinase and S6 peptide kinase in cultured rat cardiac myocytes. *J Biol Chem,* 268**,** 12069-76.

YAN, W., WU, F., MORSER, J. & WU, Q. 2000. Corin, a transmembrane cardiac serine protease, acts as a pro-atrial natriuretic peptide-converting enzyme. *Proc Natl Acad Sci U S A,* 97**,** 8525-9.

YANCY, C. W., KRUM, H., MASSIE, B. M., SILVER, M. A., STEVENSON, L. W., CHENG, M., KIM, S. S. & EVANS, R. 2008. Safety and efficacy of outpatient nesiritide in patients with advanced heart failure: results of the Second Follow-Up Serial Infusions of Nesiritide (FUSION II) trial. *Circ Heart Fail,* 1**,** 9-16.

YANDLE, T. G., RICHARDS, A. M., NICHOLLS, M. G., CUNEO, R., ESPINER, E. A. & LIVESEY, J. H. 1986. Metabolic clearance rate and plasma half life of alpha-human atrial natriuretic peptide in man. *Life Sci,* 38**,** 1827-33.

YANG, F., LIU, Y. H., YANG, X. P., XU, J., KAPKE, A. & CARRETERO, O. A. 2002. Myocardial infarction and cardiac remodelling in mice. *Exp Physiol,* 87**,** 547-55.

YANG, L., LIU, G., ZAKHAROV, S. I., BELLINGER, A. M., MONGILLO, M. & MARX, S. O. 2007. Protein kinase G phosphorylates Cav1.2 alpha1c and beta2 subunits. *Circ Res,* 101**,** 465-74.

YELLON, D. M. & HAUSENLOY, D. J. 2007. Myocardial reperfusion injury. *N Engl J Med,* 357**,** 1121-35.

YONG, A. S. & FEARON, W. F. 2013. Coronary microvascular dysfunction after ST-segment-elevation myocardial infarction: local or global phenomenon? *Circ Cardiovasc Interv,* 6**,** 201-3.

YOUSEF, Z. R., REDWOOD, S. R. & MARBER, M. S. 2000. Postinfarction left ventricular remodeling: a pathophysiological and therapeutic review. *Cardiovasc Drugs Ther,* 14**,** 243-52.

YU, Y., RICCIOTTI, E., SCALIA, R., TANG, S. Y., GRANT, G., YU, Z., LANDESBERG, G., CRICHTON, I., WU, W., PURE, E., FUNK, C. D. & FITZGERALD, G. A. 2012. Vascular COX-2 modulates blood pressure and thrombosis in mice. *Sci Transl Med,* 4**,** 132ra54.

YUSUF, S., PITT, B., DAVIS, C. E., HOOD, W. B. & COHN, J. N. 1991. Effect of enalapril on survival in patients with reduced left ventricular ejection fractions and congestive heart failure. *N Engl J Med,* 325**,** 293-302.

ZATTA, A. J. & HEADRICK, J. P. 2005. Mediators of coronary reactive hyperaemia in isolated mouse heart. *Br J Pharmacol,* 144**,** 576-87.

ZEYMER, U., SURYAPRANATA, H., MONASSIER, J. P., OPOLSKI, G., DAVIES, J., RASMANIS, G., LINSSEN, G., TEBBE, U., SCHRODER, R., TIEMANN, R., MACHNIG, T. & NEUHAUS, K. L. 2001. The Na(+)/H(+) exchange inhibitor eniporide as an adjunct to early reperfusion therapy for acute myocardial infarction. Results of the evaluation of the safety and cardioprotective effects of eniporide in acute myocardial infarction (ESCAMI) trial. *J Am Coll Cardiol,* 38**,** 1644-50.

ZHANG, D., GAUSSIN, V., TAFFET, G. E., BELAGULI, N. S., YAMADA, M., SCHWARTZ, R. J., MICHAEL, L. H., OVERBEEK, P. A. & SCHNEIDER, M. D. 2000. TAK1 is activated in the myocardium after pressure overload and is sufficient to provoke heart failure in transgenic mice. *Nat Med,* 6**,** 556-63.

ZHANG, Q., MOALEM, J., TSE, J., SCHOLZ, P. M. & WEISS, H. R. 2005a. Effects of natriuretic peptides on ventricular myocyte contraction and role of cyclic GMP signaling. *Eur J Pharmacol,* 510**,** 209-15.

ZHANG, R., KHOO, M. S., WU, Y., YANG, Y., GRUETER, C. E., NI, G., PRICE, E. E., JR., THIEL, W., GUATIMOSIM, S., SONG, L. S., MADU, E. C., SHAH, A. N., VISHNIVETSKAYA, T. A., ATKINSON, J. B., GUREVICH, V. V., SALAMA, G., LEDERER, W. J., COLBRAN, R. J. & ANDERSON, M. E. 2005b. Calmodulin kinase II inhibition protects against structural heart disease. *Nat Med,* 11**,** 409-17.

ZHANG, T., MAIER, L. S., DALTON, N. D., MIYAMOTO, S., ROSS, J., JR., BERS, D. M. & BROWN, J. H. 2003. The deltaC isoform of CaMKII is activated in cardiac hypertrophy and induces dilated cardiomyopathy and heart failure. *Circ Res,* 92**,** 912-9.

ZHANG, W., ANGER, T., SU, J., HAO, J., XU, X., ZHU, M., GACH, A., CUI, L., LIAO, R. & MENDE, U. 2006. Selective loss of fine tuning of Gq/11 signaling by RGS2 protein exacerbates cardiomyocyte hypertrophy. *J Biol Chem,* 281**,** 5811-20.

ZHANG, Z., XIAO, Z. & DIAMOND, S. L. 1999. Shear stress induction of C-type natriuretic peptide (CNP) in endothelial cells is independent of NO autocrine signaling. *Ann Biomed Eng,* 27**,** 419-26.

ZHENG, B., ZHANG, Z., BLACK, C. M., DE CROMBRUGGHE, B. & DENTON, C. P. 2002. Ligand-dependent genetic recombination in fibroblasts : a potentially powerful technique for investigating gene function in fibrosis. *Am J Pathol,* 160**,** 1609-17.

ZHENG, M., DILLY, K., DOS SANTOS CRUZ, J., LI, M., GU, Y., URSITTI, J. A., CHEN, J., ROSS, J., JR., CHIEN, K. R., LEDERER, J. W. & WANG, Y. 2004. Sarcoplasmic reticulum calcium defect in Ras-induced hypertrophic cardiomyopathy heart. *Am J Physiol Heart Circ Physiol,* 286**,** H424-33.

ZHOU, H. & MURTHY, K. S. 2003. Identification of the G protein-activating sequence of the single-transmembrane natriuretic peptide receptor C (NPR-C). *Am J Physiol Cell Physiol,* 284**,** C1255-61.

ZHOU, J., LI, Y. S. & CHIEN, S. 2014. Shear stress-initiated signaling and its regulation of endothelial function. *Arterioscler Thromb Vasc Biol,* 34**,** 2191-8.

ZOLK, O., FLESCH, M., NICKENIG, G., SCHNABEL, P. & BOHM, M. 1998. Alteration of intracellular Ca2(+)-handling and receptor regulation in hypertensive cardiac hypertrophy: insights from Ren2-transgenic rats. *Cardiovasc Res,* 39**,** 242-56.

ZOU, Y., HIROI, Y., UOZUMI, H., TAKIMOTO, E., TOKO, H., ZHU, W., KUDOH, S., MIZUKAMI, M., SHIMOYAMA, M., SHIBASAKI, F., NAGAI, R., YAZAKI, Y. & KOMURO, I. 2001. Calcineurin plays a critical role in the development of pressure overload-induced cardiac hypertrophy. *Circulation,* 104**,** 97-101.